Université Mohamed Khider – Biskra		**جامعة محمد خيضر بسكرة**
Faculté des Sciences et de la technologie		**كلية العلوم و التكنولوجيا**
Département de Génie Civil et Hydraulique		**قسم الهندسة المدنية و الري**
Réf :………………		**المرجع: ....**

Thèse de Doctorat LMD
Spécialité : GENIE CIVIL
Option : MATERIAUX DE CONSTRUCTION

Formulation et caractérisation des blocs de terre comprimée à base de déchets de palmiers dattiers

---

Présentée par :
ATIKI Elhoussine

Soutenue publiquement le : 03/11/2022

Devant le jury composé de :

CHEBILI Rachid	**Professeur**	**Président**	**Université de Biskra**
TAALLAH Bachir	**Professeur**	**Rapporteur**	**Université de Biskra**
BOUAZIZ Ahmed	**Professeur**	**Examinateur**	**Université de Biskra**
NECERA Brahim	**Maître de Conférences 'A'**	**Examinateur**	**Université de Djelfa**
FEIA Sadok	**Maître de Conférences 'A'**	**Invité**	**Université de Biskra**

الجمهورية الجزائرية الديمقراطية الشعبية

People's Democratic Republic of Algeria

وزارة التعليم العالي والبحث العلمي

Ministry of Higher Education and Scientific Research

Mohamed Khider University - Biskra

Faculty of Science and Technology

Department: Civil and Hydraulic
Engineering
Ref: ... ...

جـــامعة محمد خـيضر بـــسكرة

كـلية الـعلــوم و التكـــنولوجـيا

قـسـم : الهندسـة المـدنيـة و الـري

المرجع: ....

Thesis presented with a view to obtaining

LMD Doctorate in Civil Engineering

Option: CONSTRUCTION MATERIALS

Formulation and characterization of compressed earth blocks based on date palm waste

Presented by:

Elhoussine ATIKI

Publicly supported on: 03/11/2022

The jury composed of:

Rachid CHEBILI	**Professor**	**President**	**University of Biskra**
Bachir TAALLAH	**Professor**	**Supervisor**	**University of Biskra**
Ahmed BOUAZIZ	**Professor**	**Examiner**	**University of Biskra**
Brahim NECERA	**Lecturer 'A'**	**Examiner**	**University of Djelfa**
Sadok FEIA	**Lecturer 'A'**	**Invited**	**University of Biskra**

DEDICATION

To my dear parents, to my future wife and to all my family

Elhoussine ATIKI

ACKNOWLEDGMENTS

Abstract

Today, it is widely admitted that improved comfort conditions and reduced costs related to air conditioning and heating using environmentally friendly and low cost energy sources are some of the most urgent priorities that must be taken. In order to achieve this aim, it is required to develop new building materials and use renewable resources that could help to cut down the energy costs in buildings. Recently, the scientific community has been able to shed light on raw earth building materials and is working to make them a promising, clean, and economical alternative to cement and fired brick materials. The present study provides interesting data regarding the incorporation of date palm waste into the soil matrix for the development of environmentally friendly building materials. It is an experimental study conducted firstly to study the mechanical, thermal, physical and microstructure properties of CEB filled with date palm waste aggregate (DPWA) as thermal insulator. In this framework, quicklime, used as a stabilizer, and date palm waste were added to the CEB compositions. Five waste contents, i.e. 0.1%, 0.2%, 0.3%, 0.4% and 0.5%, were incorporated into the mixtures that were compacted with a static loading by applying a compaction-induced stress of 10MPa. Secondly, it examined the effect of the type of date palm waste on the flexural behavior of compressed earth blocks (CEBs) using digital image correlation technique (DIC) and the mechanical properties of CEB. In this context, quicklime as a stabilizer and three different kinds of date palm waste were added to the CEB composites: DPWA, date palm mesh (DPM) and date palm spikelet (DPS). Three waste weight contents (0%, 0.2% and 0.5%) were incorporated in the mixtures compacted with a static loading. The results show an interesting improvement of thermal insulation performances of blocks incorporating DPWA. The total water absorption, swelling and capillary absorption of the blocks increased with an increase in the DPWA ratio. the values of the flexural strength was higher for the mixtures with DPWA than for those with DPM or DPS. The addition of 0.5% DPS increases the ductility of the bricks, resulting in some residual force and increasing the deflection at failure. The increase in compaction pressure from 2 MPa to 10 MPa compaction pressures resulted in an increase in flexural strength of about 262.73% for the control block (samples without date palm waste). In addition, it was found that for a block containing 0.5% DPWA, increasing the compaction pressure from 2 MPa to 10 MPa leads to an increase in the bending strength of about 371.68%. The results of ε_{xx} show very high localized strains at the middle of block at the bottom of the samples under tension. The strain concentration zone increases as the fiber content increases. The decrease in compaction pressure from 10 MPa to 2 MPa resulted in a decrease in thermal conductivity of about 21.96% for the block containing 0.5% DPWA. Fortunately, this block gives approximately the same result (0.694 W/m.K) as the adobe block without date palm waste (0.677 W/m.K).

Keywords: Compressed earth block, Date palm waste, thermal conductivity, mechanical behavior, swelling

الملخص

اليوم، من المسلم به على نطاق واسع أن تحسين ظروف الراحة وخفض التكاليف المتعلقة بالتكييف والتدفئة باستخدام مصادر طاقة ووسائل صديقة للبيئة ومنخفضة التكلفة هي من أكثر الأولويات إلحاحًا التي يجب اتخاذها. لتحقيق هذا الهدف، يلزم تطوير مواد بناء جديدة واستخدام موارد متجددة يمكن أن تساعد في خفض تكاليف الطاقة في المباني. في الآونة الأخيرة، تمكن المجتمع العلمي من إلقاء الضوء على مواد البناء الترابية الخام ويعملون على جعلها بديلاً واعداً ونظيفًا واقتصاديًا لمواد الأسمنت والطوب المحروق. تقدم الدراسة الحالية بيانات مثيرة للاهتمام فيما يتعلق بدمج مخلفات النخيل في مصفوفة التربة لتطوير مواد بناء صديقة للبيئة. إنها دراسة تجريبية أجريت أولاً لدراسة الخصائص الميكانيكية والحرارية والفيزيائية والبنية المجهرية للبنات التربة المضغوطة(CEB) المملوءة بركام مخلفات نخيل التمر (DPWA) كعازل حراري. في هذا السياق، تمت إضافة الجير الحي، المستخدم كمثبت كيميائي، ومخلفات نخيل التمر إلى مكونات لبنات التربة المضغوطة. تم دمج خمسة محتويات نفايات، أي 0.1٪، 0.2٪، 0.3٪، 0.4٪ و0.5٪، في الخلائط التي تم ضغطها مع تحميل ثابت عن طريق تطبيق ضغط قدره 10 ميجا باسكال. ثانيًا، فحص تأثير نوع نفايات النخيل على سلوك الانحناء للكتل الترابية المضغوطة (CEBs) باستخدام تقنية ارتباط الصور الرقمية (DIC) والخصائص الميكانيكية لـ CEB. في هذا السياق، تمت إضافة الجير الحي كمثبت وثلاثة أنواع مختلفة من مخلفات نخيل التمر إلى مكونات الكتل: DPWA، وشبكة نخيل التمر (DPM) وسنبيلات نخيل التمر (DPS). تم دمج ثلاثة محتويات من وزن النفايات (0٪، 0.2٪ و0.5٪) في الخلائط المضغوطة مع تحميل ثابت. تظهر النتائج تحسنًا مثيرًا للاهتمام في أداء العزل الحراري للكتل التي تتضمن DPWA. زاد الامتصاص الكلي للماء والتورم والامتصاص الشعري للكتل مع زيادة نسبة DPWA. كانت قيم مقاومة الانحناء للخلائط مع DPWA أعلى مقارنة بتلك التي تحتوي على DPM أو DPS. تؤدي إضافة 0.5٪ DPS إلى زيادة ليونة الطوب، مما ينتج عنه بعض القوة المتبقية وزيادة الانحراف عند الفشل. أدت الزيادة في ضغط العينات أثناء الصنع من 2 ميجا باسكال إلى 10 ميجا باسكال إلى زيادة مقاومة الانحناء بحوالي 262.73٪ للكتلة الشاهدة (عينات بدون نفايات نخيل التمر). بالإضافة إلى ذلك، وجد أنه بالنسبة للكتلة التي تحتوي على 0.5 ٪ DPWA، فإن زيادة الضغط من 2 ميجا باسكال إلى 10 ميجا باسكال يؤدي إلى زيادة مقاومة الانحناء بحوالي 371.68٪. تظهر نتائج ε_{xx} تشوهات موضعية عالية جدًا في منتصف الكتلة في أسفل العينات تحت الشد (المنطقة المشدودة). تزداد شدة تركيز التشوه مع زيادة محتوى الألياف والركام النباتي. أدى الانخفاض في الضغط من 10 ميجا باسكال إلى 2 ميجا باسكال إلى انخفاض في التوصيل الحراري بحوالي 21.96٪ للكتلة التي تحتوي على 0.5٪ DPWA. لحسن الحظ، تعطي هذه الكتلة نفس النتيجة تقريبًا (0.694 واط / مللي كلفن) مثل كتلة اللبن بدون نفايات نخيل التمر (0.677 واط / مللي كلفن).

كلمات مفتاحية: لبنات التربة المضغوطة، نفايات نخيل التمر، الناقلية الحرارية، السلوك الميكانيكي، الانتفاخ

.

Résumé

Aujourd'hui, il est largement admis que l'amélioration des conditions de confort et la réduction des coûts liés à la climatisation et au chauffage utilisant des sources d'énergie respectueuses de l'environnement et à faible coût sont parmi les priorités les plus urgentes à prendre. Pour atteindre cet objectif, il est nécessaire de développer de nouveaux matériaux de construction et d'utiliser des ressources renouvelables qui pourraient contribuer à réduire les coûts énergétiques dans les bâtiments. Récemment, la communauté scientifique a pu faire la lumière sur les matériaux de construction en terre crue et travaille à en faire une alternative prometteuse, propre et économique aux matériaux en ciment et en briques cuites. La présente étude fournit des données intéressantes concernant l'incorporation de déchets de palmier dattier dans la matrice du sol pour le développement de matériaux de construction respectueux de l'environnement. Il s'agit d'une étude expérimentale menée dans un premier temps pour étudier les propriétés mécaniques, thermiques, physiques et microstructurales du bloc de terre comprimée BTC rempli par d'agrégat de déchets de palmier dattier (DPWA) comme isolant thermique. Dans ce cadre, de la chaux vive, utilisée comme stabilisant, et des déchets de palmier dattier ont été ajoutés aux compositions de BTC. Cinq teneurs en déchets, soit 0,1 %, 0,2 %, 0,3 %, 0,4 % et 0,5 %, ont été incorporées dans les mélanges qui ont été compactés avec un chargement statique en appliquant une contrainte induite par le compactage de 10 MPa. Deuxièmement, il a examiné l'effet du type de déchets de palmier dattier sur le comportement en flexion des blocs de terre comprimée (BTC) en utilisant la technique de corrélation d'images numériques (DIC) et les propriétés mécaniques du BTC. Dans ce contexte, la chaux vive comme stabilisant et trois types différents de déchets de palmier dattier ont été ajoutés aux composites BTC : DPWA, maille de palmier dattier (DPM) et épillet de palmier dattier (DPS). Trois teneurs pondérales en déchets (0%, 0,2% et 0,5%) ont été incorporées dans les mélanges compactés avec un chargement statique. Les résultats montrent une amélioration intéressante des performances d'isolation thermique des blocs incorporant du DPWA. L'absorption totale d'eau, le gonflement et l'absorption capillaire des blocs ont augmenté avec une augmentation du rapport DPWA. Les valeurs de la résistance à la flexion étaient plus élevées pour les mélanges avec DPWA que pour ceux avec DPM ou DPS. L'ajout de 0,5 % de DPS augmente la ductilité des briques, entraînant une certaine force résiduelle et augmentant la déflexion à la rupture. L'augmentation de la pression de compactage de 2 MPa à 10 MPa a entraîné une augmentation de la résistance à la flexion d'environ 262.73% pour le bloc témoin (échantillons sans déchets de palmier dattier). De plus, il a été constaté que pour un bloc contenant 0,5 % de DPWA, l'augmentation de la pression de compactage de 2 MPa à 10 MPa conduit à une augmentation de la résistance à la flexion d'environ 371.68%. Les résultats de ε_{xx} montrent des déformations localisées très élevées en milieu de bloc en bas des échantillons sous tension. La zone de concentration de déformation augmente à mesure que la teneur en fibres augmente. La diminution de la pression de compactage de 10 MPa à 2 MPa a entraîné une diminution de la conductivité thermique d'environ 21,96 % pour le bloc contenant 0,5 % de DPWA. Heureusement, ce bloc donne approximativement le même résultat (0,694 W/m.K) que le bloc d'adobe sans déchets de palmier dattier (0,677 W/m.K).

Mots clés : Bloc de terre comprimée, déchets de palmiers dattiers, conductivité thermique ; comportement mécanique, gonflement.

CONTENTS TABLE

LIST OF FIGURES

LIST OF TABLES

LIST OF ABBREVIATIONS AND SYMBOLS

CEB	Compressed Earth Blocks
DPWA	Date Palm Waste Aggregate
DPM	Date Palm Mesh
DPS	Date Palm Spikelet
UPV	Ultrasonic Pulse Velocity
DCS	Dry compressive strength
WCS	Wet compressive strength
E	Elastic modulus
σ_f	flexural stresses
E_d	Dynamic modulus of elasticity
C_b	Capillary water absorption coefficient
λ	Thermal conductivity
C	Volumetric heat capacity
α	Thermal diffusivity
e	Thermal effusivity
C_p	Specific heat
ρ	Density of the material
g	Acceleration due to gravity
V	Volume of the sample
M	Mass of the sample

CHAPTER 1

GENERAL INTRODUCTION

1. General introduction

1.1 Research background

The current development of technology has led engineers to carry out increasingly complex projects with deferential building materials, such as steel, concrete, and wood in the construction field. However, earth construction is an older technique in human history. It has been used in most countries of the world, especially in ancient civilizations on a worldwide scale, and it is still widely used today[1]. In recent years, climate change is one of the biggest threats facing the world and a challenging economic and environmental problem [2]–[4]. In 2018, the world had 315 natural disasters, the majority of which were caused by climate change. Storms, floods, wildfires, and droughts affected around 68.5 million people, resulting in $131.7 billion in economic losses, with storms, floods, wildfires, and droughts accounting for roughly 93 % of the total[3]. In light of the global economic and environmental threat, countries will be forced to return to renewable and clean resources using renewable energies and the abandonment of petroleum products as a source of energy, as well as the use of renewable raw materials in basic industries such as the construction materials industry. In this context, the building sector must work to convert its construction practices to improve the energy performance of new and existing buildings but also to offer innovative materials that meet the new requirements of users in terms of environmental, health impact, and comfort. Recently, the scientific community has been able to shed light on raw earth building materials and is working to make them a promising, clean and economical alternative to cement and fired brick materials. On the other hand, Cement and cement-based materials are in higher demand because of global urbanization. The accompanying CO_2 emissions from its manufacture are becoming a source of concern as its consumption grows[5]. In Algeria, energy consumption in the construction sector represents approximately 42% of the total energy consumption and is the largest energy-consuming sector[6]. Moreover, by 2023, Algeria's housing industry will have grown at an average rate of 7.7%, resulting in a consumption of 94,795 GWh. Heating and/or air conditioning to maintain a good ambient temperature in residences that are typically poorly thermally insulated account for over 80% of national energy consumption in this sector. This alarming finding leads to a new and objective look at the necessity to insulate homes thermally[7]. Improving comfort conditions and reducing costs associated with air conditioning

and heating by environmental means at a low cost of energy today are absolute priorities, which have led to the search for building materials and the use of renewable resources that contribute to reducing the costs of comfort in buildings[8]. Earth construction is a significant solution to conserve the environment and reduce energy costs [9]. Earth is a cheaper, eco-friendly and available building material, and currently, around 30% of the global population lives in earth-based housing [10]. Among the many raw earth materials, the compressed earth block (CEB) has several advantages, in particular its resistance to compression, which allows it to reduce the thickness of the walls for characteristics identical to the other techniques and to allow the realization many forms of construction (niches, arches, friezes, etc.).

To the best of our knowledge, heavy materials are poor insulators, so the thermal insulation of CEB is lower than that of an adobe wall of the same thickness. Nevertheless, in order to improve the thermal performance of CEB while accepting a certain reduction in its mechanical resistance, bio-sourced materials of plant origin can be incorporated into the mixture, for example: wood, cork, straw, hemp. Earth is a good insulation material and can store heat compared to cement building materials, and adding plant waste to earth materials improves this thermal insulation [10].

Nevertheless, some problems linked to durability against water and mechanical strength of earth-based construction materials must be seriously addressed. For this, it was decided to add lime, cement or both as chemical stabilizers[11]–[14]. Note that the cement production process, which necessitates huge amounts of energy, engenders very negative impacts on the environment. However, the production of quicklime requires heating raw limestone that contains calcium carbonate ($CaCO_3$) at about 900 °C only. Therefore, using quicklime as a stabilizer is more advantageous with regard to environment protection and energy consumption reduction. Lime is a traditional chemical binder, and its properties are compatible with soil, especially when clay and fine particles are present[15]. Moreover, lime stabilization of natural soils is a low-cost sustainable technology that may be used to enhance their strength performance and diminish their swelling[16].

1.2 Aims of the thesis

In Algeria, palm trees produce huge amounts of waste every year. Farmers usually burn it in the palm groves and this engenders negative consequences on the environment. Nevertheless, this waste may be valorized for the formulation of earthen materials, such as compressed earth blocks

(CEBs) which have become quite popular due to their low cost and good energy efficiency. These earth-based products represent a sustainable material for the construction industry. Indeed, palm tree residues taken from different parts have been used in many researches in building materials, either as natural fibers[17]–[24], as bio-aggregates[25], [26], or as wood ash[27]. Previous studies have proven that the addition of palm fibers or aggregates improves the tensile, bending [19]and thermal properties[23], [24], [26] of building materials and increases the ductility of brittle materials[25].

To the best of our knowledge, only a few studies have been conducted on the use of date palm fibers in the preparation of compressed earth blocks [18], [19]. It should be noted that the fiber-forming process requires considerable effort and time. The present study tempts to circumvent the problems linked to the use of fibers, which necessitate a lot of effort and time in their preparation, by using aggregates or particles obtained through the grinding of wastes resulting from the maintenance operation of palm groves. The main purpose of this work is to study the effect of incorporating date palm waste in the formulation of CEBs on their thermal, physical, and mechanical properties, and to carry out their microstructural analysis, in order to develop blocks possessing attractive mechanical properties, with enhanced thermal insulation features in order to provide highly insulating walls intended for housing construction. Measurement of strains under bending loads is considered complicated compared to tensile or compressive loads. This is because flexural loads result in two types of strains, tensile strains and compression strains. For this reason, this study was based on the modern method using the digital image correlation method (DIC) to measure the strains resulting from the bending loads. The second main objective of this work is to evaluate the flexural behavior of compressed earth blocks (CEBs) based on different types of date palm waste fibers using the digital image correlation (DIC) technique.

1.3 Structure of the thesis

Five chapters compose this thesis. Its content can be summarized as follows:

The first chapter provides a general overview of the thesis as well as its goals. The research background, the issues at hand, and the work's goals were all outlined.

Recent research papers on the utilization of plant aggregates and fibers in the reinforcing of compressed earth block materials are reviewed in the second chapter. To begin with, it provides an

overview of raw earth-based materials, clay minerals, plant aggregates, and fibers, as well as their properties. The microstructure properties, mechanical behavior and thermo-physical parameters of compressed earth blocks made from various types of plant aggregate and fiber are summarized after that.

The third chapter explains the thesis's research strategy and methods. The first section of this chapter will cover the characterization of the basic materials used in the production of compressed earth blocks. These are the physicochemical, mechanical and mineralogical characteristics of soil, crushed sand, and aggregate and fibers of date palm waste. The manufacturing techniques, mixing sequences, and conservation of various test pieces are then followed. This chapter also presents the mixtures, the mode of preservation, and the experimental test procedures used in this study.

The results obtained from the study are presented and analyzed in chapter four. These results show the effect of date palm waste on the mechanical behavior, thermo-physical and microstructure characteristics of compressed earth bricks stabilized by lime.

The general conclusion of the thesis are presented in chapter five, along with suggestions for further research in the topic of study.

CHAPTER 2

LITERATURE REVIEW

CHAPTER 2: LITERATURE REVIEW

2.1 Introduction

Over the last few decades, countries, economic players, and civil society have become more conscious of the negative effects of human activities on the environment and the need to eliminate these effects as soon as possible. As a result, incentives and limitations for integrating projects into a sustainable development approach are becoming stronger at the international level, particularly in the domains of industry, energy, transportation, and building. Thus, building with local materials that are less expensive and less polluting to the environment is a promising and effective solution. Earthen matrix-based building materials are one of the most prominent solutions, especially in dry desert areas. Earth construction is common in less developed countries. However, the temptations towards more polluting building techniques based on fired bricks and reinforced concrete are likely to favor a change towards a clear unsustainable pattern[28].

The chapter reviews the recent research papers, which focused on the use of plant aggregates, and fibers in the reinforcement of compressed earth block materials. Firstly, it represents a general overview of raw earth-based materials, clay minerals, plant aggregates and fibers and their properties. Thereafter, the mechanical behavior and thermo-physical properties of compressed earth block based on various types of plant aggregate and fiber are summarized.

2.2 Energy, environment, and sustainable building materials

The rapid development of technology has led to the use of energy in huge quantities for manufacturing the requirements of man in a modern way, especially the main requirements such as building materials. The great demand for the building materials industry is increasing, especially in recent decades due to the rapid population increase that has caused a chronic shortage of housing. The production of building materials is increasing to meet the ever-increasing demand for housing. The production of traditional building materials such as cement, fired bricks, steel, wood, and aluminium consumes a lot of electrical and thermal energy, thus polluting the land, air, and water. Energy consumption in buildings worldwide represents approximately 40% of the total energy consumption, responsible for 25% of the total CO_2 emissions [29]. In Algeria, energy consumption in the construction sector represents approximately 42% of the total energy consumption and is the

largest energy-consuming sector[6]. Energy demand should have grown by about 40% to 16.8 billion tons of equivalent petroleum between 2007 and 2030[28]. The increasing demand for energy worldwide is a major reason for the unsustainable development of the world.

In recent years, climate change is one of the biggest threats facing the world, as well as a difficult economic and environmental problem. In highly industrialized countries, the beginning of the 21st century was marked by a general awareness of the need to limit the impacts of human activity on the environment. The results of the **2009 United Nations Climate Change Conference** (the World Climate Summit in Copenhagen) showed that we are still far from the international consensus on the means that must be implemented to reduce the impacts of human activity on the environment[30]. However, it is no longer possible to ignore the incentives and constraints that lead to the integration of projects, whatever the sector of activity in the approach to sustainable development. Given the critical importance, the construction sector has to effectively address environmental issues including, waste generation, greenhouse gas (GHG) emissions, energy consumption, and consumption of non-renewable resources. Energy consumption during the life of a building depends on various factors: construction materials, construction, use, maintenance, and demolition or end of life[31]. Because of their widespread use as basic building materials, concrete and cement production results in significant emissions of greenhouse gases and places strain on the availability of natural resources, such as water (see Fig.2.1). Cement accounts for 36% of all emissions related to construction activities and 8% of total anthropogenic CO_2 emissions[32]. Concrete production worldwide contributes about 4.8% of sulfur oxide emissions, 7.8% of nitrogen oxide emissions, 5.2% of particulate matter emissions smaller than 10 microns and 6.4% of particulate emissions smaller than 2.5 microns[2]. In addition, the concrete industry was responsible for 9% of global industrial water withdrawals in 2012[4]. Its production results in high emissions of greenhouse gases, which is the primary focus of research and mitigation strategies in the building materials industry[2].

a The building stock

GHG emissions (kg CO$_2$ per m^2)

2,000 / 100 / 50 / 0

Existing buildings / New construction

- Heating over lifetime
- Construction and maintenance

b One building

Relative contribution to CO$_2$ emissions (%)

100 / 80 / 60 / 40 / 20 / 0

- Other
- Sanitary equipment
- Electrical equipment
- Finishing
- Insulation
- Windows
- Bricks
- Steel reinforcement
- Concrete

c One cubic metre concrete

Relative contribution to CO$_2$ emissions (%)

100 / 80 / 60 / 40 / 20 / 0

Concrete placement
- On-site placement
- Transport to construction site

Concrete production
- Concrete mixing
- Transport raw material

Material production
- SCM processing
- Cement production
- Gravel production
- Sand production
- Admixture production

d One cement bag

Relative contribution to CO$_2$ emissions (%)

100 / 80 / 60 / 40 / 20 / 0

Cement final production
- Cement grinding
- SCM production

Direct kiln emissions
- Limestone decarbonation
- Fuel burnt

Material production
- Fuel production and transport
- Raw material transport and preparation

Fig.2. 1.The contribution of cement and concrete production to global warming[32].

The construction industry may be the most widely used field for sustainable development, since scientific awareness has led to the valorization of industrial and natural waste in the production of sustainable building materials. According to Miller[5], alkali-activated materials produced with calcined clay or industrial waste products appear to be a scalable technology. Due to raw material inputs, these materials would likely only contribute to mitigation of CO_2 emissions if the emissions from the alkali-activator could be reduced. Currently, industrial and agricultural waste are commonly used in the production of cement, mortar, concrete and earth building materials (see Fig.2.2). Many studies have recently concentrated on waste recycling and its application in the building materials sector to develop less costly, environmentally friendly and sustainable building materials[26], [27], [33]–[40].

Agricultural waste	Industrial waste	Municipal waste
Bagasse ash	Fly ash	Waste rubber
Sawdust ash	Silica fume	Waste plastic
Rice husk ash	Tailing	Construction and demolition waste
Palm oil fuel ash	Nuclear waste	Municipal solid incineration ash
Corn cob ash	Slag	Paper sludge
Coconut shell	Coal gangue	Waste glass
Natural fiber	Red mud	Sewage sludge ash
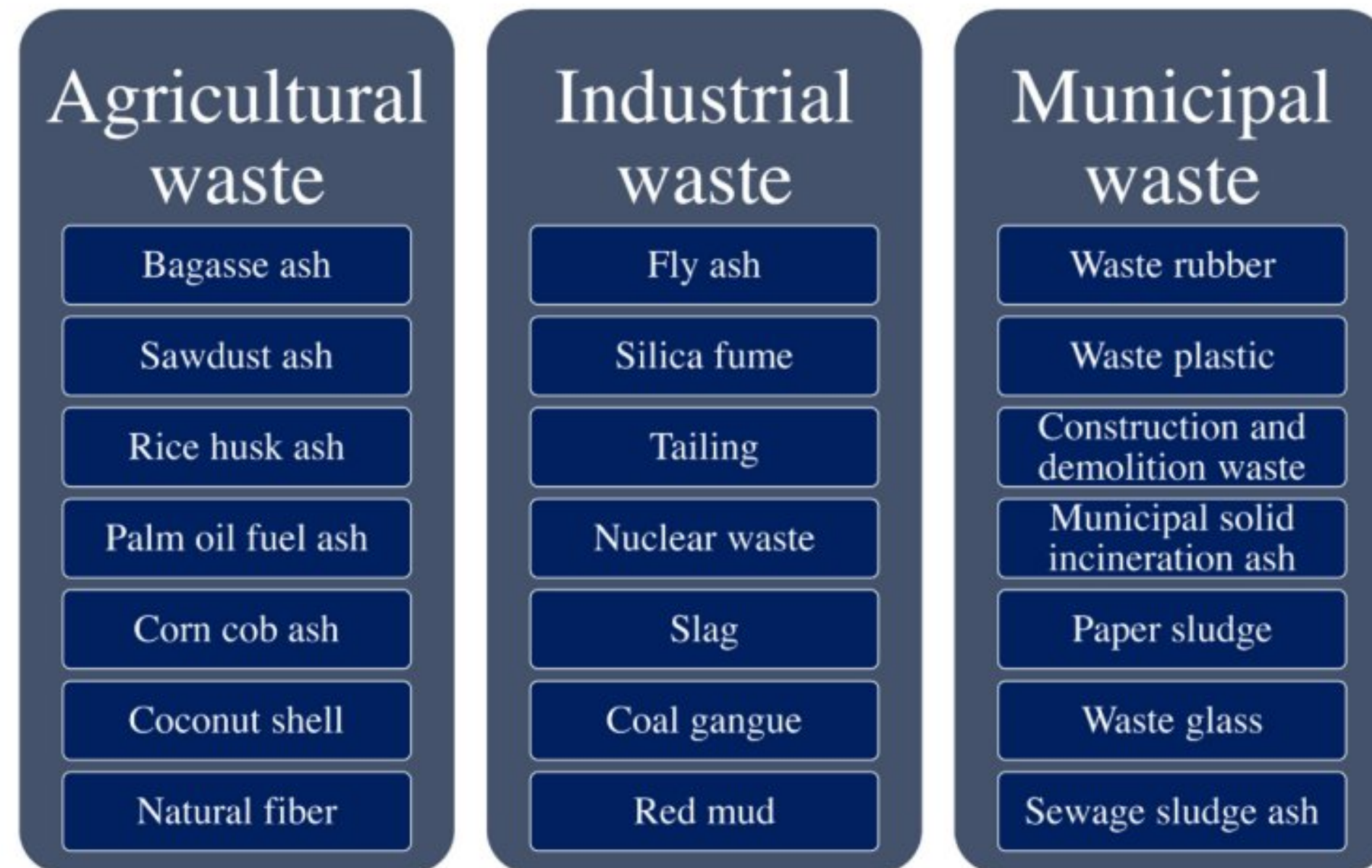
Fig.2. 2. Types of waste materials used in building materials[41].

2.3   Earth-based building material

2.3.1   Background of earth-based buildings

The scientific community has increased interest in earth construction in the last decade, evidenced by the tenfold increase of the published research articles compared to the previous decade[28]. There is no consensus about when humanity began to use earth as a building material. The earliest known uses of earth as a building material, according to Minke[10], extend back more than 9,000 years, based on the discovery of earth block (adobe) based homes in Turkmenistan dating from between 8000 and 6000 BC. The oldest adobe blocks discovered in the Tigris River basin date from 7500 BC, implying that earthen construction has been utilized for nearly 10,000 years. Even the Great Wall of China whose construction began about 3000 years ago has extensive parts built by rammed earth.[28].
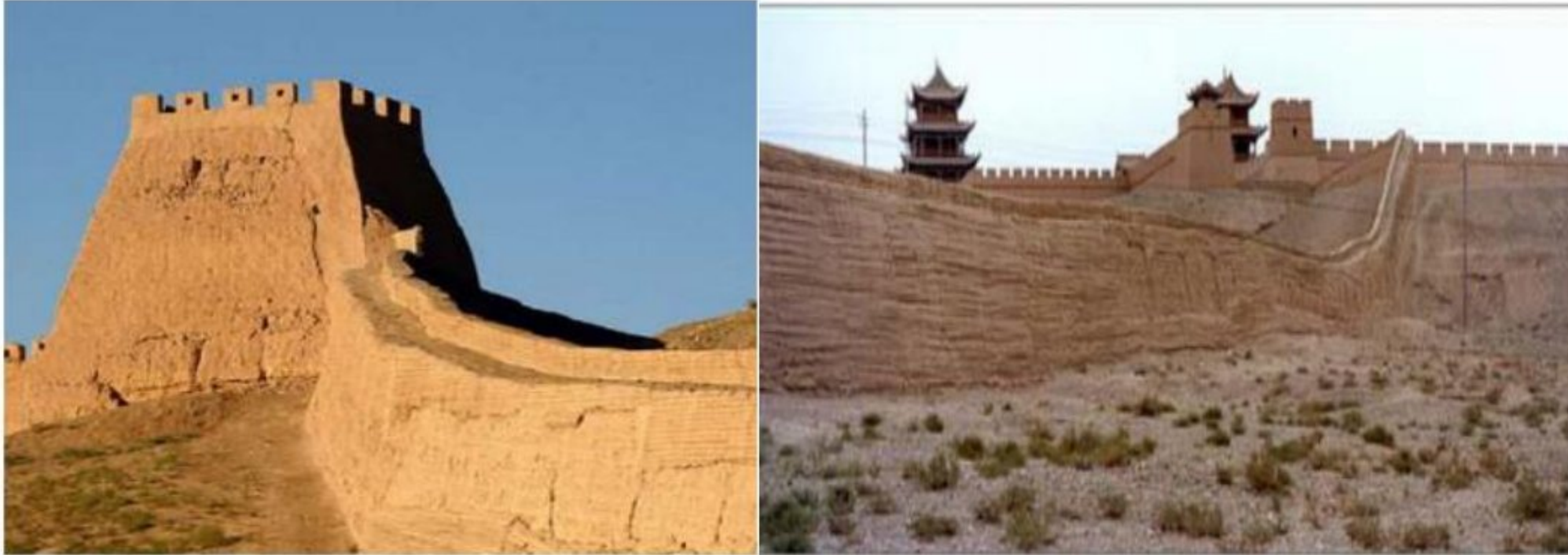
Fig.2. 3. Parts of the Great Wall of China made by rammed earth[42].

Fig 2.4 show the town of Shibam in Yemen with multi-story earth buildings (about 11 stories and up to 8 reaching 30 meters) was built 100 years ago and is considered the oldest skyscraper city in the world [28]. The south of Algeria is characterized by a dry and hot climate, so the people living in these areas used earthen construction in the past centuries, and it is still widely used today, especially in rural areas. Algeria contains many Ksour (local name) of earthen buildings that are among the heritage of the country and have remained as a witness to this type of construction (Fig.2. 5 and Fig.2.6). In the city of Adrar (Algeria), architect Michel Luyekx designed a regional hospital in 1943, which was the first model of an earthen public building.

Fig.2. 4. The town of Shibam with multi-story earth buildings, Shibam, Yemen (Internet sources: Google.com).

Fig.2. 5. Ksar of Mougheul sited in the city of Bechar (south-west Algeria) [43].

Fig.2. 6. Hotel "Ksar Massine" (Timimoune, Algerie) (Internet sources: Google.com).

Nearly half of the world's population now lives in earth-based dwellings. The majority of earth construction is found in less developed countries, but it is also found in Germany, France, and the United Kingdom, which has over 500,000 earth-based dwellings. Earth construction has increased significantly in the United States, Brazil, and Australia, owing to the sustainable construction agenda, in which earth construction plays a key role. The French laboratory CRATerre, formed in 1979 and related to the Grenoble School of Architecture, was able to sustain a strong and constant action in the promotion of earth construction after receiving institutional recognition from the French Government in 1986[28].

○ UNESCO world heritage sites
● Regions of recorded traditional earth construction

Fig.2. 7. Map of the traditional earth-construction regions around the world, with the locations of the UNESCO world heritage sites[44].
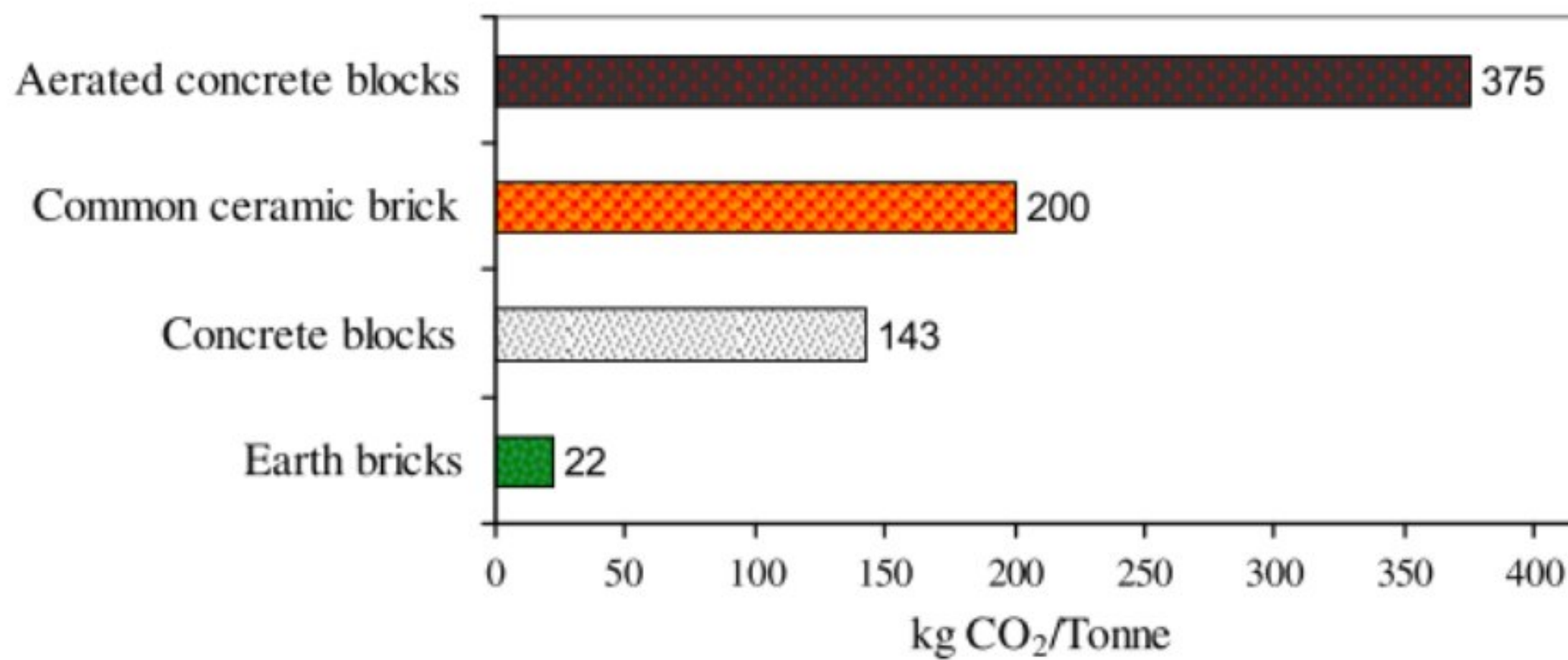
Fig.2. 8. Embodied carbon in different masonry materials[28].

There are three main advantages of raw earth construction. From a socio-economic point of view, one of the first advantages of this type of construction is the fact that the base material is widely available and often immediately available to users. In addition, before the rise and expansion of modern materials such as concrete and steel, every region of the world had a long history of general construction. The ancient built heritage and archaeological remains are immortal witnesses. Thanks to its wide availability, raw soil material is found in constructive culture in different regions of the world. In 2011, it was estimated that about 10% of the share of earthen construction is in the World Heritage. The cost of producing and transporting modern building materials, in this case, concrete, makes them unavailable to people in developing countries. The environmental aspect of raw earth construction is one of the most promoted advantages in the current context of combating global warming. The environmental impact of transportation is limited by the principle of availability of materials near the construction site and it's almost infinitely recyclable[45].

Recently, a certain number of intrinsic properties of raw earth material, which have been used for a long time in old buildings, are nowadays of particular interest to those involved in the building industry. Thanks to its hygroscopic capacities, the raw earth material is able to naturally regulate the humidity of the air and consequently the temperature inside the building. First, the natural adjustment of indoor humidity limits the risks of pathologies linked to prolonged condensation such as the appearance of molds and respiratory diseases for residents. In addition, the resulting thermal inertia would reduce the energy costs of heating and air conditioning homes depending on the climate of the region[10], [28]. Thus, earth-based materials allow better balance and control of the interior thermal and acoustic climate compared to usual construction materials.

Proper selection of building materials can decisively contribute to reducing energy consumption in the construction sector. Therefore, priority should be given to the use of local materials such as earth. For a three-room house of 92 m^2 made of earthen walls, the values represent a reduction of 7 tons of CO_2 compared to ceramic bricks and a reduction of 14 tons of CO_2 in the case of using aerated concrete blocks (see Fig. 2.8.). Replacing just 5% of the concrete blocks used in UK construction by earth masonry would mean a reduction in CO_2 emissions of approximately 100,000 tons[28]. In 1993 in Algeria, the Scientific Research Center CNERIB produced a guide on building by stabilized earth concrete. A prototype was produced within the CNERIB in 2007, which they named "energy efficient house". This prototype is fitted with solar panels (Fig.2.9).

Fig.2. 9. Energy efficient house, prototype produced at CNERIB, Algeria(Internet sources: Google.com).

2.3.2 The main unfired earth construction techniques

Earthen construction techniques have been used for thousands of years with several methods of manufacture. The most important earthen construction techniques are Wattle and daub – cob, Adobe (moulded bricks), and Rammed earth that have been used for a long time in the world. The compressed earth block (CEB) is the most modern technique compared to other techniques.

↓ Adobe

Adobe is a fairly simple earthen construction technique that was used in most ancient structures. These bricks are obtained from a mixture of clay soil and water as basic materials. Adobe is derived from the Arabic word "Attob," which meaning sun-dried brick. The process of making adobe bricks involves filling wooden molds with moist earth and drying them in the sun. Because shrinkage fractures in adobe's surface can occur when it dries, several authors[46] recommend using straw or other vegetable fibers to prevent this.

↓ Wattle and daub – cob

The wattle and daub technique (torchis in French, tabique in Portuguese) are used for almost 6000 years. In the wattle and daub technique, the earth is pressed against a woven lattice of wooden strips. As to the cob technique (bauge in French) it involves mixing earth with straw and water to form layer by layer masonry walls (cob is an old Englishword for loaf)[1], [28].

Fig.2. 10. Cob house in Devon, UK[47].

Rammed earth

Rammed earth is a process of building mud walls, compacted in a formwork in successive layers using a pestle. Rammed Earth (RE) has different names such as taipa (in Portuguese), tapial (in Spanish) and pise/de terre (in French)[48].
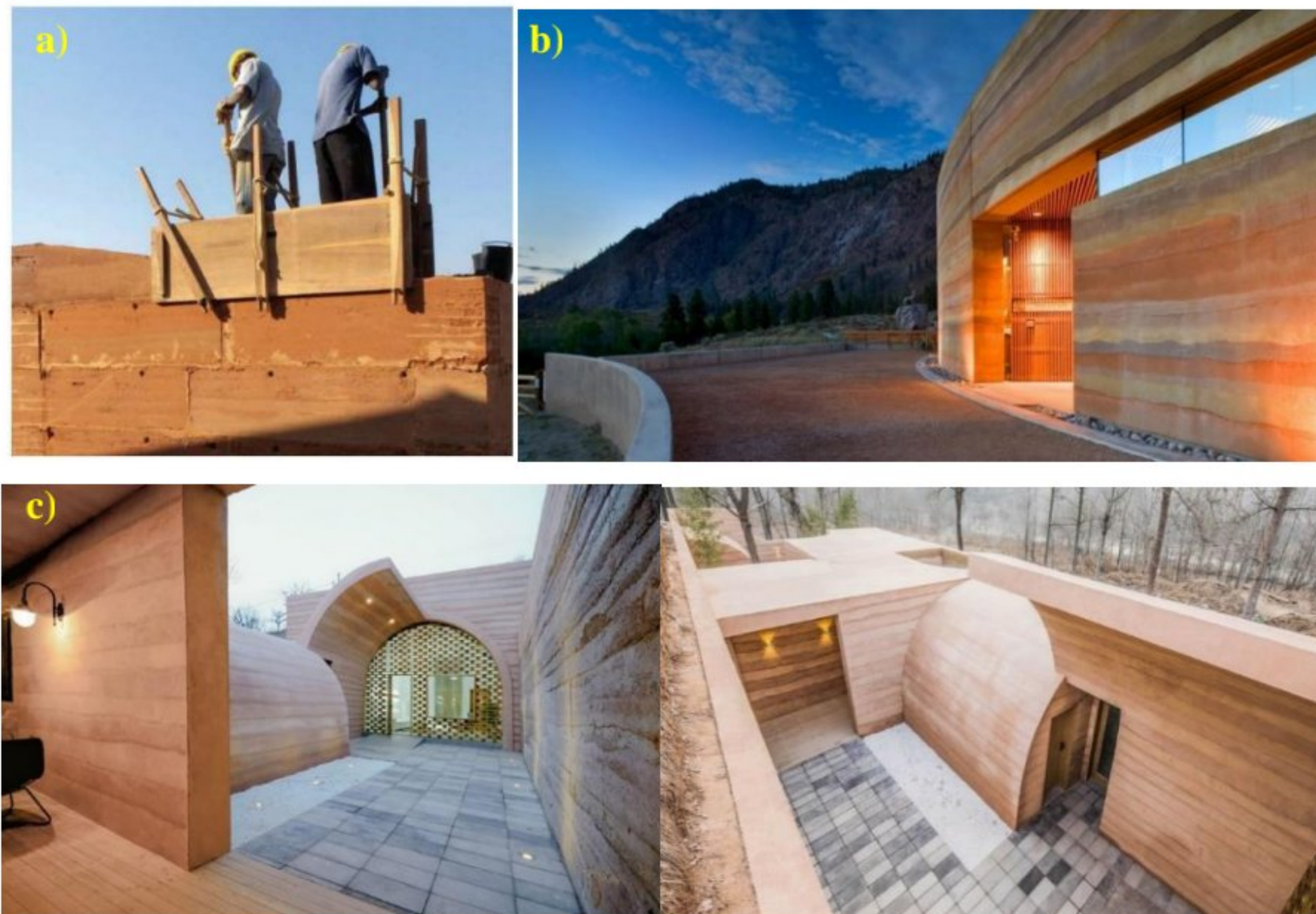
Fig.2. 11.a) Manufacture of a rammed earth wall; b) Desert Cultural Centre (Osoyoos Indian Band); c) Contemporary house made of Rammed earth (China) (Internet sources: Google.com).

14

♣ Compressed earth blocks

The use of compressed earth blocks in masonry was first adopted in the middle of the twentieth century. It is now, ahead of rammed earth, the most widespread contemporary technology of construction with raw earth. The blocks are manufactured by pressing soil into block moulds with a manual, mechanical, or hydraulic press[1]. Among the many earth materials techniques, compressed earth block (CEB) has several advantages, notably its compressive strength, but the thermal resistance of CEB is lower compared to adobe wall of the same thickness. CEBs are a modern evolution of the adobe. The CEB technique is considered as one of the most promising techniques of building materials and can serve as a suitable alternative to the conventional fired clay brick. In fact, CEBs have been successfully built in both developing and developed countries. In addition, CEB technology is a relatively recent development in construction and has become more popular over the last 50 years[49]. Fortunately, CEBs are used as elements in the construction of load-bearing walls or partition walls of residential or industrial buildings. CEBs also allow the construction of special structures (arches, and domes). Today, the building materials market has a wide and different range of compressed earth products (see Fig. 2.13). CEB products come in a variety of shapes and sizes, and they are employed in a variety of public and building projects.

Fig.2. 12. Contemporary house made of compressed earth blocks (Internet sources: Google.com).

1 300*150*100mm	2 300*150*100mm	3 150*150*100mm	4 300*150*100mm	5 300*150*100mm
6 150*150*100mm	7 300*150*100mm	8 300*150*100mm	9 150*150*100mm	10 300*150*100mm
11 300*150*100mm	12 300*150*100mm	13 250*175*100mm	14 250*175*100mm	15 300*150*100mm
16 300*150*100mm	17 230*180*115mm	18 230*220*115mm	19 230*220*115mm	20 230*220*115mm
21 230*140*115mm	22 245*107*60mm	23 250*60mm Diagonal	24 200*100*60mm	25 200*100*60mm
26 200*100*60mm	27 260*160*100mm	28 300*150*100mm	29 300*150*100mm	30 250*125*60mm

Fig.2. 13. Types of compressed earth block products(Internet sources: Google.com).

2.3.3 Background of soil

It is known that soil, especially clay soil, is a raw material for the manufacture of earth-based building materials. Soil is a natural resource of mineral grains that can be separated[50], [51]. However, soil is considered a composition of four basic types: gravel (>2mm), sand (0.06–2 mm), silt (0.002–0.06 mm) and clay (less than 0.002 mm)[52].

16

The term "clay" has no universal definition. Thus, the word "clay" has two meanings: one is linked to grain size, and the other is related to mineralogy. However, any mineral with a particle size of less than 2 micrometers is considered "clay" by geologists. In addition, clay is a natural binder that helps earth materials particles bond when they reacted with water.

2.3.2.1 Clay minerals

Clay is a product of the erosion of feldspar and other minerals. Feldspar contains aluminium oxide, a second metal oxide and silicon dioxide. One of the most common types of feldspar has the chemical formula $Al_2O_3 \cdot K_2O \cdot 6SiO_2$[10]. Clays are alumino-silicates with a laminated (or lamellar) structure formed by the stacking of hexagonal layers: tetrahedron SiO_4 and compact layers: octahedron Al_2O_6. All clay minerals consist of two basic sheets which are characteristically stacked and which have certain cations in the tetrahedron and octahedron sheets. In the field of engineering, only the most common clay minerals contained in so-called clay soils are noted. The main groups of clay minerals are thus characterized by a constant number of these layers forming a set of sheets; the thickness of the sheets being an essential characteristic of the mineral.

Non-clay mineral particles such as quartz and calcite may also be present in clay compositions[53]. The minerals kaolinite, illite, and montmorillonite are the three main minerals of crystalline components that make up clays[50], [51]. Clay minerals are also found mixed with other chemical compounds, particularly with hydrated iron oxide ($Fe_2O_3 \cdot H_2O$) and other iron compounds, giving the clay a characteristic yellow or red color. Manganese compounds impart a brown color; lime and magnesium compounds give white, while organic substances give a deep brown or black color. Clay minerals usually have a hexagonal lamellar crystalline structure. Furthermore, there may be isomorphic substitutions in the tetrahedral ($Si^{4+} \rightarrow Al^{3+}$, Fe^{3+}) and/or octahedral ($Al^{3+} \rightarrow Mg^{2+}$, Fe^{2+}, or $Mg^{2+} \rightarrow Li^+$) layers[54]. These substitutions lead to a charge deficit which is compensated, outside the sheet, by compensating cations. These lamellas consist of different layers that are usually formed around silicon or aluminium cores[10]. The classic classification is based on the thickness and structure of the sheet. There are four groups[55]:

❖ **1/1 or T-O type minerals**: the sheet is made up of a tetrahedral and octahedral layer. Its thickness is around 7 A° (angstrom). Each sheet is connected to another sheet through labile

hydrogen bonds. The property of this bond is to allow the cohesion of the crystal while leaving the possibility of cleavage of the different sheets.

❖ **Minerals of the 2/1 or T-O-T type**: the sheet is framed by two tetrahedral layers. Its thickness is about 10 A°. The tetrahedral layers can either contain silicon and oxygen atoms or have a partial substitution of silicon atoms by aluminum atoms. In this case, the layers present a deficit in positive charges (substitution $Si4+$ by $Al3+$).

❖ **Minerals of the 2/1/1 or T-O-T-O type**: the sheet consists of an octahedral layer flanked by two tetrahedral layers. Its thickness is about 14 A°.

❖ **Interstratified minerals**: these minerals result from the regular or irregular mixture of clays belonging to the above groups. The thickness of the sheet is variable.
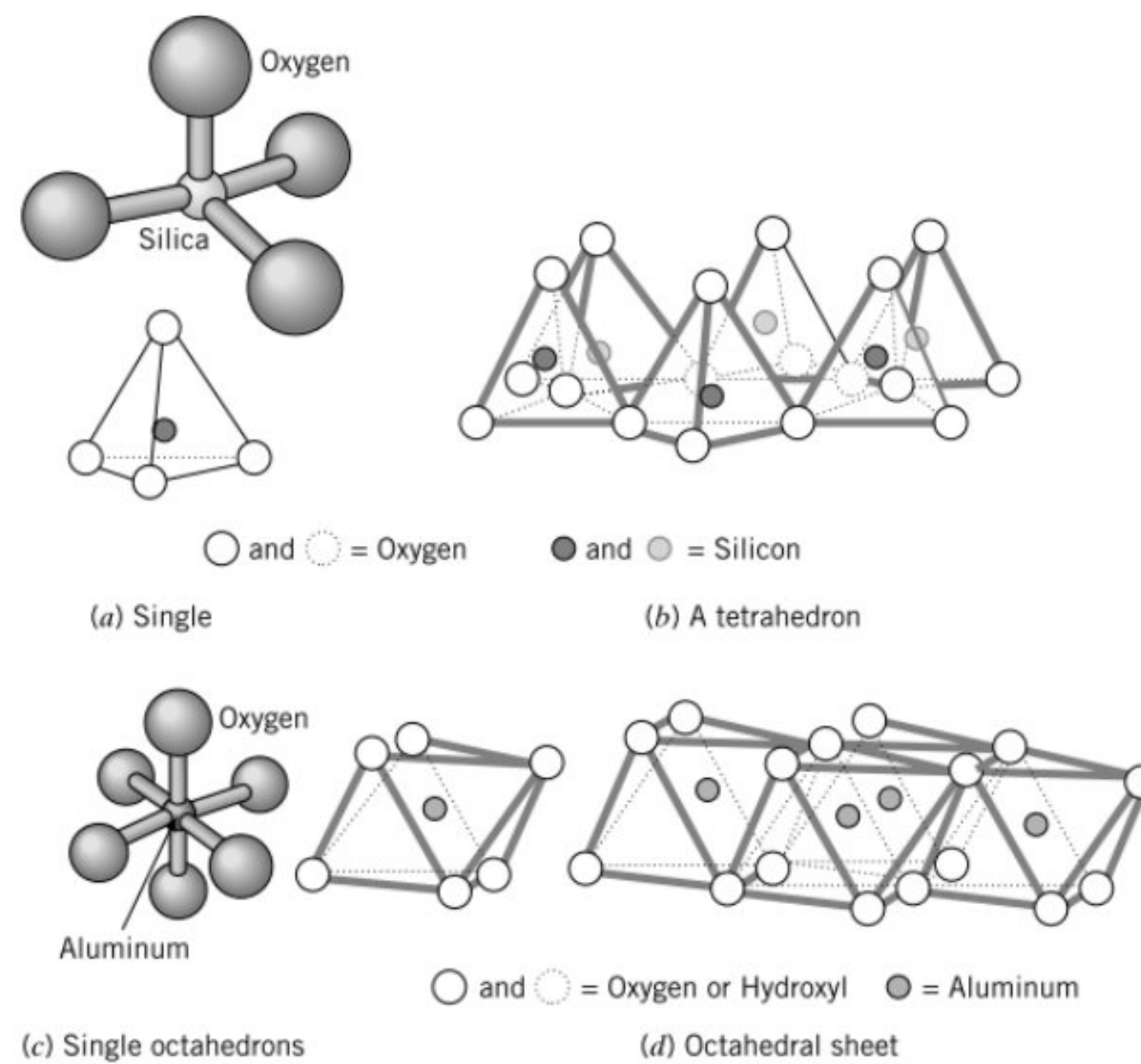
Fig.2. 14. (a) Silica tetrahedrons, (b) silica sheets, (c) single aluminum octahedrons, and (d) aluminum sheets[51].

18
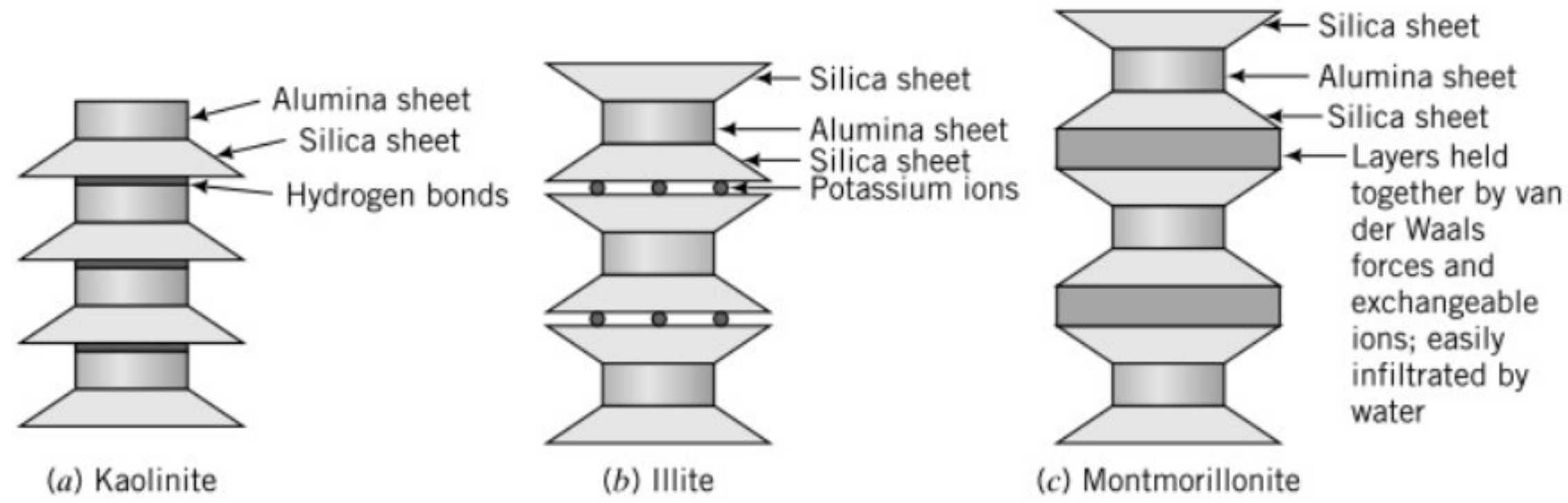
Fig.2. 15. Structure of kaolinite, Illite, and Montmorillonite[51].

Table.2. 1. Clay minerals[56].

	Name of mineral	Structural formula
I.	Kaolin group	
	1. Kaolinite	$Al_4Si_4O_{10}(OH)_8$
	2. Halloysite	$Al_4Si_4O_6(OH)_{16}$
II.	Montmorillonite group	
	Montmorillonite	$Al_4Si_8O_{20}(OH)_4nH_2O$
III.	Illite group	
	Illite	$K_y(Al_4Fe_2.Mg_4.Mg_6)Si_{8-y}$
		$Al_y(OH)_4O_{20}$

✦ Kaolinite

Kaolinite is one of the most common clay minerals in sedimentary and residual soils. A unit sheet of kaolinite, which is approximately 0.7 nm thick, is composed of one aluminum octahedral layer and one silicon tetrahedral layer, joined together by shared oxygens[50]. Thus, Kaolinite is a two-layer mineral T-O. Its structure is stable, so it does not swell when there is water. Kaolin clay is currently used in a variety of industries, including the pharmaceutical industry. Kaolinite is used in the paper industry both as a filler in the mass of paper and as a surface coating. In addition, it is used to treat certain digestive disorders. Thus, kaolinite is excellent for stomach problems. Calcined kaolinite is used as a mineral addition (metakaolin) in the production of building materials and in agriculture (including organic farming).

O Oxygen atoms ◎ Hydroxyl ions
○ Silicon atoms tetrahedrally ● Aluminium atoms octahedrally
coordinated coordinated
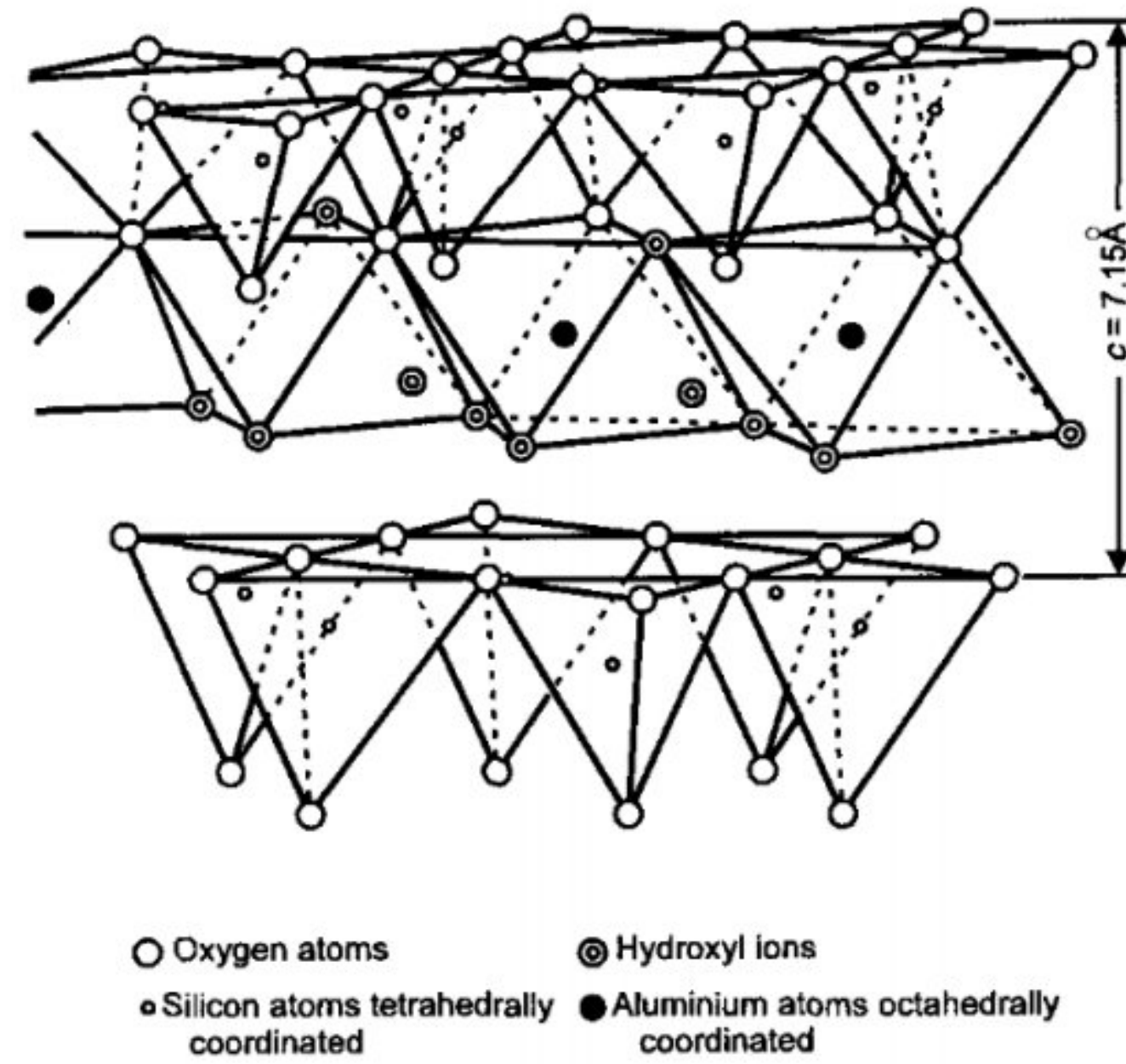
Fig.2. 16. Structure of Kaolinite[57].
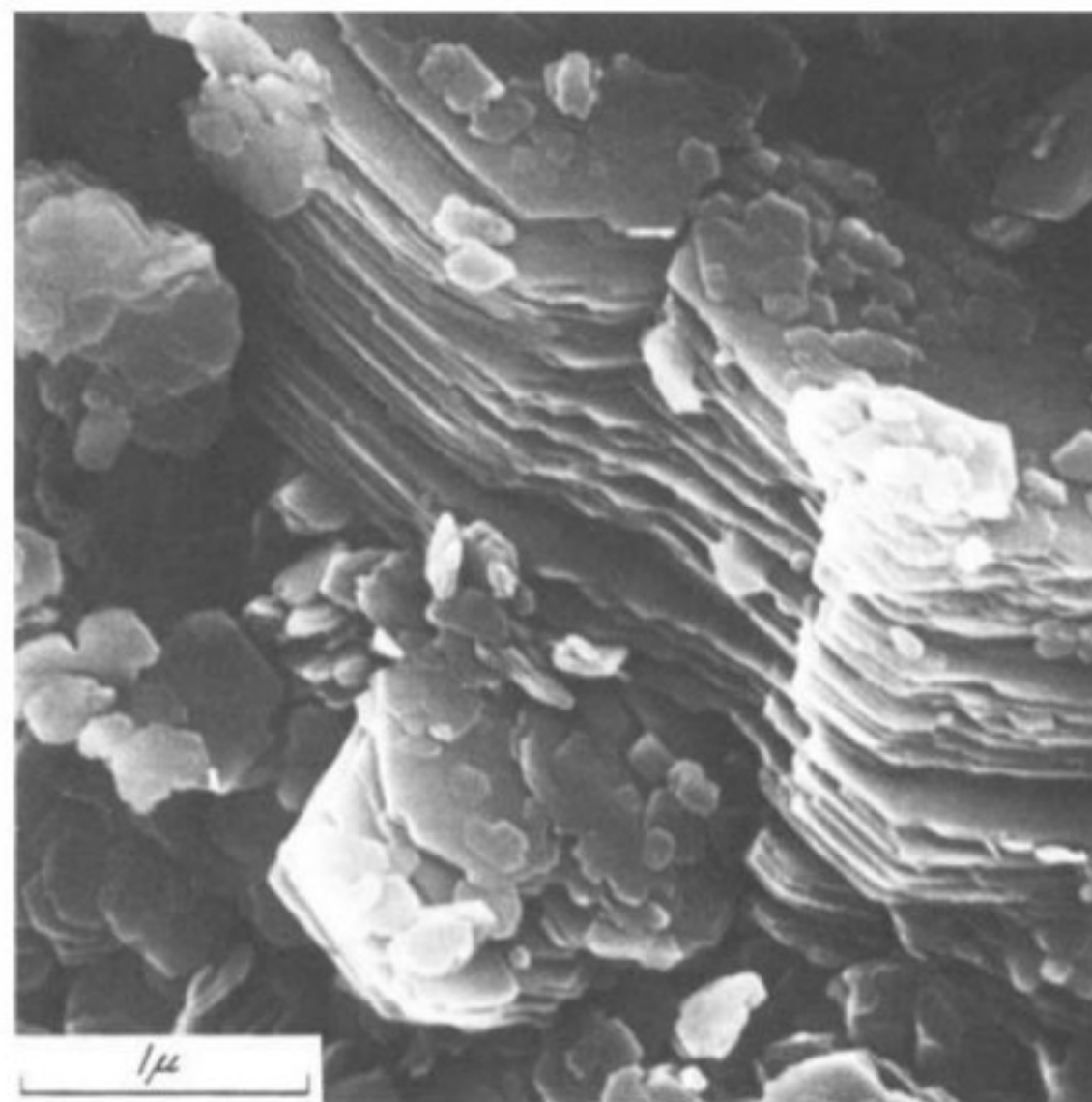
Fig.2. 17. Scanning electron microscope (SEM) photograph of kaolinite[50].

Illite

Illite is the most common clay mineral in stiff clay sand shales as well as in postglacial marine and lacustrine soft clay and silt deposits[50]. The mica-type mineral found in argillaceous sediments was given the name illite by Grim, Bray, and Bradley in 1937[58]. It is often present, some-times interstratified with other sheet silicates, in sedimentary and residual soils, except in residual soils derived from amorphous volcanic material. Illite is also referred to as fine-grained mica and

weathered mica. However, in microscopic illite particles the stacking of the sheets is not so regular as in well-crystallized micas, and weathering may remove intersheet K^+ from the edges of the plates. The resulting illite particles, with terraced surfaces where one or more unit sheets terminate, have frayed and tattered edges are flexible and elastic, are 10 to 30 nm in thickness, have a breadth/thickness of 15 to 30, and have a specific surface of 80 to 100 m^2/g. A SEM photomicrograph of illite particles is shown in Fig. 2.19[50].
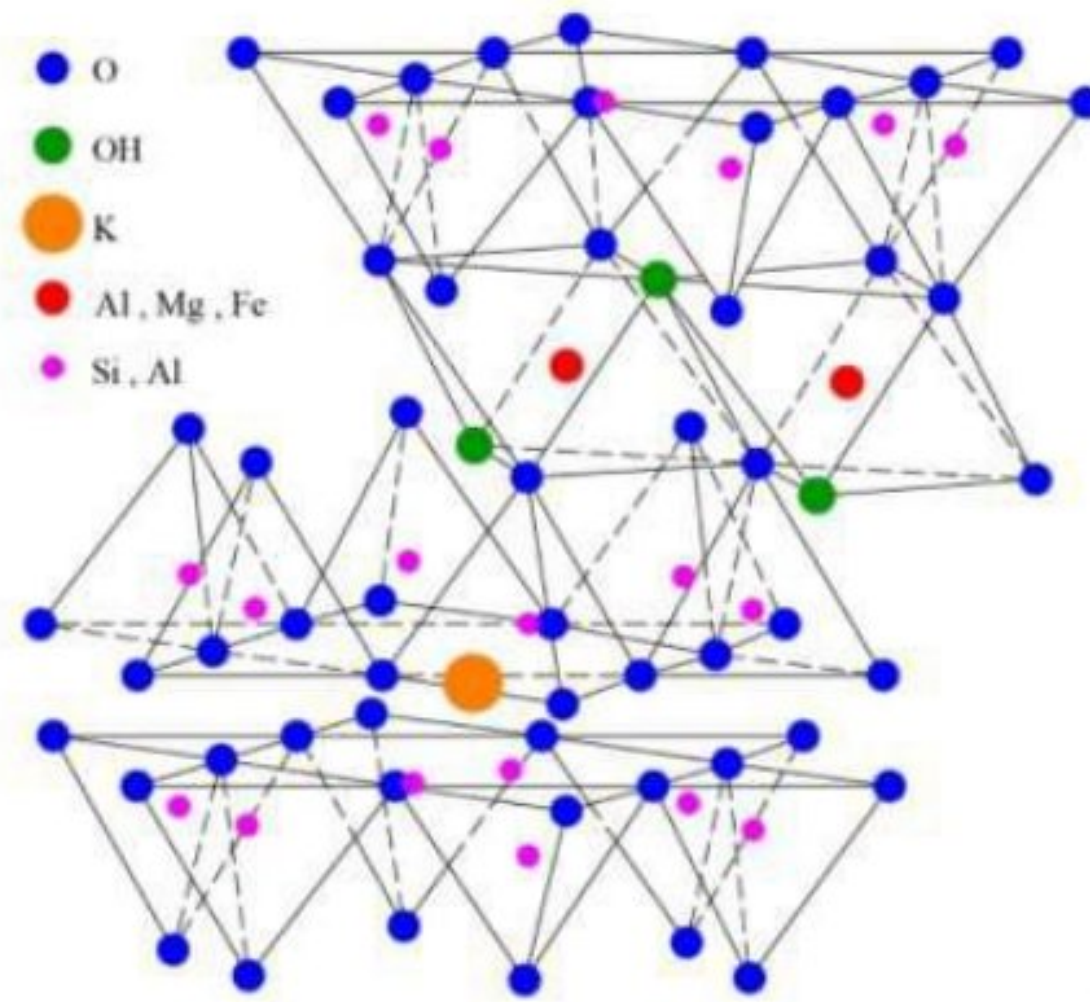
Fig.2. 18. Structure of illite[59].

Fig.2. 19. Scanning electron microscope (SEM) photograph of illite [50].

✚ Montmorillonite

Montmorillonite, the most common member of a group of clay minerals known as smectites, is the dominant clay mineral in some clays and shales and in some residual soils derived from volcanic ash. Relatively pure seams of montmorillonite are found in some deposits, and bentonite being the best-known example. A unit sheet of montmorillonite is similar to that of the micas. In montmorillonite, octahedral Al is partially replaced by Mg atoms. Each isomorphous replacement produces a unit negative charge at the location of the substituted atom, which is balanced by exchangeable cations, such as Ca^{+2} and Na^+ situated at the exterior of the sheets. In a packet of montmorillonite in the anhydrous state, where as many as 10 unit sheets are in contact, the stacking of the sheets is disordered in the sense that the hexagonal cavities of the adjacent surfaces of two neighboring sheets are not matched face-to-face. In a hydrous environment, water molecules penetrate between the sheets and separate them by 1 nm (i.e., four molecular layers of water)[50]. Montmorillonite clays are composed of extremely small units of indefinite shape, which disperse in water into very thin flakes[53].
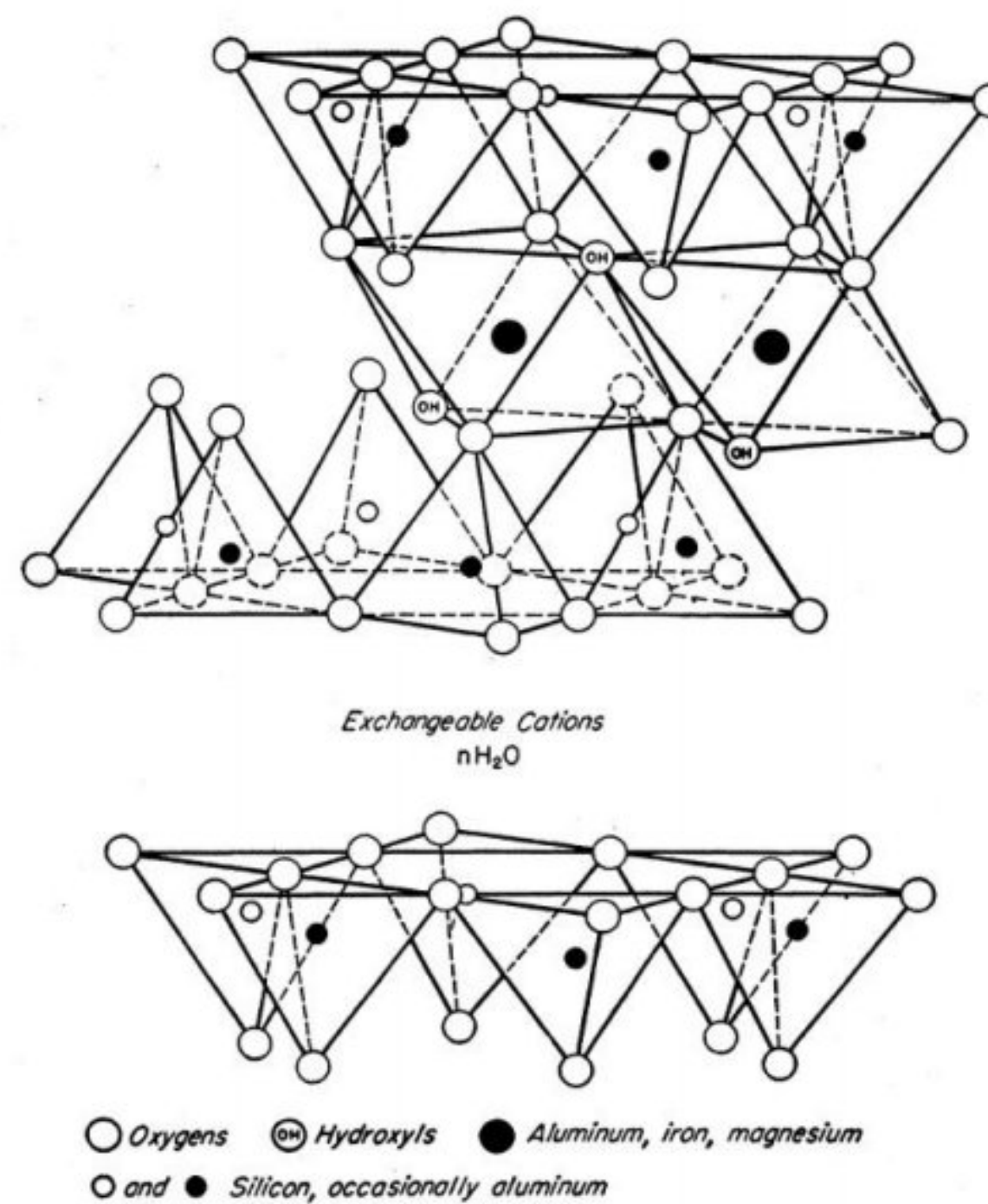
Fig.2. 20. Structure of montmorillonite. According to Grim[53].
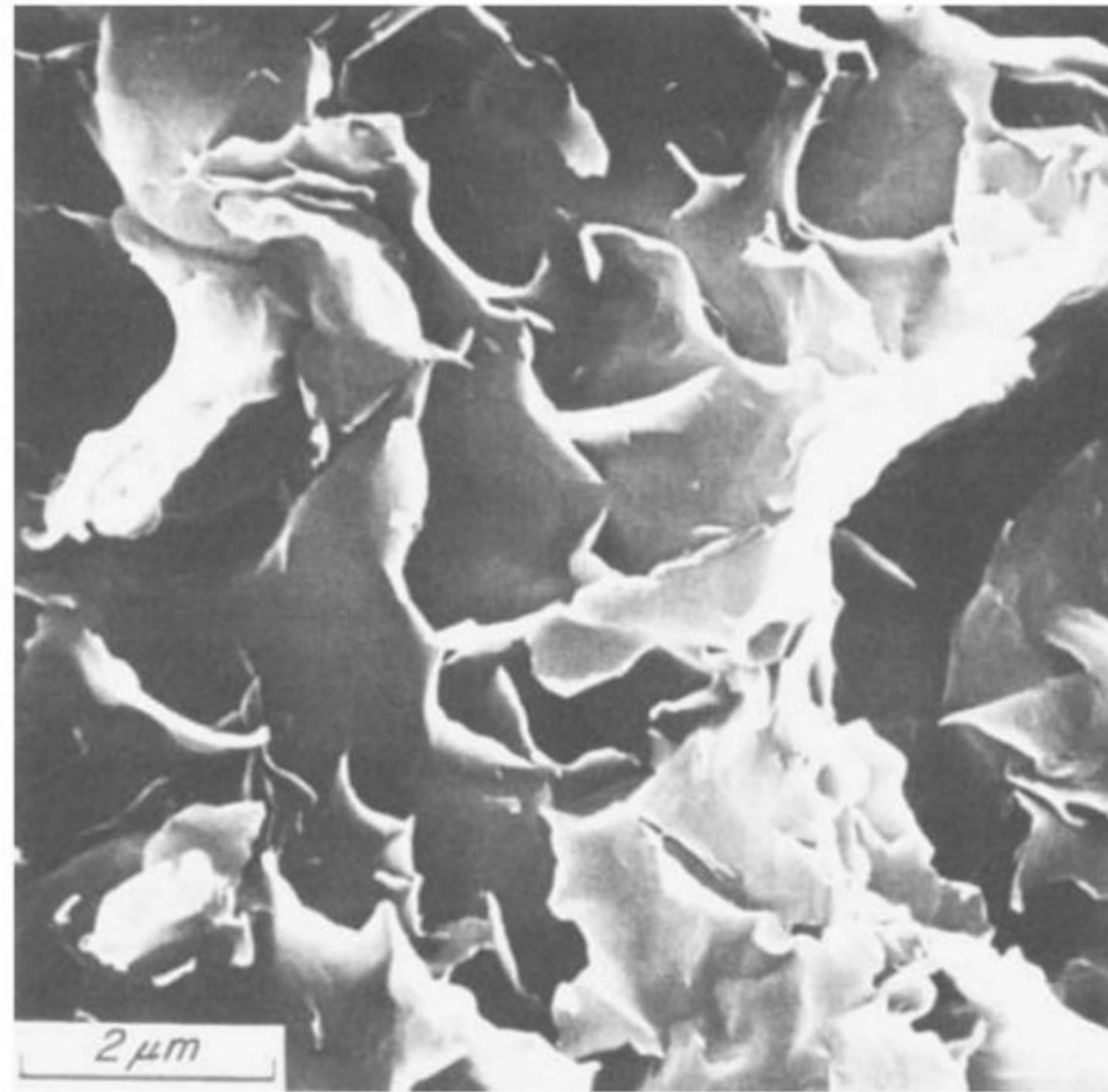
Fig.2. 21. Scanning electron microscope (SEM) photograph of montmorillonite [50].

2.4   Soil selection for earth building materials

The characterization of soils is important because not all soils are suitable for earth building. There are several tests to identify the characteristics of a soil, the objective of which is the correct selection for earth building. These characteristics include chemical composition, particle size distribution (Texture), Atterberg limits, and mineralogical composition. The type of earth (i.e. soil gradation and its plasticity) is one of the important factors that decide the properties of compressed earth block.

2.4.1 Texture

The content of the different sizes of particles or fractions that make up the soil is known as texture or granularity. Wet sieving and a sedimentation test are used to determine the particle size distribution (for the fineness of the soil). It is very important to respect the minimum clay content for all techniques (see Fig. 2.22). There is always a minimum clay content that can be established, in 5% based upon the information offered. It has been found that for clays (particles under 0.002 mm), all recommendations include contents of 10–22% for CEB and 10–15% for rammed earth. A silt content (0.002 and 0.06 mm) common to all recommendations would be 10–25% for CEB[60].
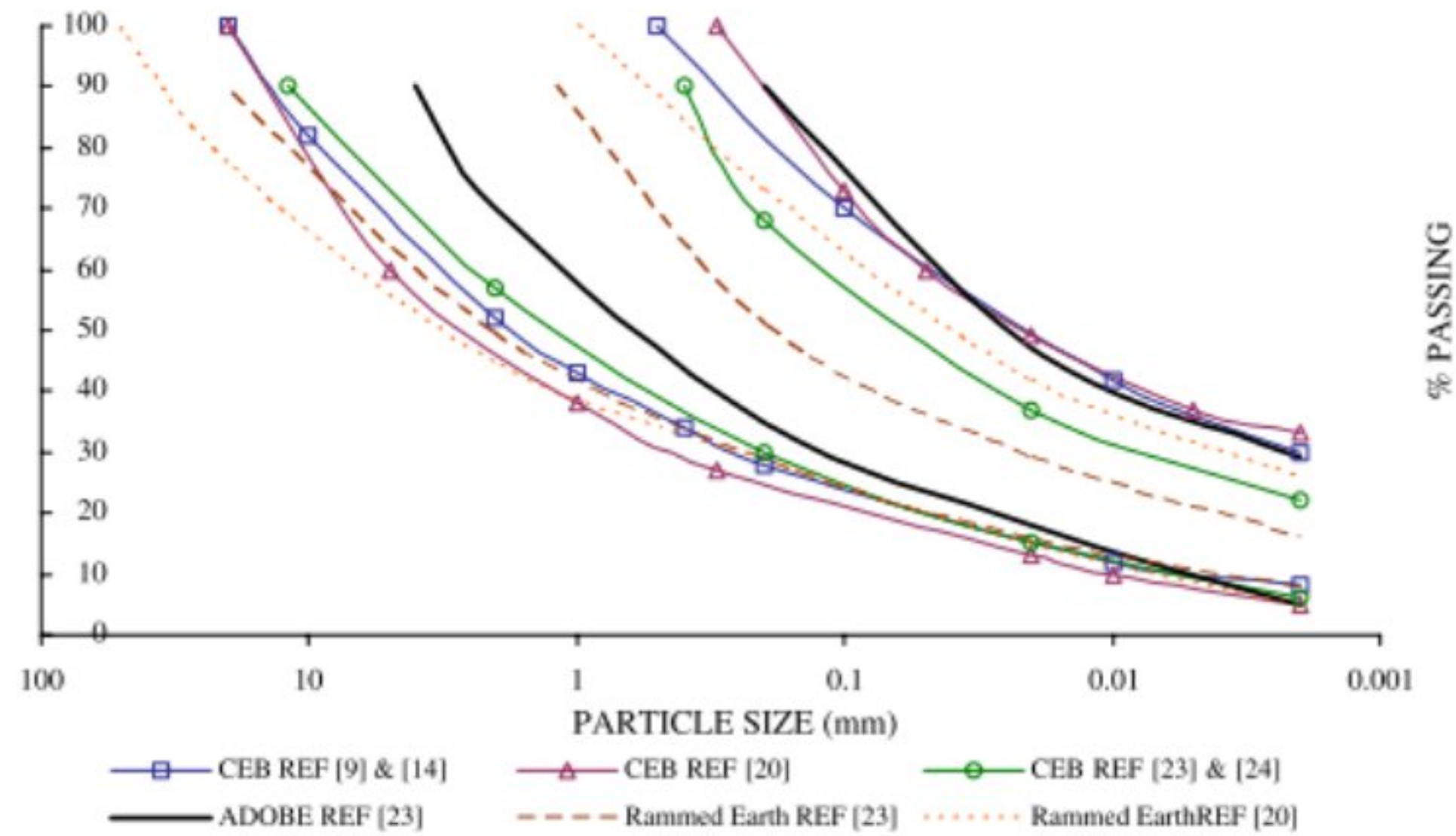
Fig.2. 22. Granularity nomograms showing recommended areas for particle size distribution of soils for adobe, rammed earth and compressed earth blocks[60].

It has been discovered that there is always an optimum clay content corresponding to the lowest void ratio in a given soil mix. With this clay content in cement stabilized soil bricks, the maximum compressive strength is obtained. Optimum clay content is found to be 10% and 14% for fine-grained and coarse-grained soils, respectively. Moreover, it is reported that, soils with clay content of 15–30% are most suitable in blocks making. However, suitability of the soils also depends upon the variation of cement content. Further increase in clay content impairs the effectiveness of cement due to presence of unstabilized cohesive soils, which reduces the bonding between cement and soil [61].
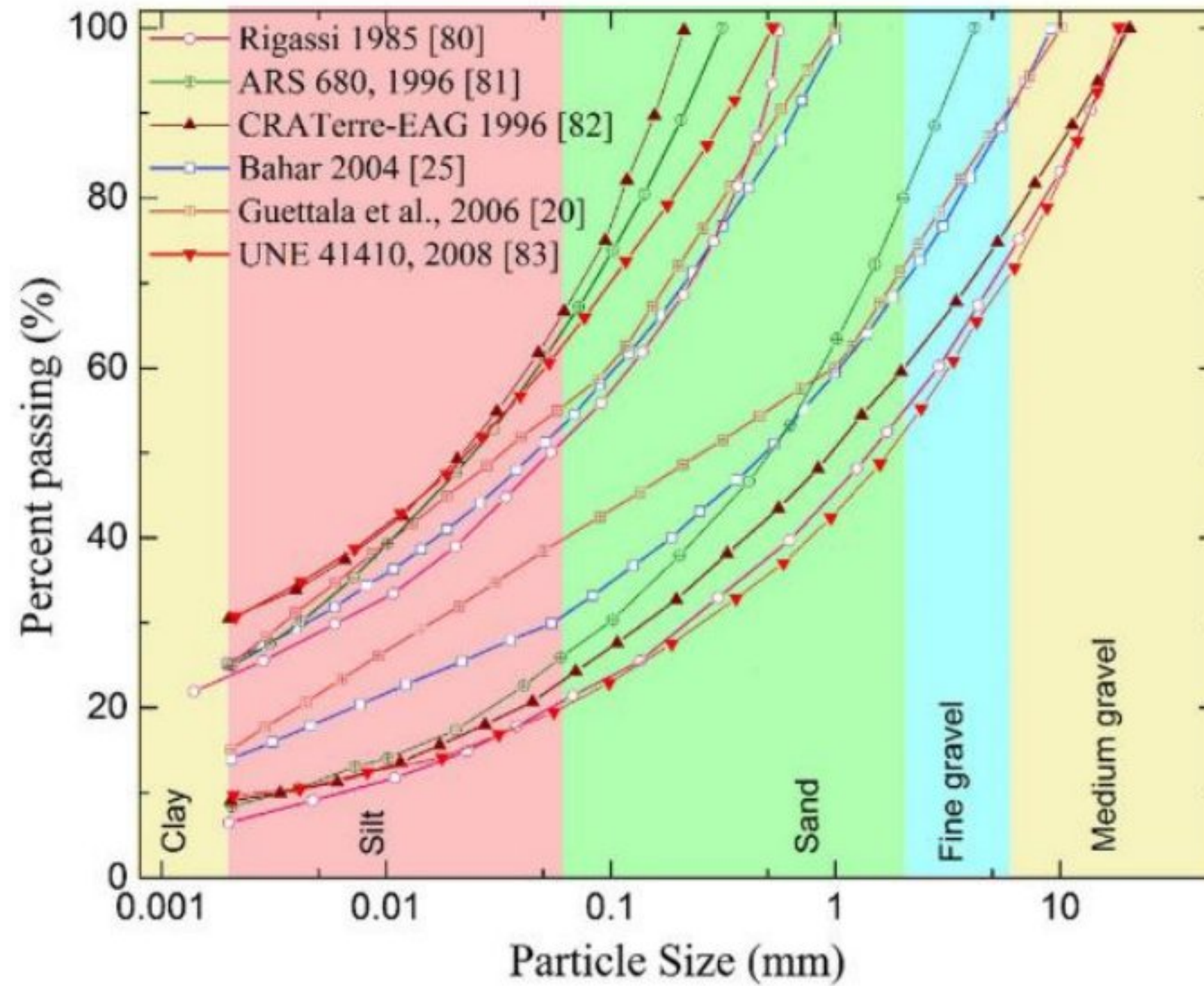
Fig.2. 23. Suitable gradation of soil for stabilized compressed earth block (CEB) [61].

2.4.2 Plasticity

The plasticity is the ability of materials to keep a deformation without breaking. As more water is added, soils transition from dry to plastic and fluid states, depending on the water concentration. Plasticity markers such as Atterberg limits are often used. The liquid limit (LL), plastic limit (PL), and plasticity index, PI (PI= LL – PL) are laboratory test standards that are commonly used in earth building. They are suggested that soils with PI and LL within the region common to all the proposed graphs, shown in Fig. 2.24, with PI of 16-28 and LL of 32-46, are good soil for earth building in general. [60].
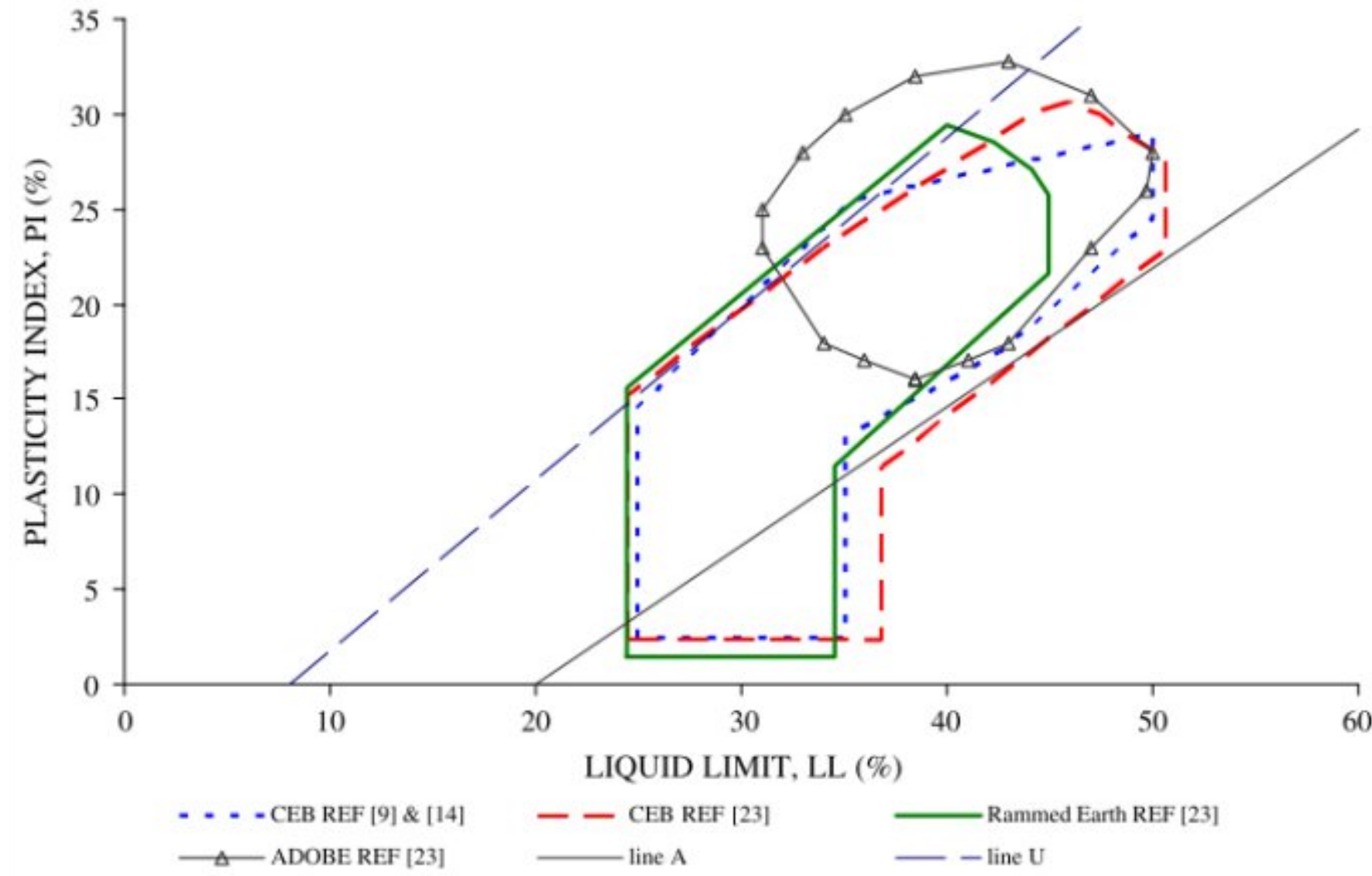
Fig.2. 24. Plasticity nomograms showing recommended areas of PI/LL of soils for adobe, compressed earth blocks or rammed [60].

Much variation was observed in the soil plasticity used or recommended by various researchers, irrespective of the stabilizing methods adopted. However, almost all the soils lie in between the A-line [PI = 0.73 (LL-20), which separates the more clay like materials from silty materials and the organics from inor- ganics] and U-Line [PI = 0.9 (LL-8), representing the upper bound for general soils][61] (see Fig.2.25).
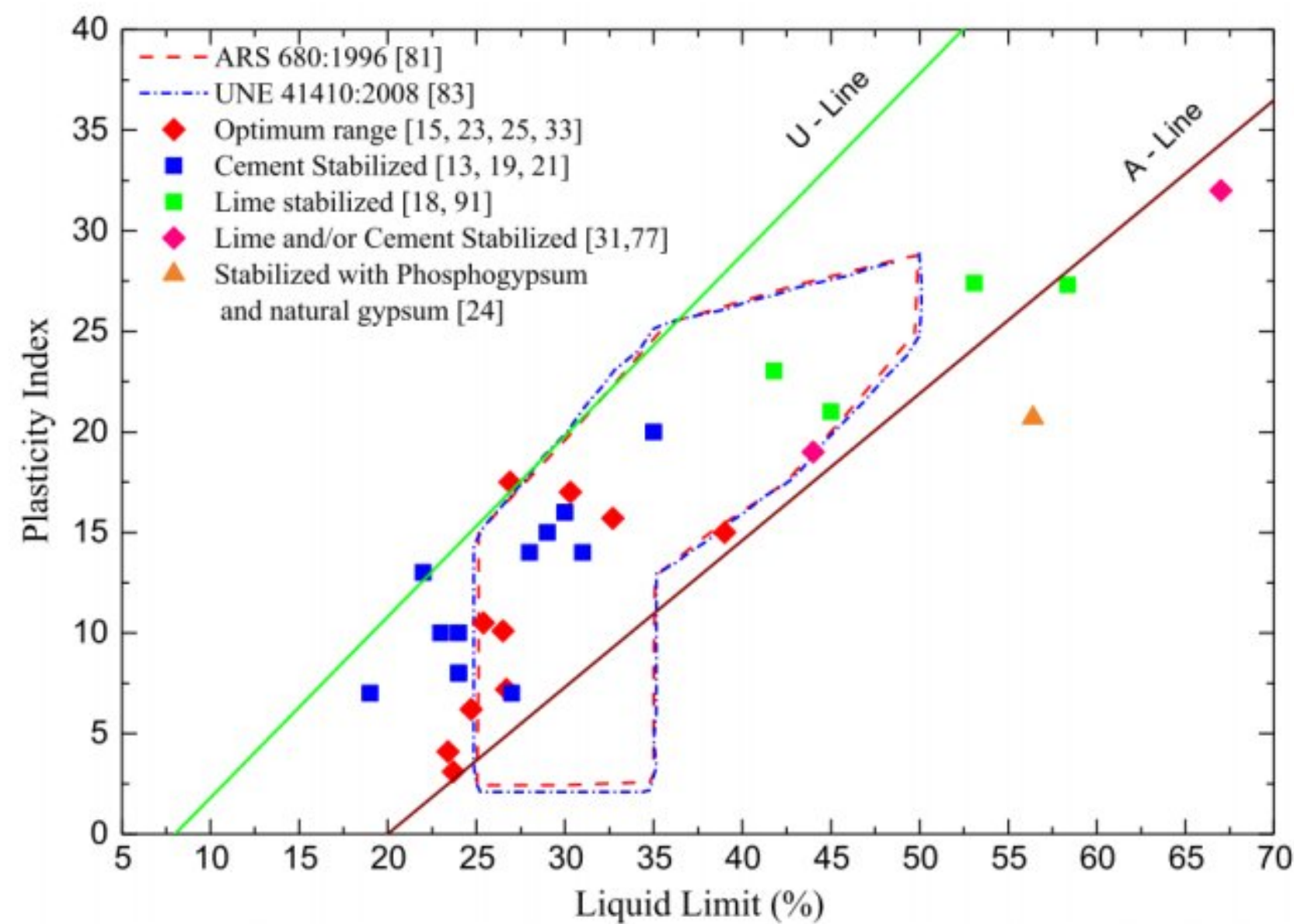
Fig.2. 25. Soil plasticity recommended for brick production[61].

2.5 Techniques for stabilizing earthen materials

Earth is an inexpensive, renewable natural resource that is suitable for making environmentally friendly building materials. However, problems in the construction with earth are to ensure its durability against water and mechanical strength. For this reason, lime, cement or both are added as chemical stabilizers[11]–[14]. There are three main stabilization methods: (1) mechanical stabilization, (2) physical stabilization and (3) chemical stabilization.

2.5.1 Mechanical stabilization

The mechanical stabilization of the soil is by compacting it, which changes its compressibility, density and porosity. However, the idea of compacting the soil to improve the properties of molded earthen blocks is old, and the first compacted earthen blocks were produced with wooden pestles[62]. Soil compaction allows to obtain a material with high mechanical properties. Three types of compaction are used to improve the engineering properties of soil: dynamic, static and vibratory[63]. Guettala *et al.*[64] investigated the influence of compacting force on the properties of CEB. They[64] mentioned that the compressive strength, capillary absorption, and durability properties of the CEB block improve as the compaction stress increases. On the other hand, It was found that for specimens without fibers the increase in compaction pressure from 1.5 MPa to 5 MPa (about 330%) resulted in a very important increase in dry compressive strength of about 240%, and from 5 MPa to 10 MPa (100%) compaction pressures there is an increase in strength about 120%[18].
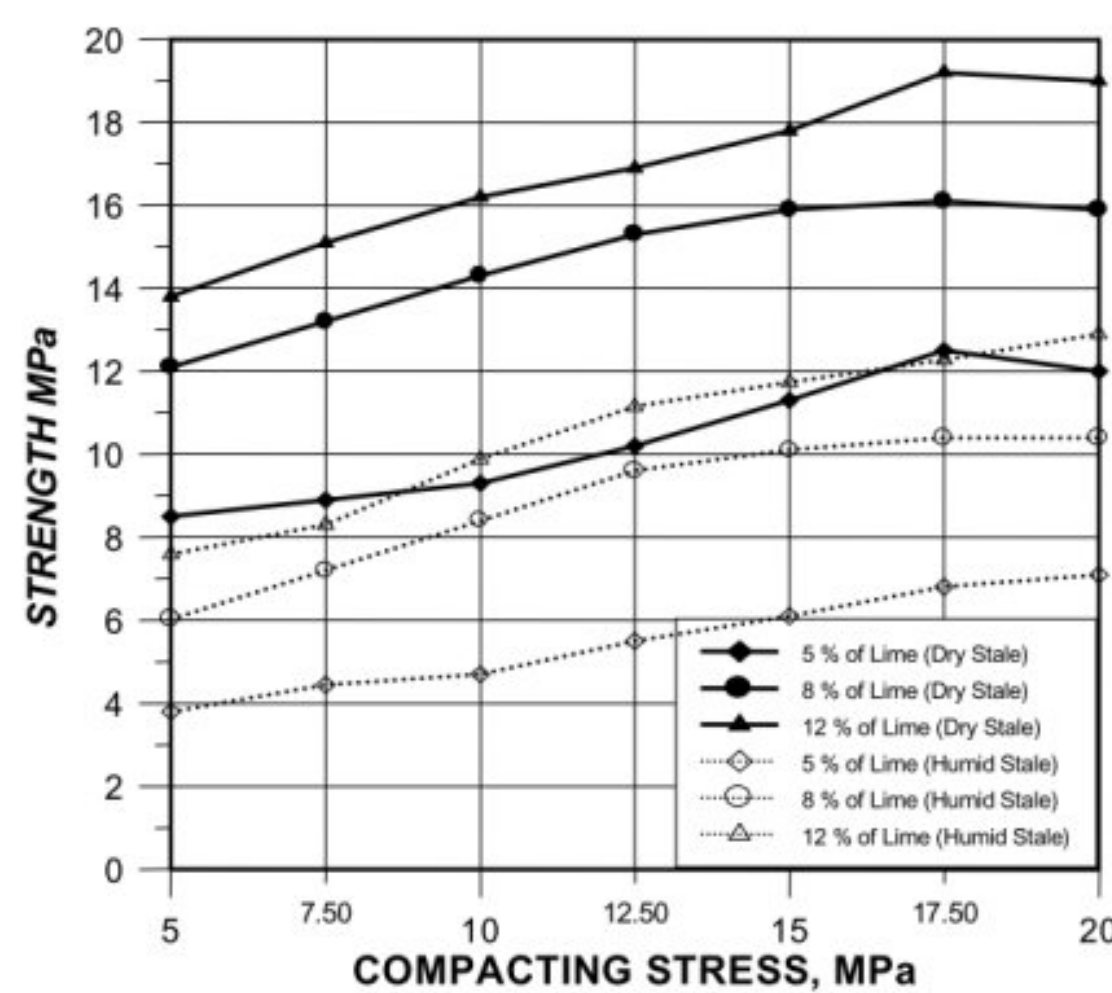
Fig.2. 26. Influence of compacting stress on the compressive strength of CEB[64].
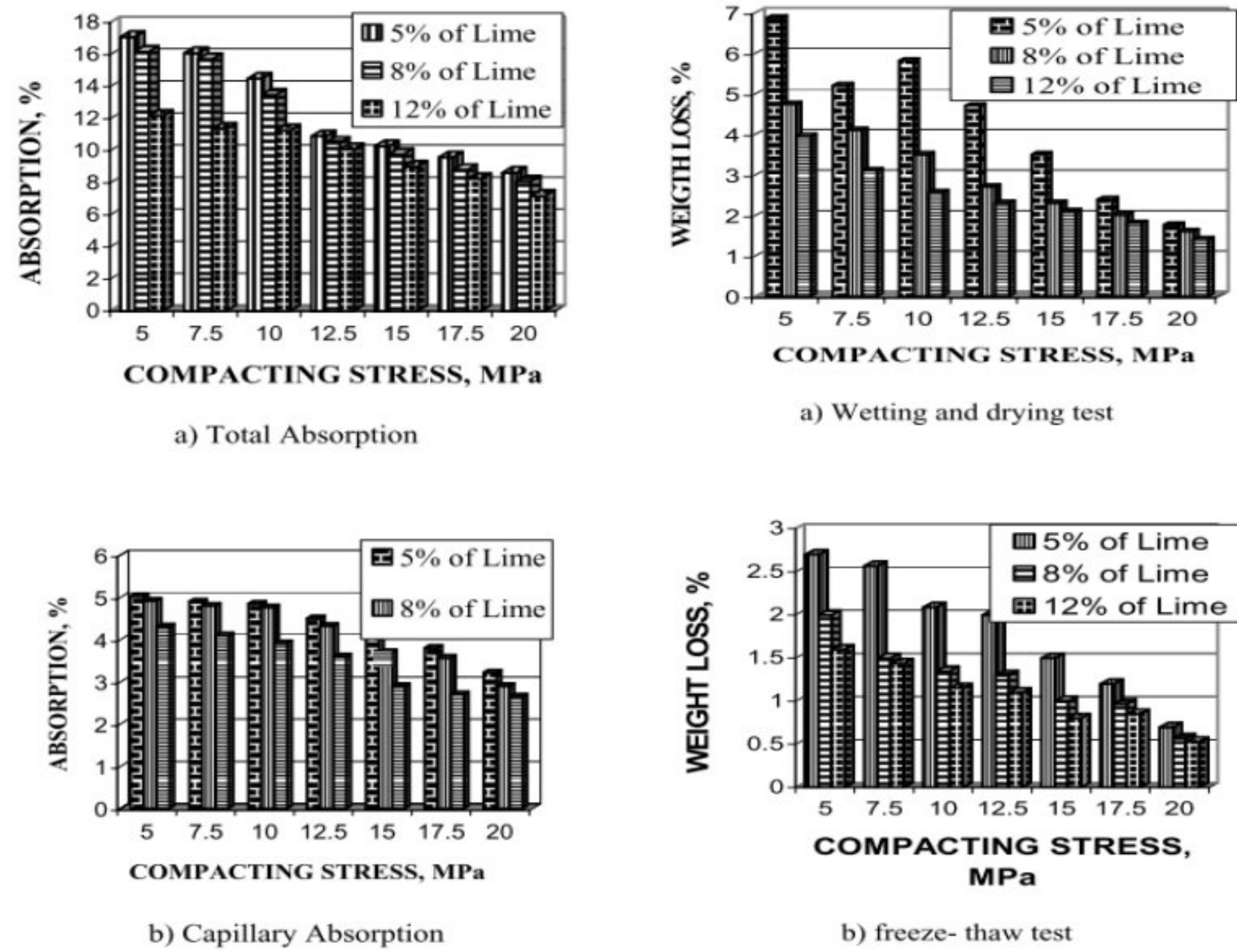
Fig.2. 27. Influence of the compacting stress and lime content on the absorption and the weight loss of CEBs [64].
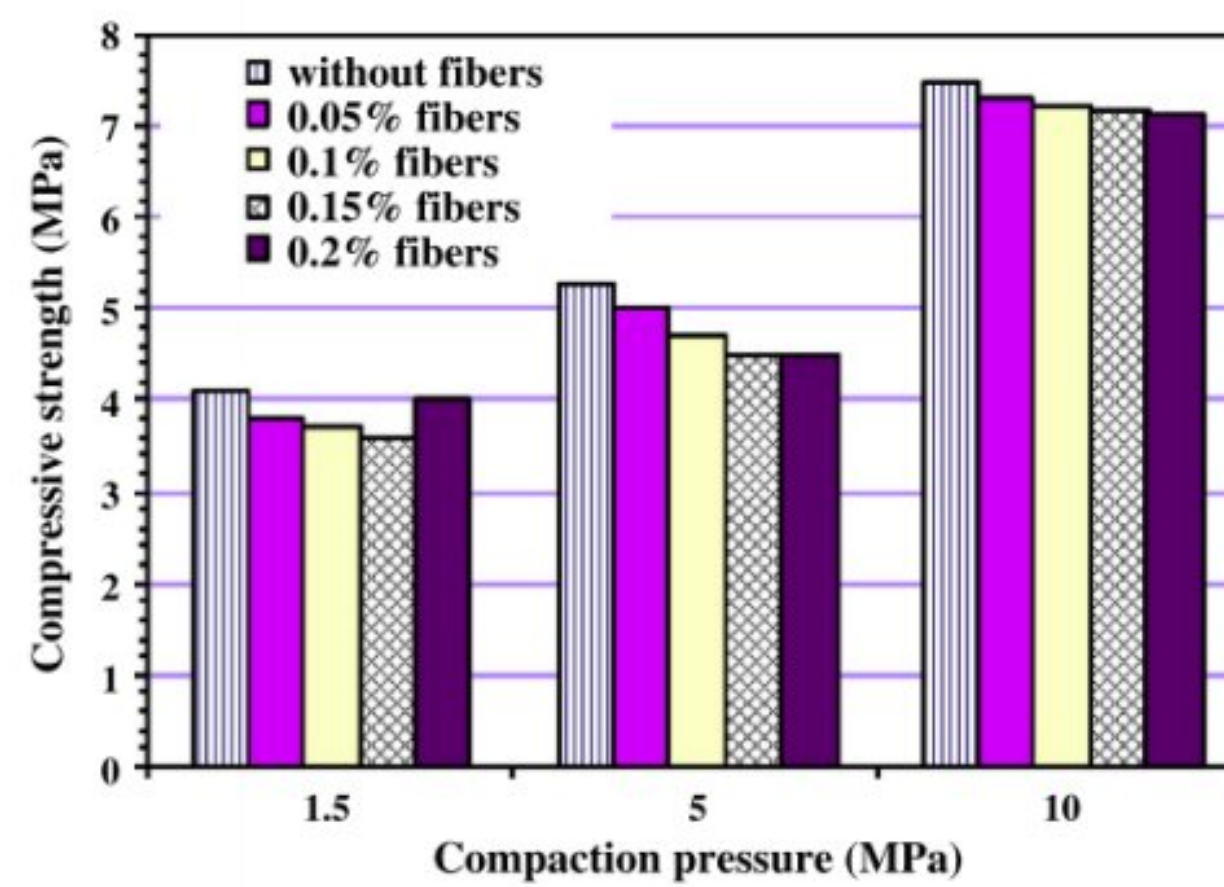
Fig.2. 28. Effect of compaction pressure on the dry compressive strength of CEB with fibers stabilized by 5% cement[18].

2.5.2 Physical stabilization

Physical stabilization can take two forms: either modifying the soil's qualities through enhancing the material's properties, or correcting the grain. In this case, the action is conducted directly on the texture, and the resulting combination reduces the plasticity of the basic soil by adding sand, or gives it a certain consistency by adding granules. Fibers can also be added to clay soil. As the clay shrinks as the soil dries up, this improves the material's structure by preventing it from cracking. According to Guettala et al.[64], the compressive strength in the dry and wet state increases with increasing sand concentration. For 30% sand content, there is a development of compressive strength in the dry and wet state about 24% and 28%, respectively. Indeed, Bouhicha et al. [46] suggested that the linear and volumetric shrinkage decreased when both the amount and length of plant fibers in soil augmented. On the other hand, Millogo et al. [65] observed that integrating short kenaf fibers allowed reducing the propagation of cracks in earth blocks.
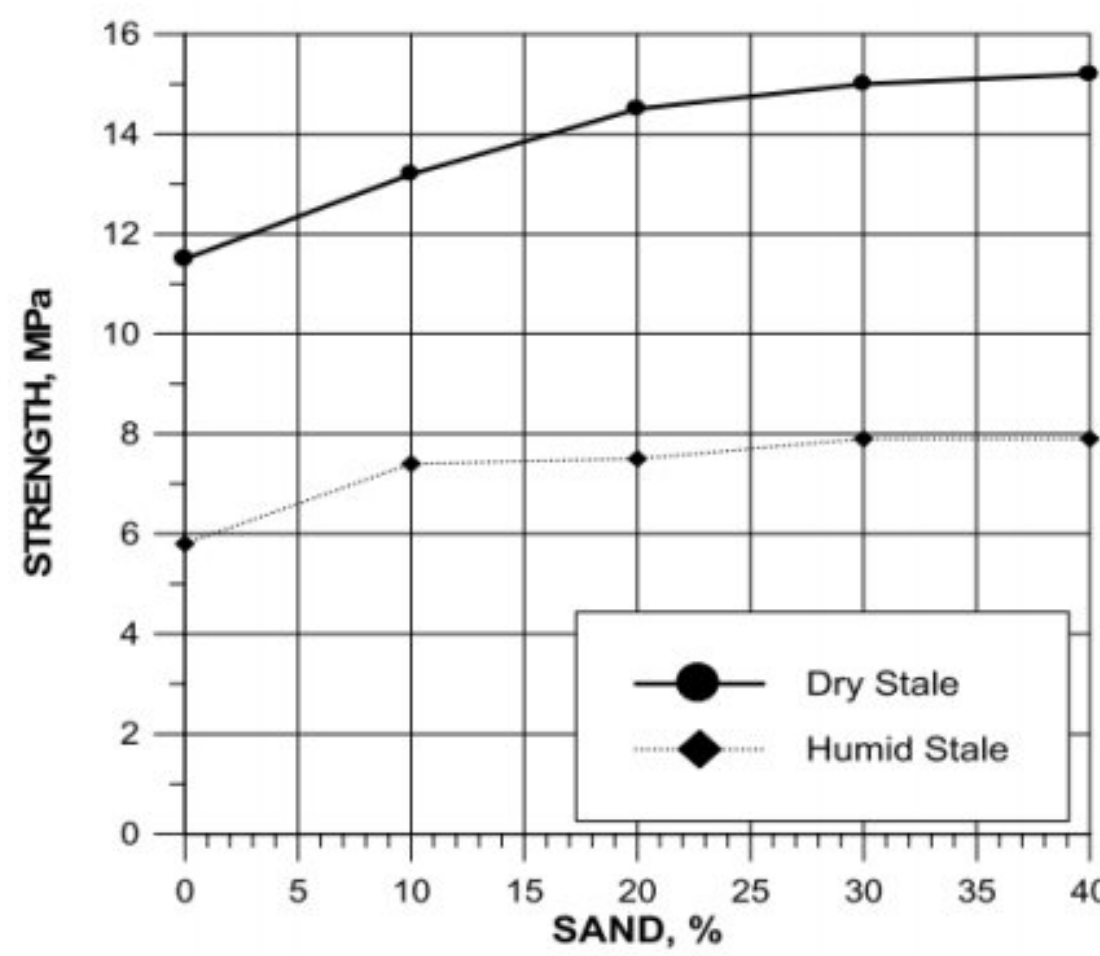
Fig.2. 29. Influences sand content on compressive strength[64].
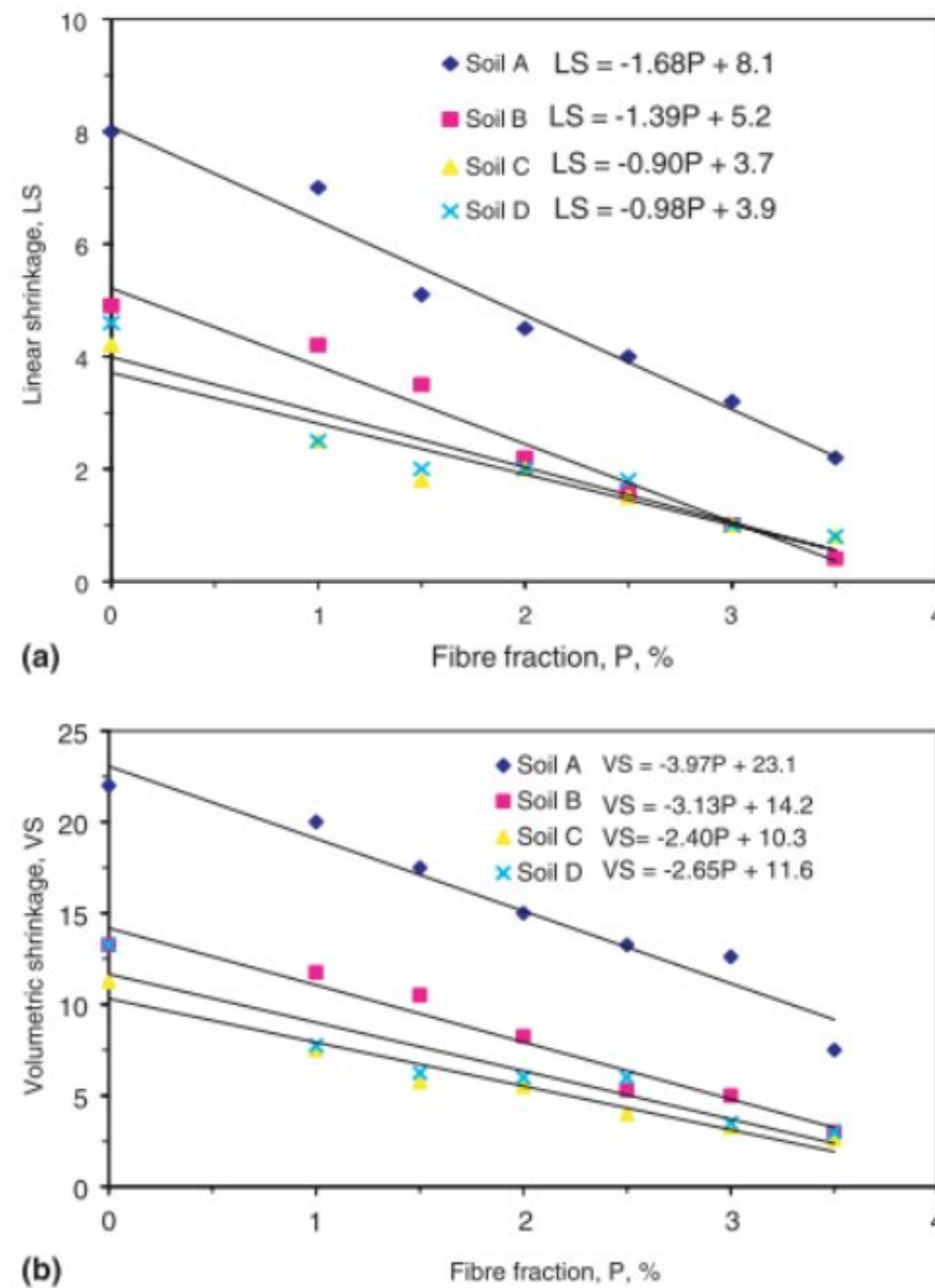
Fig.2. 30. Linear and volumetric shrinkage variation with fiber fraction[46].

2.5.3 The main chemical stabilizers of earthen materials

2.5.3.1 Cement

Portland cement is composed of four major oxides: CaO, SiO_2, Al_2O_3 and Fe_2O_3. Portland cement is made by firing a mixture of clay and limestone as raw materials at about 1450 °C, and the clinker is produced. The clinker is mixed with a small amount of $CaSO_4$ to obtain the cement. This process of calcination liberates CO_2 from the $CaCO_3$ to form CaO (quicklime) and other cementitious compounds[66]. Portland cement is a multi-component system, in which the clinker phases C_3S, C_2S, C_3A and C_4AF are the major compounds. According to the literature, increasing the cement content in earthen blocks improves mechanical strength and durability[12], [18], [67].

2.5.3.2 Lime

Quicklime production needs only heating raw limestone that contains calcium carbonate ($CaCO_3$) at about 900 °C, which makes the use of quicklime preferred as a stabilizer to protect the environment and reduce energy consumption compared to cement. Lime is a traditional chemical

binder, and its properties are compatible with soil, especially when clay and fine particles are present[15]. In addition, treatment of soil with lime is one of the economical techniques to improve the strength characteristics and reduce soil swelling [16]. Four types of reactions can take place during the stabilization of soil with lime: (1) cation exchange, (2) flocculation and particle aggregation, (3) lime carbonation, and (4) pozzolanic reactions between lime, silica and alumina. Reactions 1 and 2 lead to improvement in soil plasticity and workability. Reactions 3 and 4 lead to the formation of cementing products and are responsible for long-term increase in durability and soil strength [68].

✦ Cation exchange and flocculation

These reactions result from the replacement of univalent sodium (Na^+) and hydrogen (H^+) from the earth with divalent ions, calcium ions (Ca^{2+}) from lime. Cationic exchange causes cations (Ca^+) to adsorb to the surface of particles and decrease their electronegativity, thereby promoting flocculation. The action of calcium ions begins immediately after the addition of lime to the soil. A decrease in the plasticity of the soil occurs, it then becomes brittle and breaks easily. The reaction usually takes place within 96 hours[69].

✦ Pozzolanic reaction

After the reaction with lime, the silica and alumina present in the clay particles promote the formation of calcium silicate hydrates (C-S-H) and or calcium aluminates hydrates (C-A-H) as indicated in reactions (2.1), (2.2) & (2.3).

$$CaO + H_2O \rightarrow Ca\,(OH)_2 \qquad\qquad (2.1)$$

$$Ca\,(OH)_2 + SiO_2 \rightarrow CaO - SiO_2 - H_2O\ (C\text{-}S\text{-}H) \qquad\qquad (2.2)$$

$$Ca\,(OH)_2 + Al_2O_3 \rightarrow CaO - Al_2O_3 - H_2O\ (C\text{-}A\text{-}H) \qquad\qquad (2.3)$$
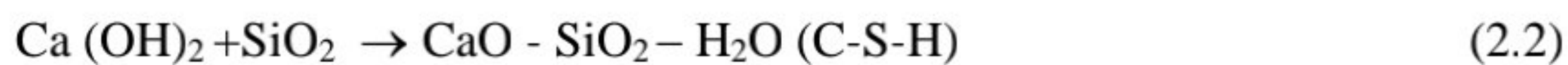
The pozzolanic reaction is the most important in stabilization. At temperatures below 55 °C, these reactions slow down and may continue for several years, while temperatures above 55 °C accelerate them[69]. The solubility of fine quartz in the medium is linked to the increase of pH, due to lime additions. In this condition, the calcium silica hydrate formed (C-S-H). Thus, the high pH basic medium increases the solubility and reactivity of silica and alumina present in clay particles. It is

postulated that calcium ions combined with dissolved silica and alumina in the clay network to form additional cementitious material (C-S-H and C-A-H)[13].

A schematic model describing the physicochemical process initially proposed by Ingles and Metcalf (1973) and later modified by Choquette (1988) to take into account the results for high water content soils is presented in Fig.2.31. This model illustrates how the reaction products are disseminated within the soil matrix, creating bridges between or on soil particles. This cementation process is responsible for the increase in strength and acts primarily on the cohesion component of the shear strength parameters of the soil. On the long term, a high water content soil may even perform better than a soil with a low water content, likely because movement of solutes is eased within the porous space (Fig.2.31)[68].
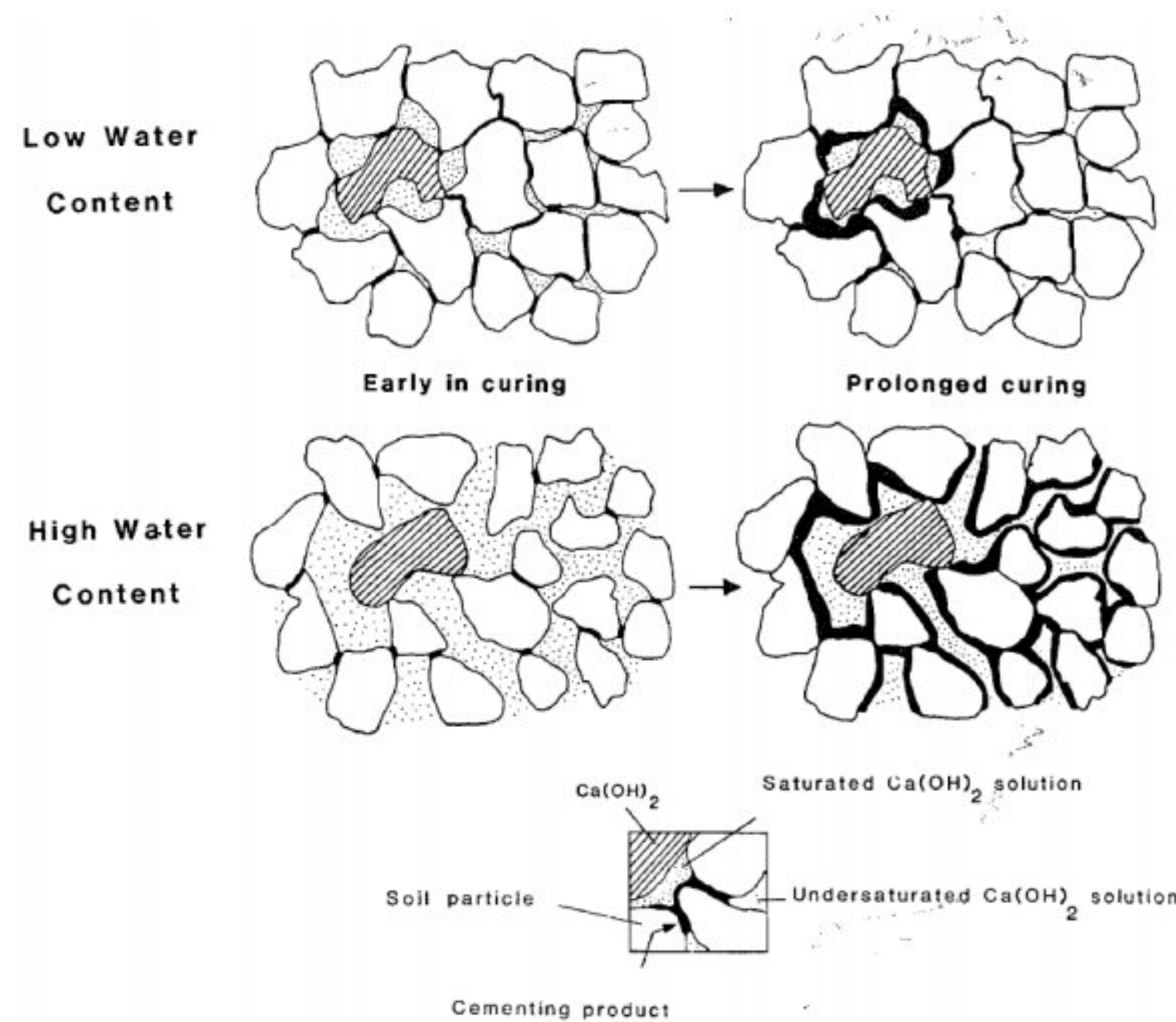
Fig.2. 31. The model proposed for lime stabilization of clays[68].

🞣 Carbonation

The lime carbonation process is made by a reaction between the lime and CO_2 coming from the air to form limestone ($CaCO_3$) [10]. The reverse reaction occurs when lime is produced from limestone, and should be avoided since the calcium and magnesium carbonates formed prevent resistance from developing. Carbonation also occurs when the soil does not contain a sufficient amount of pozzolanic clay, or because too much lime has been added. $CaCO_3$ increases soil plasticity and binds to lime so that it cannot react with pozzolanic materials. Therefore, adding a

lot of lime to the soil does not lead to beneficial results[69]. Millogo et al. [13] mentioned that the contribution of the pozzolanic reaction, involving kaolinite (the unique clayey constituent of the raw material), to C-S-H formation seems to be insignificant. The development of C-S-H together with the formation of minor amounts of calcite, in <10 wt% lime samples, improved the mechanical strength and the compactness of adobe bricks (Fig.2.32). The development of calcium silicate hydrates (C-S-H) and formation of minor amounts of portlandite ($Ca(OH)_2$) and calcite ($CaCO_3$) lead to improvement in the mechanical properties and the compactness of CEB. C-S-H is originated from the chemical reaction between SiO_2 (fine grains of quartz) and CaO (quicklime). However, higher quicklime additions, the quasi-absence of C-S-H and formation of higher amounts of portlandite have negative effects on the mechanical properties of CEB [13].
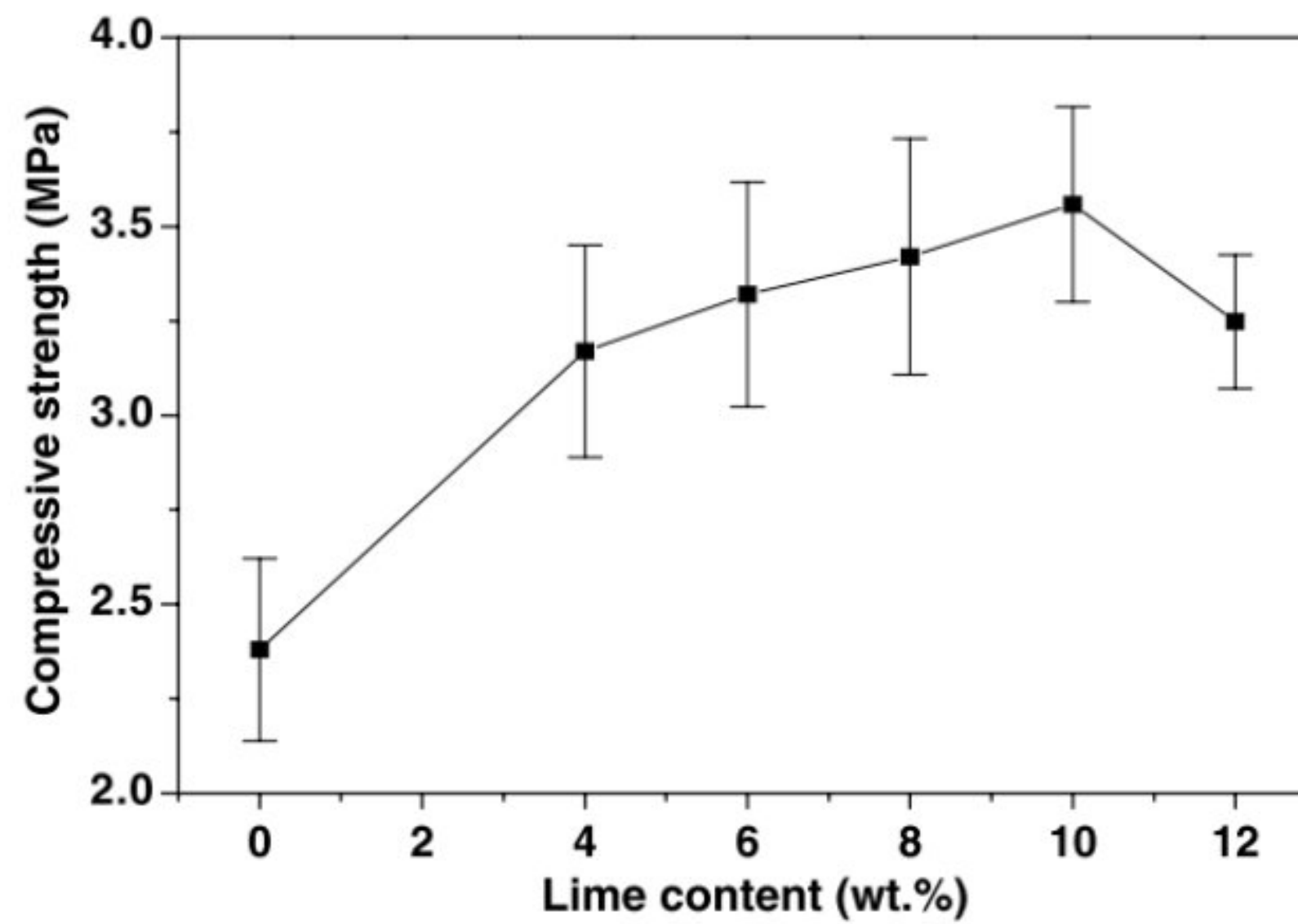
Fig.2. 32. Evolution of the compressive strength of clayey adobe bricks as function of lime content[13].
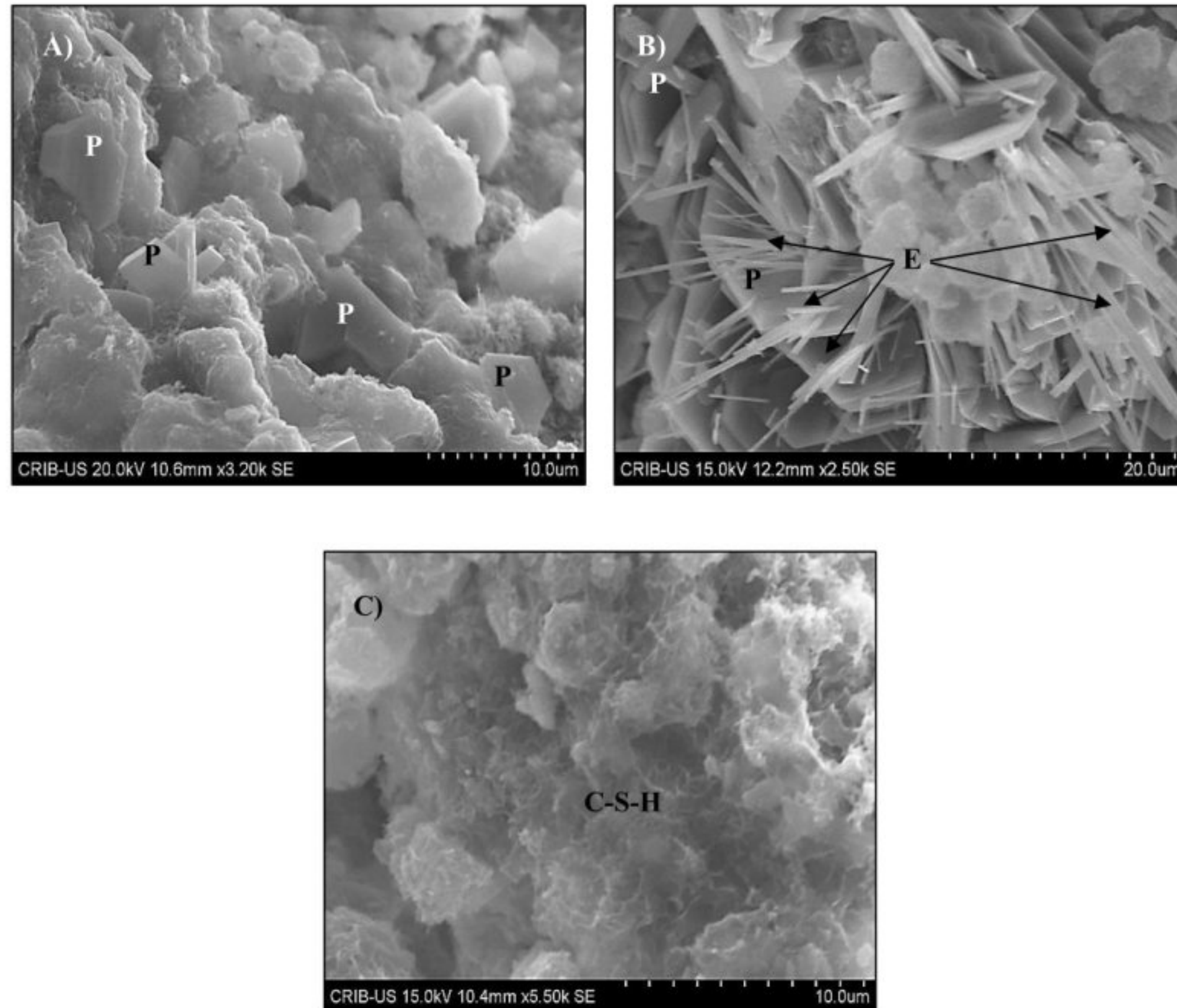
Fig.2. 33. Product of hydration of cementitious materials by SEM (P = Portlandite, E = Ettringite, C-S-H = hydrated calcium silicate)[70].

According to Millogo et al. [13], SEM examinations performed on free lime and 4 wt.% lime samples (Fig. 2.34 a and b) showed a heterogeneous structure consisting of isolated particles of kaolinite Calcium-rich zones, manifesting as bright areas (Fig. 2.34 b – Zone D), developed in 4 wt.% lime sample. When the lime content increased to 6 wt.%, the tiny filiform free silica disappeared and linkage between particles developed, resulting thus in the occurrence of a homogeneous microstructure (Fig. 2.34 c). In this case, isolated featureless particles (Fig. 2.34 e-Zone E), identified as C-S-H were developed. On the other hand, it is worth noting that coarse grains of quartz displayed surficial pits (Fig. 2.34 d-Zone F), which apparently constituted preferential sites for C-S-H and/or calcite nucleation. However, it appears that K-feldspar grains (Fig. 2.34 e-Zone G) were unaltered. As the lime content increased to 12 wt.%, portlandite and calcite, which manifested as bright areas (Fig. 2.34 f-Zone H), were extensively formed. The excessive carbonation resulted in the occurrence of a heterogeneous microstructure.
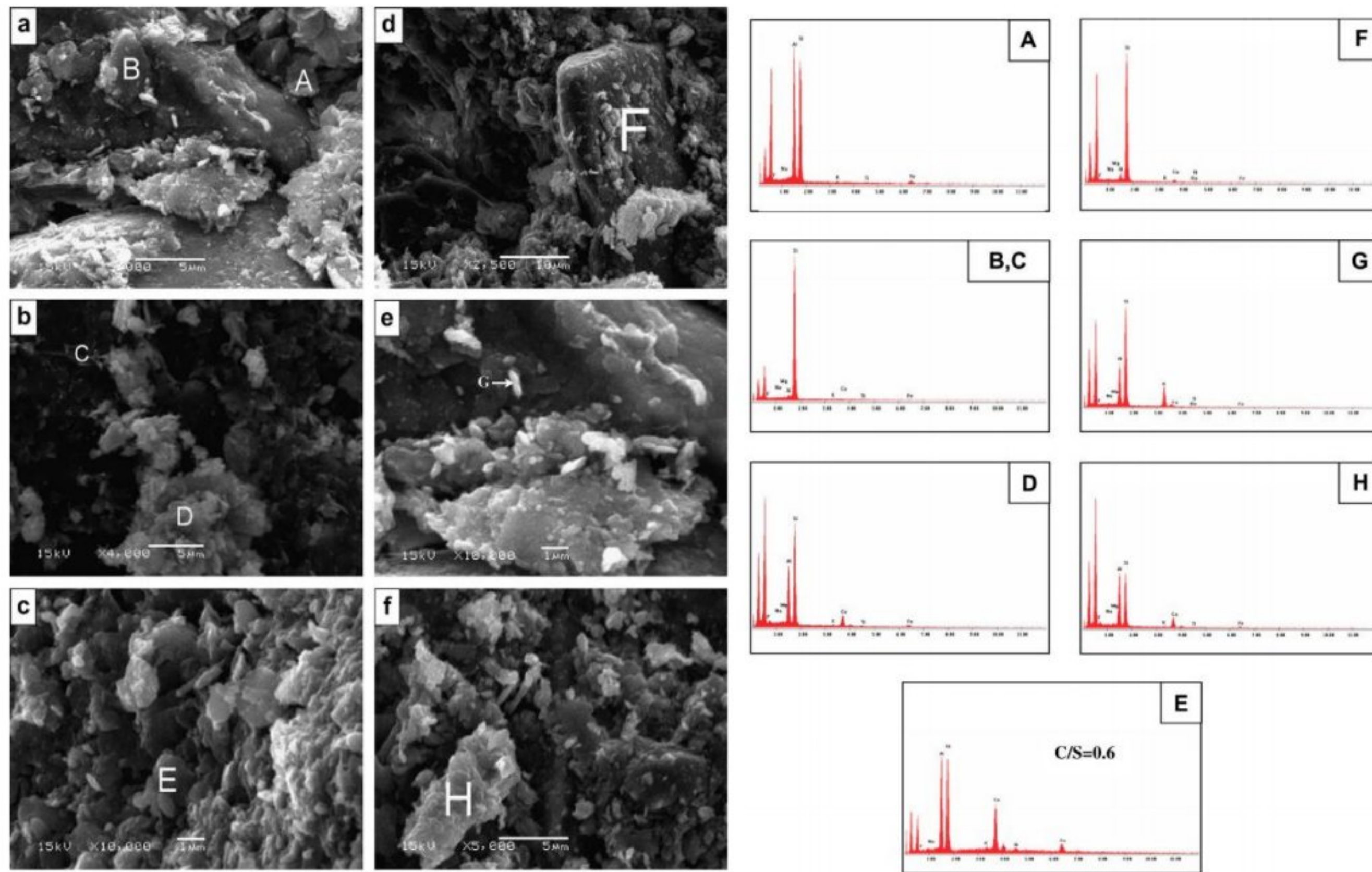
Fig.2. 34. SEM micrographs of adobe clayey bricks samples and EDS analyses of areas quoted. (a) Lime free sample, (b) 4 wt.% lime, (c) 6 wt.% lime, (d and e) 10 wt.% lime and (f) 12 wt.% lime[13].

2.5.3.3 Other promising chemical stabilizers

- **Geopolymer**

Discovered in the 1970s, geopolymers can be synthesized at low temperatures (25–80 °C) using an alkaline solution and an alumino-silicate material. Materials including amorphous silica, alumina, and alkali hydroxide (NaOH/KOH) are commonly used in the synthesis. For the synthesis of the binder, a variety of aluminosilicate materials can be employed. Metakaolin, rice husk ash, fly ash, and volcanic slag are among them. Metakaolin appears to be the most extensively utilized aluminosilicate material for manufacturing the geopolymer binder because its raw material (kaolin) is easy to synthesis without CO_2 emissions, and it has excellent chemical and mineralogical qualities (amorphous phase, silica and alumina content)[71]. It is a more environmentally friendly alternative to conventional Portland cement. It reduces the carbon footprint of cement manufacturing by relying on little processed natural resources or industrial wastes, while simultaneously being highly resistant to many common building materials durability issues[71]–

[74]. Omar Sore et al[71]. mentioned that geopolymerization of compressed earth blocks (CEBs) significantly improved their mechanical performance and gave them thermal properties that were very similar to those of non-stabilized blocks. For a 15% geopolymer content, these materials displayed properties comparable to those of Portland cement-stabilized CEBs, in particular with regard to their stability in water.
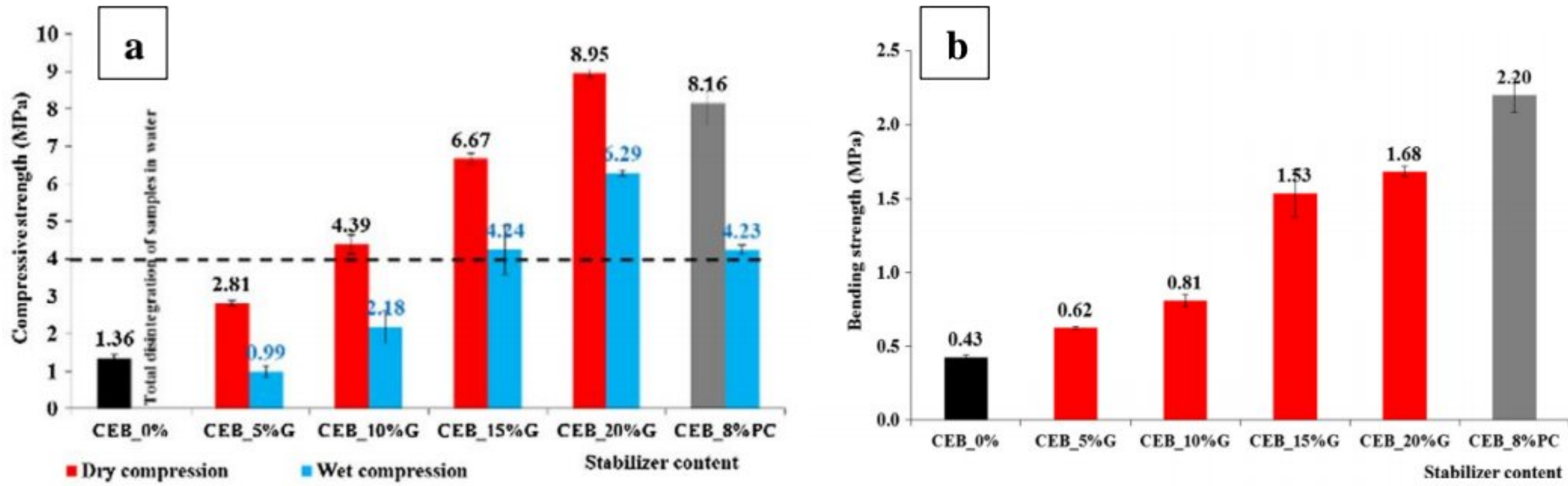
Fig.2. 35. a) Dry and wet compressive strength of CEB samples; b) Bending strength of CEB samples[71].
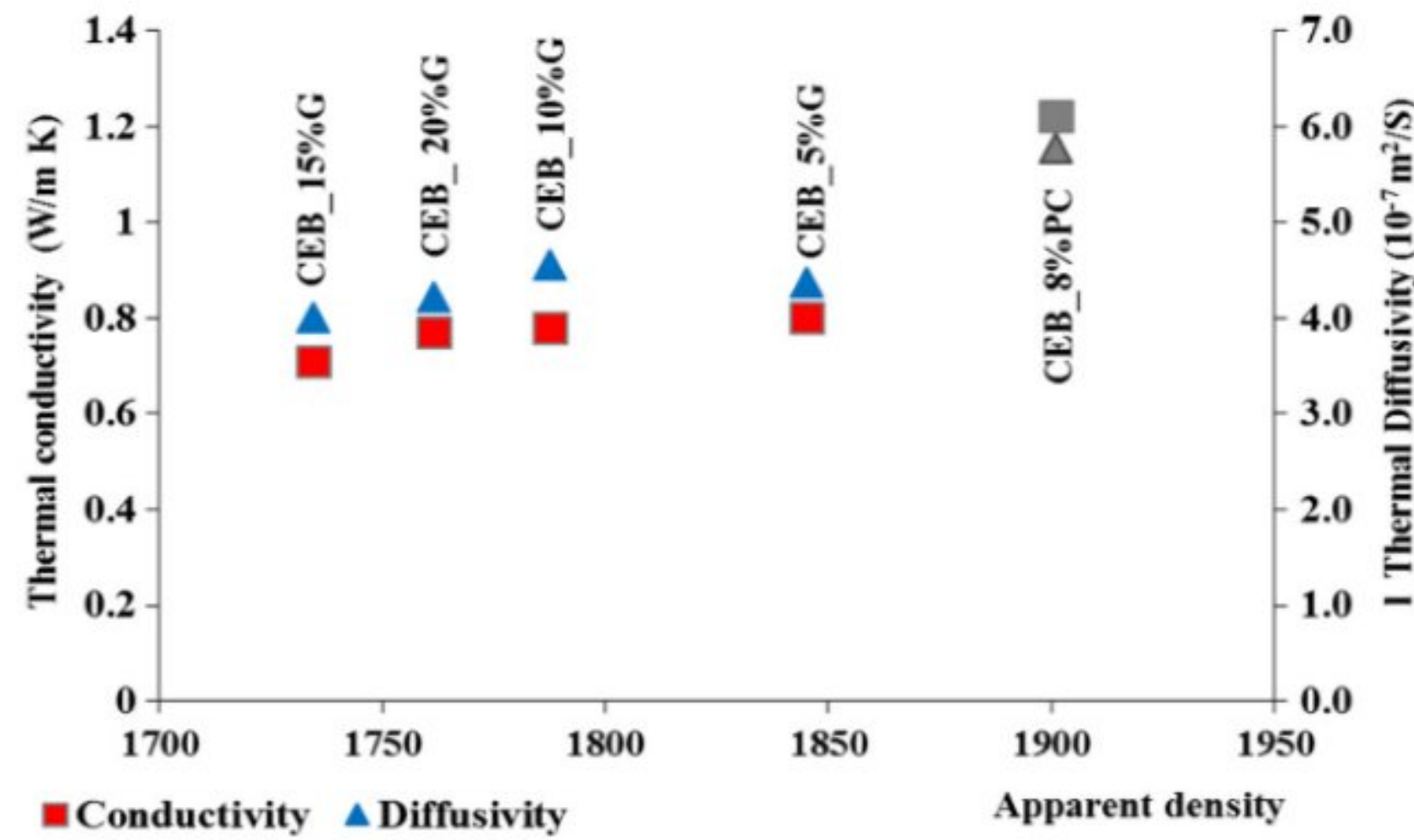
Fig.2. 36. Thermal properties according to the apparent density[71].

- **Biopolymer**

Biopolymers are produced from living beings and they can have very different features: plant or animal origin, hydrophilic, hydrophobic, or amphiphilic behavior. Since prehistoric times, natural polymers have been tried for soil stability. Natural Polymers were extracted from plants and trees. In fact, solid additives (such as cow dung and vegetable residues) and liquids or powders are mainly

used as biopolymers stabilizers[75]. Some tribes in Africa use proteins to provide an enzyme type reaction to stable soil-based constructions. In the country of Mali wet mud is fermented with natural polymers and rested for several days former to make earth walling blocks. It was found that South African tribes dated 49,000BC used animal milk to stable soil and color pigments. Another similar material is the cellulose properties of termite mound (White ant saliva) makes polymeric binder used by white ants to make termite castles[76]. The findings of the study by Udawattha et al.[76] revealed that, while natural polymers such as Pines resins exhibit favorable outcomes in terms of strength development in earth blocks, they also have a number of disadvantages. The most significant disadvantage is the high water absorption rate.

▪ **Bio-cementation**

Bio-cementation is a new environmentally friendly biochemical process that improves the physical and mechanical properties of soil, which has attracted attention in the twenty-first century due to its significant advantages over traditional reinforcement methods. This process is carried out by a catalyst (urease enzyme) and other chemical solutions as a source of calcium and carbon (urea-$CaCl_2$). These reactions lead to the precipitation of calcium carbonate ($CaCO_3$) in the form of solid crystals, which increase the adhesion between the seeds of soil and increase the rigidity and the mechanical resistance of the soil. The bio-cementation method is a difficult method to apply in the practical field due to its high cost and the fact that it relies on enzymes and living organisms that only perform under perfect conditions. These disadvantages must be overcome in the future.
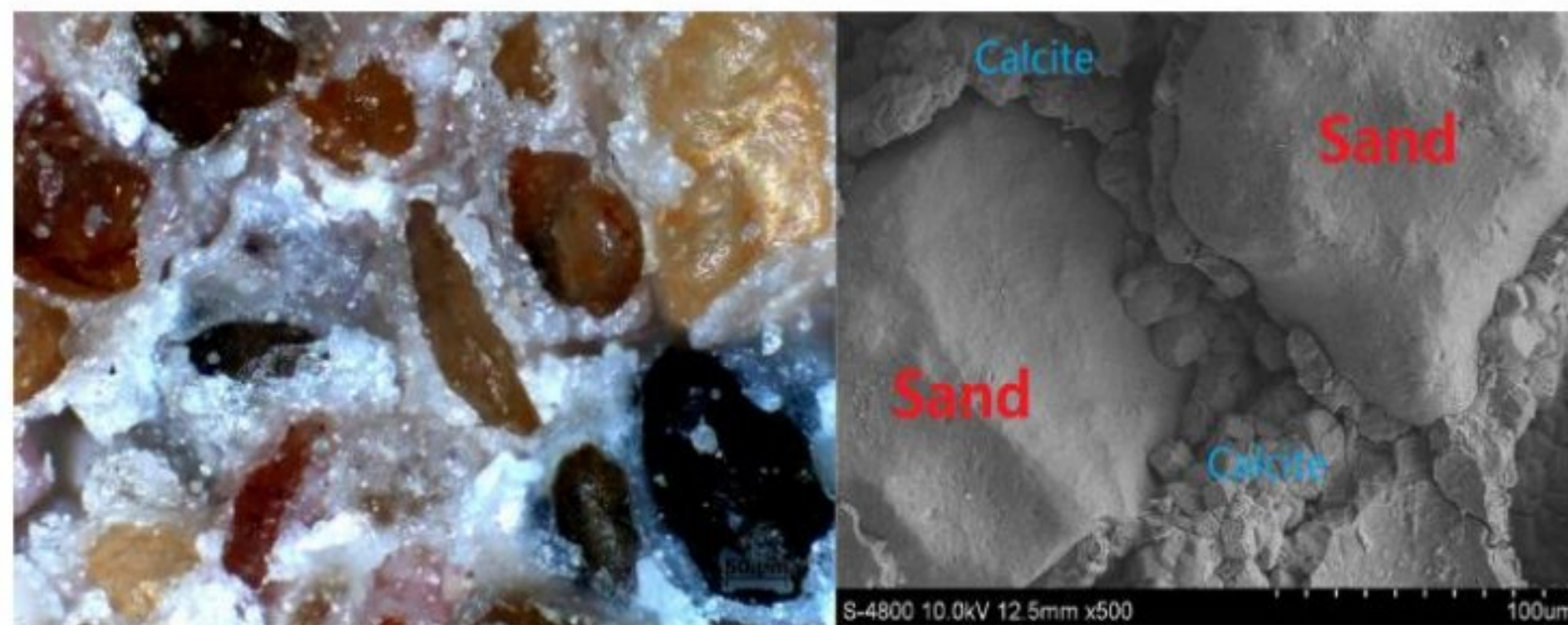
Fig.2. 37. Optical microscopy and SEM images of bio-cemented sand[77].

2.6. The use of plant aggregates and fibers in the formulation and elaboration of compressed earth blocks

2.6.1 Background of the plant aggregates and fibers

Natural fibers such as date palm, kenaf, flax, jute, hemp, and sisal are still gaining increasing interest after decades of high-tech development of artificial fibers such as carbon, and glass. In recent years, because of the large consumption of non-renewable resources, the scientific community began to search for appropriate solutions for the environment, and reduce the depletion of non-renewable resources and replace them with renewable and sustainable resources. Recently, scientific interest in natural fibers has increased as a component of building applications. The use of plant fibers as a raw material is a return to ancient civilizations. For example, in Egypt 3000 years ago, walls were constructed by strengthening clay with straw[78]. The plant aggregates and fibers are used in building materials according to their abundance in the study location. Plants waste can be used as alternative fibers to traditional fibers, such as steel, carbon and glass fibers or as plant aggregate in composite materials, especially those used in the construction field in order to improve its ductility as well as thermal and mechanical properties. The use of natural waste in building materials helps to reduce environmental pollution, saves natural resources and energy production processes. Compared to synthetic fibers, natural fibers are very cheap, promising and abundant.

Date palm tree are one of natural source of fibers, these fibers considered as plant waste with no economic value. The date palm is commonly found in dry and hot regions of the world, especially the North Africa, Middle East, and there are about 100 million date palm trees in the world[20]. Algeria is a land famous for dates production, because it has a large desert area and a large number of palm trees that yield over 800 date varieties in its oases in the south and there are more than 18.7 million trees in Algeria[20], [21]. Palm trees produce huge amounts of waste every year. Farmers usually burn it in the palm groves, which negatively affects the environment. However, this waste can be valorized in the earth materials production like compressed earth blocks (CEB) or adobe by the incorporation of date palm waste as thermal insulator or reinforcement in the formulation of CEB for the production the ecofriendly CEB as building materials.
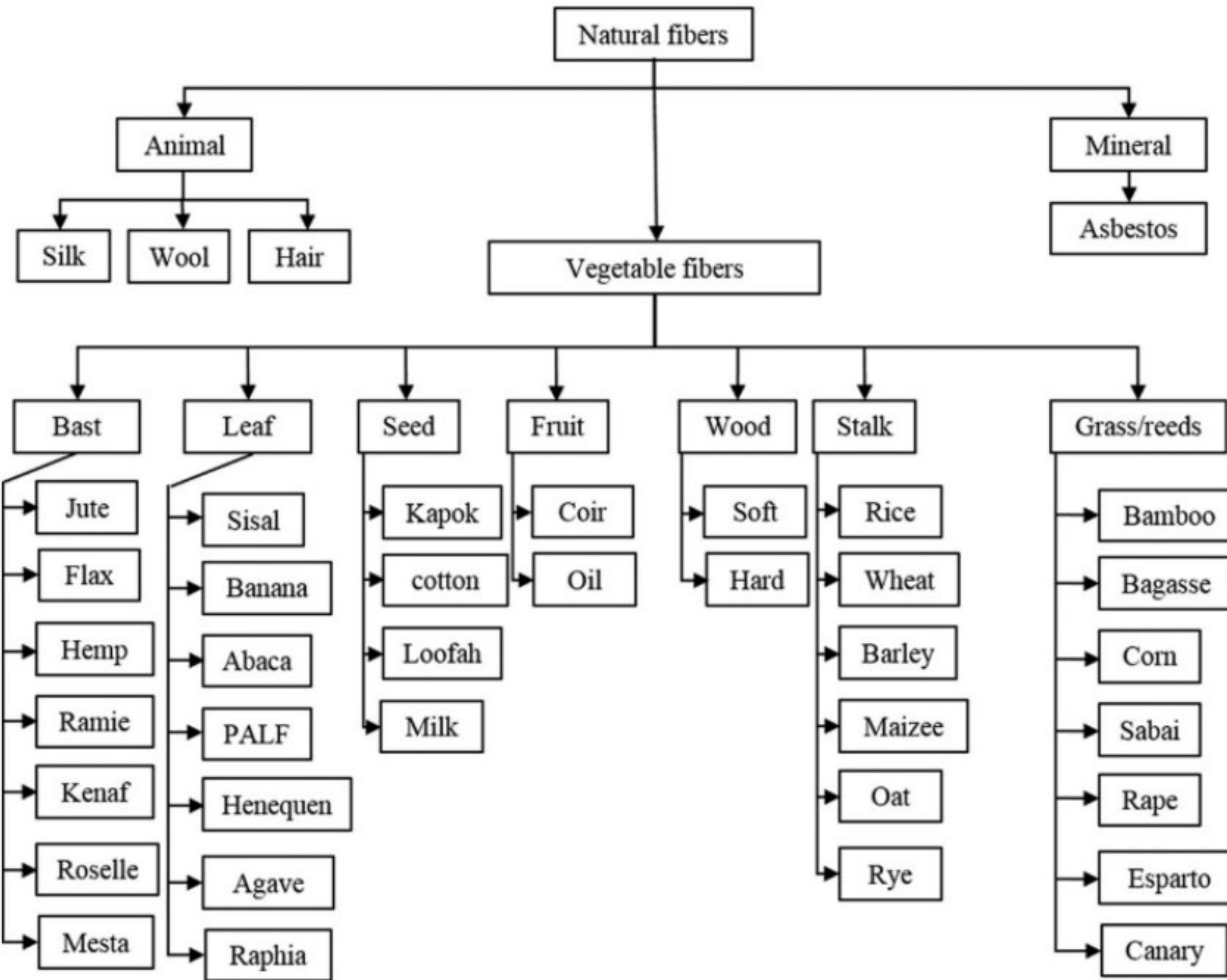
Fig.2. 38. Classification of natural fibers[78].

2.6.2 Properties of date palm fiber and other fibers

Currently, natural fibers and bio-aggregate attract the attention of researchers and builders in the construction industry, as they are eco-friendly, lightweight, cost-effective, and renewable resources. The inclusion of natural fibers in the cement concrete or mortar and earth based materials will contribute to solving the environmental problems associated with dumping or burning them and improve the properties and durability of building materials[43], [73], [87]–[89], [79]–[86].

The date palm (Phoenix dactylifera l.) is one of the oldest fruit trees cultivated for millennia in the Middle East and North Africa region which produces around 2.6–2.8 million tons of waste, deposited annually in landfills[90]. Date palm has an enormous importance in Saharan agriculture and the main livelihood of populations living there. According to the 2018 data from the Food and Agriculture Organization of the United Nations (FAO), Algeria is the fourth largest date producer in the world and the second in Africa after Egypt, with 1,904,700 tons of dates harvested and a cultivation area of 168,855 ha[91].
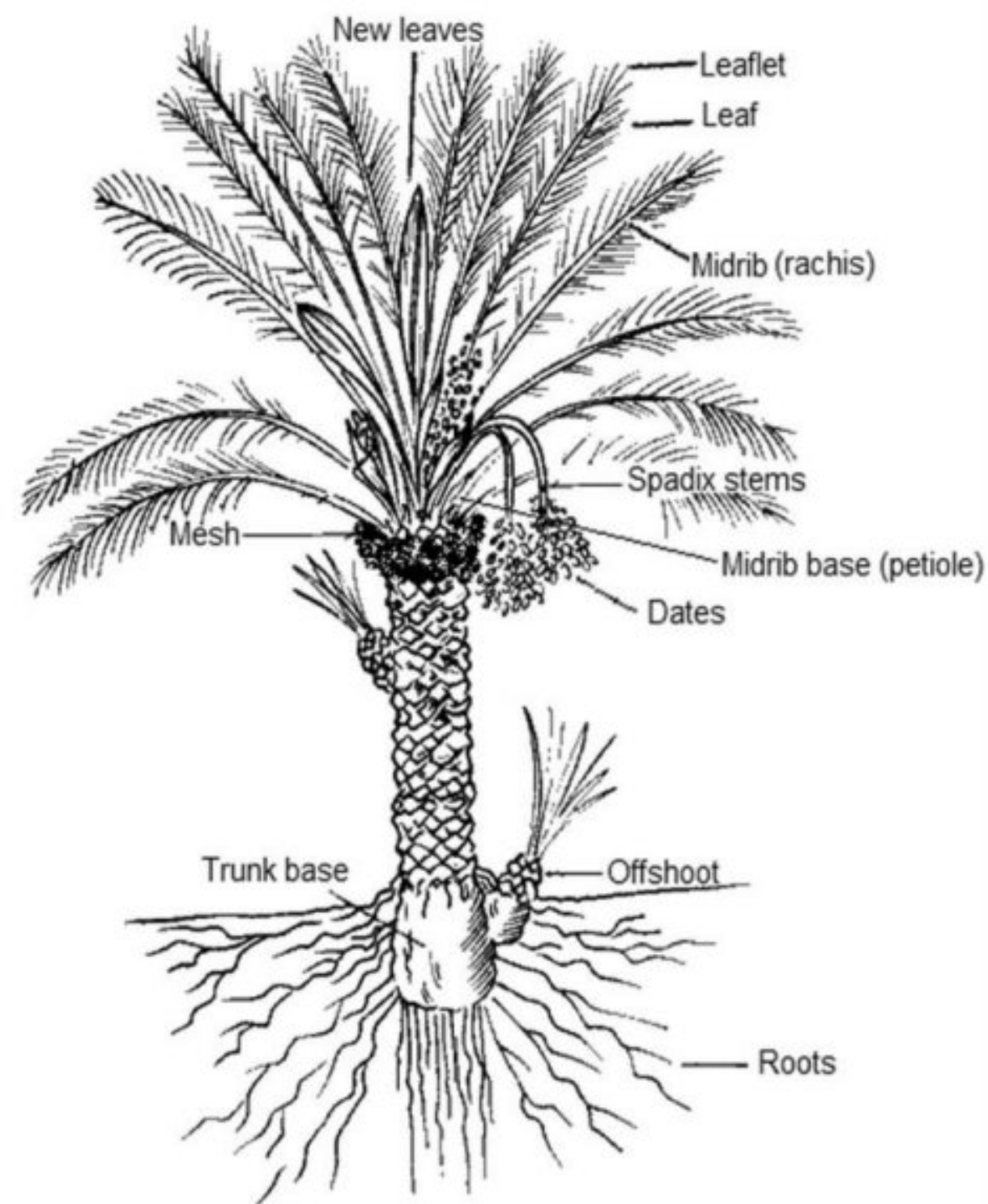
Fig.2. 39. Date palm tree[90].

A statistical study perfermed among farmers and agricultural organizations in the region of Biskra has estimated that approximately 47.57 kg of palm residues is obtained per tree annually. This quantity of residues is made up of 28.7% Leaflets, 27% Rachis, 23.9% Petioles, 6.3% Fibrillium, 5% Spathes, 4.9% Bunches, 3.3% Pedicels, and 0.8% Thorns[92]. In fact, this natural resource can be exploited sufficiently as many other natural fibers such as jute, flax, ramie, hemp and sisal which are used as reinforcement in many industrial applications. Utilizing date palm fiber and date palm bio-aggregate for industrial applications as a reinforcement in building materials, polymeric and inorganic matrices is relatively a new application.

Fig.2. 40. Different parts of date palm wood: (a) Rachis, (b) Thorns, (c) Leaflets, (d) Petiole, (e) Spathe, (f) Bunch, (g) Pedicels, (h) Fibrillium[92].

Each palm tree can grow up to 100 years with an average 35 kg of palm residues per year. The estimated annual palm tree raw fiber production is around 4200 tons. Fig. 2.41 gives a direct comparison between the annual production of different natural fibers. From this figure, one can realize that the annual estimated palm fiber production bests all other sources with more than 10 times of sisal fibers. The price of plant fiber is determined by the quantity available and the market demand for these fibers. The annual production of date palm and hemp fibers, for example, is 4,200,000 tons and 214,000 tons, respectively. Date palm fibers are 60 times cheaper than hemp fibers due to the difference in production ratio, with a market value of around $20 per ton (down to no >0.02$/kg)[93].

World production (10³ ton)
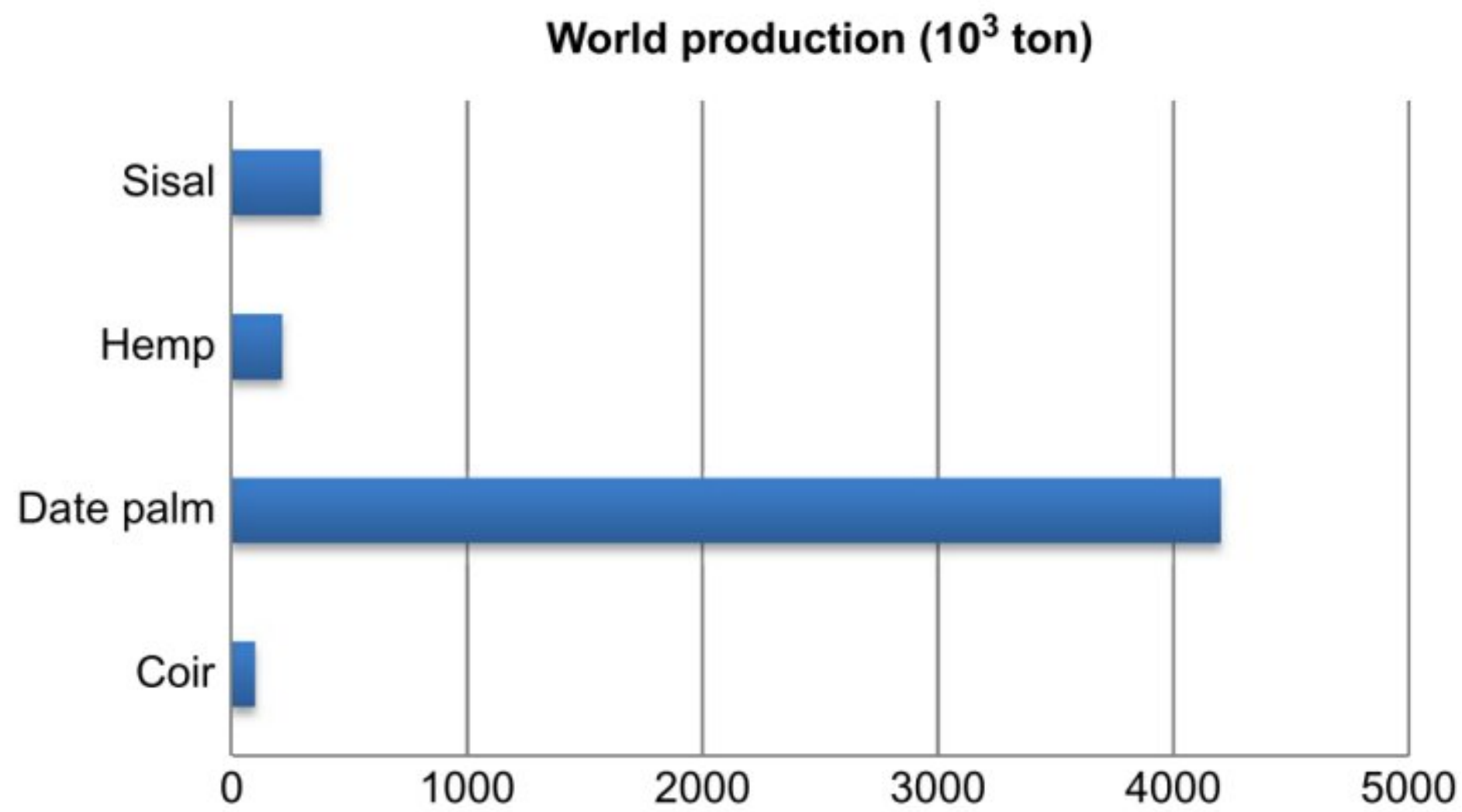
Fig.2. 41. The annual production of some natural fibers[93].
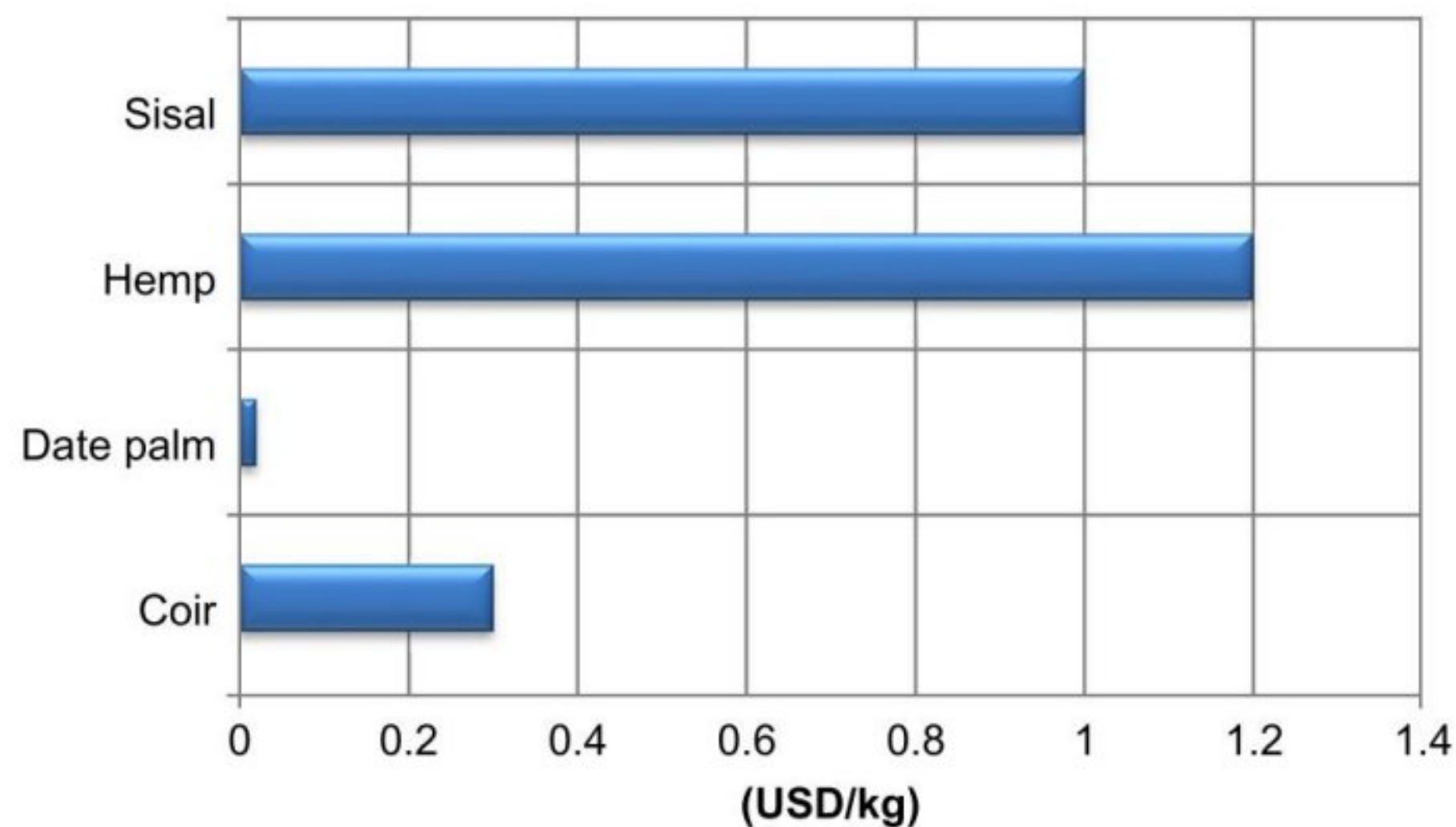
Fig.2. 42. Comparing the price of some natural fiber types used in the automotive industry with date palm fibers[93].

2.6.2.1 Chemical properties

The biological structures of vegetable fibers (date palm, sisal, hemp, cotton, jute, flax, kenaf, coconut, wood, etc.) are mostly made up of cellulose, hemicelluloses, and lignin. Cellulose is a polymer with a largely crystalline structure, unlike the other components of the fiber, which have an amorphous structure. If the absorbed water is ignored, the main elements of cellulose-based reinforcements are three types of chemicals: cellulose (about half), hemicellulose and lignin (about a quarter). Pectin and waxes are two further extractives found in plant sources[94].
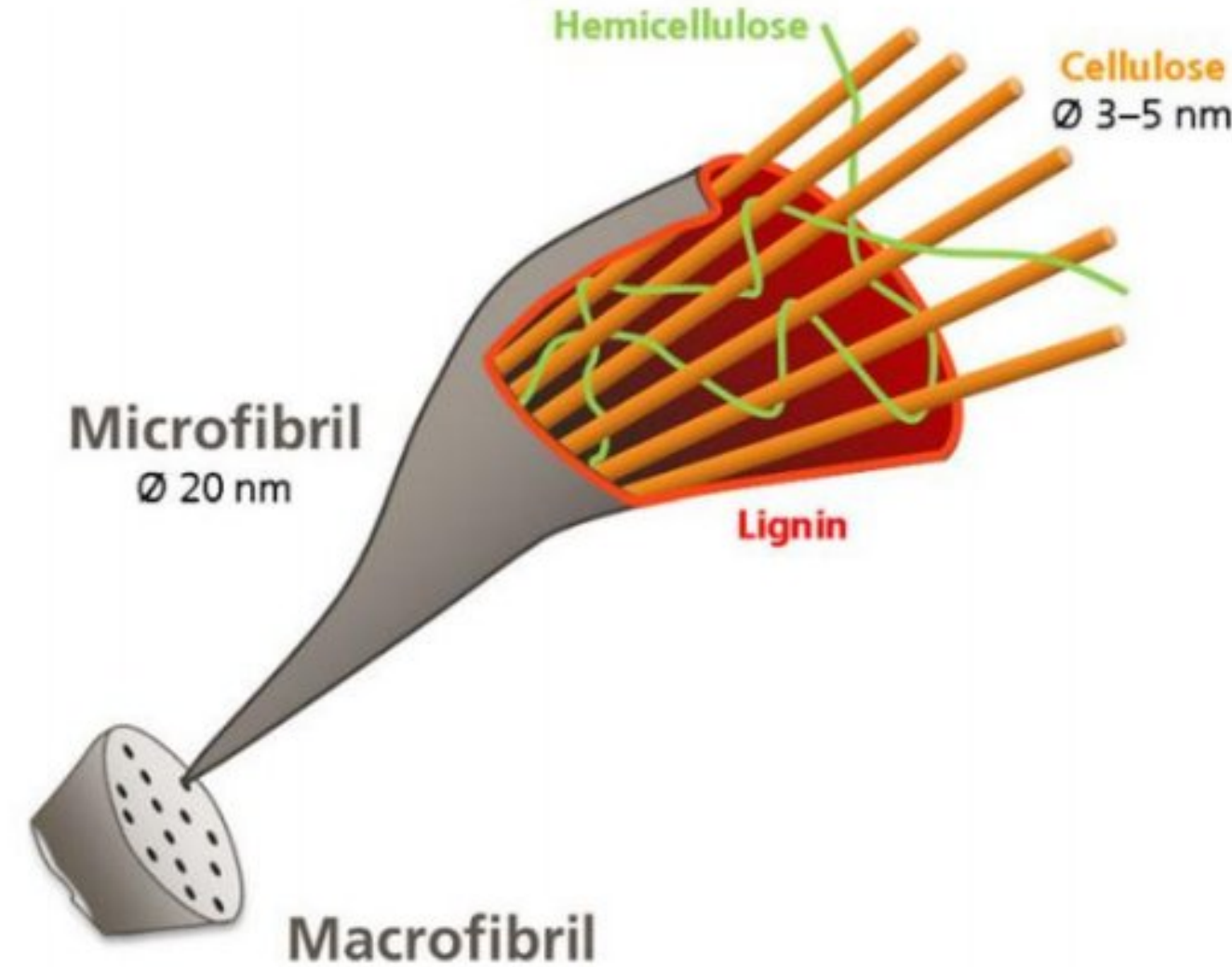
Fig.2. 43. Schematic structure of a vegetable fiber[95].

✚ Cellulose

Cellulose is a natural polymer that is the most widely available biopolymer on earth. Cellulose is a chemical starting material for synthetic textiles, adhesive films, and a variety of other products. It is utilized in a variety of industries, including packaging, textiles, and paper, as well as a food additive. Cellulose has been and continues to be the intriguing subject of a vast amount of research[96]. Its crystalline structure giving it a modulus of elasticity of roughly 136 GPa, compared to 75 GPa for glass fibers. Vegetable fiber is comparable to a composite material reinforced by cellulose fibrils[78]. Anselm Payen discovered cellulose as a common material in plant cell walls for the first time in 1838. A natural polymer consisting of D-glucose ($C_6H_{12}O_6$) monomer units, cellulose contains glucose units which link together to form long unbranched chains. Fig. 2.44 shows a schematization of the cellulose structure. There are roughly 4,000 to 8,000 glucose molecules strung together. The polymer chains in cellulose have a linear structure due to the beta 1,4-β glycosidic linkages[94]. The cell unit form of cellulose is known in literature by different names, such as microfibrils, elementary fibrils, and proto- fibrils. Such a configuration of different cellulose components is shown in Fig.2.45[78].
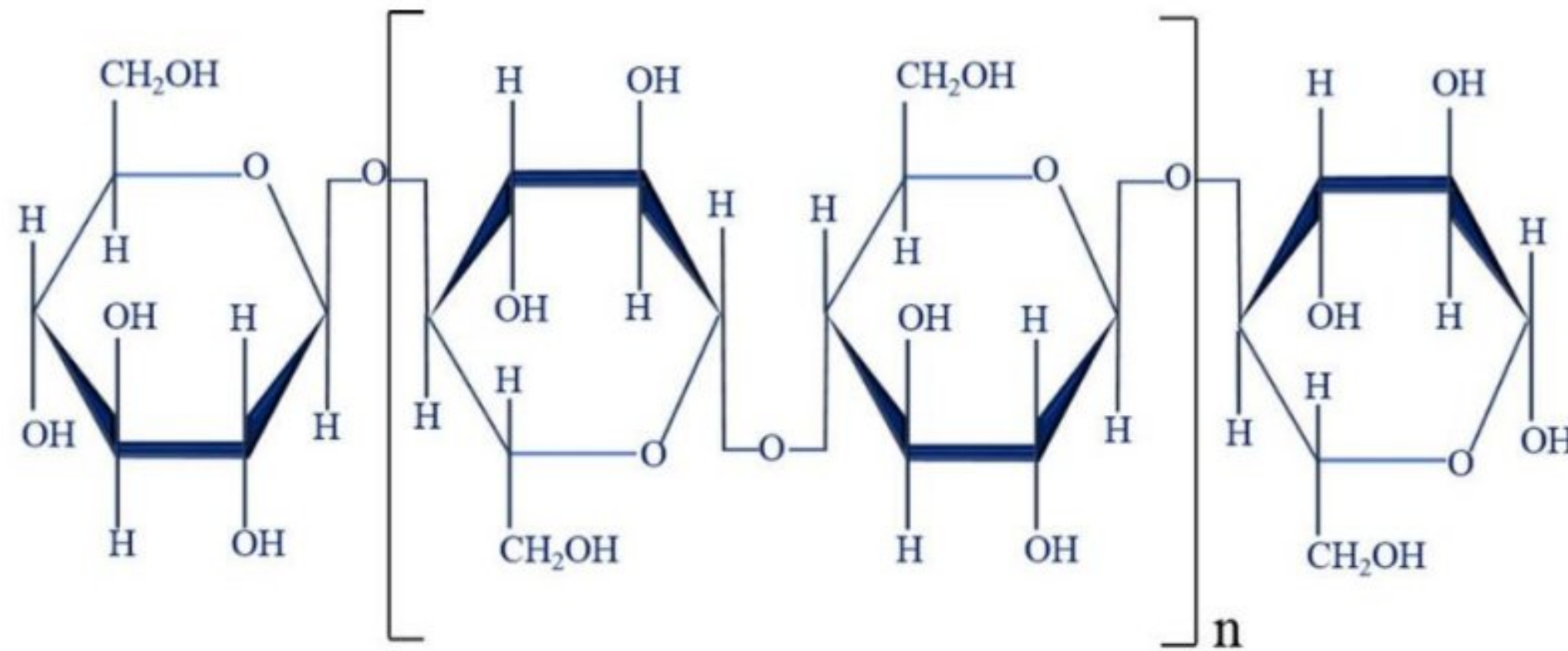
Fig.2. 44. Cellulose molecule[78].
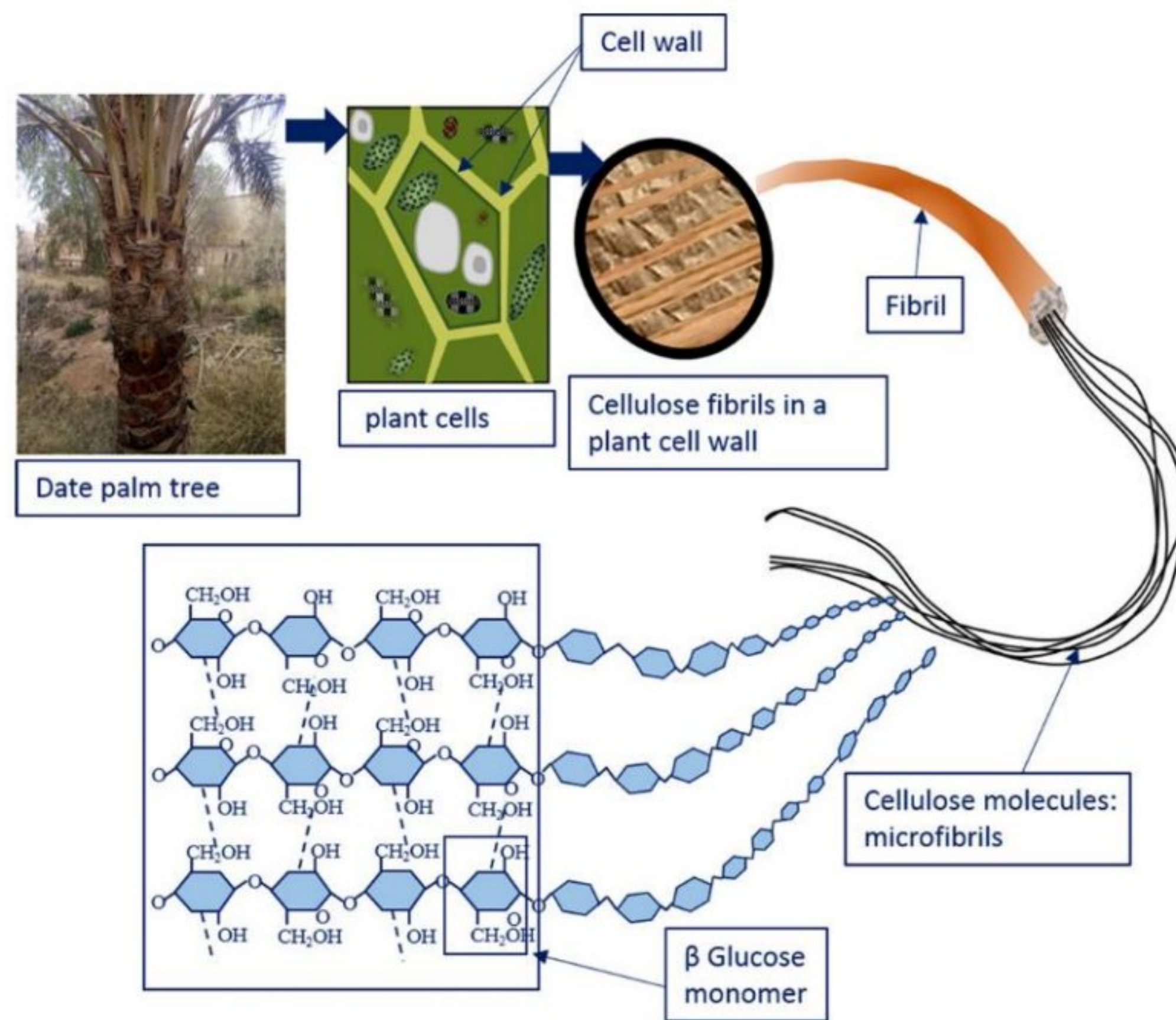
Fig.2. 45. Organization of cellulose components in the cell wall of a typical plant fiber[78].

According to Almi et al[92]. there is no significant difference between the samples on the contents of cellulose, hemicellulose, and lignin. Nevertheless, it can be noted that lignin content in Rachis is relatively high compared to the lignin contents in the other samples. This may be related to the climate conditions and to the soil chemical composition in which the plants are growing. Furthermore, the high content of cellulose brute in Fibrillium and Pedicels indicates that these

varieties are more resistant in acid and alkaline environment which makes them more suitable to reinforce alkaline matrix.

Compared to the chemical composition contents of natural fibers (Fig. 2.46), date palm wood contains lower amount of cellulose. Nevertheless, the cellulose content in Leaflets, Bunch, Rachis, Spathe, and Fibrillium is close to that of coconut and bamboo, and it belongs to the range of 38–45% which is compatible to the reported cellulose content of softwoods (40–52%) and hardwoods (38–56%). Cellulose contents in this range make these parts of palm tree a suitable raw material for the paper and pulp industry. It can be noted also from Fig. 2.46, that date palm wood is rich in lignin and it is close to lignin content of coconut. Like in coconut wood, the higher lignin content makes palm wood very tough and stiffer compared to the other natural fibers and contributes to its flexibility and its hydrolysis rate. The structural rigidity of the palm wood makes it a valuable building material[92].
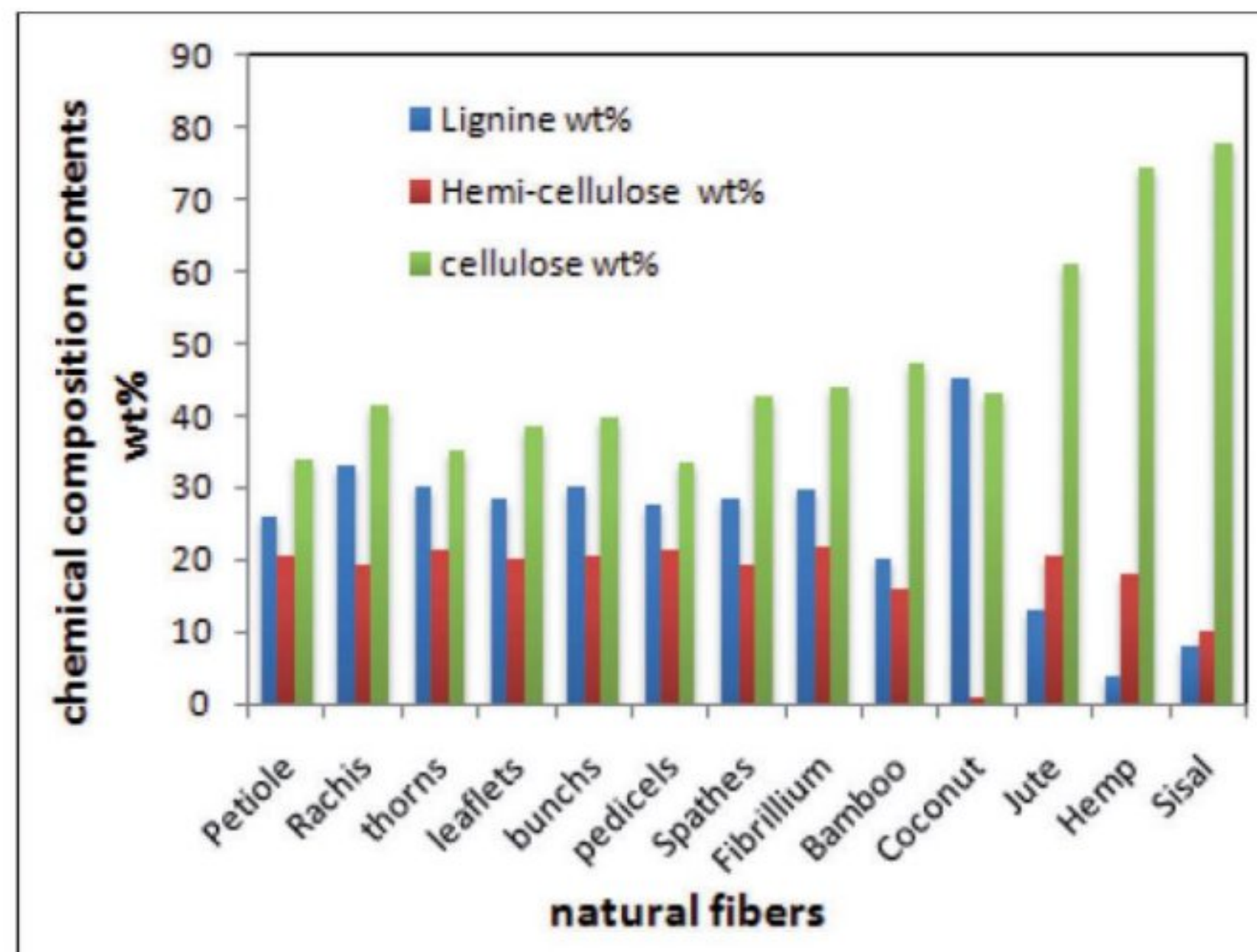
Fig.2. 46. Chemical composition of date palm wood compared to other natural fibers[92].

✦ **Hemicellulose**

Carbohydrate monomers are assembled in various quantities into relatively short and generally branching polymers to form hemicelluloses in the woody tissue of trees. Wood is generally composed of 25–35% hemicelluloses by dry weight. Because hemicelluloses have a more open structure than cellulose, they are more hygroscopic (i.e., they attract water molecules more readily)

and are considerably more soluble. Their structure also makes them more heat-labile, that is, more prone to thermal degradation, as compared to cellulose. Hemicelluloses are soluble in dilute alkali (e.g., 1% sodium hydroxide) and are also hydrolyzed by weak acids. Some may even be solubilized by hot water[96]. A fourth form of sugar polymers found in biomass is hemicellulose. Hemicellulose consists of short, highly branched chains of sugars (Fig.2. 47). It contains five-carbon sugars (usually D-xylose and L-arabinose), six-carbon sugars (D-galactose, D-glucose and D-mannose) and uronic acid[94].
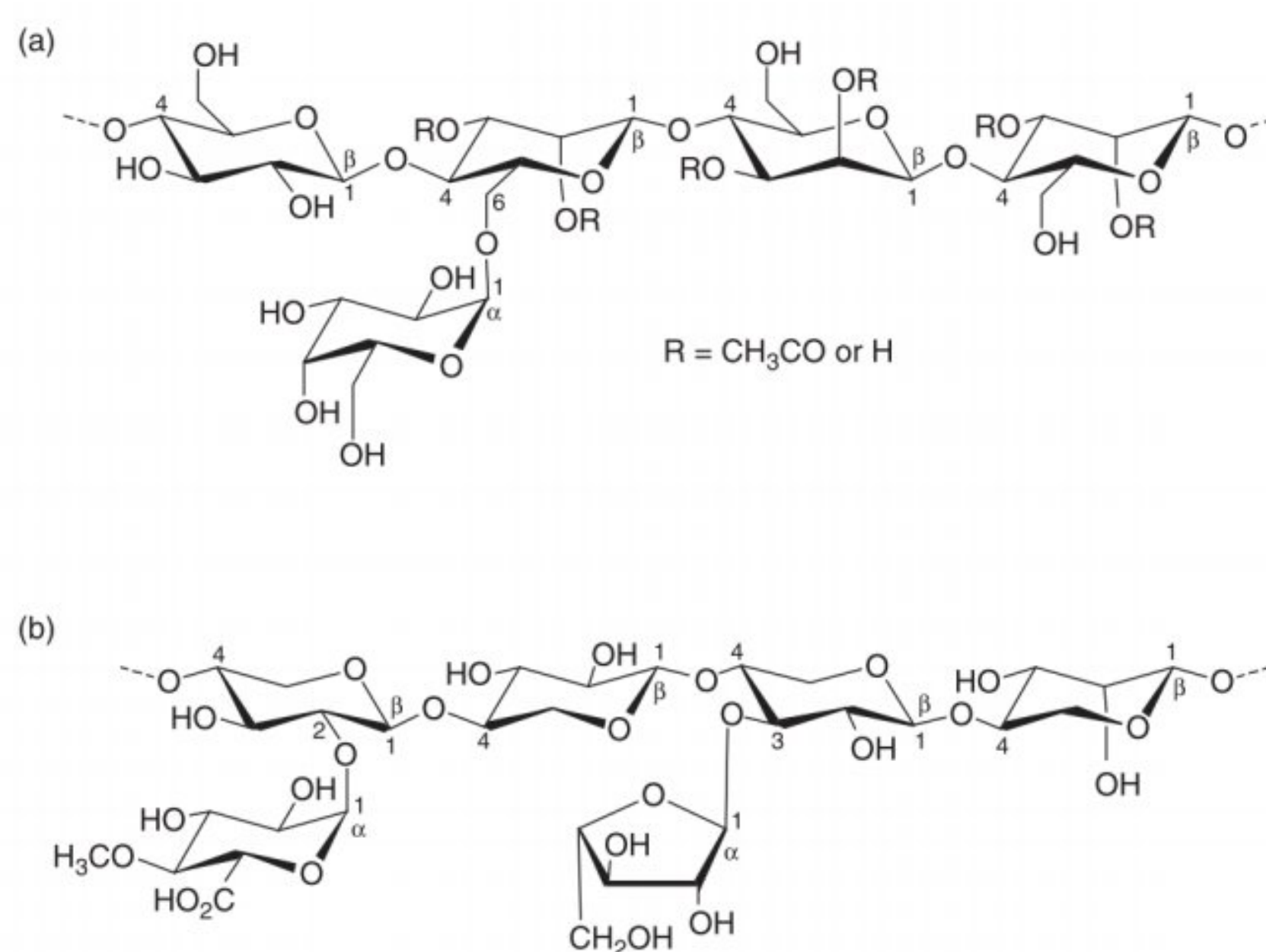
Fig.2. 47. Structures of major hemicelluloses found in the wood[96].

🞦 Lignin

Lignin is the second most common renewable organic material on earth after cellulose. Lignin is an extremely heterogeneous macromolecule that represents about 30% of the organic carbon in the biosphere. Unlike other carbohydrate-containing cellulose and hemicellulose, lignin is totally amorphous and has a role in structural stiffness, which helps protect cell walls from harmful organisms.[78], [97]. Lignin is formed by the removal of water from sugar to create aromatic structures. Lignin has an aromatic structure represented by three precursors: p-coumaryl, sinapyl, and coniferyl alcohol (see Fig. 2.48) [96]. The amount of lignin in a vegetable fiber can range from 2% to 45%[93].
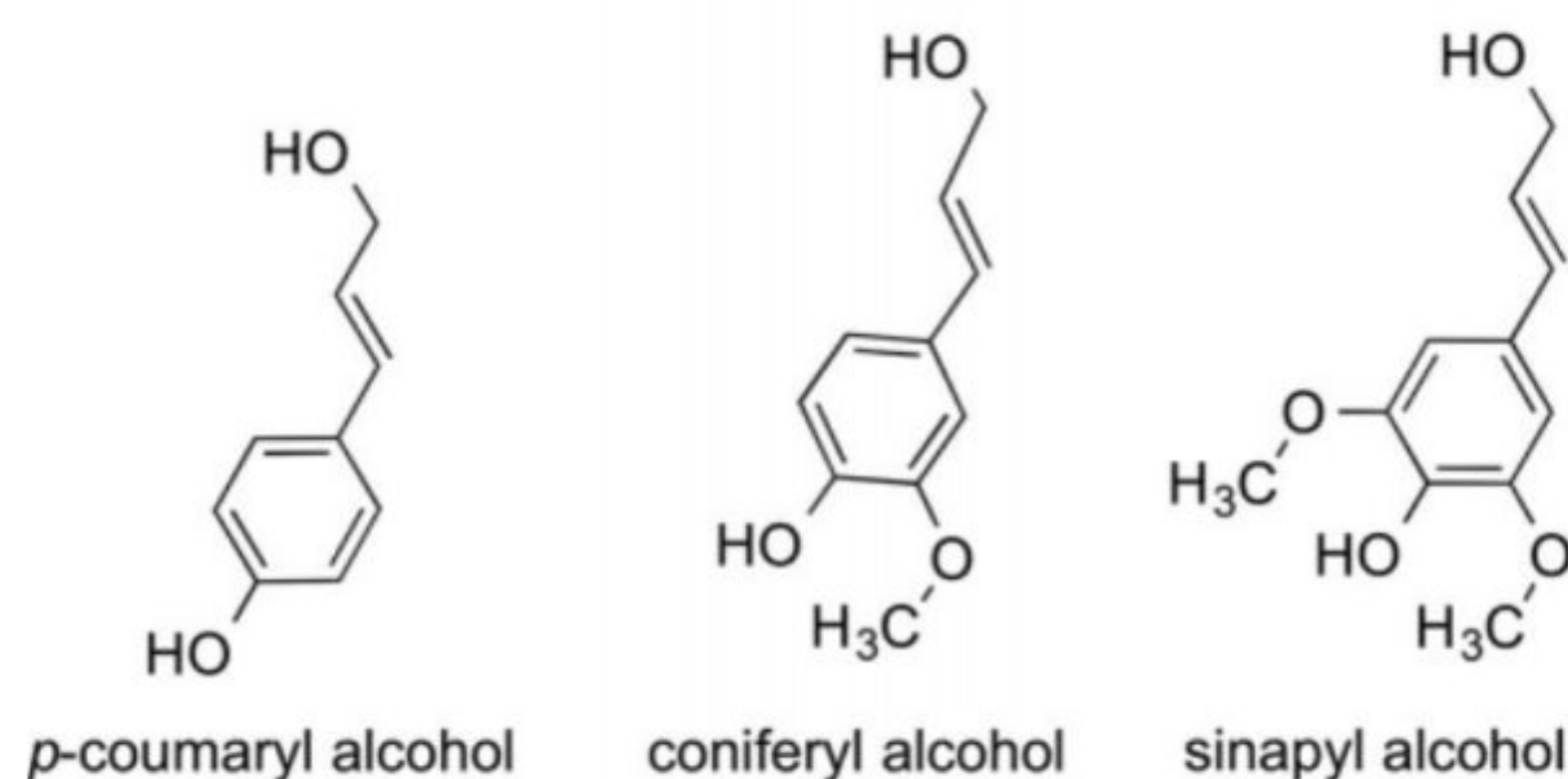
Fig.2. 48. Lignin precursors or monolignols[96].

2.6.2.2 Physical properties

Date palm fiber (DPF) average density was determined by several researchers and it was noticed to range between 0.199 and 1.98 (g/cm3), mainly lower than many other natural fibres such as hemp, sisal and coir, this may give an added value in the development of composite materials. This value may be important in developing light weight composite structures that may be suitable for space and automotive applications[90]. Rachis and Bunch wood are considered as light wood 500–650 kg/m3. While Petiole, Fibrillium, Spathe, Leaflets, Pedicels, and Thorns wood are classified as very light wood (<500 kg/m3), which makes them soft and easy to handle. Concerning the rate of water absorbed after 24 h by mass, the results show that Petiole, Spathe, and Fibrillium have relatively high values compared to other parts. Petiole's rate reached 140%, is lower than mean rate of absorption of sisal 230%, and higher than that of coconut, which was 100%. The mean rate of absorption of Rachis, Thorns, Pedicels, Bunch, Leaflets was lower than that of coconut, and this could have a beneficial effect on the chemical treatment consumption to reduce the moisture absorption of the fibers especially of the Rachis 36.88%. Results of thermal analysis show that Leaflets variety provides the highest resistance to thermal degradation; its main degradation occurred at 360 °C.[92].

2.6.2.3 Mechanical properties

Generally, date palm fiber mechanical properties such as tensile strength, tensile strain and Young's modulus usually increase as cellulose content and cell length increases. The mechanical properties of the eight date palm tree residues ranged slightly, according to the findings. Rachis has the highest tensile strength and Young's modulus, which may be attributable to its chemical and

physical features (relatively high cellulose content and lower porosity rate) [92]. Almi et al. [92] have concluded from the experimental study that the results show that Rachis variety exhibits relatively high values of tensile strength and Young's modulus; they attained 213 MPa and 8.5 GPa, respectively. In contrast, Petiole variety exhibits relatively high values of specific mechanical properties. This is due to its low value of bulk density, which is 0.160 g/cm3. Fig.2.49 shows that Young's modulus values of date palm fibers are close to that of coconut fibers and are considerably lower than those of most vegetable fibers. This can be explained by the physical structure of the natural fibers such as the crystal structure, the degree of crystallinity, the degree of polymerization, the porosity content, and the size of the lumen in addition to the chemical composition[92].
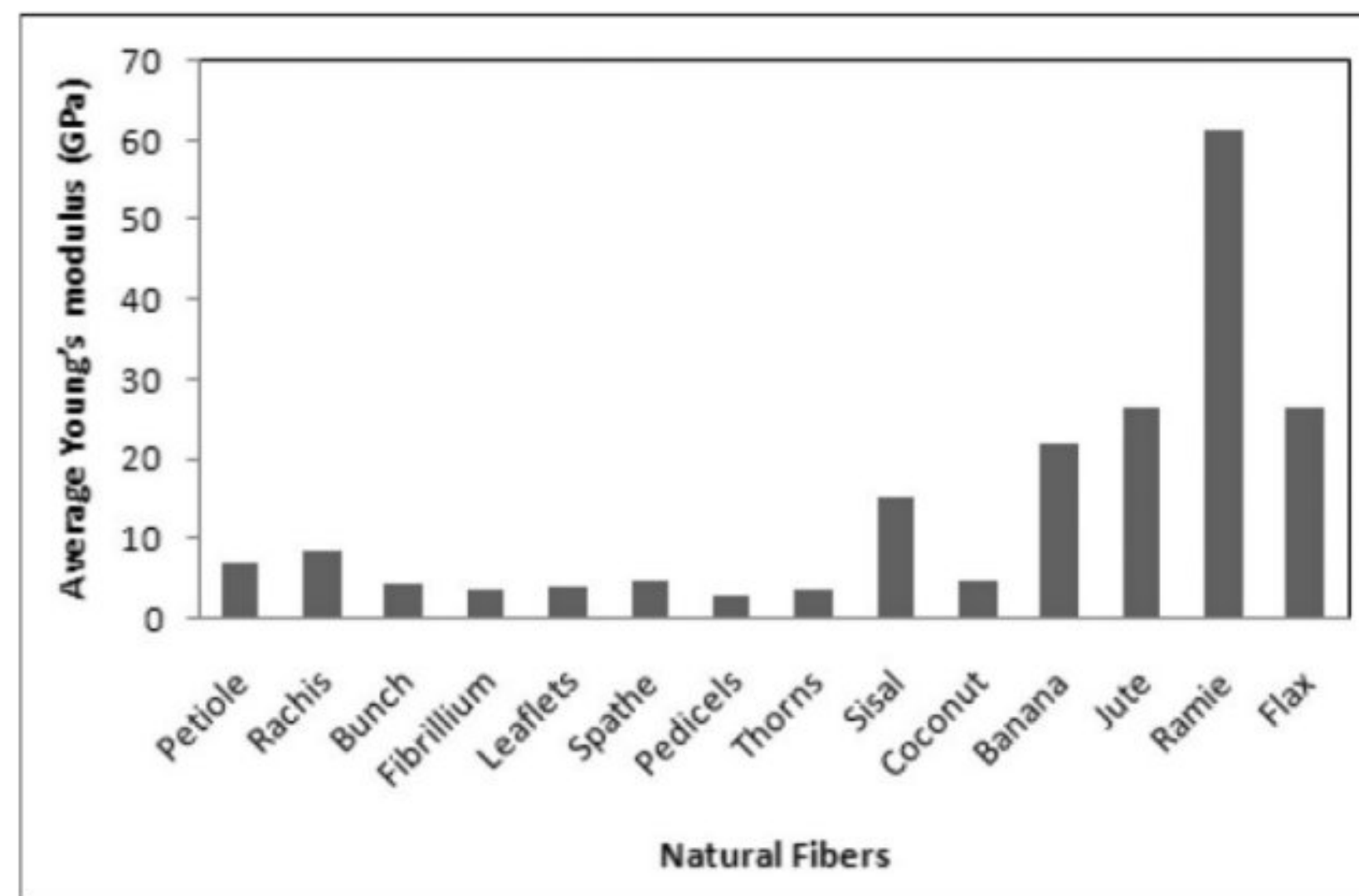
Fig.2. 49. Average Young's modulus of date palm fibers compared to other natural fibers[92].

2.6.2.4 Thermal conductivity

Other essential criterion in the building materials sector, particularly in the interior design of structures, are excellent thermal and acoustic insulation capabilities. This requires materials used in the buildings to have low thermal conductivity. Results had shown that date palm fiber has a thermal conductivity coefficient of 0.083 (W/m K)[98], which is lower than that of hemp (0.115 W/m K) and very near to that of sisal (0.07 W/m K). However, results show that coir has the lowest thermal conductivity coefficient with (0.047 W/m K). Fig. 2.50 summarizes these results. When considering its appropriate thermal properties as well as its lower density, date palm fiber can be a possible choice for building materials applications[93].
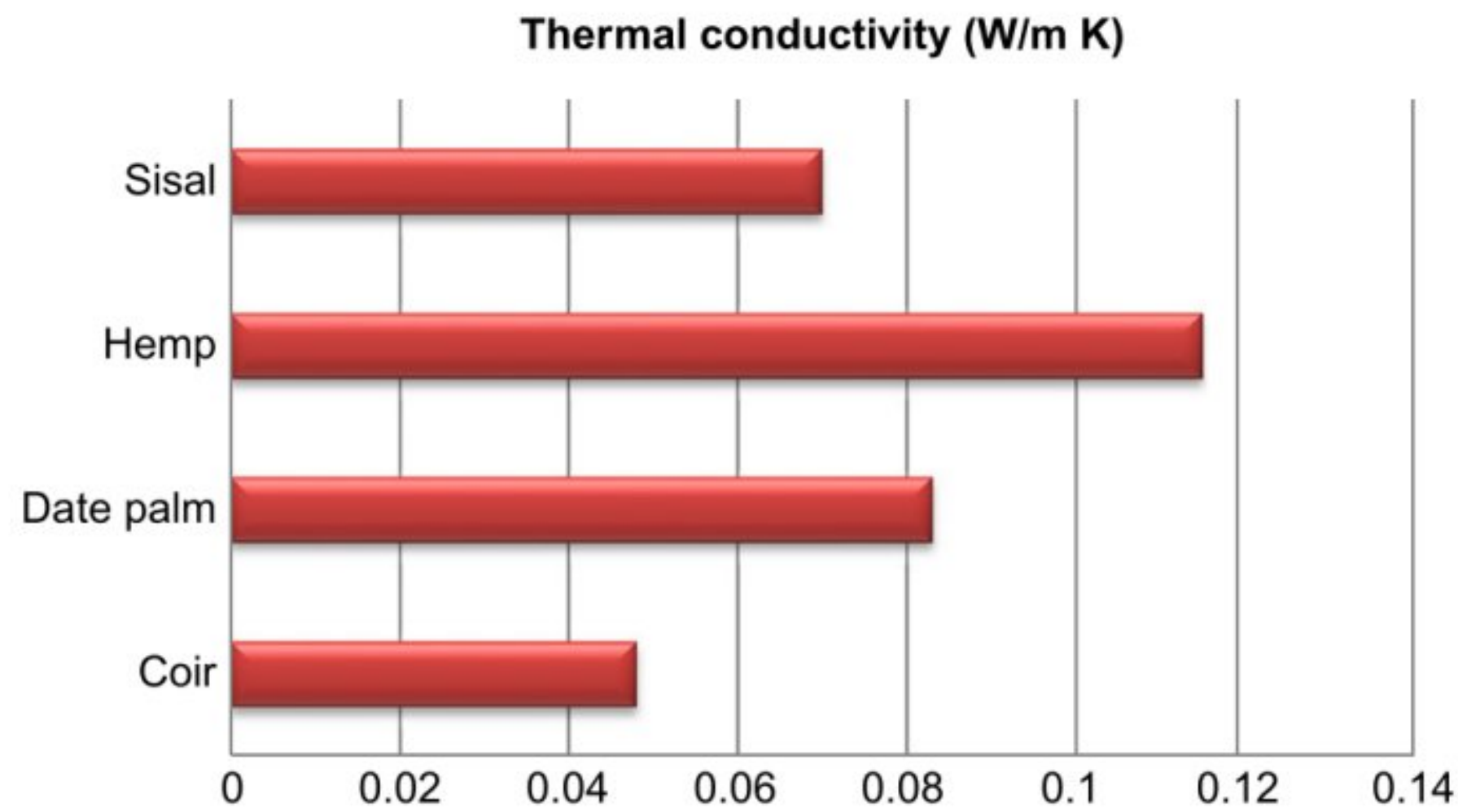
Fig.2. 50. Date palm's thermal conductivity with respect to other natural fiber types[93].

2.6.3 Properties of Compressed Earth Blocks (CEBs) materials modified with plant aggregates or fibers

2.6.3.1 Effects of plant aggregates and fibers on the mechanical properties of compressed earth blocks

2.6.3.1.1 Compressive strength

In recent decades, several research programs have been performed to investigate the effect of using plant fibers, such as sisal, kenaf, banana and date palm fibers on mechanical properties of CEB [18], [19], [49], [99]. Mostafa and Uddin[49] investigated the effect of the use of banana fibers. They concentrated on the effect of fibers' length on the compressive and bending strength of CEB. Laibi et al. [99] evaluated the effect of the length of kenaf fibers on the mechanical properties and thermal conductivity of CEB. Taallah et al. [18], and Taallah and Guettala [19] presented an experimental investigation to study the effects of the use of male date palm surface fibers on the mechanical strength and physical properties of CEB. Other researchers studied the effect of the use of plant aggregate on the properties of earth bricks, including corn cob, barley straw and hemp shiv [100], [101]. For example, Laborel-Préneron et al. [101] investigated the effect of the use of hemp shiv, corn cob and barley straw on the mechanical characteristics of earth bricks. Laborel-Préneron et al. [100] also carried out an investigation to study the effect of hemp shiv, corn cob and barley straw addition on the hygrothermal properties of earth bricks. According to many researchers [19], [101], [102], the compressive strength of earth blocks materials is negatively affected by the

incorporation of raw plant fibers. However, others found an increase in the compressive strength of banana fibers with length varying from 50 mm to 60 mm [49], of kenaf fibers with length varying from 10 mm to 20 mm [99], and of date palm fibers with 8% cement, and a compaction pressure of 10 MPa and 0.05% of fibers [18].
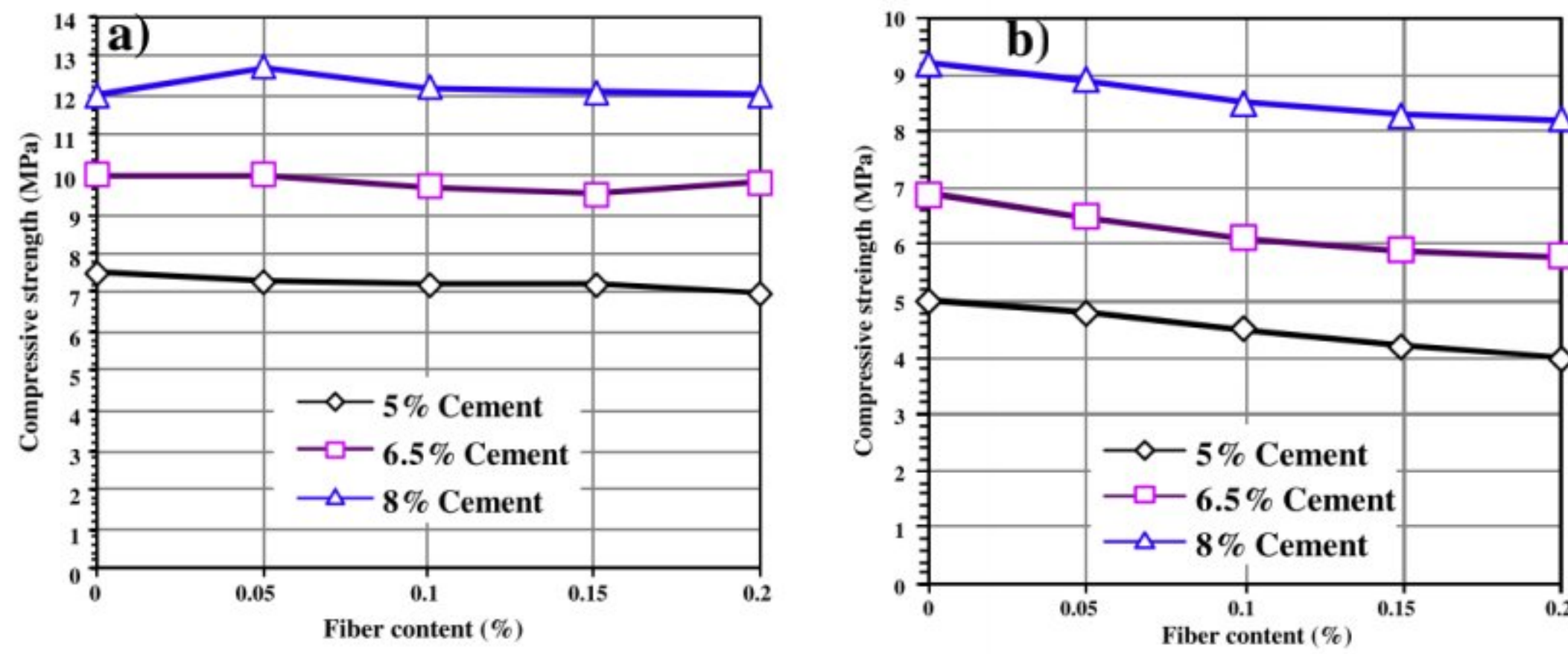
Fig.2. 51. a) Dry compressive strength of CEB as a function of fiber content; b) Fig. 6. Wet compressive strength of CEB as a function of fiber content[18].
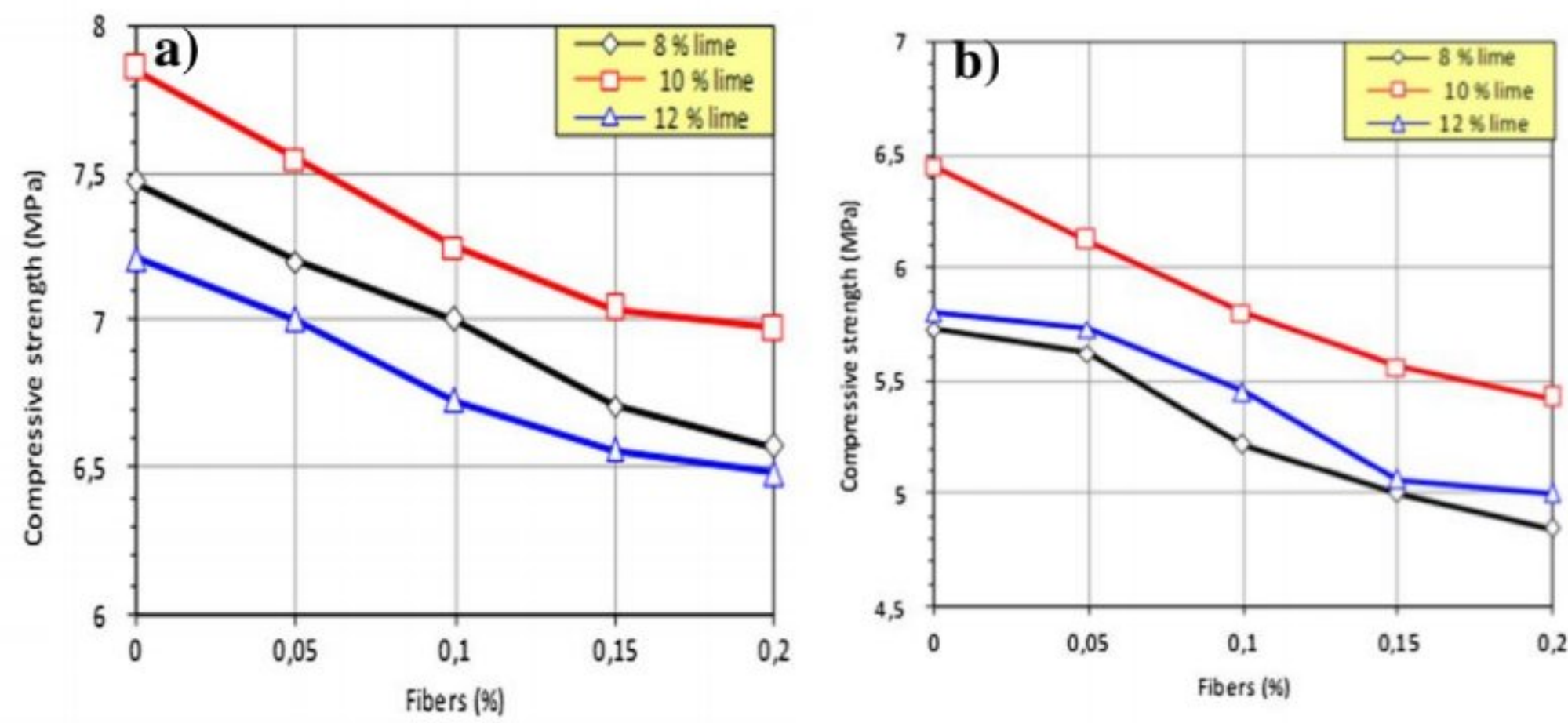
Fig.2. 52. a)dry compressive strength of CEB after 28 .b)wet compressive strength of CEB after 28 days[19].
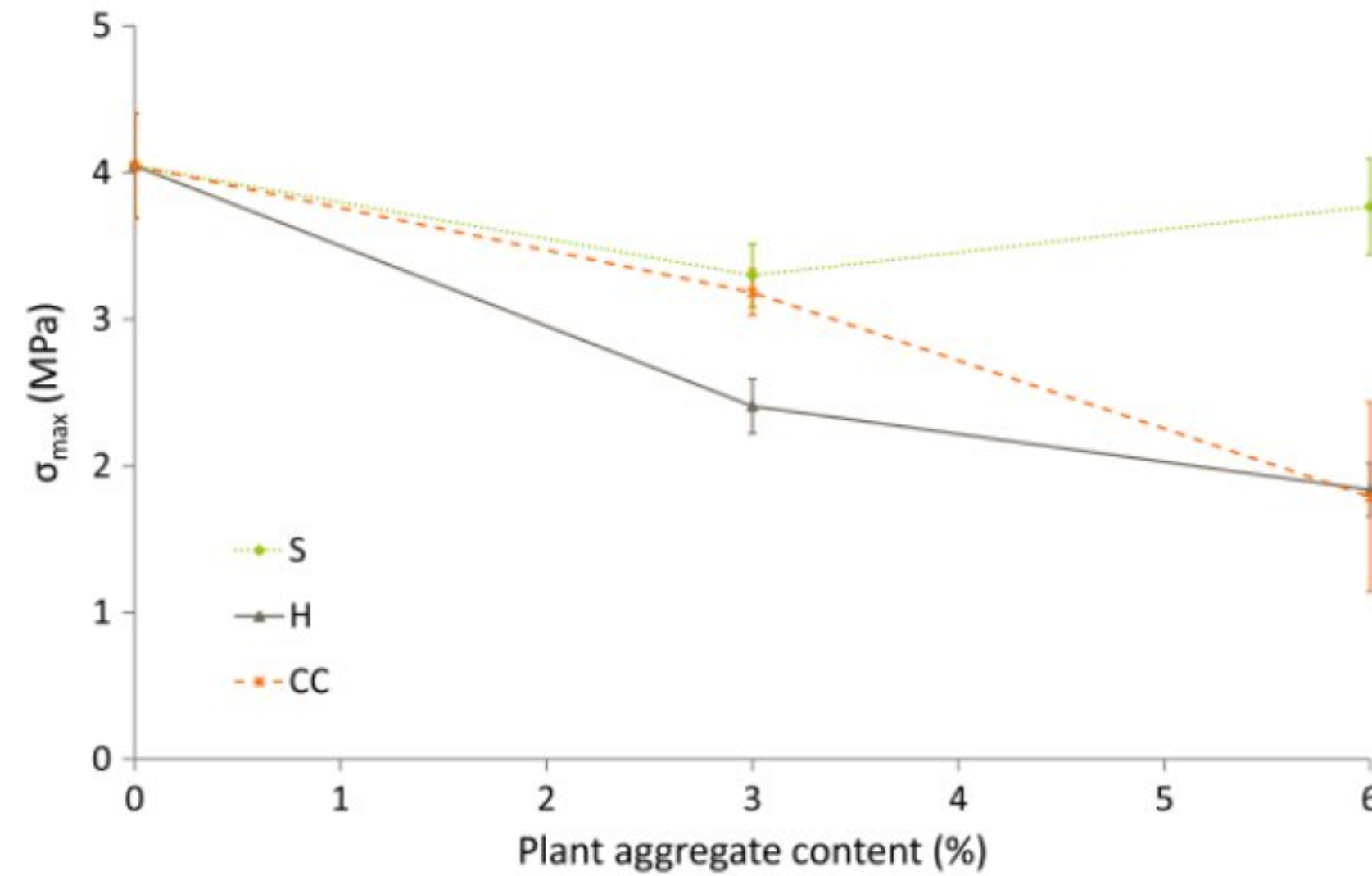
Fig.2. 53. Results for compressive strength test[101].

2.6.3.1.2 Tensile and flexural strength

The addition of natural fibers is used in the manufacture of products of earth in order to reduce shrinkage cracking and improve the tensile and flexural strength. The addition of fibers to mixtures of CEB caused a decrease in tensile strength with the increase of the fibers content, and the lowest value is found for 0.2% fibers content for all cement content used in the study of Taallah et al. [18]. For this work, the decrease in tensile strength compared to CEB without fibers is 23.5%, 18.5% and 14% for 5%, 6.5% and 8% cement content, respectively[18].

Some authors have focused on the bending strength of earth blocks. An increase in bending strength was observed in these studies with an addition of plant waste, for example, Bouhicha et al. [46] with barley straw fibers and Mostafa and Uddin [49] with banana fibers with length varying from 50 mm to 70 mm. Taallah and Guettala[19] mentioned that in the case of 0.05% fiber content and 8% and 12% lime content, there are slight increase in tensile strength. However, a general slight decrease in tensile strength with increasing the fibers content.
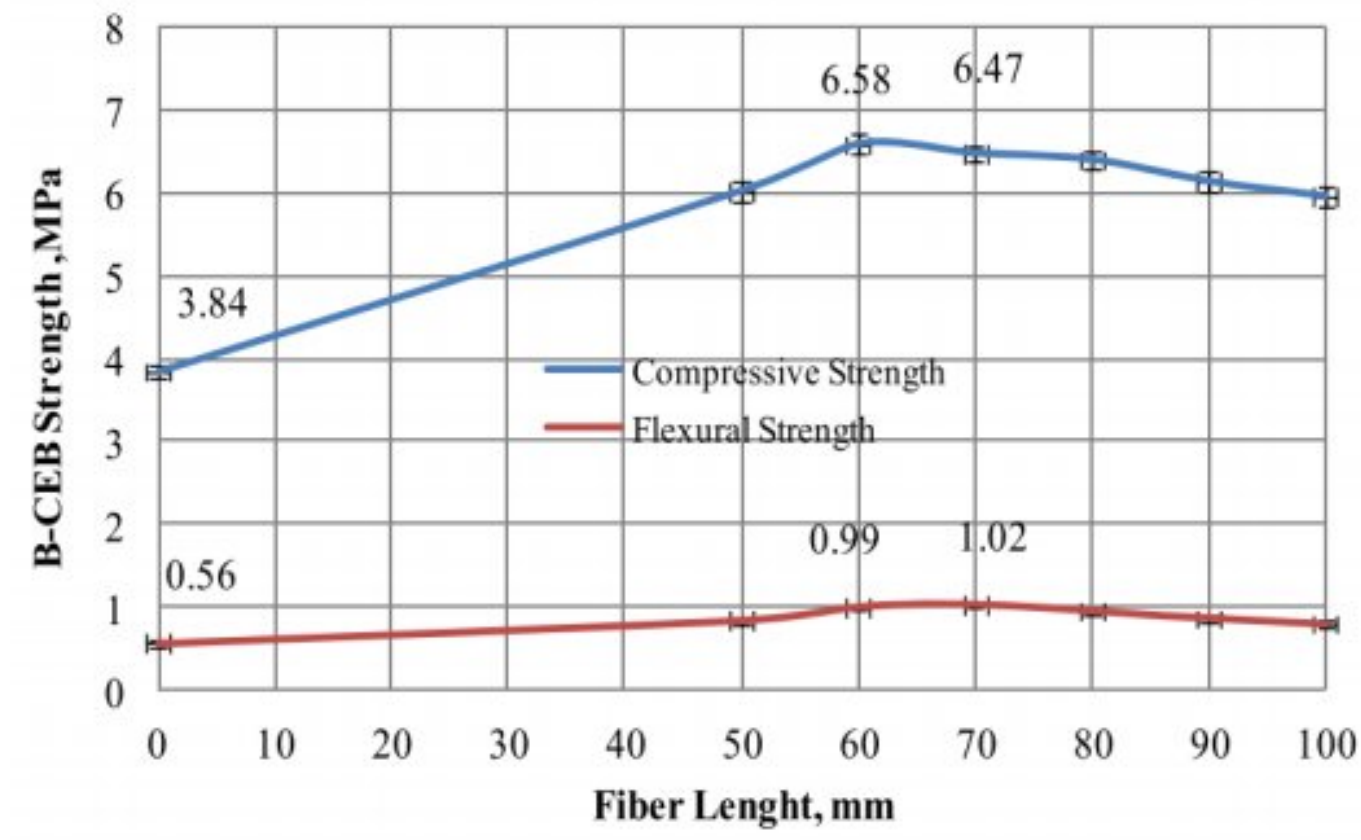
Fig.2. 54. Compressive and Flexural Strength of B-CEB[49].
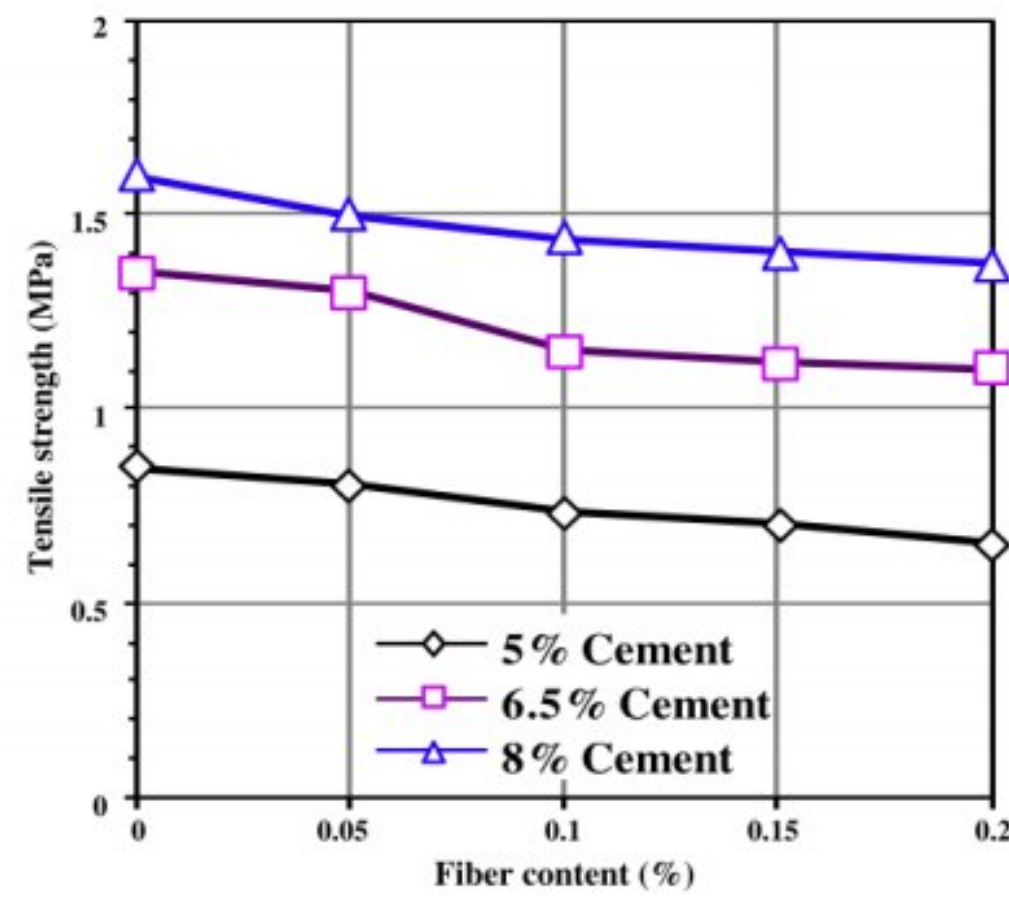
Fig.2. 55. Dry tensile strength of CEB as a function of fiber content [18].
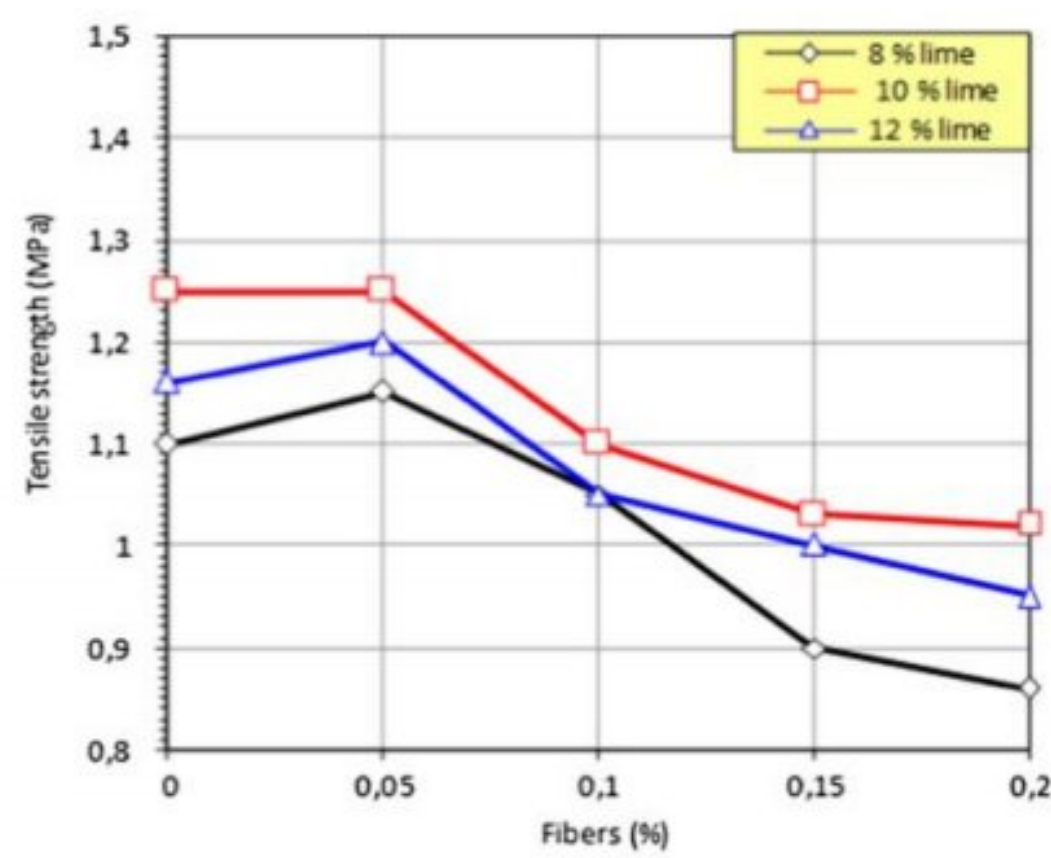
Fig.2. 56. Dry tensile strength of CEB after 28 days [19].

2.6.3.1.3 Mechanical behavior

In order to evaluate the effect of the plant fiber or bio-aggregates on mechanical behavior and ductility of materials, stress–strain or load–deflection curves were studied. Studies carried out on compressed earth blocks based on plant fibers show a modification of the mechanical behavior of the composite. According to Laborel-Préneron et al.[101], the reference specimens (FWAS) show brittle failure, whereas the ultimate strain is high for the specimens containing plant aggregates, especially those with 6% (Fig.2.57). Although these specimens are weaker than FWAS specimens, they are also more ductile, with a larger zone of plasticity. Ductility of the composite is thus increased by the addition of plant aggregates. The load-deflection curves illustrate that the addition of plant aggregates increases the ductility, giving some residual strength and increasing the deflection at failure of bricks (see Fig.2.58)[101].
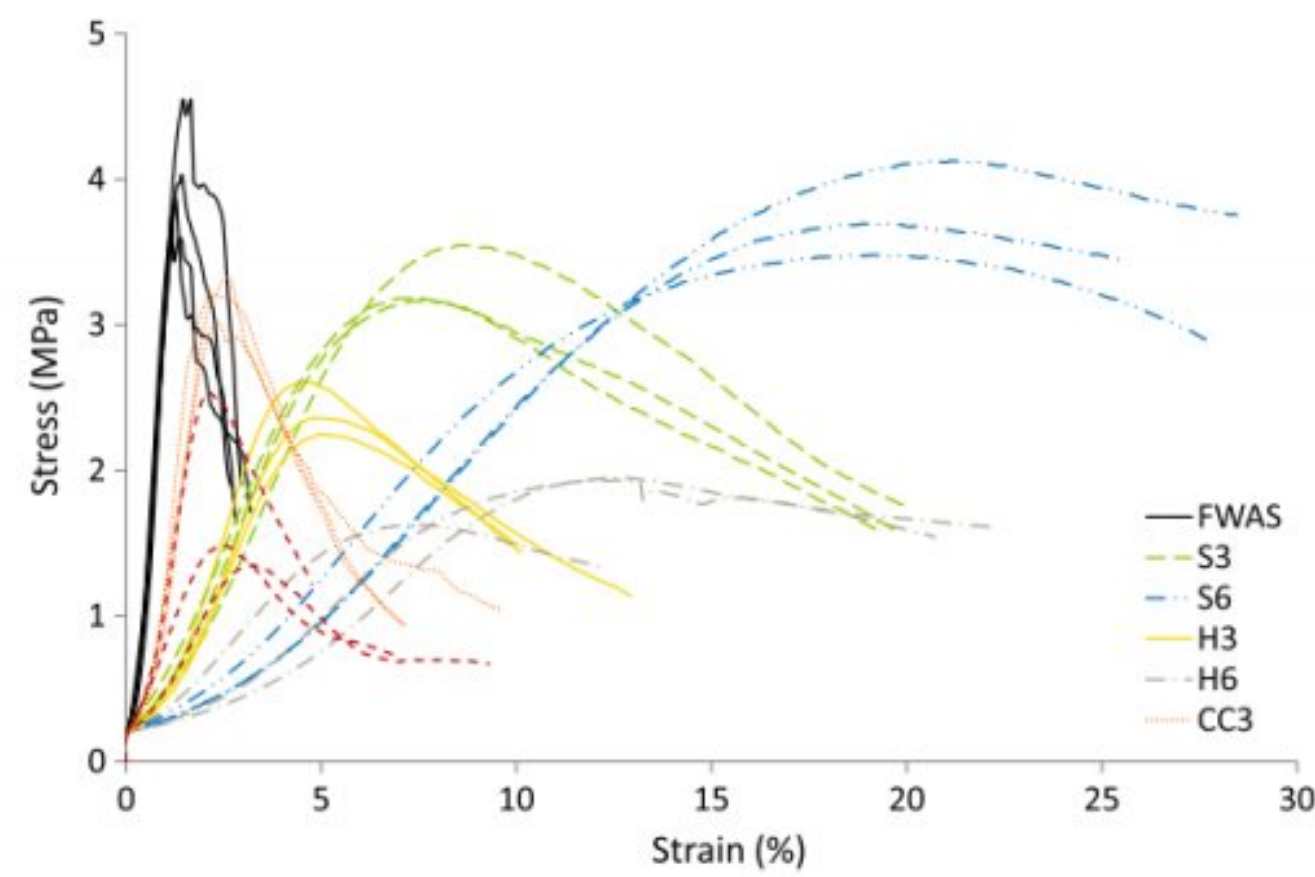
Fig.2. 57. Strain–stress diagram for all the specimens[101].
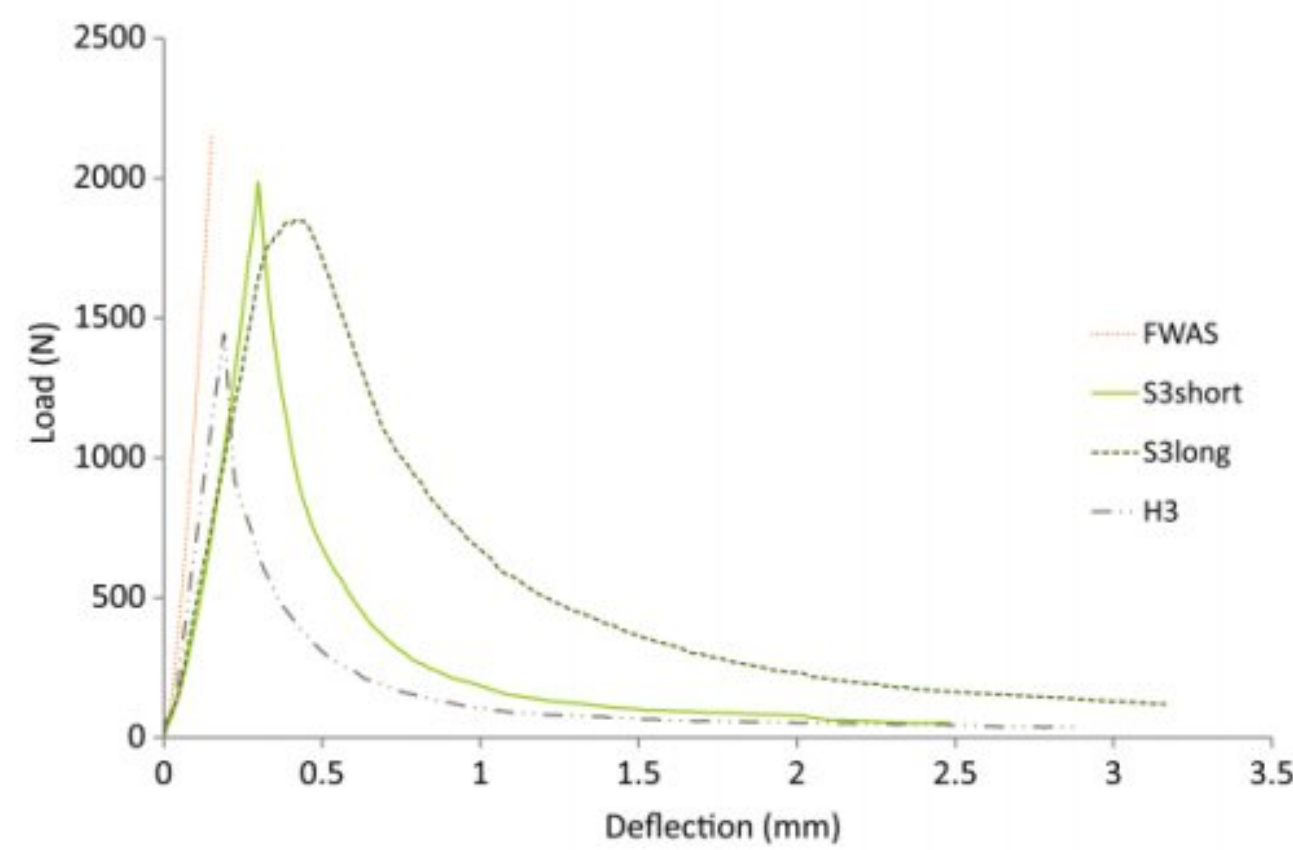
Fig.2. 58. Typical load-deflection curves[101].

Mesbah et al. [103] developed a direct tensile behavior test for compacted earth blocks reinforced with natural sisal fibers. Mesbah et al. [103] reported that the advantages of using natural fibers as reinforcement in a compacted earth block include both an improvement in tensile ductility compared to a block without reinforcement and prevention of the propagation of tensile cracks after their initial formation. According to the authors, before cracking, the fibers have not significantly modified block behavior[103].
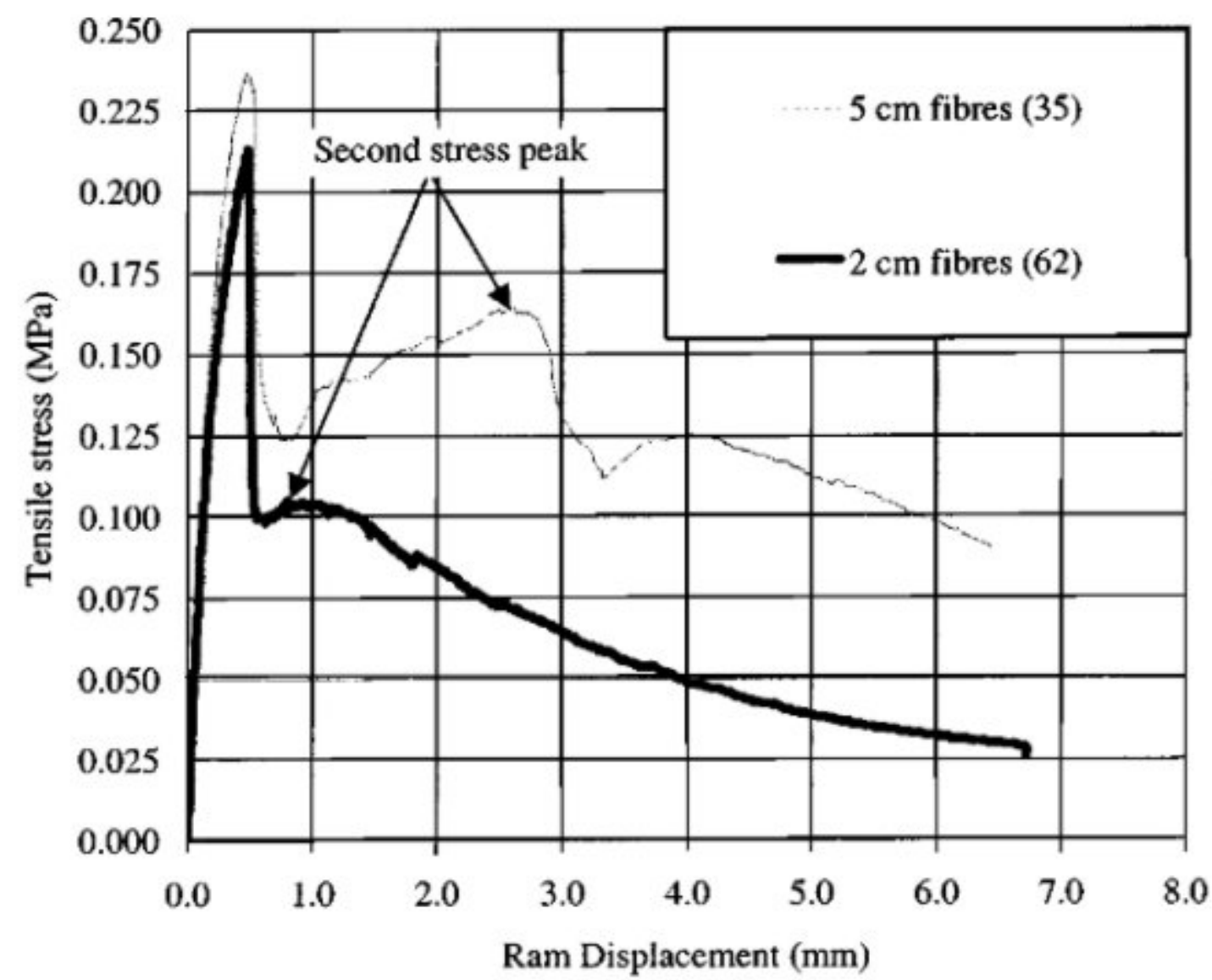
Fig.2. 59. Tensile behavior of fiber-reinforced blocks Tests[103].

Laibi et al.[99] reported that the unreinforced material A0 is characterized by an elastic linear behavior up to catastrophic failure (domain I). In the case of formulation A3 (1.2% fiber content and 30 mm fiber length), two additional domains can be distinguished. First, the domain of elastic linear behavior is followed by domain II in which occurs a more or less pronounced decrease of the stress (this first damage is identified as matrix cracking), then stress recovery extends up to the maximum value. Beyond this level occurs stable crack propagation in domain III.
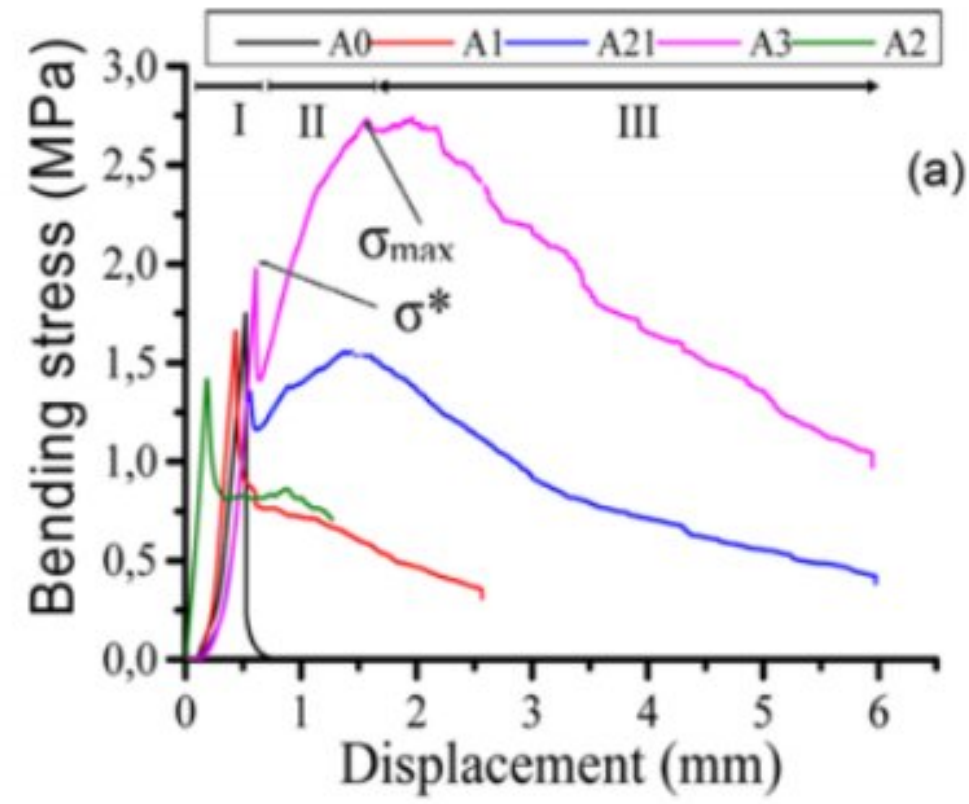
Fig.2. 60. Bending stress-displacement curves of CEB based on Kenaf fibers [99].

2.6.3.1.4 Modulus of elasticity

The modulus of elasticity is one of the most important mechanical properties. The elastic modulus is measured by mechanical destructive experiments such as compressive, tensile and bending tests. The modulus of elasticity (Young's modulus) is calculated to define the material mechanically. Young's modulus is used in simulating complex structures using numerical methods such as the finite elements method. There are many studied on the influence of the plant fiber or bio-aggregates on the modulus of elasticity of compressed earth blocks. In this context, Laborel-Préneron et al.[101] evaluated the effect of plant aggregates on the modulus of elasticity of unfired earth bricks. This study showed that the modulus of elasticity from the compressive and flexural test decreases when the percentage of plant aggregates (wood aggregates) in the earth material increases[101].
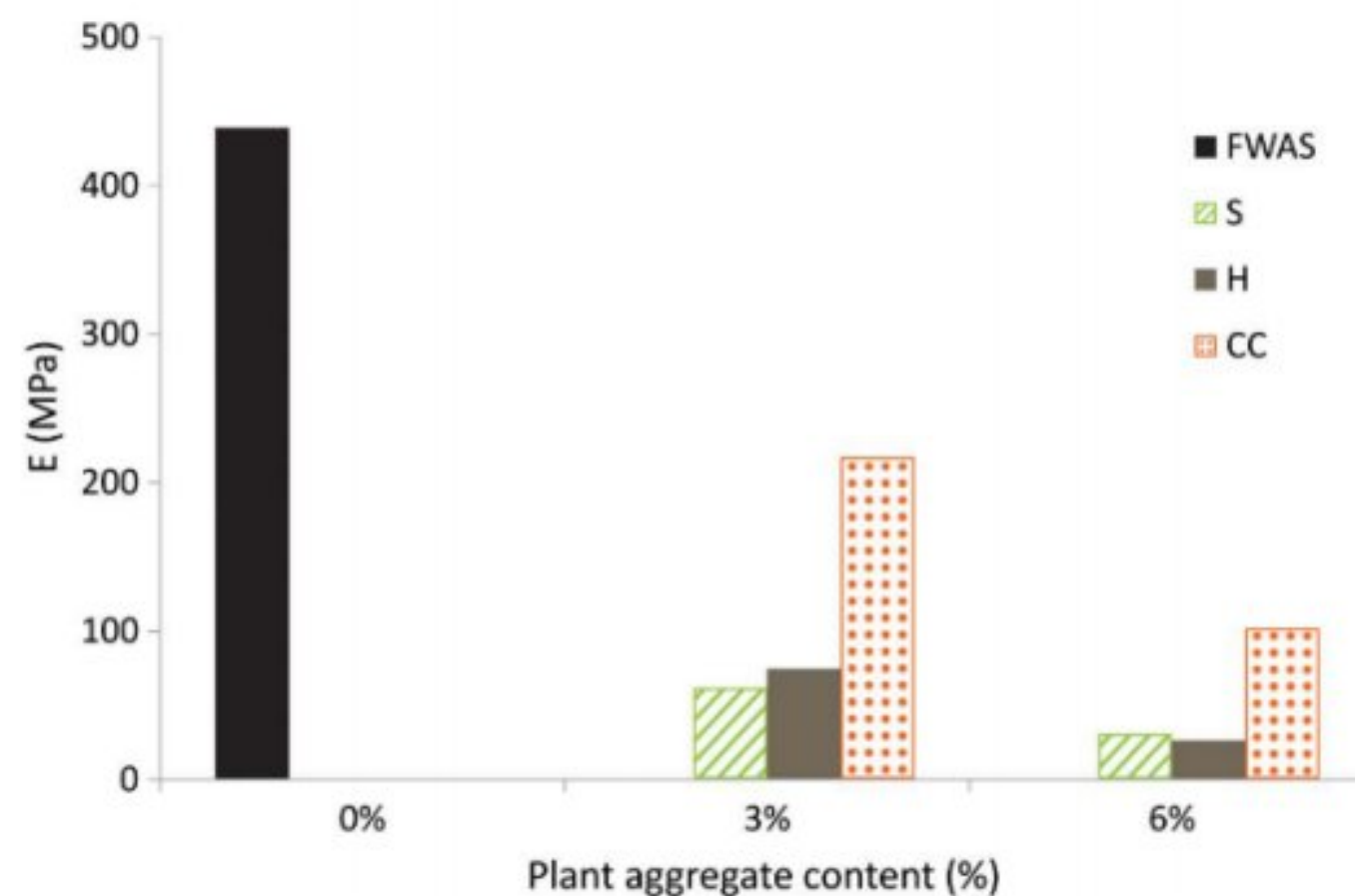
Fig.2. 61. Young's modulus from compressive test as a function of the plant aggregate content[101].

2.6.3.2 Effect of plant fiber and bio-aggregate content on physical and hygroscopic properties of CEB

2.6.3.2.1 Bulk density

Several authors mentioned that the bulk density decreases due to the incorporation of plant fibers or plant aggregate into the mixture of blocks [19], [101], [104]. Bouchefra et al.[105] mentioned that the inclusion of raw and treated doum fiber from 0 to 2% has caused a decrease of density by 15.2% and 16.6% respectively.
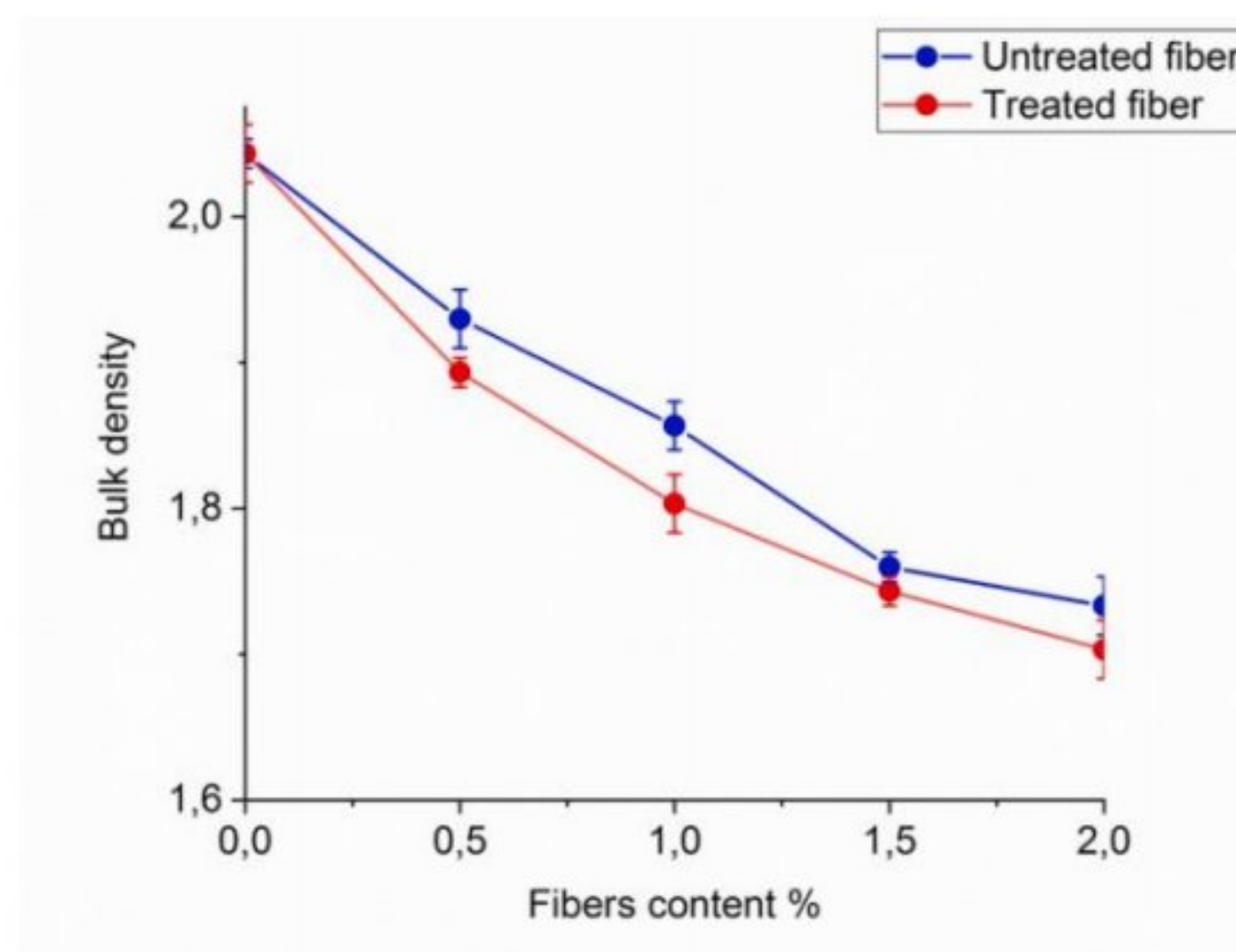
Fig.2. 62. Effect of raw and treated fibers content on bulk density of stabilized CEB by 9% of lime[105].

Laborel-Préneron et al.[101] mentioned that the bulk density decreased as the aggregate content increased for the three kinds of plant aggregates. In addition, the bulk density was higher for the mixtures with corn cob than for those with straw or hemp. This difference may have been because of the huge variability of the particle bulk densities: 497 kg m^{-3} for corn cob against 57 and 153 kg m^{-3} for straw and hemp shiv, respectively[101], [106].
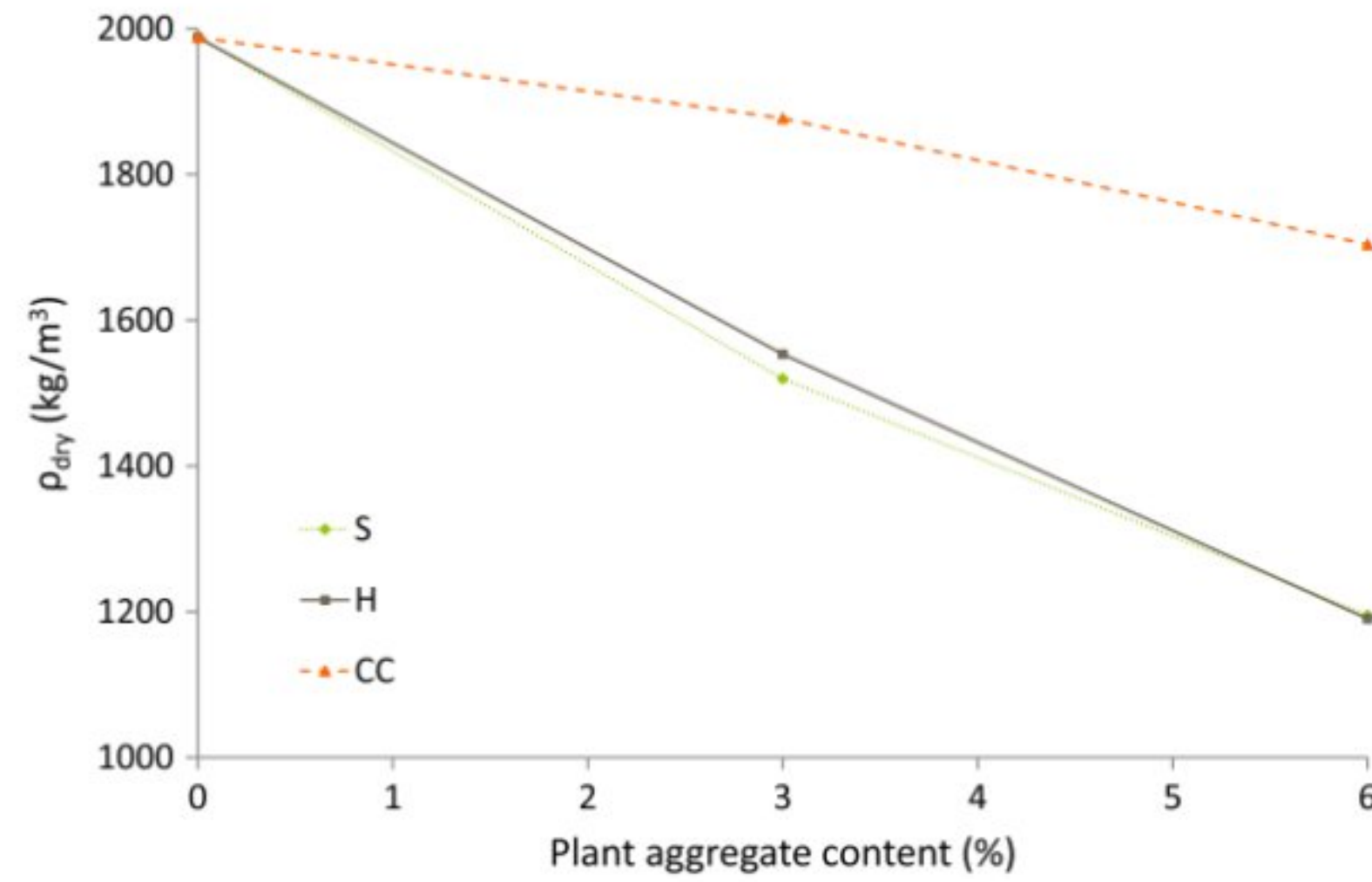
Fig.2. 63. Bulk density as a function of the plant aggregate content[101].

2.6.3.2.2 Total water absorption, capillary absorption and swelling

The hygroscopic properties of earth materials are a very important indicator of the durability and quality of this type of material. It is well known that wood has a high water-absorbent capacity. However, the addition of plant fibers in building materials negatively affects the hygroscopic properties of these materials, and this hypothesis has been experimentally proven. According to several researchers[18], [19], [105], swelling and water absorption in CEB blocks increase with the increase in natural fiber content.
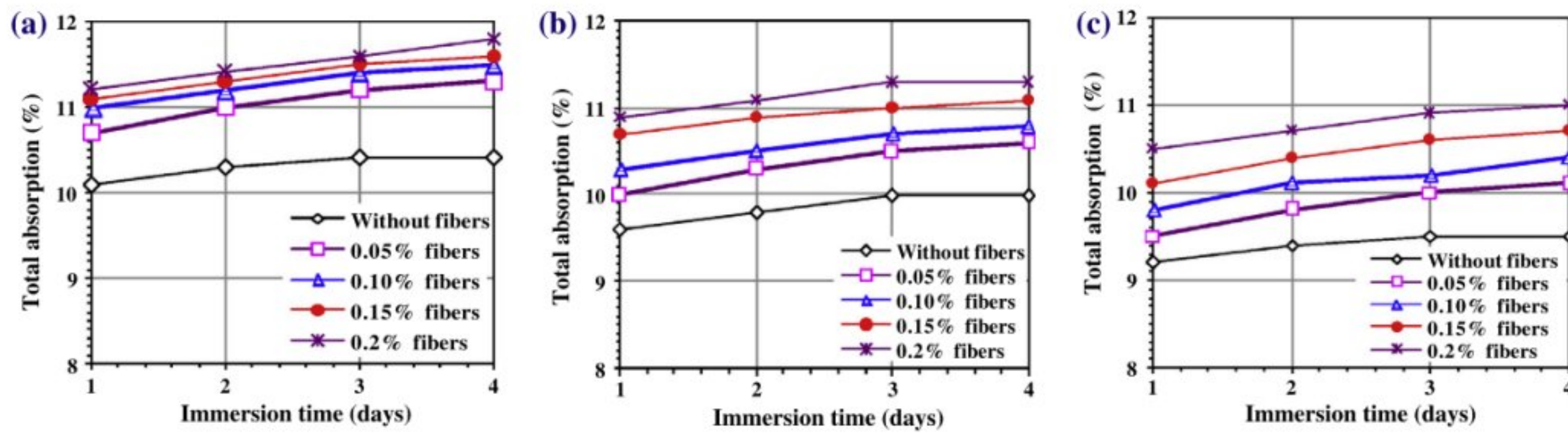
Fig.2. 64. Effect of fibers content on the total absorption in time of CEB (with 10 MPa of compaction pressure): (a) 5% cement; (b) 6.5% cement; (c) 8% cement[18].
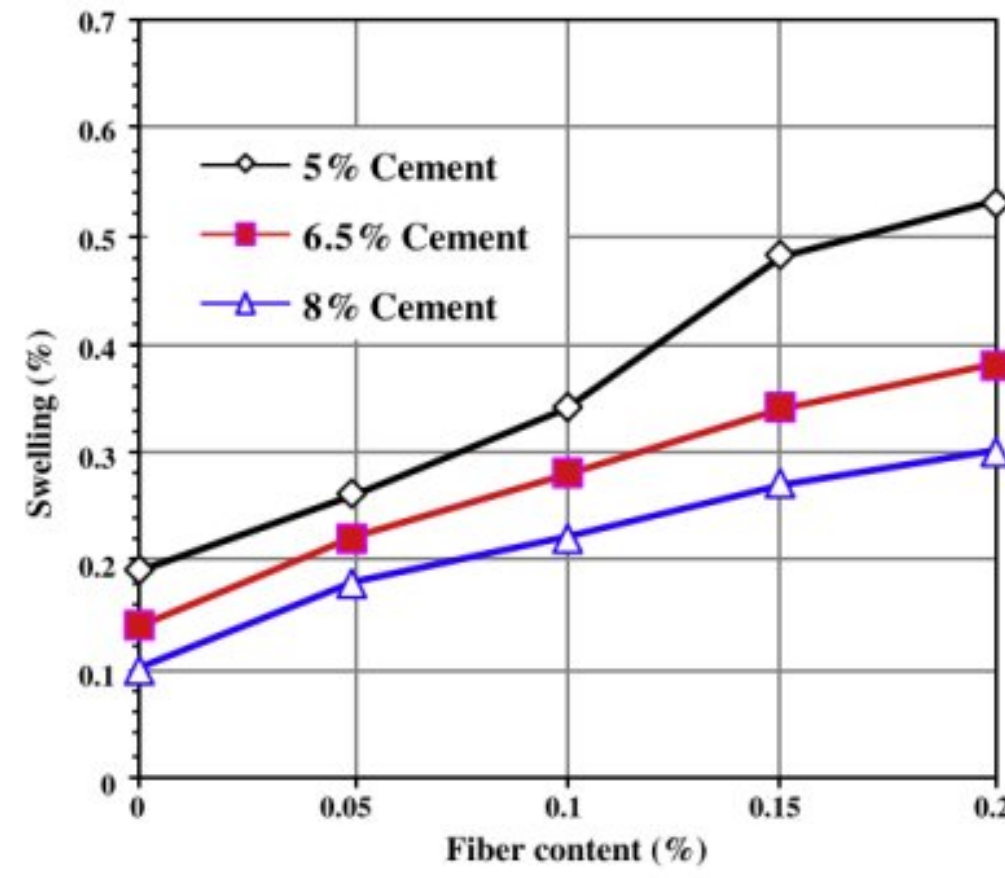
Fig.2. 65. Swelling by immersion of CEB as a function of fiber content (with 10 MPa of compaction pressure) [18].
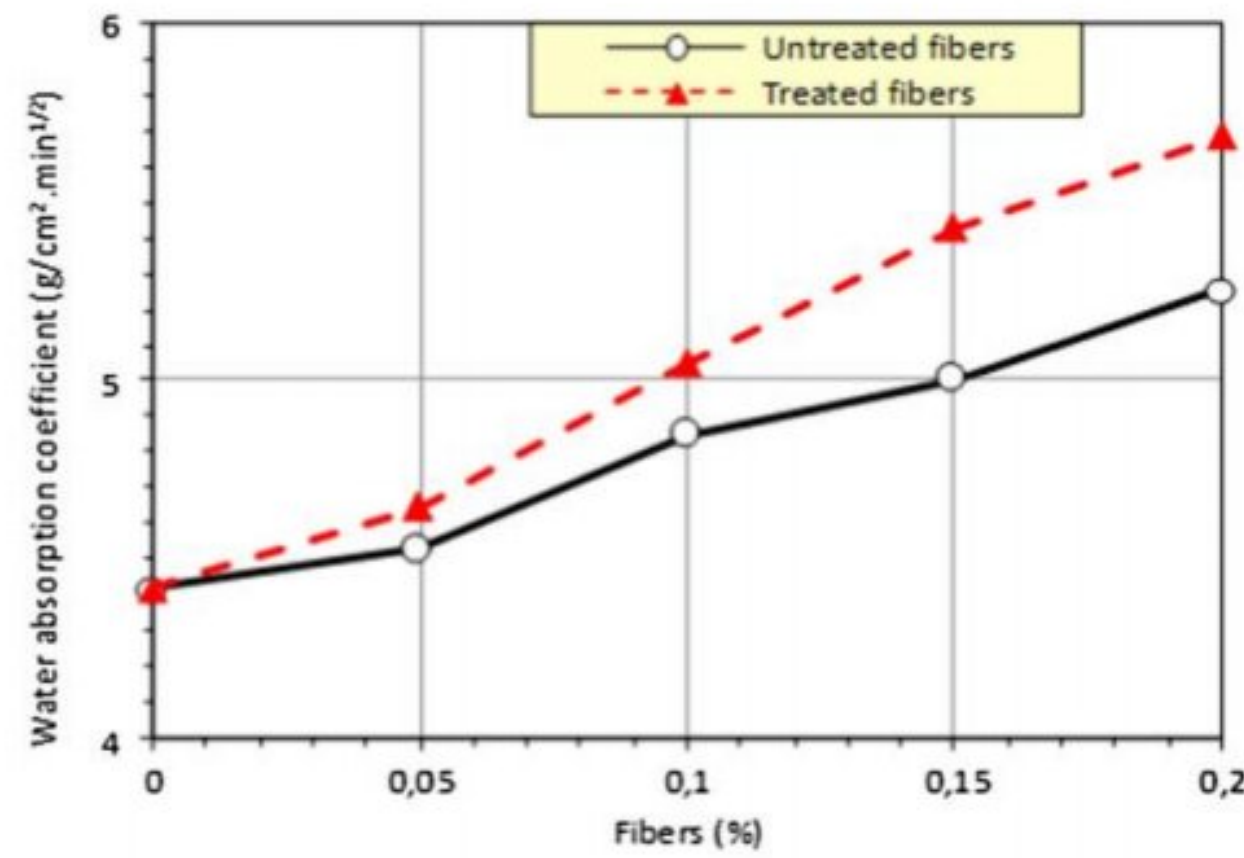
Fig.2. 66. Effect of varying the fibers content on water absorption coefficient Cb of CEB stabilized with 10% of quicklime after 7 days of oven curing[19].
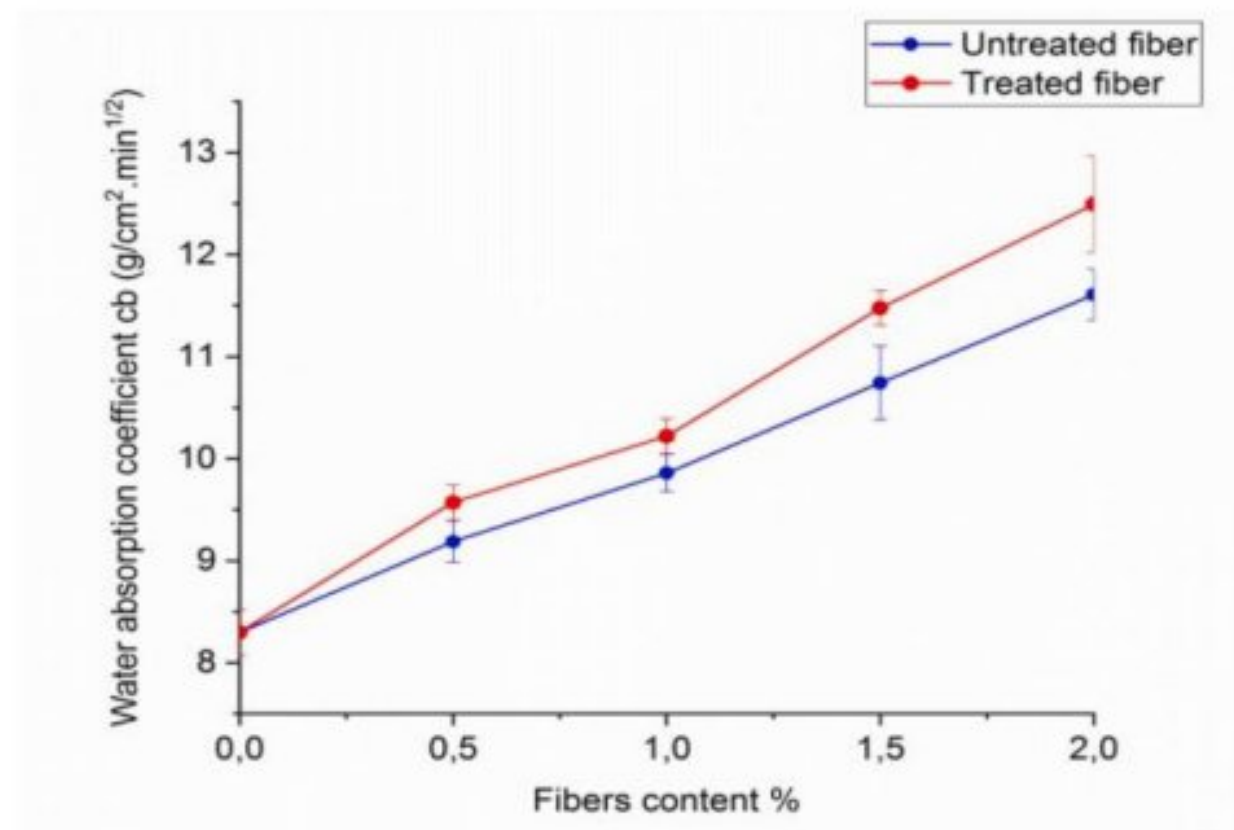
Fig.2. 67. Effect of untreated and treated doum fibers on water absorption co- efficient of CEB stabilized by 9% of lime[105].

58

2.6.3.3 Effect of plant fiber and bio-aggregate content on thermo-physical properties of CEB

2.6.3.3.1 Thermal conductivity

Laborel-Préneron et al. [100] also carried out an investigation to study the effect of hemp shiv, corn cob and barley straw addition on the hygrothermal properties of earth bricks. The addition of 6% of straw decreased the thermal conductivity by 75% in comparison with an FWAS specimen whereas the decrease was only 55% in the case of an addition of 6% of corn cob[100].
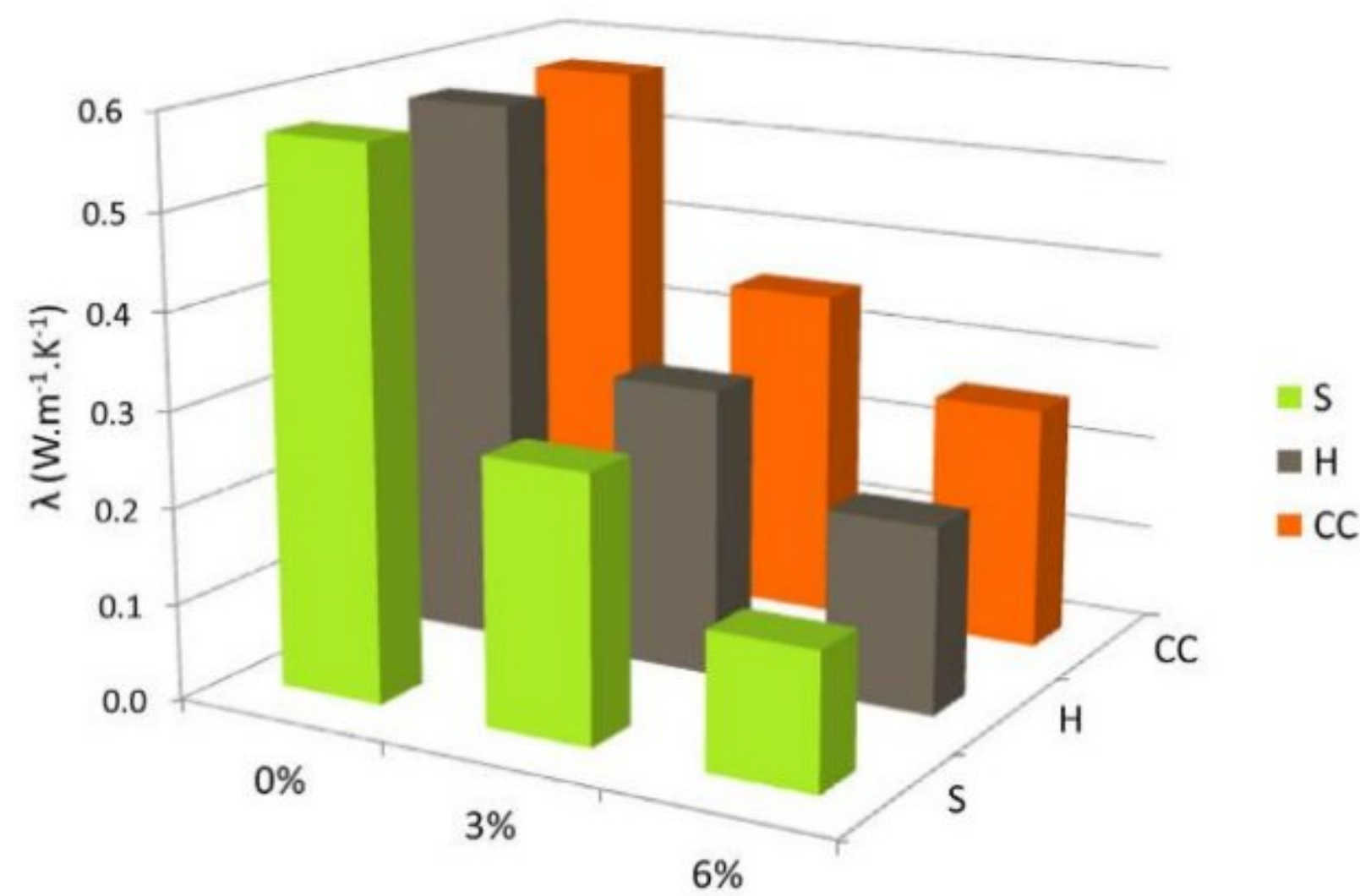
Fig.2. 68. Thermal conductivity of the different materials[100].

The results of the study of Taallah and Guettala [19] illustrate that increasing fibers content from 0% to 0.2% caused a decreasing of thermal conductivity percentage to 11.4% and 6.2% for untreated and treated fibers respectively. Increasing fiber's length and content had a positive impact on the thermal conductivity of CEB. Also, the thermal conductivity of CEB decreases from 0.63 W/m.K to 0.57 W/m.K when the length of fibers increases from 0.4 cm to 2.5 cm and the thermal conductivity of treated fibers is higher than that of the untreated fibers [105].
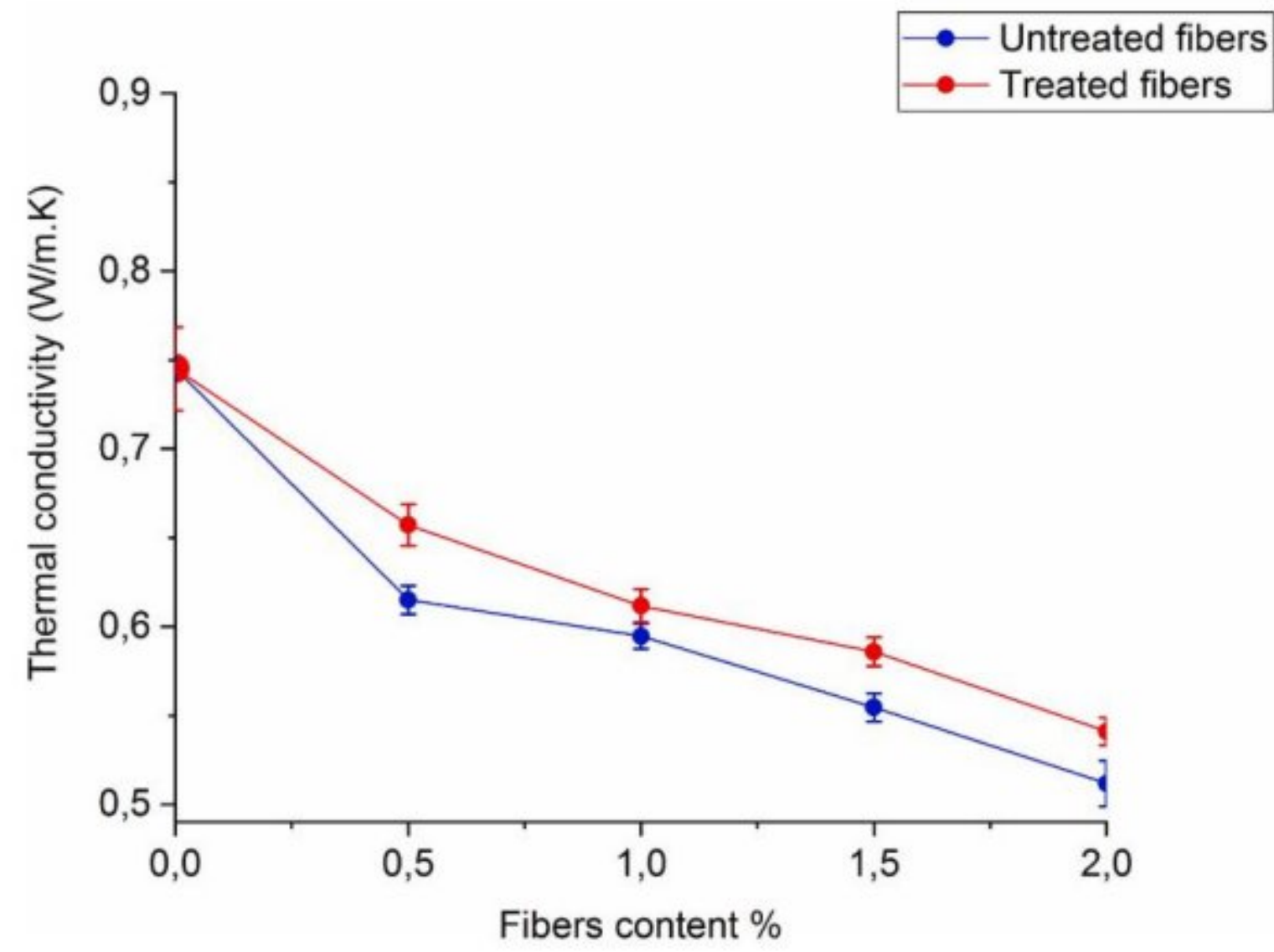
Fig.2. 69. Effect of varying the fibers content on thermal conductivity of CEB stabilized by 9% of lime[105].
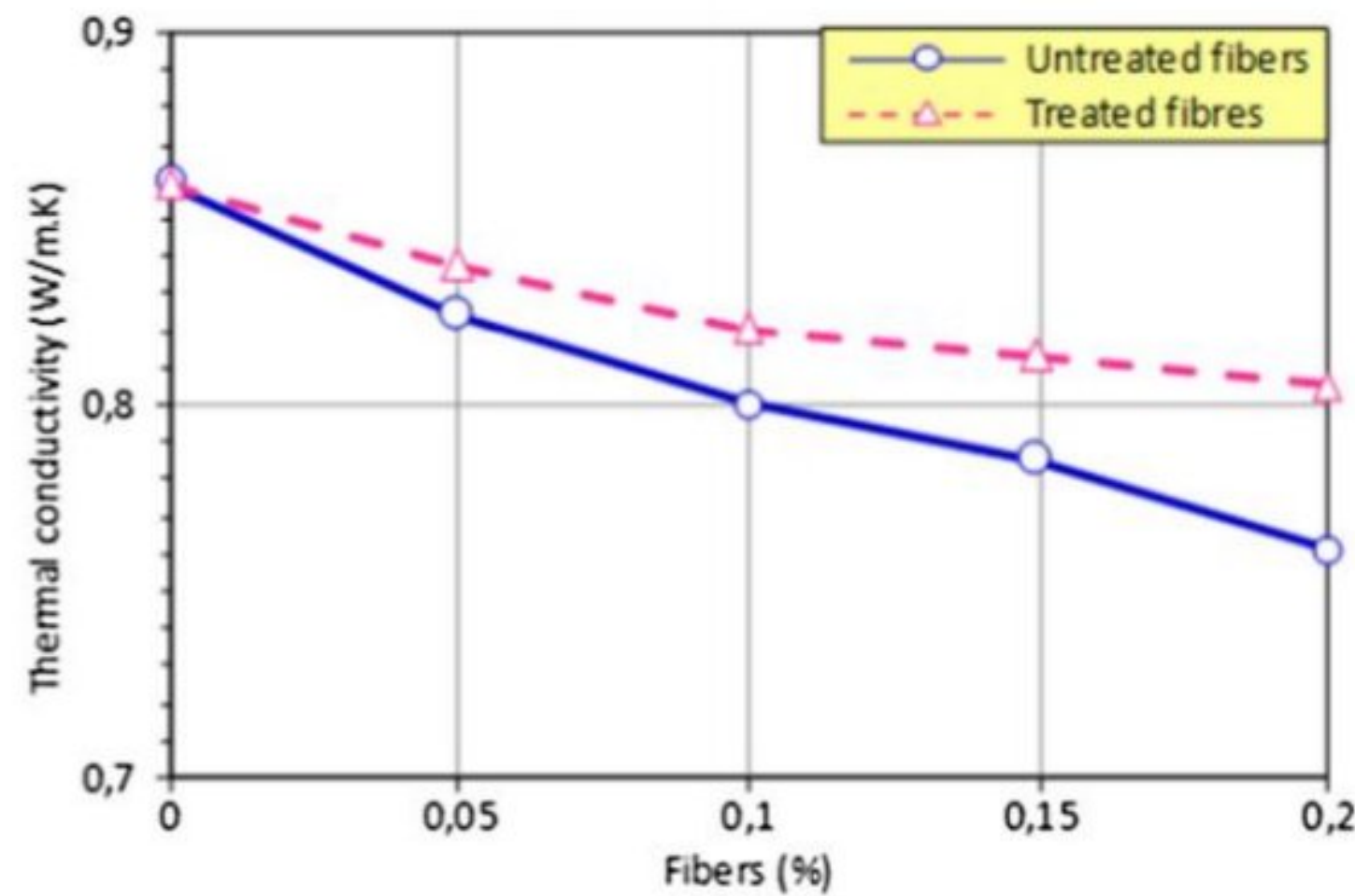
Fig.2. 70. Effect of varying the fibres content on thermal conductivity of CEB stabilized with 10% of quicklime after 7 days of oven curing[19].

The study of Khoudja et al [25] shows a quasi-linear decrease in thermal conductivity with the increase in the DPW content, which induces a gain in thermal insulation performance estimated at 49% for the case of an adobe containing 10% of DPW corresponding to a thermal conductivity of 0.342 W/ m.K which is smaller than that of control adobe whose thermal conductivity is equal to 0.677 W/m.K.

2.6.3.3.2 Thermal diffusivity and thermal effusivity

The addition of the plant aggregates engenders a decrease of the thermal effusivity values. The diffusivity is also affected by the introduction of plant aggregates, it decreases when the plant content increases[100].

Table.2. 2. Specific heat capacity (C_p), volumetric heat capacity ($\rho_d \cdot C_p$), calculated effusivity (E) and calculated diffusivity (D) of the earth matrix and of the composite materials[100].

	c_p (J kg^{-1} K^{-1})	$\rho_d.c_p$ (J m^{-3} K^{-1})	E (J K^{-1} m^{-2} s$^{-1/2}$)	D x 10^{-7} (m^2 s^{-1})
FWAS	774	1463,634	913	3.9
S3	786	1208,700	582	2.3
H3	791	1201,592	600	2.5
CC3	790	1320,745	680	2.7
S6	800	879,555	351	1.6
H6	809	1028,455	454	1.9
CC6	808	1264,254	573	2.1

2.6.3.3.3 Specific heat capacity

The specific heat capacity (Cp) values of the composites (with plant aggregates) are only slightly higher than earth material alone[100]. Khoudja et al [25] mentioned that when the date palm waste (DPW) content went from 0% to 2%, the specific capacity increased from 1168.83 J/kg K to 1197.14 J/kg K, which is a 2.4%increase. This was followed by a decrease in the specific heat occurred to reach the lowest value of 1010.45 J / kg K for the highest DPW content (10%).
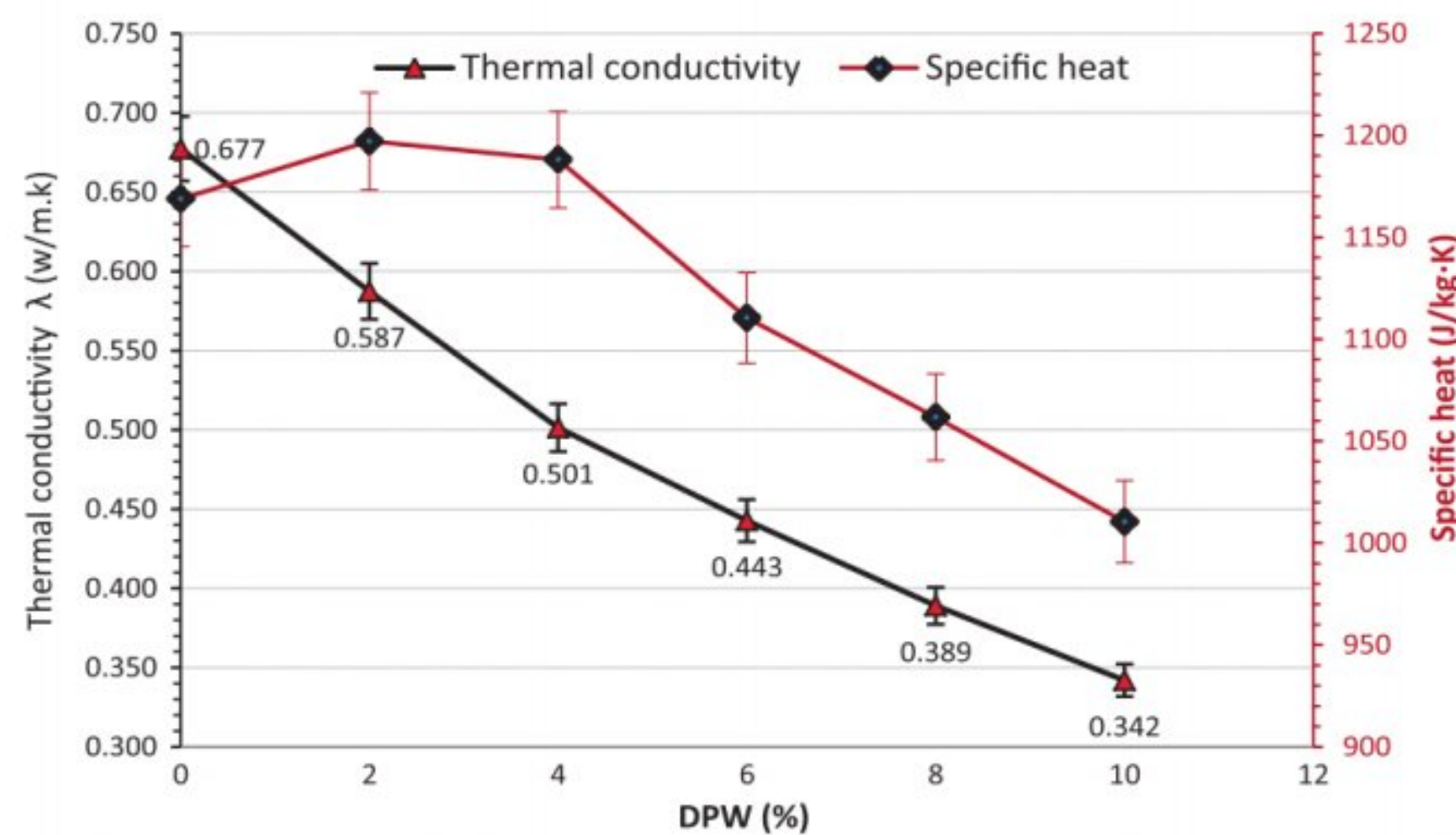
Fig.2. 71. Thermal conductivity and Specific heat as a function of DPW content[25].

Table.2. 3. Characteristics of CEBs based on plant fiber.

References	Type of fibers	Type of Chemical stabilization	Dosage [%]	Length of fibers [mm]	Compressive strength (Min and Max) [MPa]	Thermal conductivity (Min and Max) [W/mk]
Taallah et al.,[18]	Date palm	Cement	0, 0.05, 0.1, 0.15, 0.2	2cm	High value=12.8 with 0.05% of fiber content, 8%cement content and 10 MPa of compaction pressure. Less value=3.6 with 0.15% of fiber content, 5%cement content and 1.5 MPa of compaction pressure. Improvement with 0.05% of fiber content, 8% cement content and compaction pressure of the 10MPa. A gradual decrease with the increase of fibers.	_
Taallah and Guettala[19]	Date palm	quicklime	0, 0.05, 0.1, 0.15, 0.2	2cm	High value=7.9 Less value=6.5 A gradual decrease with the increase of fibers.	Less value=0.761, high value=0.851. A gradual decrease with the increase of fibers.
Mostafa and Uddin[49]	Banana	Cement	_	0, 50, 60, 70 80, 90 100	Less value=3.84, high value=6.58. Improvement with fiber length of 60 mm.	_
Laibi et al.,[99]	Kenaf	_	0 and 1.2	10, 20 and 30	Less value=4, high value=6. Improvement with fiber length of 30 mm.	Less value=0.8 high value=2 The thermal conductivity decreases when the fiber length is increased.

Table 2.3 summarizes the most important mechanical and thermal properties obtained from the literature for compressed earth blocks incorporated by plant fibers.

2.6.3.4 Effect of plant fiber and bio-aggregate content on microstructural properties of CEB

Microstructural analysis of the samples was performed by scanning electron microscopy (SEM) in the study of Laibi et al.[99]. Microscopic analyzes are carried out in order to confirm the apparent results of the effect of adding plant fibers and bio-aggregates. The microscopic study of Laibi et al. [99] showed that the fibers strengthen the matrix after the first damage. However, when cracks spread, the fibers slide against the matrix (Fig.2.72). The high tensile strength of natural fibers compared to cement matrices, but the presence of these fibers rarely improves the tensile strength of the reinforced materials. The reason for the decrease in the tensile and bending strength of building materials reinforced with natural fibers as commonly assumed in the literature is the poor adhesion between the matrix and the fibers. [18], [78], [101]. Water absorption by aggregates and fibers has a significant impact on their matrix adherence. The soil is pushed away by the swelling of the particles caused by water absorption over the first 24 hours. When the volume of the particles reduces after drying, voids are created around them, as seen in Fig.2.73[88], [107], [108].
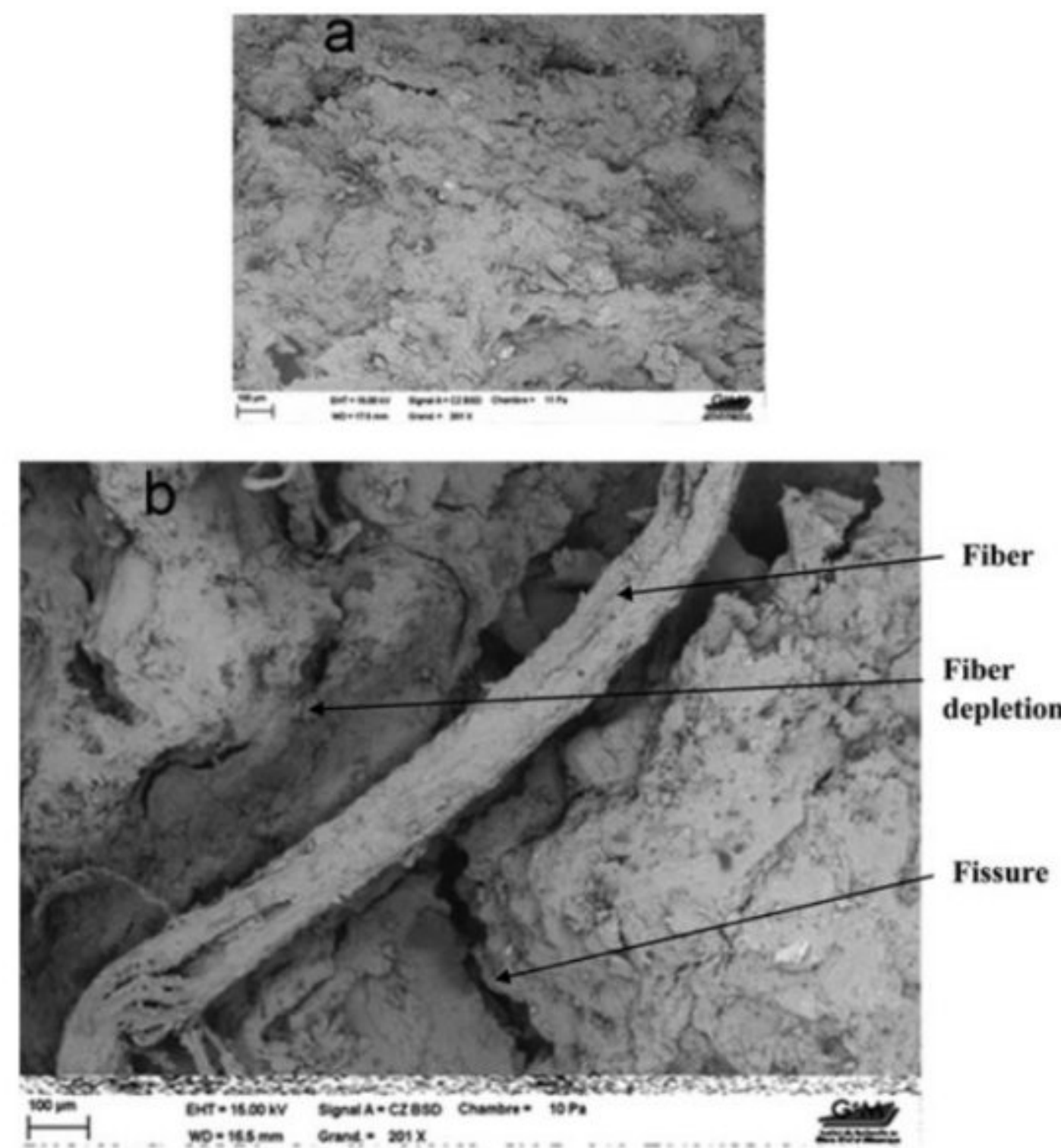
Fig.2. 72. SEM Image of the Fracture Surfaces of CEB (a) and Fiber- reinforced CEB (b)[99].
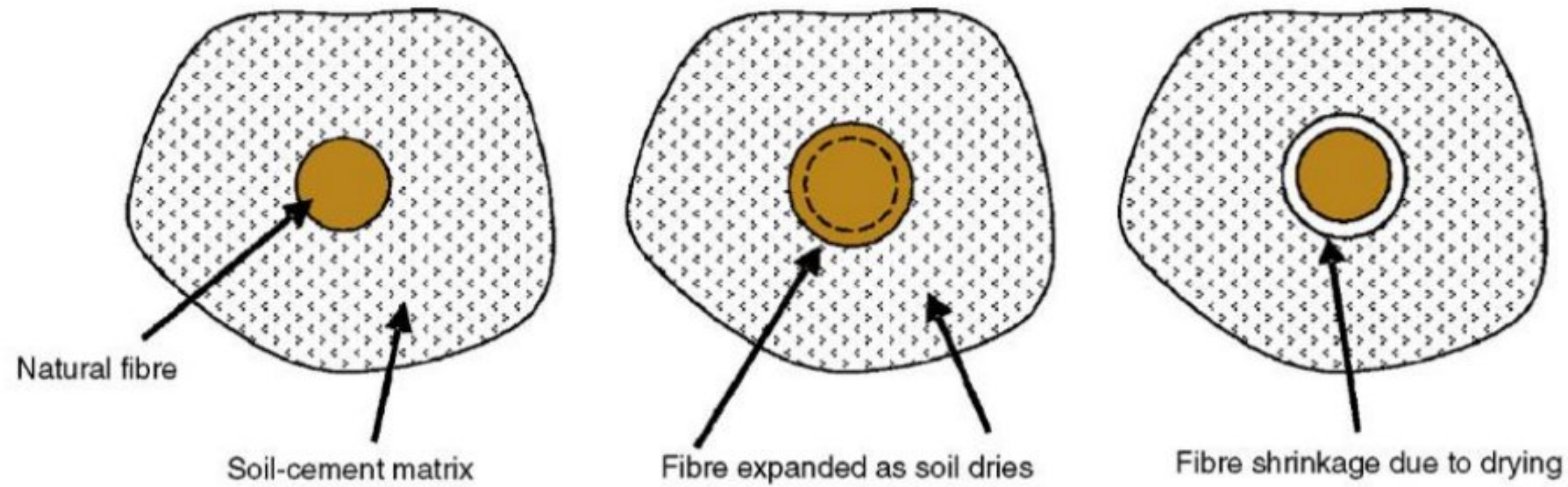
Fig.2. 73. Interaction between natural aggregate or fiber and soil matrix after drying [107].

2.7 Digital Image Correlation technique (DIC)

Digital Image Correlation (DIC) is an important and widely used non-contact technique for measuring material deformation[109]. In the field of experimental mechanics, digital image correlation (DIC) is an effective and practical tool for full-field deformation measurement that has been widely accepted and used[110]. DIC uses image registration algorithms to track the relative displacements of material points between a reference (typically, the undeformed) image and a current (typically, the deformed) image[109]. Many recent studies [111]–[119]have focused on the use of DIC technique to measure the deformation of materials while they are subject to forces. Araya-Letelier et al[40] mentioned that the plain adobe beam presented small values of the horizontal strains ε_{xx}, which was consistent with its collapse right after the maximum load, whereas the fiber-reinforced adobe beams presented significant larger (with respect to the plain adobe beam) values of ε_{xx} right before collapse, and these increment were larger as fiber dosages increased (see Fig.2.74).
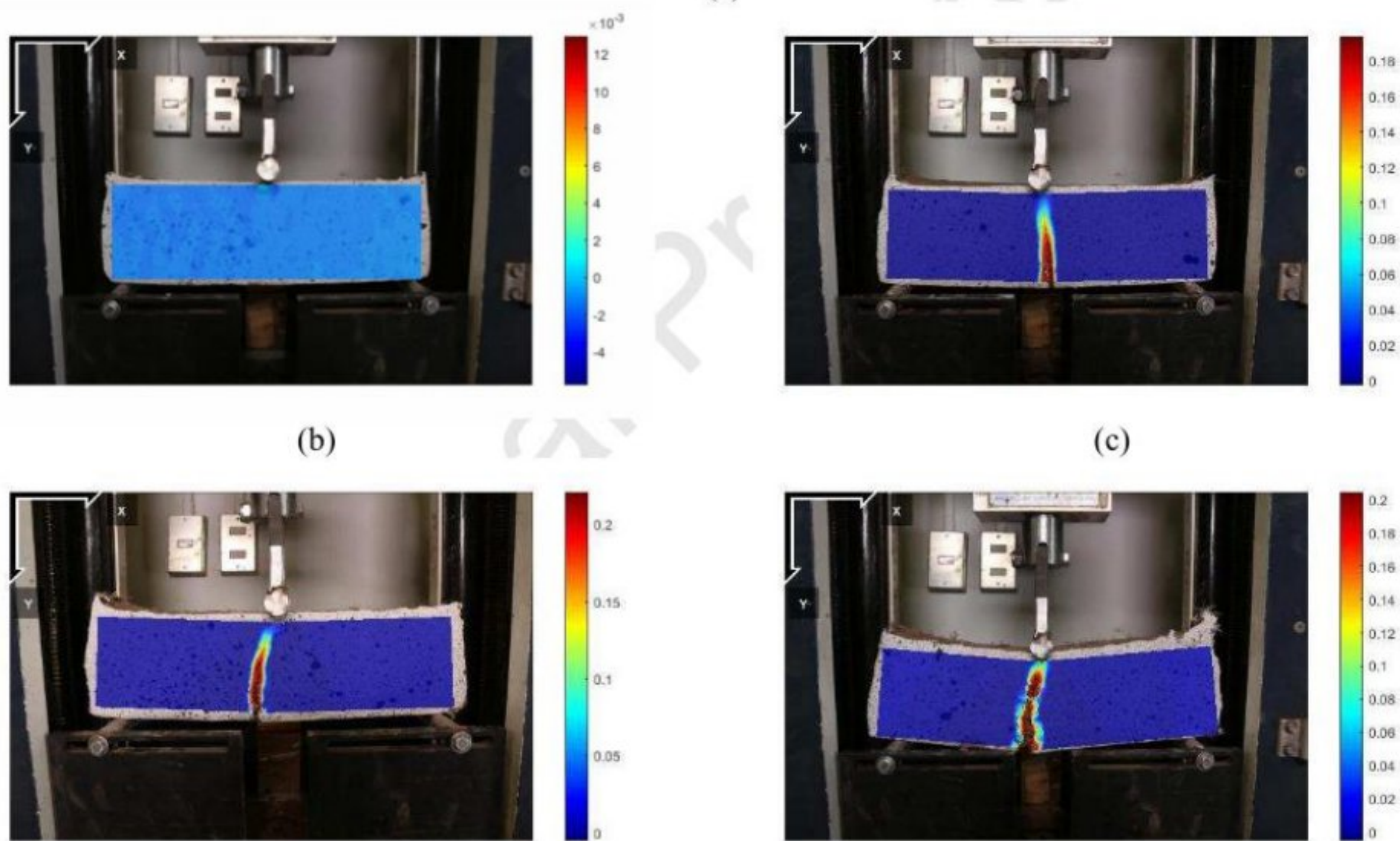
Fig.2. 74. Flexural toughness: (b) ε_{xx}DIC of CFF0.0, (c) ε_{xx} DIC of CFF0.25, (d) ε_{xx} DIC of CFF0.5, and (e) ε_{xx} DIC of CFF1.0 (DIC images were taken right before collapse)[40].
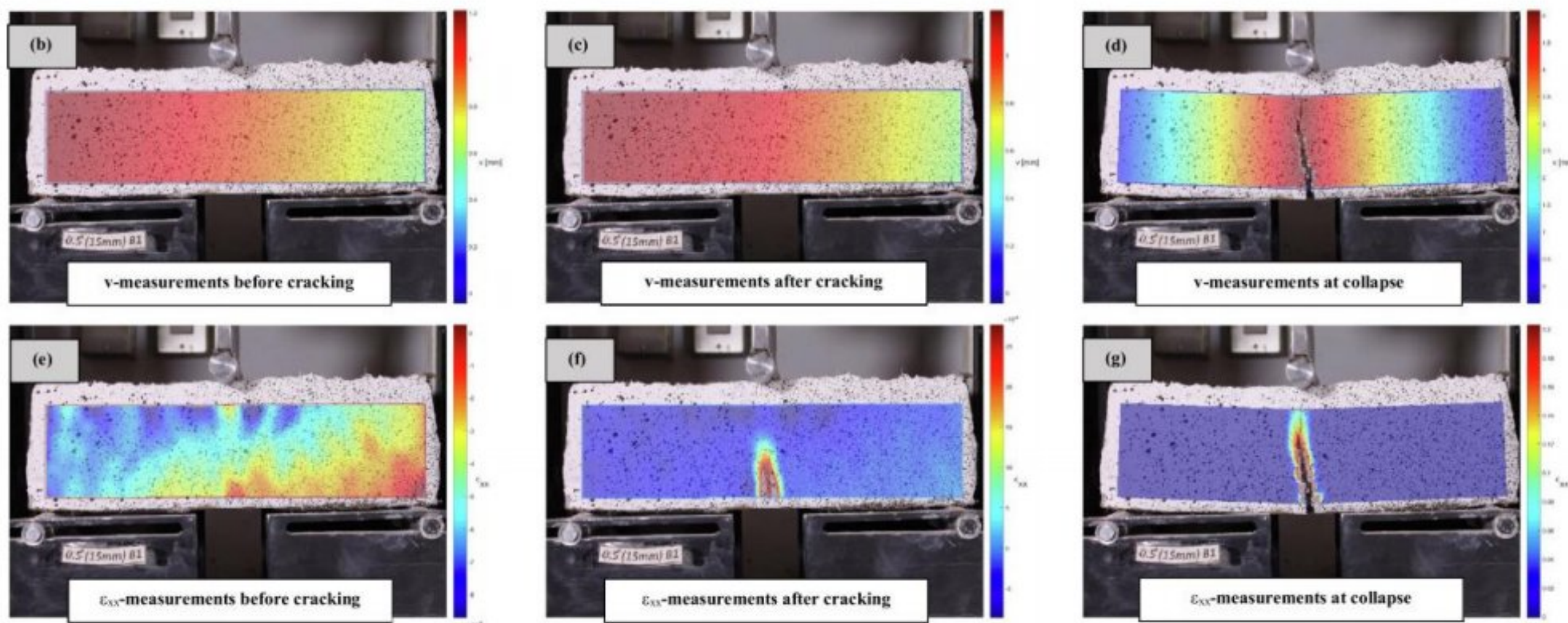
Fig.2. 75. (b)-(d) DIC vertical displacement measurements before cracking, after cracking and at collapse, respectively, and (e)-(g) DIC ε_{xx} measurements before cracking, after cracking and at collapse, respectively[120].

2.8 Conclusion

This chapter has focused on the use of natural fibers and aggregates, particularly as reinforcement in earth material, as building materials. Through this bibliographic research, it was noted that many research works have confirmed that the use of mineral binders (cement, lime) as stabilizers improves the mechanical resistance and water insensitivity of CEB. To the best of our knowledge, there is no study related to the effect of the partial replacement of soil and crushed sand with date palm waste aggregate and fiber on the thermo-physical, microstructure and mechanical behavior of oven cured compressed earth blocks stabilized by lime. Although many important studies have been published, several gaps in information remain, especially regarding the thermo-physical and microstructure properties of oven-cured compressed earth bricks stabilized by lime. To fill this knowledge gap, this research will study the effect of the partial replacement of soil and crushed sand with date palm waste on the thermo-physical, microstructure properties and mechanical behavior of oven-cured compressed earth blocks stabilized by lime.

CHAPTER 3

RAW MATERIALS AND EXPERIMENTAL METHODS

Chapter 3: Raw materials and experimental methods

3.1 Introduction

The research plan and methodology for this thesis are described in this chapter. The characterization of the fundamental ingredients for the manufacturing of compressed earth blocks will be presented in the first portion of this chapter. These are the physicochemical, mechanical and mineralogical characteristics of soil, crushed sand, and aggregate and fibers of date palm waste. Following that, manufacturing procedures, mixing sequences, placement, and conservation of different test pieces. In the second part, we described the materials and methods used in the investigation.

3.2 Materials

In our study, local materials were used for making date palm waste-based CEB as follows: soil and crushed sand as a main matrix, quicklime as a chemical stabilizer, three kinds of date palm waste (DPWA, DPM and DPS) and water.

3.2.1 Soil

In this study, the soil of Biskra region, located in southeastern Algeria was used, and it was selected on the basis of its availability and its abundance in the region. Analyzes of the chemical and mineralogical compositions were carried out in the laboratory of the Center for Studies and Technological Services of the Construction Materials Industry CETIM in Boumerdès (Algeria). The chemical composition on this raw soil shown in Table 3.1 was carried out by X-ray fluorescence. The mineralogical composition on this raw soil presented in Table 3.2 was performed by X-ray diffraction. The mineralogical composition shows that the soil has a high content of calcite, dolomite and quartz, and a low concentration of illite and gypsum. The particle size distribution of the soil presented in Fig. 3.2 was determined by wet sieving and sedimentation, according to NF P 18-560 and NF P 94-057 successively. Absolute density is 2400 kg m^{-3} and bulk density is 1240 kg m^{-3}. The Atterberg limits were: liquid limit (LL = 29%), plastic limit (PL=21%) and plasticity index (PI = 8%).
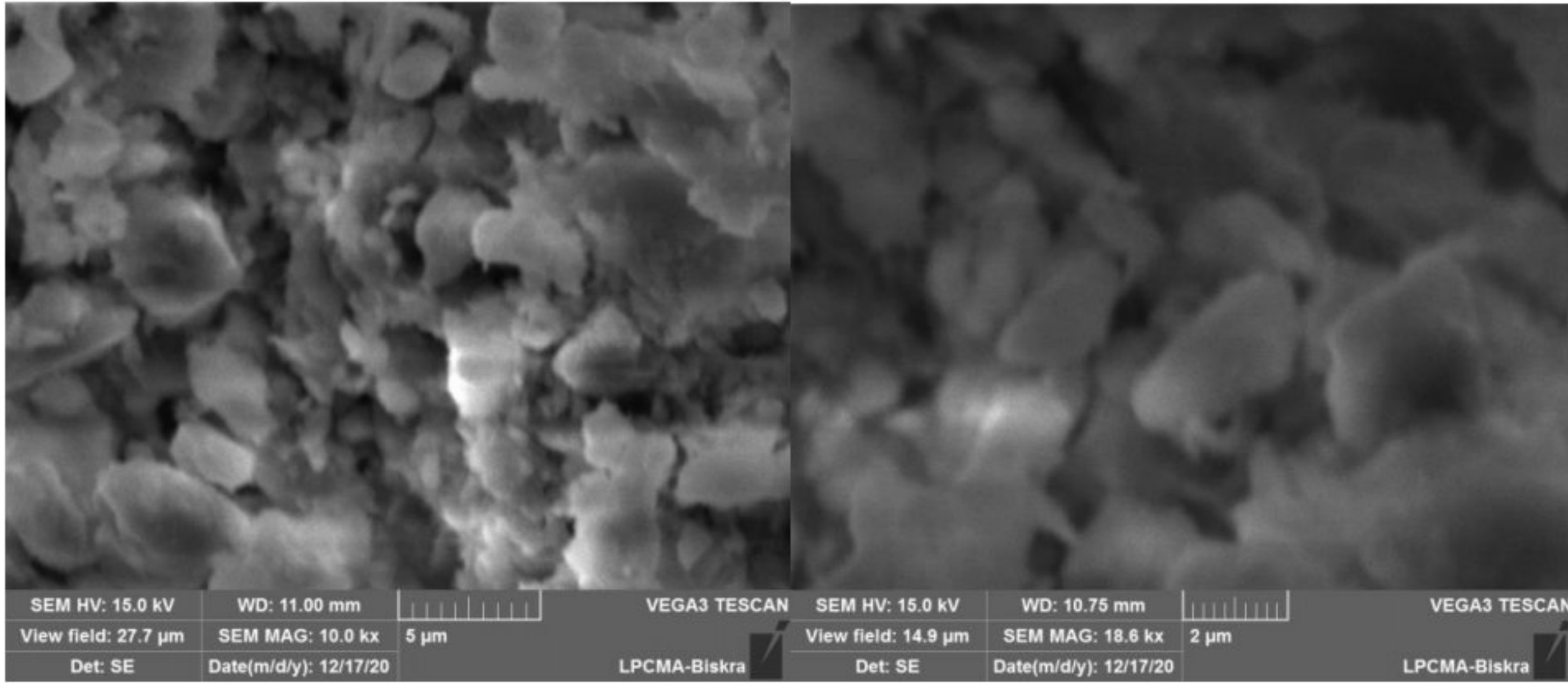
Fig.3. 1. SEM of the soil used in this study.

Table.3. 1. The chemical analysis of used soil.

Content (%)										
SiO_2	Al_2O_3	Fe_2O_3	CaO	MgO	SO_3	K_2O	Na_2O	P_2O_5	TiO_2	LOI
35.29	5.25	2.38	27.46	2.09	0.38	0.88	0.21	0.12	0.33	25.62

Table.3. 2. Mineralogical composition of soil.

	Minerals				
	Gypsu	Quartz	Calcite	Dolomite	Illite
Mineralogical composition (%)	1	24	38	29	8
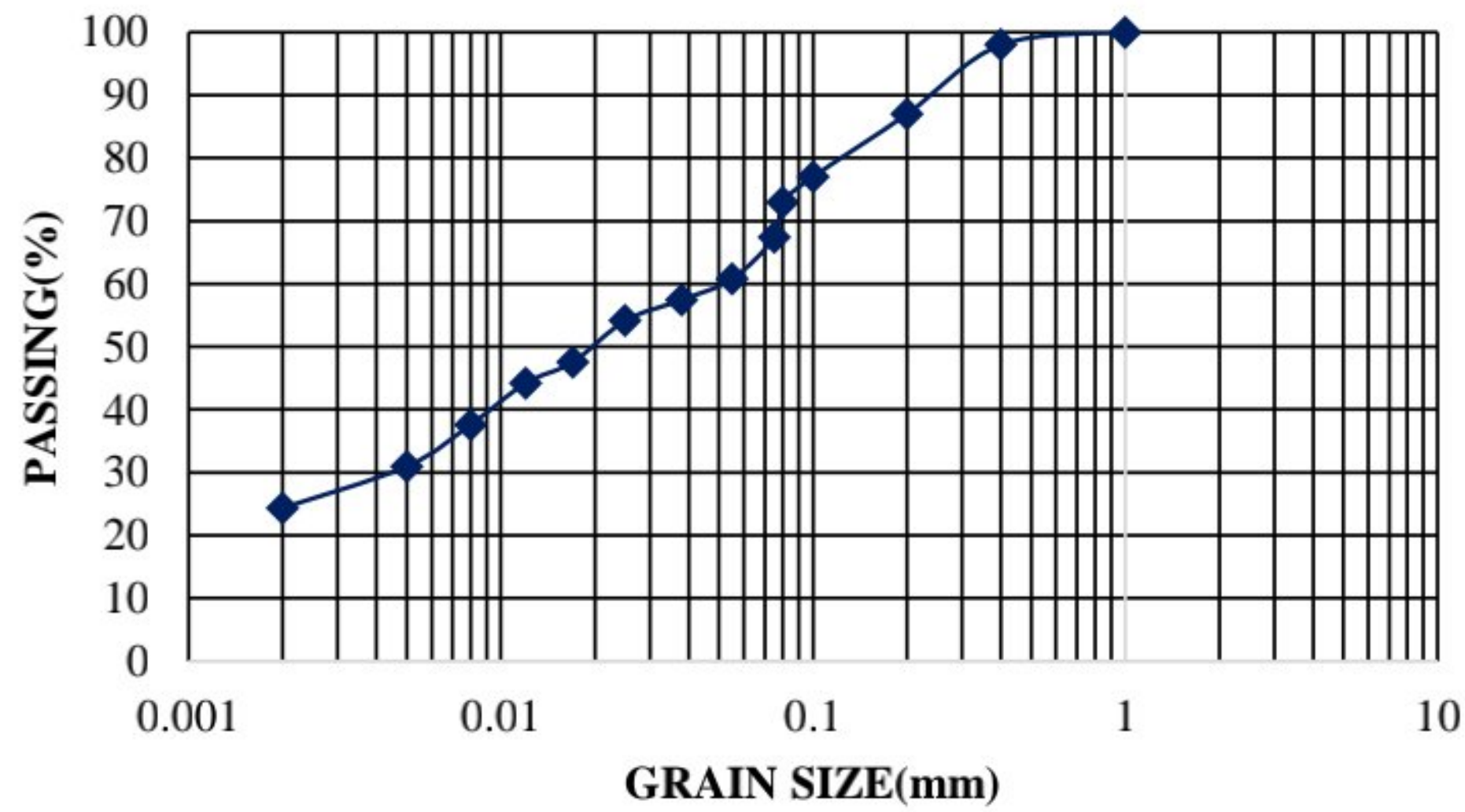
Fig.3. 2. Grain size curve of soil.

3.2.2 Crushed sand

The crushed sand used in this investigation came from Biskra region (Algeria), passing through a 5 mm sieve. Absolute density is 2600 kg m^{-3}, bulk density is 1570 kgm^{-3} and fineness modulus is 2.31. The particle size distribution of this sand is determined by sieving, according to NF P 18-560.The test results are presented in Fig. 3.3. Chemical composition of crushed sand is shown in Table 3.3.
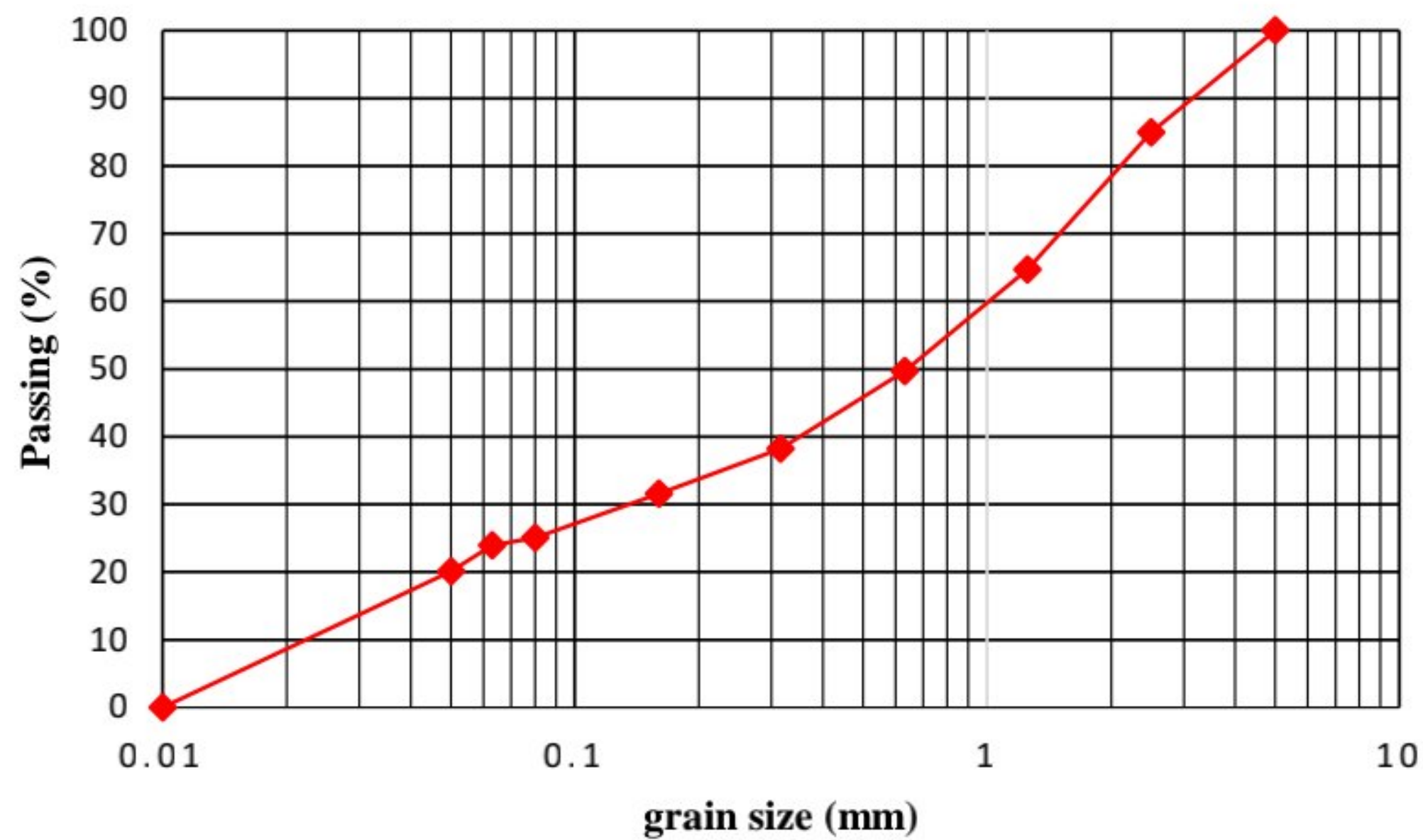
Fig.3. 3. Grain size curve of crushed sand.

Table.3. 3. Chemical composition of crushed sand (%).

SiO$_2$	Al$_2$O$_3$	Fe$_2$O$_3$	CaO	K$_2$O	SO$_3$	Na$_2$O	MgO	Loss on ignition
0.87	0.30	0.15	54.70	0.07	0.08	0.04	0.66	43.20

3.2.3 Lime

Commercially abundance quicklime produced by the lime unit of Saida (Algeria) was used in this study. The chemical and physical properties of quicklime according to its technical sheet are presented in Tables 3.4 and 3.5.

Table.3. 4. Chemical properties of quicklime according to the technical sheet of this quicklime.

			Content (%)					
SiO_2	Al_2O_3	Fe_2O_3	CaO	MgO	SO_3	$CaCO_3$	Na_2O	CO_2
<2.5	<1.5	<2	<83.3	<0.5	<0.5	<10	0.4–0.5	<5

Table.3. 5. Physical properties of quicklime according to the technical sheet of this quicklime.

Physical properties	
Physical appearance	Dry white powder
Specific gravity	2
Over 90 µm (%)	<10
Over 630 µlm (%)	0
Insoluble material (%)	<1
Bulk density (g/l)	600–900

3.2.4 Date palm fibers

In this investigation, three types of date palm waste were used: date palm waste aggregate (DPWA), Date palm mesh (DPM) and date palm spikelet (DPS) (Fig. 3.4).
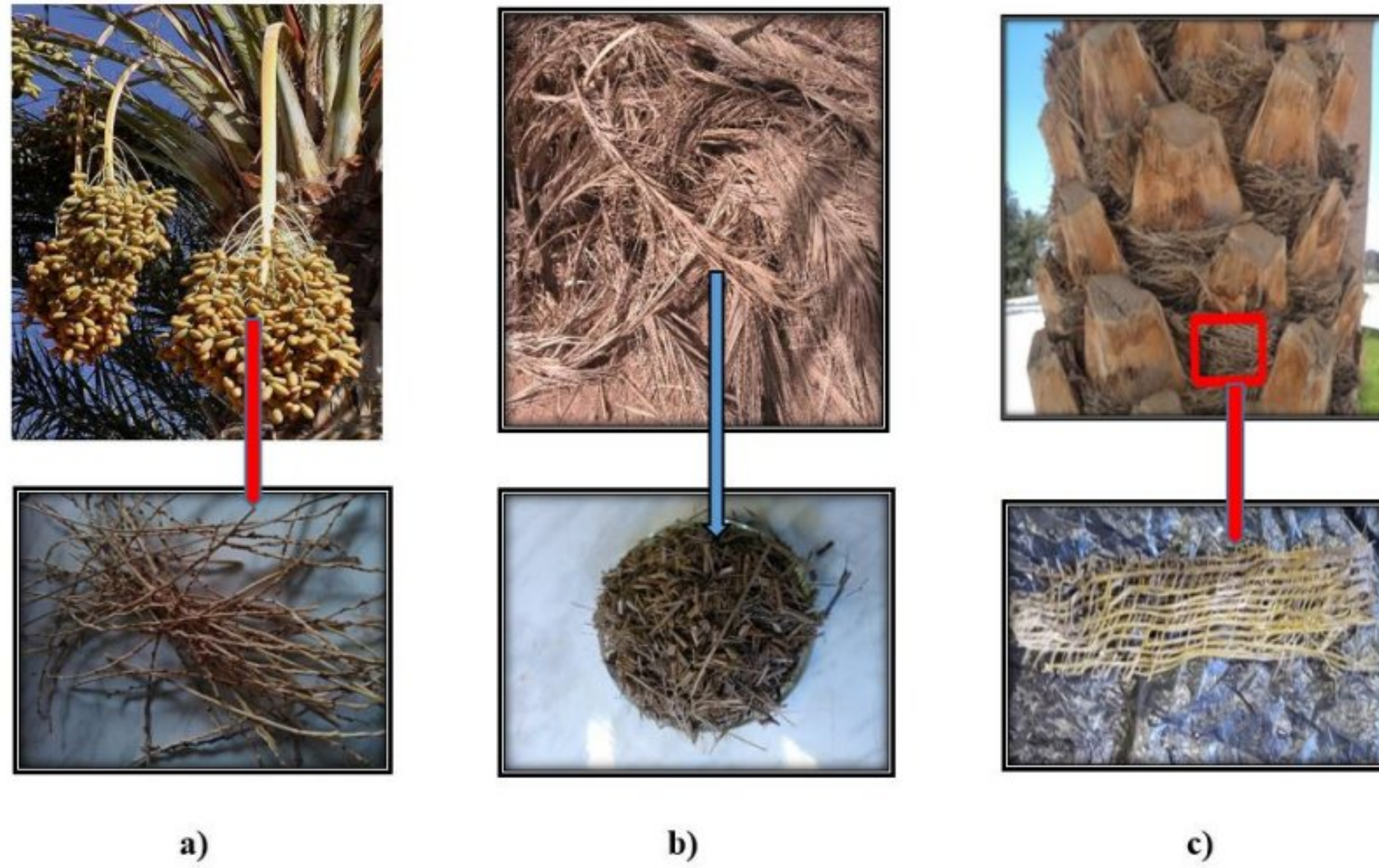
Fig.3. 4. Date palm waste used in this study: a) DPS, b) DPWA and c) DPM.

• **Date Palm Waste Aggregate (DPWA)**

Date palm waste is the product of maintenance operations on palm groves. In the DPWA type, two kinds of date palm waste (leaves and petiole) were mixed together. This waste was brought back from the Technical Institute for the Development of Agriculture in the Desert, Ain bin Nawi Biskra, Algeria. The mechanical characteristics (Table 3.6) of two kinds of date palm fibers (leaves and petiole) were taken from the experimental study performed by Djoudi et al [22]. The physical properties of DPWA are presented in Table 3.7. Bulk density of DPWA samples was performed by a balance with an accuracy of ±0.1%, by the gravimetric method based on the Archimedean principle [92]. The water absorption of DPWA was performed according to the study of Benmansour et al [23]. Fig.3.5 presents SEM images of the palm components, such as the spine, petiole and Leaflet.

Table.3. 6. Mechanical properties of date palm waste fibers (leaves and petiole) used as plant aggregates [22].

Fibers type	Tensile strength σ_{max} (MPa)	ε_{max} (mm/mm)	Modulus of elasticity E (GPa)
leaves	91.07 ± 17.9	0.008 ± 0.003	13.91 ± 0.76
Petiole	114.53 ± 7.49	0.017 ± 0.005	10.81 ± 0.28

Table.3. 7. Physical properties of DPWA (plant aggregate).

Property	Size(mm)	Bulk density(kg.m^{-3})	Water absorption (%)
Values	1-4	113.85	284
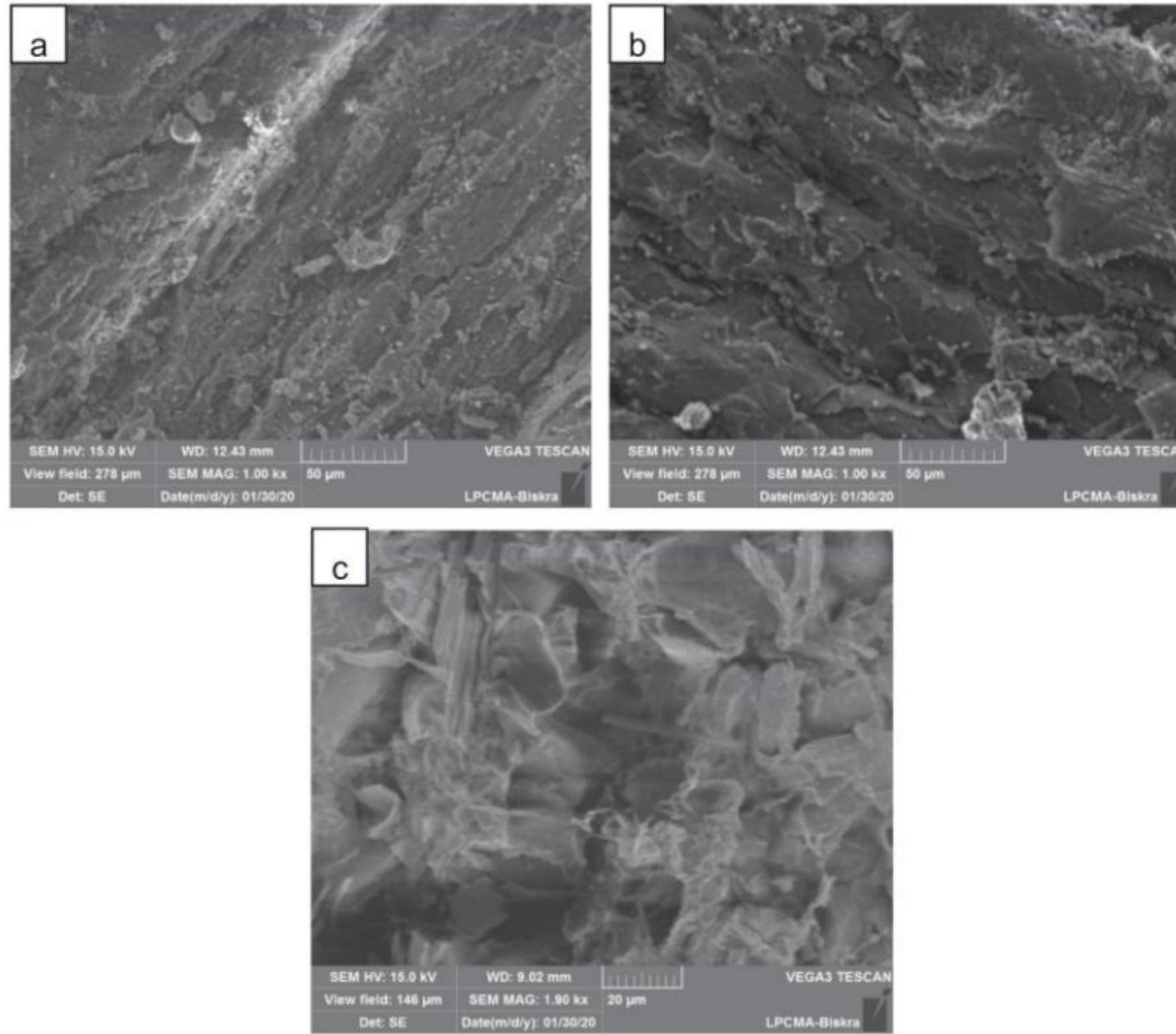
Fig.3. 5. SEM images of the components of the palm: a) Spine, b) Leaflet, and c) Petiole[25].

- **Date Palm Mesh (DPM)**

In this study, the DPM type was used in the form of a mesh that contains fibers in two perpendicular directions as tissue, and was pulled out from male date palm trunk in the form of nearly rectangular mesh (200–300 mm width and 300–500 mm length). Date palm trunk surface fibers are a natural woven (such as welded plant fibers mesh). In this work, DPM was cut with a variable length ranging between 10 cm and 18 cm and width ranging between 5 cm and 8 cm. The mechanical and physical properties (Table 3.8) were taken from the experimental study performed by Kriker et al. [21]. Fig. 3.6 presents the scanning electron micrographs of DPM; Fig. 3.6(a) and (b) show the typical transverse and longitudinal sections of DPM. The DPM section is dense with a small canal and many little pores for circulation of saliva. This confirms the porous structure and the observed absorption capacities of the DPM[21].

Table.3. 8. Physical and mechanical properties of DPM fibers [21].

Property		Values
Physical properties		
Bulk density (kg/m^3)		512.2–1088.8
Absolute density (kg/m^3)		1300.0–1450.0
Natural moisture content (%)		9.5–10.5
Water absorption after 5 min under water (%)		60.1–84.1
Water absorption to saturation (%)		96.8–202.6
Mechanical properties	Fiber length	
Tensile strength (MPa)	100(mm)	170 ± 40
	60(mm)	240 ± 30
	20(mm)	290 ± 20
Elongation (%)	100(mm)	16 ± 3
	60(mm)	12 ± 2
	20(mm)	11 ± 2
Modulus of elasticity (GPa)	100(mm)	4.74 ± 2
	60(mm)	5.00 ± 2
	20(mm)	5.25 ± 3

(a)　　　　　　　(b)　　　　　　　(c)
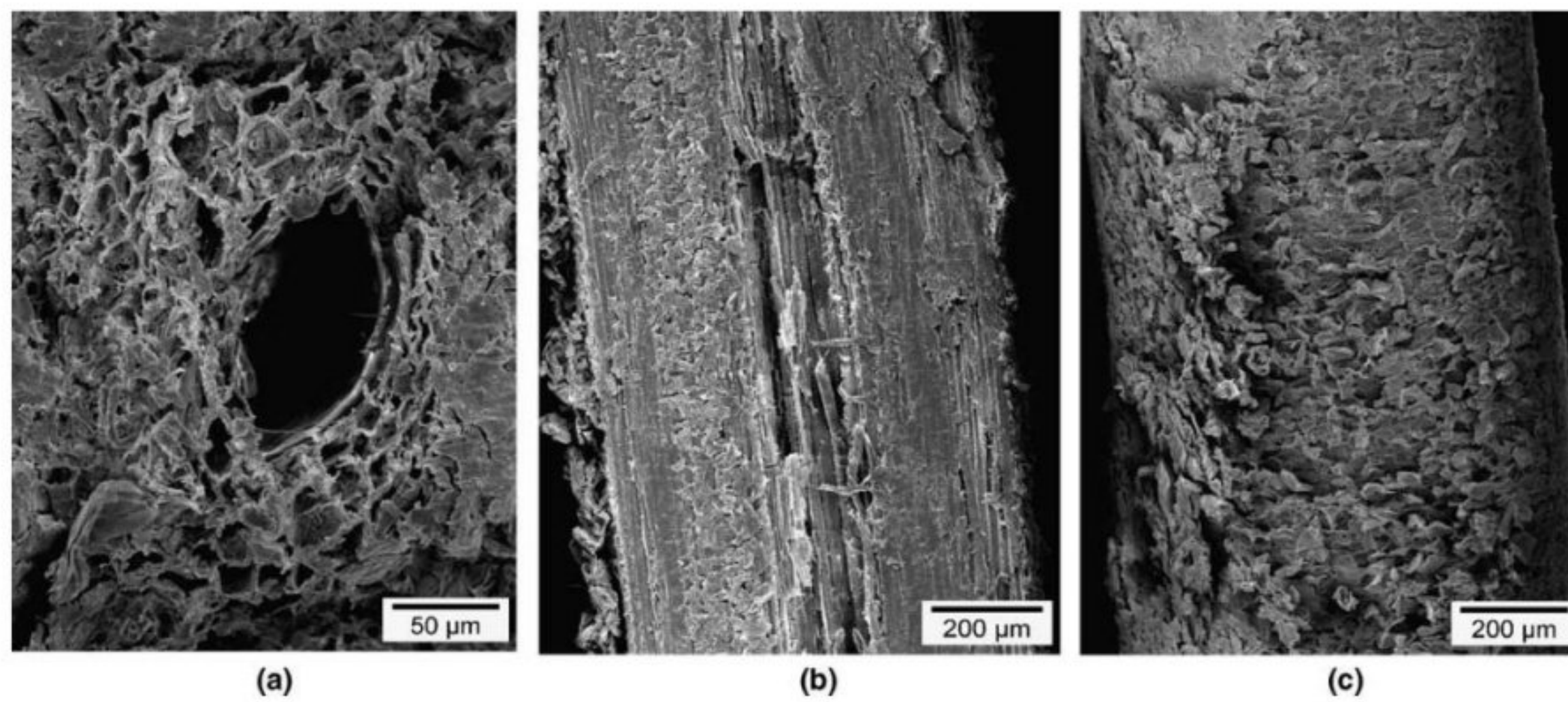
Fig.3. 6. (a) Scanning electron micrograph of typical transversal section of DPM fiber; (b) scanning electron micrograph of typical longitudinal section of DPM fiber; (c) scanning electron micrograph of longitudinal view of DPM fiber[21].

- **Date Palm Spikelet (DPS)**

The current study used DPS as the same as that used in the study of Abdelaziz et al. [17]. The spikelet was obtained from date palm waste originated from Biskra, Algeria. DPS was cut to a fixed length of 18 cm. Abdelaziz et al. [17] studied DPS and found from the tensile test of DPS that the young's modulus had an average value of 16 GPa and ranged between 8.5 GPa and 23.5 GPa. From the 3D scanner measurement, the surface topography of DPS showed that the volume of DPS is 558 mm^3 for a length of 65 mm. From the image analysis, thick samples of DPS have a diameter of 4.79 ± 2.63 mm and smaller samples have an average diameter of 2.29 ± 0.53 mm. The overall DPS diameter is 3.3 mm. Under the outer epidermis of DPS, there were a large number of fibrovascular bundles (see Fig.3.7).
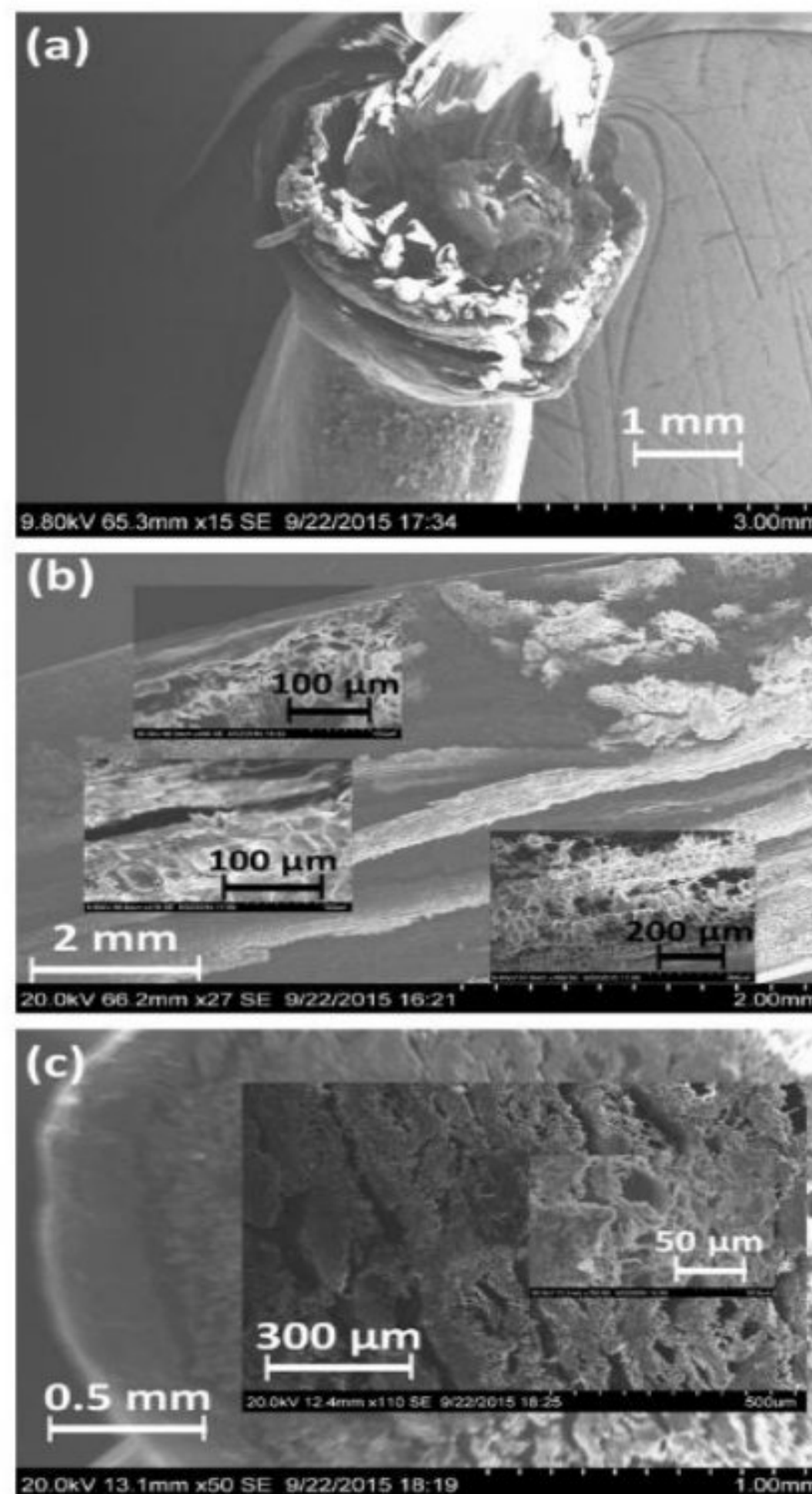
Fig.3. 7. Microstructural arrangement of the spikelet cortex revealed using SEM and showing (a) perianth morphology, (b) axial orientation of the fibers underneath, (c) transverse microscopic arrangement of the spikelet homogeneous central cylinders with fibrovascular cells[17].

The physical properties of DPS were taken from the experimental study performed by Almi et al.[92] as follows: Bulk density is 425±23.6 (kg/m^3), absolute density is 749±25.6 (kg/m^3) and water absorption is 73.78±3 (%).

3.2.5 Water

Mixing water is potable water with a temperature of 20 ± 2 °C and contains little sulfate. The quality of this potable water conforms to the requirements of NFP 18–404 standard.

3.3 Specimen preparation and curing condition

In the testing program, two types of blocks were manufactured: blocks of lime content optimization and blocks filled with date palm waste.

▪ **Manufacturing of specimen of lime optimization**

The crushed sand and soil were dried in an oven for 24 hours at 65± 2 °C. After the mixture dried (crushed sand with soil), this mixture was firstly mixed for 2 minutes in the concrete mixer, then the stabilizer (quicklime) was added. It was being mixed for 1 minute allowing the mixture to have a homogeneous color, then water was added to the mixture that was continuously being mixed for 2 minutes. The mixture obtained was placed in a steel mold of volume (100 mm x 100 mm x 200 mm), and compacted immediately with a static loading by applying compacting stress of 2 MPa. The static compaction was applied on the mixture according to the C.D.E method [121]. During all steps of this study, one curing condition was used which is the oven curing for 7 days at 65 ± 2 °C. Taallah and Guettala [19] mentioned that oven curing (7 days) led to better compressive (dry and wet) and tensile strength compared to laboratory curing (28 days) and natural steam curing (7 days).

The weight of the overall dry mixture for each block was kept constant during all the steps of this study, it was taken equal to 2000 g. In order to find the optimum moisture content for each block with different percentages of quicklime, the static compaction method proposed by C.D.E method [121] was carried out. A series of blocks were made using a mixture of 70% soil and 30% crushed sand, stabilized with four lime contents (7%, 9%, 11%, 12% and 13%) in order to find the optimum lime content in CEB (Table 3.9). For each test, three blocks of CEB were made to give average results.

Fig.3. 8. Static compaction for manufacturing of CEBs.
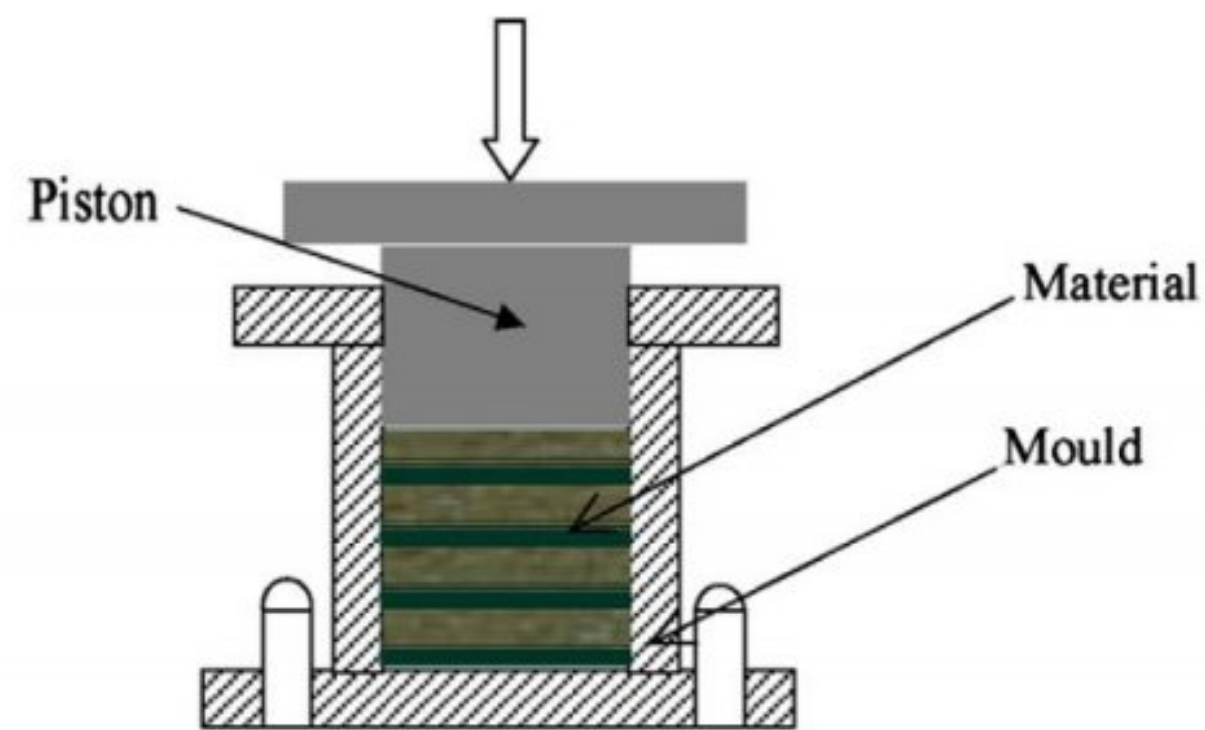
Fig.3. 9. Mould used for bricks making.

Table.3. 9. Formulation of CEB samples for optimal lime value test.

Soil (%)	70	70	70	70	70	In relation to the
Crushed sand (%)	30	30	30	30	30	dry mixture (soil–sand)
Quicklime (%)	7	9	11	12	13	In relation to the
Water (%)	10	11	13	14	15	global dry mixture

- **Manufacturing of composite specimen (filled by date palm waste)**

❖ **DPWA**

For the elaboration of the composite materials, the dry mixture (sand crushed with soil) was firstly mixed for 2 minutes in the concrete mixer, then 12% of the stabilizer (quicklime) was added and it was being mixed for 1 minute until a uniform color was gotten. Next, the optimum water content of the mixture 14% of the water was added to the mixture which was being mixed for 2 minutes. After that, date palm waste aggregate (DPWA) was added in proportions (0.1%, 0.2%, 0.3%, 0.4% and 0.5%) to the mixture in relation to the global dry mixture, then it was mixed manually. The mixture was placed in the mold and compacted immediately with a static loading by applying compacting stress of 10 MPa. Finally, the specimens were cured in an oven for 7 days at 65 ± 2 °C.

Fig.3. 10. Cured specimens in the oven.

❖ **DPM and DPS**

In the DPM and DPS types of waste, the same steps mentioned in the first type (DPWA) for making samples were done while maintaining the same proportions to do the comparison. However, the mixture of CEB was placed in the mold in two layers, and the DPM and DPS waste were introduced between the two layers. Each DPS equal to 0.1% of the total dry weight of CEB, i.e., equals 2 g. One DPS was placed in the mixture at 0.1% and with every 0.1% increase, one DPS was also increased.

Fig.3. 11. Compressed Earth Bricks (CEBs) manufactured in this study.

Table.3. 10. Formulation of CEB samples incorporated by Date Palm Waste (DPW).

Soil (%)	70	70	70	70	70	In relation to the dry mixture (soil–sand)
Crushed sand (%)	30	30	30	30	30	In relation to the dry mixture
DPW (%)	0.1	0.2	0.3	0.4	0.5	In relation to the global dry mixture
Quicklime (%)	12	12	12	12	12	In relation to the global dry mixture
Water (%)	14	14	14	14	14	In relation to the global dry mixture

3.4 Tests conducted

3.4.1 Dry and wet compressive strength test

In order to evaluate the simple compressive strength of the CEB blocks in the wet and dry state, the compressive strength test was carried out according to standard XP P 13-901. In this test, two half-blocks superposed and adhered by a joint of cement mortar were subjected to a simple compression until rupture. In the wet compressive strength test, the sample of the test was humidified by complete immersion for 2 hours, and then the sample was subjected to a simple compression until rupture.

Fig.3. 12. Experimental setup of compressive strength test.

3.4.2 Three-point bending test

A universal testing machine MTS 50 KN (MTS criterion model 45) controlled by a computer was used to study the mechanical behavior in three-point bending as can be seen in Figure. A high precision load cell with a capacity of 50 kN is used for recording the load. The specimens were loaded in bending to failure at a deflection rate of 1mm/min to ensure steady deflection and recorded easily. This procedure made it possible to draw Load–deflection diagrams, which allowed following the mechanical behavior of the material under bending at different DPWA contents (flexural strength and modulus of elasticity calculated from the linear part of the Load–deflection data). The three-point bending test was carried out on samples with dimensions (10cm x 20cm x 5.5±0.5cm), and the loading was applied at a rate of 1 mm/min. The flexural stresses (σ_f) and the elastic modulus (E) were calculated using the equations below[25]:

$$\sigma_f = \frac{3FL}{2bh^2} \tag{3.1}$$

$$E = \frac{FL^3}{48I\delta} \tag{3.2}$$

Where F is the maximum load at failure (N), δ is the deflection caused by the load F, I is the moment of inertia of the section at mid-span, h is the height (mm) of the sample, b is the width (mm) of the sample, and L is the distance between the supports (mm).

Fig.3. 13. Experimental setup of three-point bending.

3.4.3 Thermal proprieties

The thermal conductivity (λ) and the volumetric heat capacity (C) were measured using the Hot Disk device at the Laboratory of Civil Engineering Research, University of Laghouat, Algeria (Fig. 3.14). The hot disk technique has proven to be a very efficient and accurate method for measuring the thermal conductivity, specific heat, and thermal diffusivity of heterogeneous and homogeneous materials [122]. This test was carried out on samples with dimensions of 4 cm x 4 cm x 2 cm. The thermal diffusivity (α), thermal effusivity (e) ,and specific heat (Cp) were determined by the following expressions [123]:

$$\alpha = \frac{\lambda}{c} \qquad\qquad (3.3)$$

$$e = \sqrt{\lambda\,C} \tag{3.4}$$

$$Cp = \frac{C}{\rho} \tag{3.5}$$

where λ is the thermal conductivity(W.m^{-1}.K^{-1}); e is the thermal effusivity (J.s$^{-1/2}$.m^{-2}. K^{-1}); C is the volumetric heat capacity (J.m^{-3}.K^{-1}); ρ is the bulk density (Kg/m^3); Cp is the specific heat (J.kg^{-1}.K^{-1}); and α is the thermal diffusivity (m^2.s^{-1}).
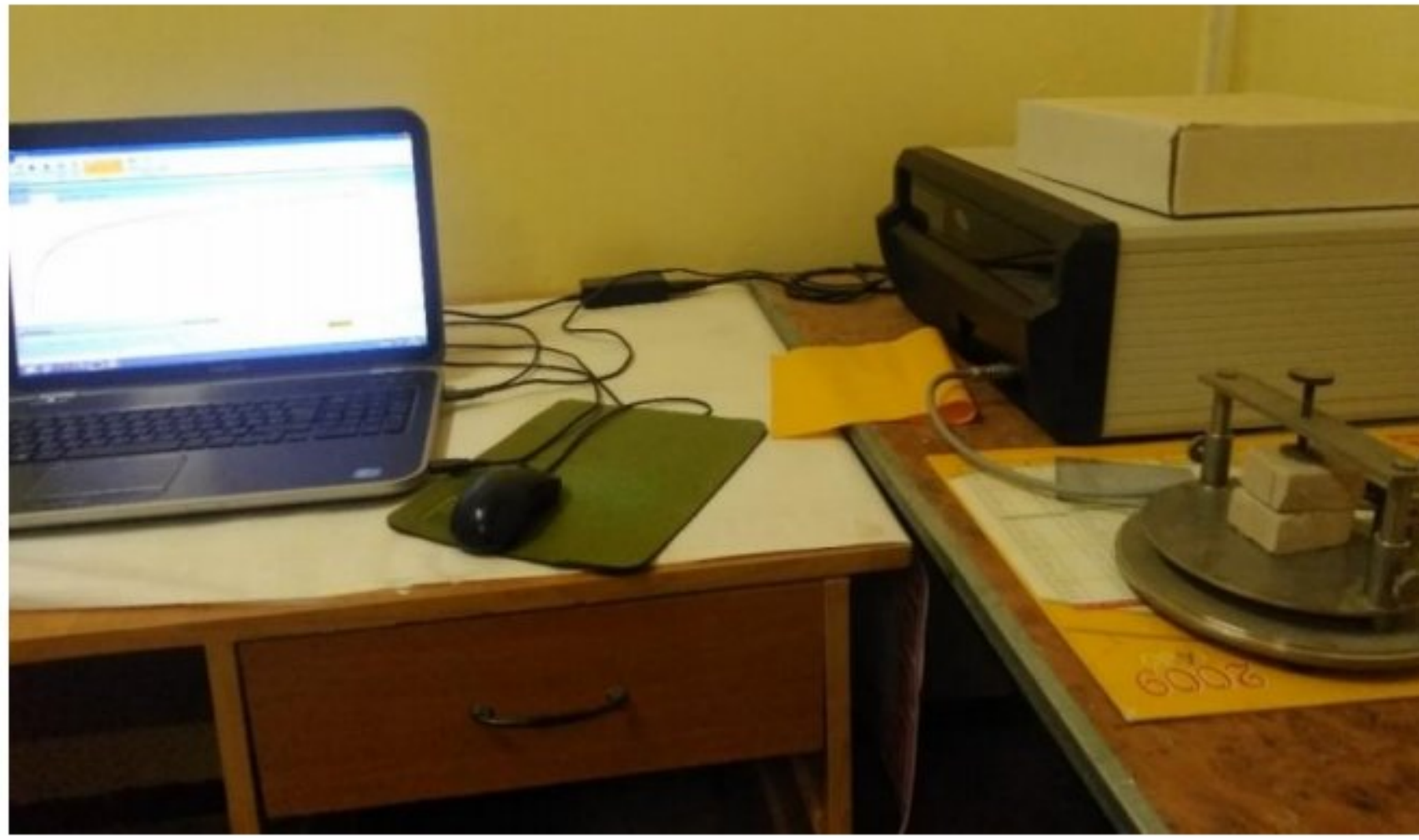
Fig.3. 14. Experimental setup of thermal properties.

3.4.4 Scanning electron microscopy and Energy-dispersive X-ray spectroscopy (*SEM-EDX*)

The *SEM-EDX* technique was used to perform a microscopic examination of the samples, with and without DPWAs, at the Laboratory of Physics of Thin Films and Applications (LPCMA) of the University of Biskra (Algeria) for the purpose of confirming the recorded macroscopic properties and examining the cohesion between the date palm waste aggregates (DPWAs) and the matrix of the samples.

3.4.5 Ultrasonic pulse velocity test (UPV)

The incorporation of the date palm waste into the compressed earth block affects the compactness and voids. In order to assess the effect of date palm waste on the compactness and also acoustic comfort of the samples, the ultrasonic pulse velocity test (non-destructive test) was performed according to standard NF EN 12 504-4. The two poles were held on either side of the block (100 mm x 200 mm x 50 mm) and the pulse velocity and transmission time were read.

Fig.3. 15. Ultrasonic pulse velocity test (non-destructive test) of CEBs blocks.

3.4.6 Capillary Absorption

This test was performed according to standard XP P 13-901. The sample was partially immersed to a depth of 5 mm for 10 min. The water absorption coefficient was calculated from the following formula:

$$Cb = 100 \text{ x } \frac{(M_1 - M_0)}{S\sqrt{t}} \tag{3.6}$$

where Cb is the capillary water absorption coefficient (g/cm min$^{1/2}$), M_1 and M_0 is the weight of the sample after and before immersion in water respectively (g), t is the immersion duration (min), and S is the surface of the face submerged of the sample (cm^2)

3.4.7 Total water absorption

To ensure that the CEB samples have good resistance and durability against water, this test was performed. The samples were immersed in a water bath for: 1, 2, 3 and 4 days. The weights of the wet samples were calculated after taking them out of the water. The relative difference between dry and wet weight of block was calculated to obtain the water absorption percentage of the sample shown in the following formula:

$$A (\%) = 100 \text{ x } \frac{(W_h - W_s)}{W_s} \tag{3.7}$$

where Wh is the wet weight of the block, while Ws is the dry weight of the block.

3.4.8 Swelling test

The swelling test was performed according to standard XP P 13-901. The samples were placed in water during 1, 2 and 3 days. The distance between two pre-installed studs was measured after drying the samples for about 10 minutes. The swelling percentage of the sample was calculated using the following formula:

$$\text{Swelling (mm/m)} = \frac{(l_1 - l_0)}{l_0} \qquad (3.8)$$

where l_0 and l_1 are the distances before and after immersion respectively.

Fig.3. 16. Total water absorption and swilling test.

3.4.9 Bulk density (ρ)

The density of each sample was calculated according to the following formula:

$$\text{Bulk density} = \frac{M}{V} \qquad (3.9)$$

Where M is the dry mass of the sample in (kg) and V is the volume of the sample in (m^3).

Fig.3. 17. Measuring the weight of block for density.

3.4.10 Dynamic modulus

The dynamic modulus of elasticity is obtained from the following expression[124], [125]:

$$E_d = \frac{V^2 \rho}{g} \times 10^{-2} \qquad (3.10)$$

Where E_d is the dynamic modulus of elasticity (GPa), V is the UPV (km/s), g is the acceleration due to gravity (9.81 m/s^2), and ρ is the density of the material (kg/m^3).

3.4.11 Digital Image Correlation (DIC) technique in measuring strain using open source Ncorr

3.4.11.1 DIC samples preparation:

One of the samples surfaces was scrubbed and was cleaned thoroughly to remove the dirt. Before the testing, the DIC samples were prepared and covered using a white paint and sprayed with a black aerosol to create a random speckle pattern, which was used for the DIC analysis.

Fig.3. 18. Sample ready for DIC test.

3.4.11.2 Fundamentals of 2D DIC

Measurement of strains under bending loads is considered complicated compared to tensile or compressive loads. This is because flexural loads result in two types of strains, tensile strains and compression strains. For this reason, this study was based on the modern method using the digital image correlation method (DIC) to measure the strains resulting from the bending loads. The three point bending tests implemented to measure strains of CEBs were also performed using open source 2D digital image correlation (DIC) software[109] analyses based on high resolution images taken by a CANON 1300D digital camera (18 Megapixels resolution). During the tests images were taken every 1 second over specimens that had been painted with a white background and a

random black paint pattern (speckle pattern).Then, images were analyzed using MATLAB and the Ncorr 2D-DIC toolbox to estimate displacements and strains fields.

Surface deformation measurement of materials and structures subjected to diverse loadings (e.g. mechanical or thermal) is a crucial problem in experimental solid mechanics. In addition to the widely used pointwise strain gauge technique, various full-field non-contact optical technologies, such as digital image correlation (DIC), have been developed and utilized for this purpose[126]. In the field of experimental mechanics, digital image correlation (DIC) is an effective and practical technology for full-field deformation measurement, which has been commonly accepted and widely used[110], [127]. Displacements are directly detected from digital images of an object's surface (specimen) in two-dimensional DIC. Fig. 3.19 shows a typical example of an experimental setup for two-dimensional DIC. A camera with an image lens is used to observe an object's planar surface. Then, the images on the surface of the object, one before and another after deformation, are recorded, digitized and stored as digital images in a computer.
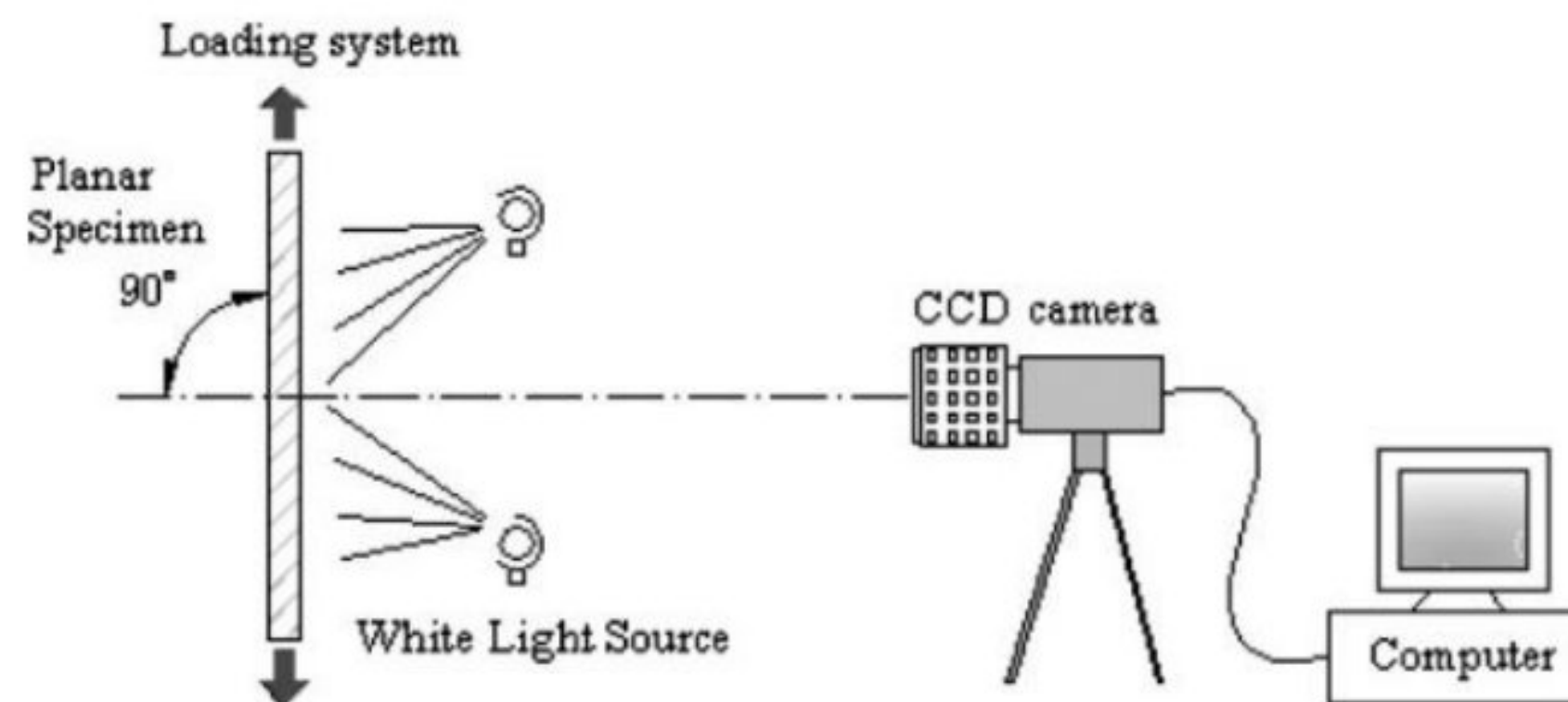
Fig.3. 19. Setup for strain measurement by the 2D DIC method[126].

The displacement of the subset on the image before deformation is found in the image after deformation by searching the area of same light intensity distribution with the subset. Once the location of this subset in the deformed image is found, the displacement of this subset can be determined. In order to complete this process, the object's surface must have a feature that allows the subset to be matched. If no feature is observed on the surface of the object, an artificial random pattern must be applied. Fig.3.18 shows a typical example of the random pattern on the surface of an object created by spraying paint[128]. In subset-based DIC algorithms, the reference image is partitioned into smaller regions referred to as subsets or subwindows. The deformation is assumed

to be homogeneous inside each subset, and the deformed subsets are then tracked in the current image. In Ncorr, subsets are initially a contiguous circular group of points that are on integer pixel locations in the reference configuration. The transformation of the coordinates of these points from the reference to the current configuration is constrained to a linear, first order transformation[109].
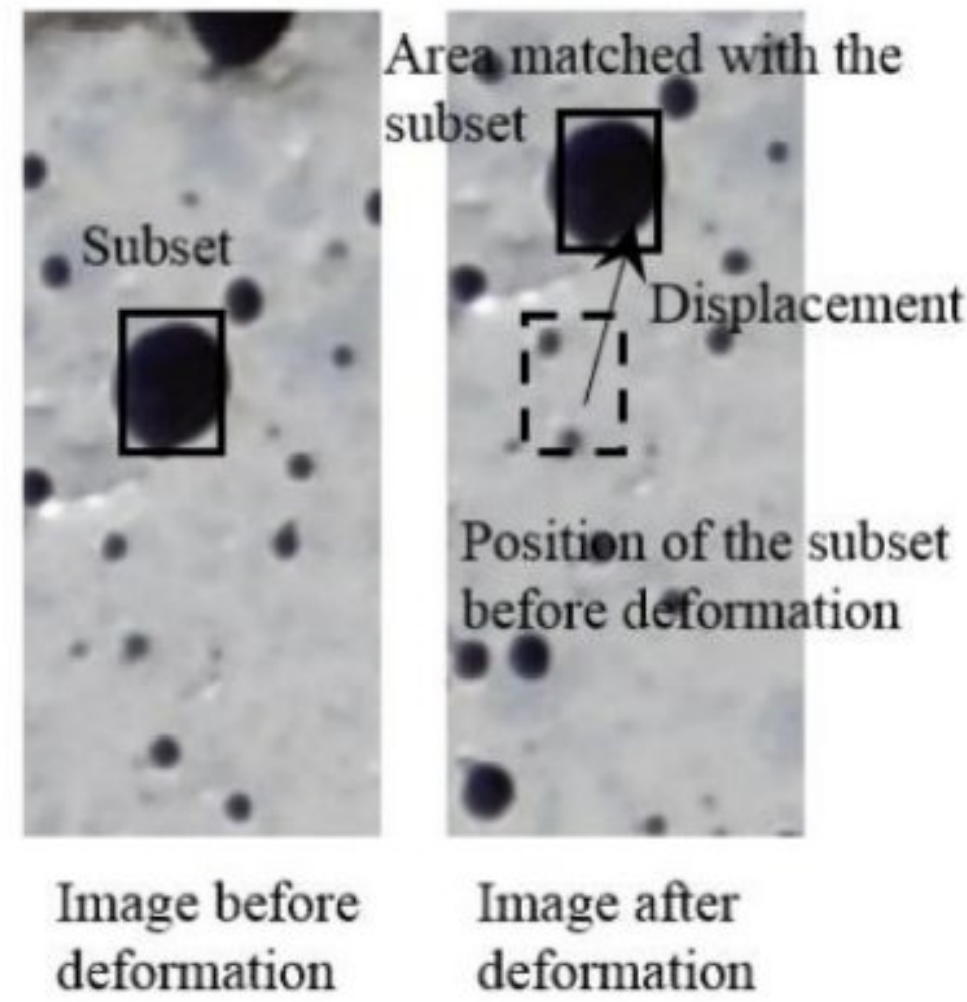
Fig.3. 20. Matching the subset before and after deformation[129].
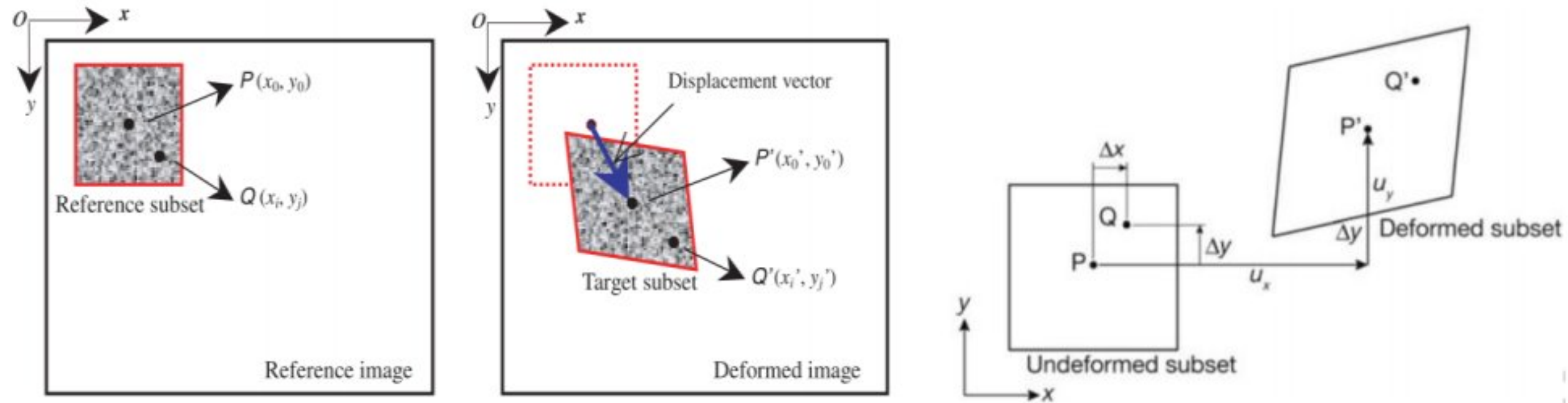
Fig.3. 21. Schematic illustration of a reference square subset before deformation and a target (or deformed) subset after deformation[126], [128].

Several functions exist to match the subset from one image to another based on the above fundamental principle. One is the magnitude of intensity value difference as:

$$\mathbf{R}\ (\mathbf{x, y, x^*, y^*}) = \sum |\mathbf{F}\ (\mathbf{x, y}) - \mathbf{G}\ (\mathbf{x^*, y^*})| \qquad (3.11)$$

and another is the normalized cross-correlation as:

$$\mathbf{C}\ (\mathbf{x, y, x^*, y^*}) = \frac{\sum \mathbf{F}\ (\mathbf{x,y})\ \mathbf{G}\ (\mathbf{x*,y*})}{\sqrt{\sum \mathbf{F}\ (\mathbf{x,y})^2 \sum \mathbf{G}\ (\mathbf{x*,y*})^2}} \qquad (3.12)$$

where F(x, y) and G(x*, y*) represent the gray levels within the subset of the undeformed and deformed images, and (x, y) and (x*,y*) are the coordinates of a point on the subset before and after deformation, respectively. The symbol of the summation represents the sum of the values within the subset. The coordinate (x*,y*) after deformation relates to the coordinate (x, y) before deformation. Therefore, displacement components are obtained by searching the best set of the coordinates after deformation (x*,y*) which minimize R(x, y, x*,y*) or maximize C(x, y, x*,y*). There are many functions except for equations (3.11) or (3.12) can be used, however, the normalized cross-correlation (Eq. (3.11)) is widely used for matching the subset in digital image correlation[128].
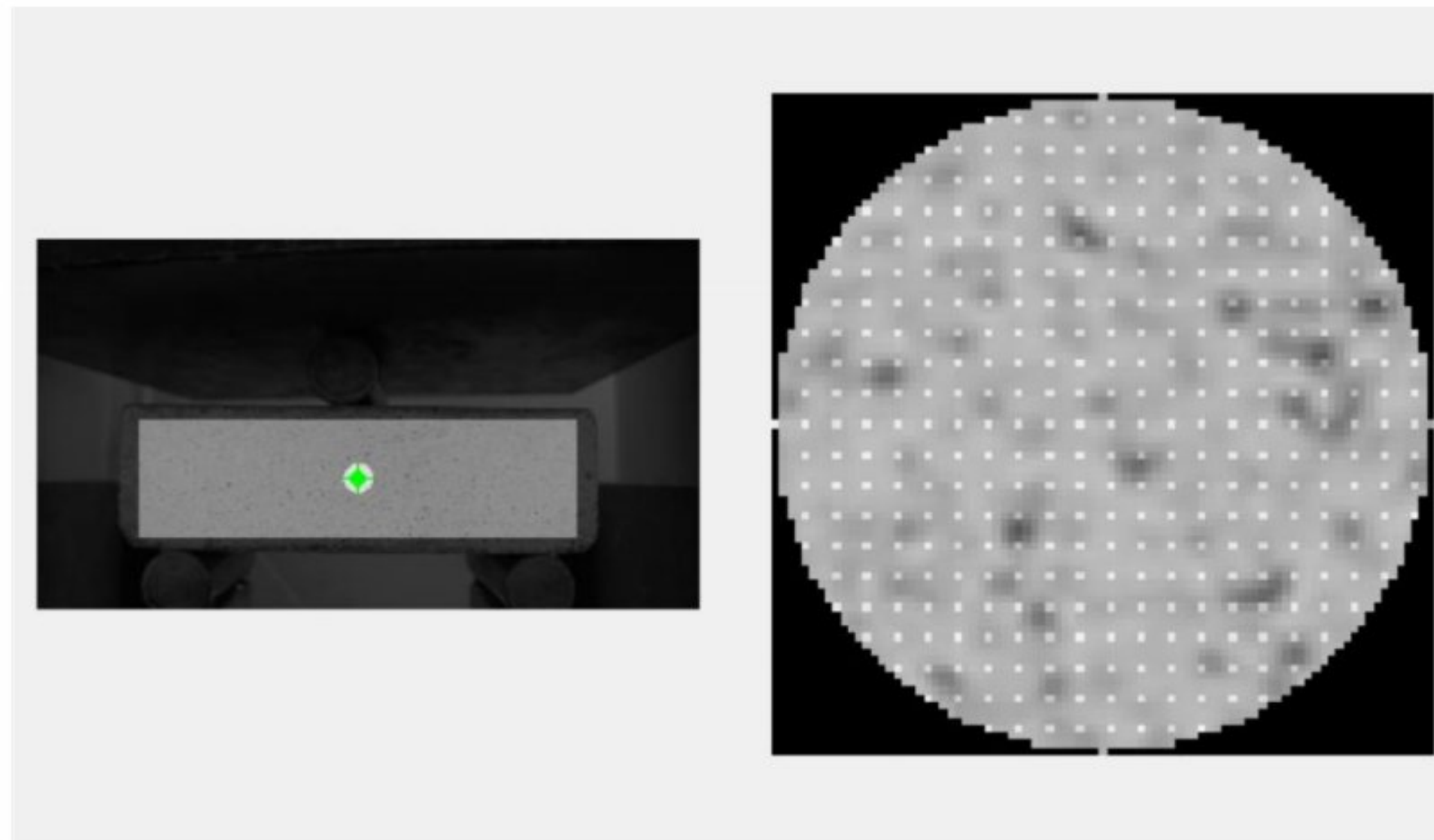
Fig.3. 22. Subset location of the tested specimen.

Strains are more difficult to resolve than the displacement fields because strains involve differentiation, which is sensitive to noise. This means any noise in the displacement field will magnify errors in the strain fields. The values of the strain computation available for in plane space are ε_{xx} (transverse direction), ε_{yy} (force direction), and ε_{xy}. Ncorr uses the Green- Lagrangian strains[109], which are obtained by using the three displacement gradients as follows:

$$\varepsilon_{xx} = \frac{1}{2}\left(2\frac{\partial u}{\partial x} + \left(\frac{\partial u}{\partial x}\right)^2 + \left(\frac{\partial v}{\partial x}\right)^2 \right) \tag{3.13}$$

$$\varepsilon_{yy} = \frac{1}{2}\left(2\frac{\partial v}{\partial y} + \left(\frac{\partial u}{\partial y}\right)^2 + \left(\frac{\partial v}{\partial y}\right)^2 \right) \tag{3.14}$$

$$\varepsilon_{xy} = \frac{1}{2}\left(\frac{\partial v}{\partial x} + \frac{\partial u}{\partial y} \quad \frac{\partial u}{\partial x}\frac{\partial u}{\partial y} + \frac{\partial v}{\partial x}\frac{\partial v}{\partial y} \right) \qquad (3.15)$$

Where (u, v) are the displacements of a point on (x, y) respectively.

When both strains and rigid body rotations are small, the quadratic terms in the Green-Lagrange strain tensor can be ignored. This leads to the well-known engineering strain tensor.

In general, the implementation of the 2D DIC method comprises the following three consecutive steps, namely (1) specimen and experimental preparations; (2) recording images of the planar specimen surface before and after loading; (3) processing the acquired images using a computer program to obtain the desired displacement and strain information[126]. The use of DIC using the Ncorr 2D-DIC toolbox to estimate the strain fields for each sample is summarized in the following points:

1. Running Ncorr program from MATLAB.
2. The reference image is loaded at zero load. The reference image means the initial/first image taken of the sample before any deformation occurs (Set Reference Image).
3. The current image(s) are loaded based on the entire force loading used for the experiment (Set Current Image(s)). (Example: Image 1 for 50N, image 2 for 100N until the force is measured).
4. Region of Interest is drawn based on the area of gauge and strain field to be determined (Set Region of Interest (ROI)).
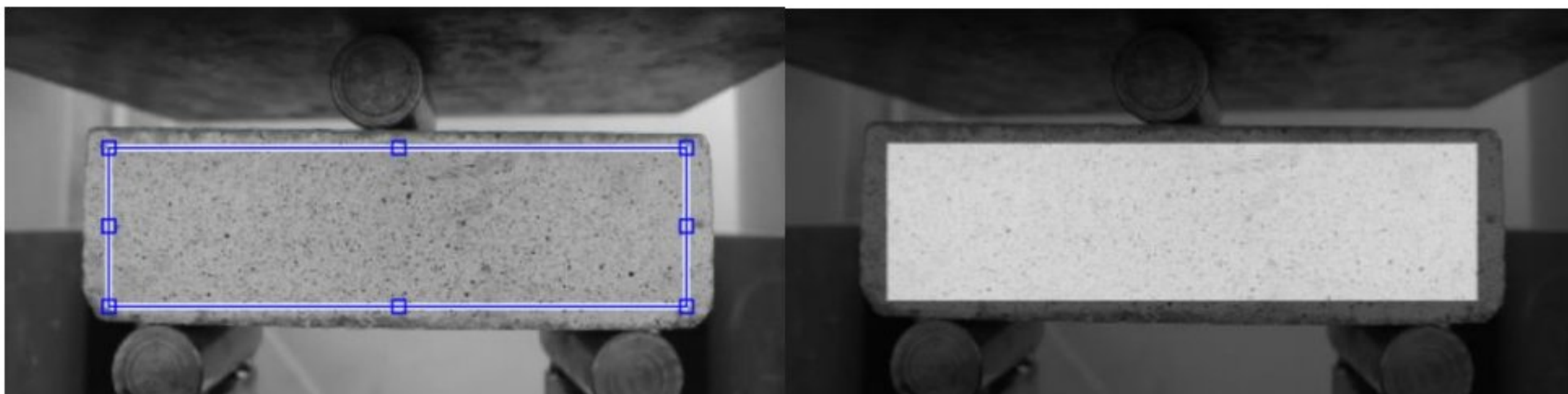
Fig.3. 23. Region of Interest (ROI) of the tested specimen.

5. Set DIC Parameters. The necessary parameters are entered at this stage before processing and calculations begin.
6. DIC Analysis. Processing and calculations begin at this step.

7. Format Displacements. The vertical and horizontal displacement forms are displayed after the processing is completed.

8. Calculate Strains. The strains can be calculated after the displacement is obtained.

3.5 Conclusion

This chapter focused on presenting the basic raw materials used in this study and their chemical, physical and mechanical properties. The proportions for the formulation compressed earth blocks, and the results of the characterization of raw materials were presented, as well as the methods and standards used to characterize the blocks manufactured from date palm waste, soil and crushed sand, which were stabilized with quicklime and cured in the oven.

CHAPTER 4

RESULTS AND DISCUSSION

Chapter 4: Results and discussion

4.1 Introduction

The previous works' synthesis has highlighted the need for further research into the effects of introducing fibers and aggregates extracted from plant wastes such as palm wastes, which are considered waste with no economic value, on the thermos-physical, microstructural, and mechanical behavior of compressed earth bricks. After defining the methods used in preparing and characterizing the properties of the composite materials produced in this work and identifying the physical, chemical, and mechanical properties of the basic raw materials. The results obtained through experimental laboratory work will be presented and analyzed in this chapter to understand the effect of incorporating date palm waste on the macroscopic properties and microstructural analyses. Microscopic analysis is carried out in order to confirm the apparent results of the effect of adding plant fibers and bio-aggregates.

4.2 Lime content optimization in CEB

In order to find the optimum value of lime in the blocks, the compressive strength as a function of lime content was carried out, as shown in the Fig.4.1. Compression strength is the most important mechanical property of brittle materials. The results shown in the Fig.4.1 showed a variation on compressive strength between 1.81 MPa and 6.62MPa. It is clear that the increase in the lime content from 7% to 12% leads to an increase in compressive strength value of about 72.60%, but after from 12% to 13% there is a reduction in resistance of 39.52%. This type of results was also noted by Millogo et al[13].The optimum compressive strength value is found in 12% of the lime content. The development of calcium silicate hydrates (CSH) and formation of minor amounts of portlandite ($Ca(OH)_2$)and calcite ($CaCO_3$)leads to improvement of the mechanical properties and the compactness of CEB. CSH is originated from the chemical reaction between SiO_2 (fine grains of quartz) and CaO (quicklime).However, higher quicklime additions (>12 %) have negative effects on the mechanical properties of CEB[13].
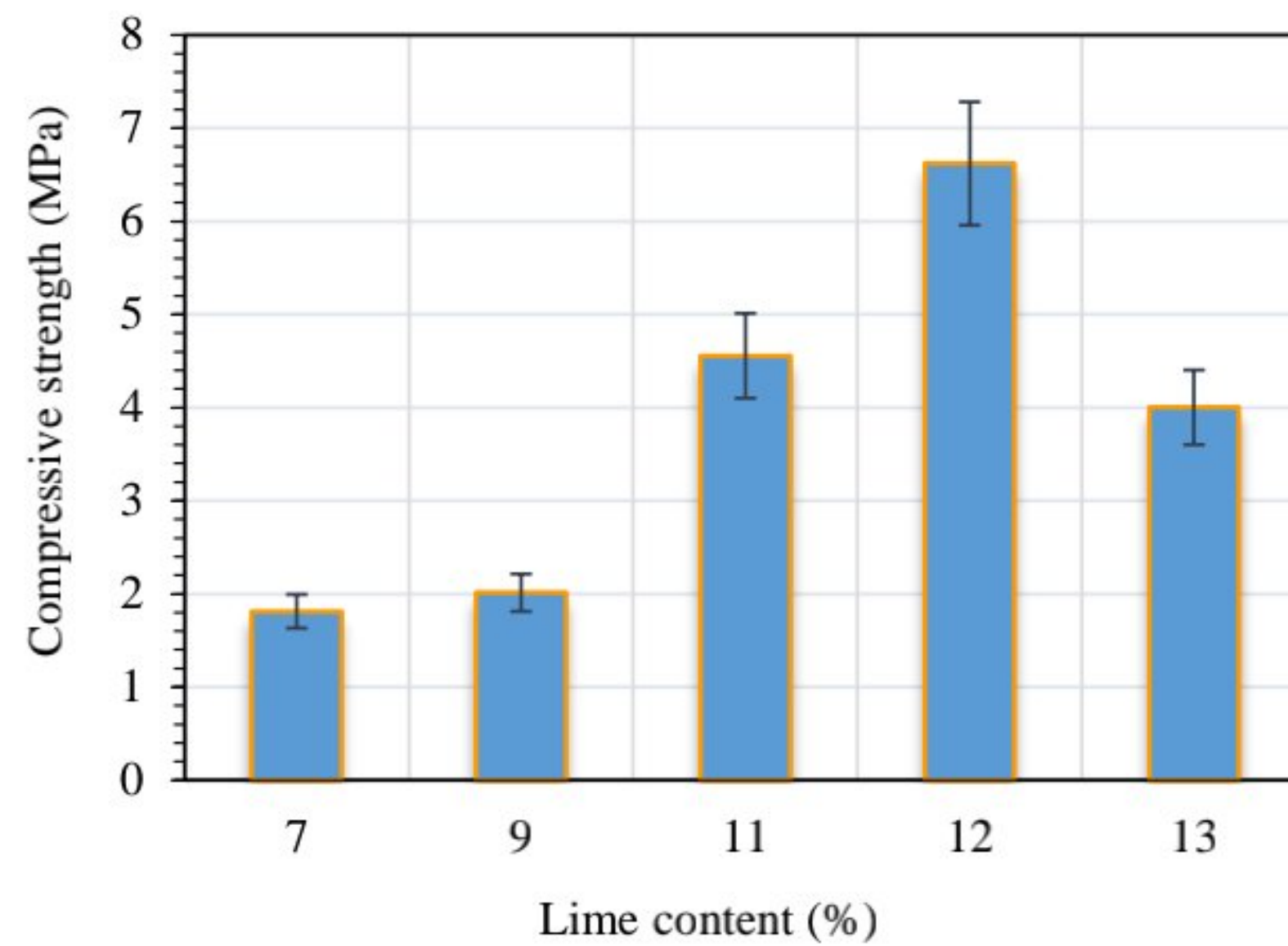
Fig 4. 1. Dry compressive strength as a function of lime content of the CEB (with 2 MPa of compaction pressure).

4.3 Effect of DPWA content on the mechanical behavior and microstructure of CEB

Fig. 4.2 presents the dry and wet compressive strengths of CEB incorporating date palm waste aggregates (DPWAs). It turned out that the compressive strength of the CEB sample without DPWAs was greater than that of all the other samples. In addition, the dry compressive strength values ranged from 9.81 to 15.84 MPa. It was found that when the DPWA content increased from 0% to 0.5%, the compressive strength of the blocks went down. This result was also reported by Chikhi et al. [24] who explored the effect of date palm fiber content on the gypsum-stabilized composite material. These same researchers indicated that when the fiber load of the composite increased the area of the interface between the fiber and matrix became larger, which engendered a smaller compressive strength value. The compressive strength drop was attributed to the addition of plant aggregates which have low compressive strength and stiffness [101]. It was shown that, in contrast with the block without DPWAs, increasing the DPWA content from 0.1% to 0.5% caused the compressive strength of the block to decrease from 15.03% to 38.09%.

On the other hand, the wet compressive strength test was carried out to investigate the effect of moisture coming from rain, flooding or groundwater upwelling. Fig. 4.2 clearly illustrates the relationships between the wet compressive strength and DPWA content. It was observed that the wet compressive strength value ranged from 5.65 to 10.03 MPa. Based on this finding, one may notice that the wet compressive strength decreases when the DPWA content increases. Unlike the block without DPWA, increasing the DPWA content from 0.1% to 0.5% caused the wet compressive strength to drop from 19.68% to 43.71%. This result may be attributed to the increase in void volume as a result of the incorporation of plant aggregates into the compressed earth block composite. When the blocks were entirely immersed, the voids were filled with water, and consequently the wet compressive strength gradually decreased as the DPWA content augmented. Note also that the void ratio and water absorption increased progressively when the DPWA level increased.

Furthermore, Fig. 4.2 illustrates the effect of DPWAs on the dry-to-wet compressive strength (DCS/WCS) ratio. Note that the CEB (DCS/WCS) ratio increases when the DPWA content grows. This same figure suggests that the highest value of the (DCS/WCS) ratio is equal to 1.88, and the recommended value for that ratio must not be greater than 2. These findings have also been encountered in numerous studies reported in the literature [18], [19]. The higher (DCS/WCS) ratio can certainly be attributed to the higher water absorption when the DPWA content increases. Moreover, a larger water absorption ratio in CEB engendered a remarkable decrease in the wet compressive strength, which caused the (DCS/WCS) ratio to augment. In addition, moisture inside the block pores induced water absorption and therefore the dispersion of the unstabilized soil grains [130].

The load–deflection curves of all the samples under study are depicted in Fig. 4.3. It was observed that all the blocks exhibited a linear elastic behavior until reaching the maximum load which was followed by brittle failure without any residual strength. It should be noted that the ultimate deflection was high for the blocks containing DPWA, especially those with 0.5% DPWA.

The test results of the elastic modulus are all summarized in Fig. 4.4 and Table 4.1. It was noted that the elastic modulus of CEB follows the same trend as the flexural and compressive strength, as can be seen in Fig. 4.2 and Fig. 4.4. This elastic modulus was equal to 809.37 MPa and 321.52 MPa for the control sample (0% DPWA) and the composite sample incorporating 0.5%DPWA, respectively. It is worth noting that the elastic modulus dropped when the percentage of replacement of natural soil and sand by date palm waste increased. Furthermore, the percentage decrease in the elastic modulus was about 11.33%, 37.71%, 41.46%, 58.04% and 60.27% for CEB containing 0.1% DPWA, 0.2% DPWA, 0.3% DPWA, 0.4% DPWA and 0.5% DPWA, respectively, in comparison with the reference CEB (0% DPWA). The literature review [101] indicated that the incorporation of plant particles into composite materials engendered lower values of the elastic modulus. In this context, Laborel-Préneron et al. [101] found out that the elastic modulus decreased with the incorporation of plant aggregates. It was also revealed that the lowest modulus of elasticity corresponded to the highest percentage of plant aggregates (DPWAs). It is widely acknowledged that the bending strength is one of the most important mechanical properties of materials. Table 4.1 and Fig. 4.4 show the effect of DPWAs on the flexural strength of CEB. It was shown that the CEB flexural strength values decreased as the DPWA content went up. Moreover, the flexural strength value ranged from 4.37 to 5.48 MPa. In comparison with CEB without DPWA, when the DPWA content increased from 0.1% to 0.5%, the flexural strength dropped from 4.01% to 20.25%. These findings are consistent with those previously published in the literature [101].

On the other hand, Taallah et al. [18] found out that the decrease in dry and wet compressive strength and flexural strength could be attributed to the weak adhesion between plant aggregates and matrix due to the decompression of CEB following unloading during its manufacture, because the plant aggregates have an elastic behavior. As illustrated in Fig. 4.5, the weak bond between date palm aggregates and the matrix engendered a higher porosity. This same figure shows the SEM images of three CEB samples with and without waste fibers. In addition, useful information about the adhesion status at the interface between DPWA aggregates and the matrix of the material is provided on that figure where voids between the date palm waste aggregates and the matrix can be observed. These voids were engendered by the shrinkage of DPWAs after drying inside the block and to the weak bond between the plant aggregates and the matrix. It should be noted that the presence of these voids were responsible for the compressive and flexural strength drop, and for the decrease in the elastic modulus as well.

Furthermore, the energy dispersive X-ray (EDX) spectroscopy allowed determining the percentages of hydrate products within the material, as seen in Fig.4.6. The results obtained indicated that incorporating DPWA aggregates induced a decrease in calcium silicate hydrates C-S-H (measured as Si). Note that the drop in Si content engendered a lower C-S-H level. Likewise, the amount of Ca in the blocks containing DPWA also decreased, as depicted in Fig. 4.6, and it is responsible for long-term carbonation ($CaCO_3$) process.

The decrease in the elastic modulus, flexural and compressive strength may be attributed to the considerable decrease in the amounts of C-S-H within blocks, which in turn are responsible for the strength of the blocks. It should be noted that the amounts of C-S-H dropped as a result of the decrease in grains mass of SiO_2 and Ca within the mixture, because part of soil and crushed sand were replaced by date palm waste aggregates (DPWA)[26].

The SEM - EDX observations and analyses allowed confirming the above mentioned results related to the mechanical properties of compressed earth blocks.
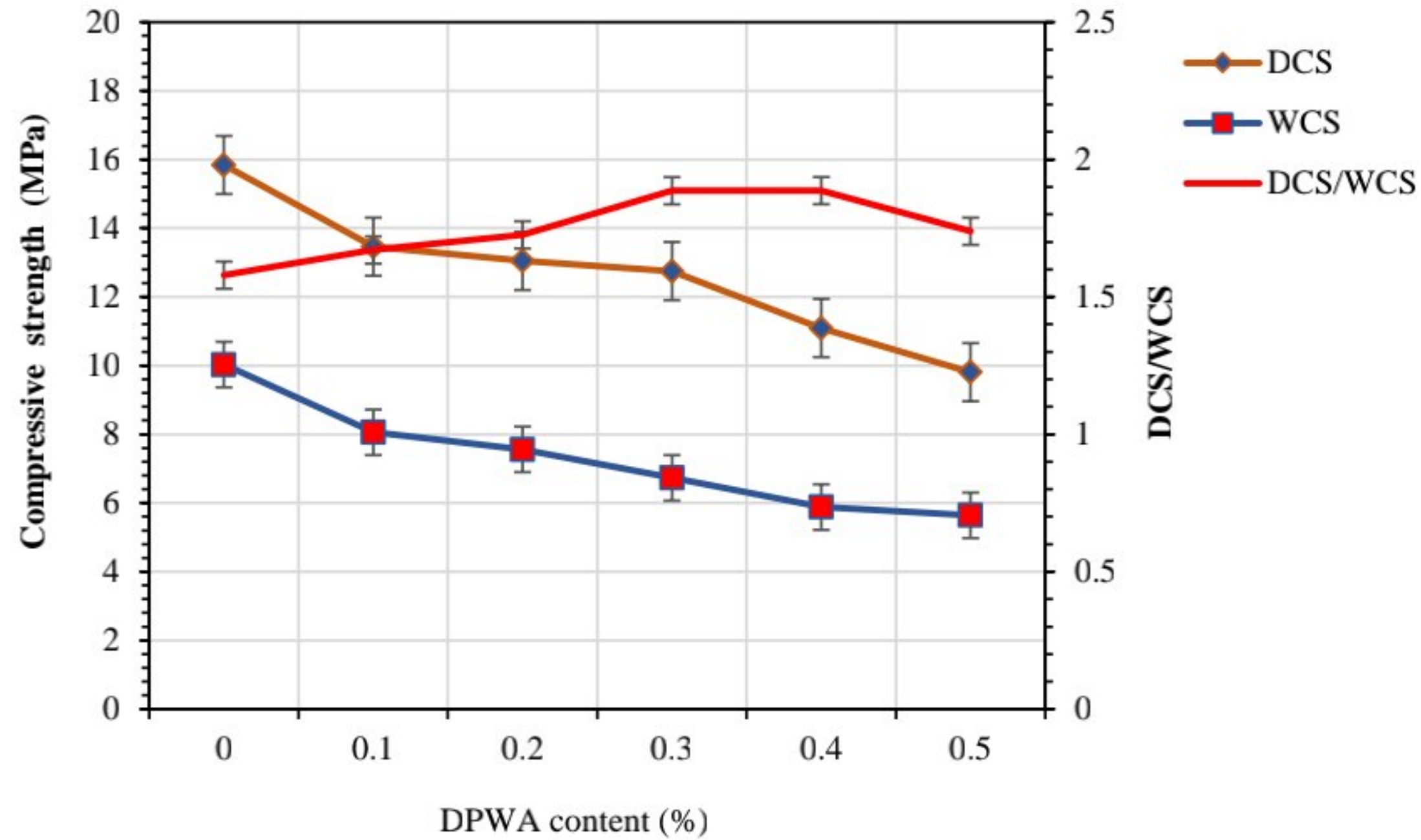
Fig 4. 2. Effect of DPWA content on dry (DCS) and wet (WCS) compressive strengths of CEB.
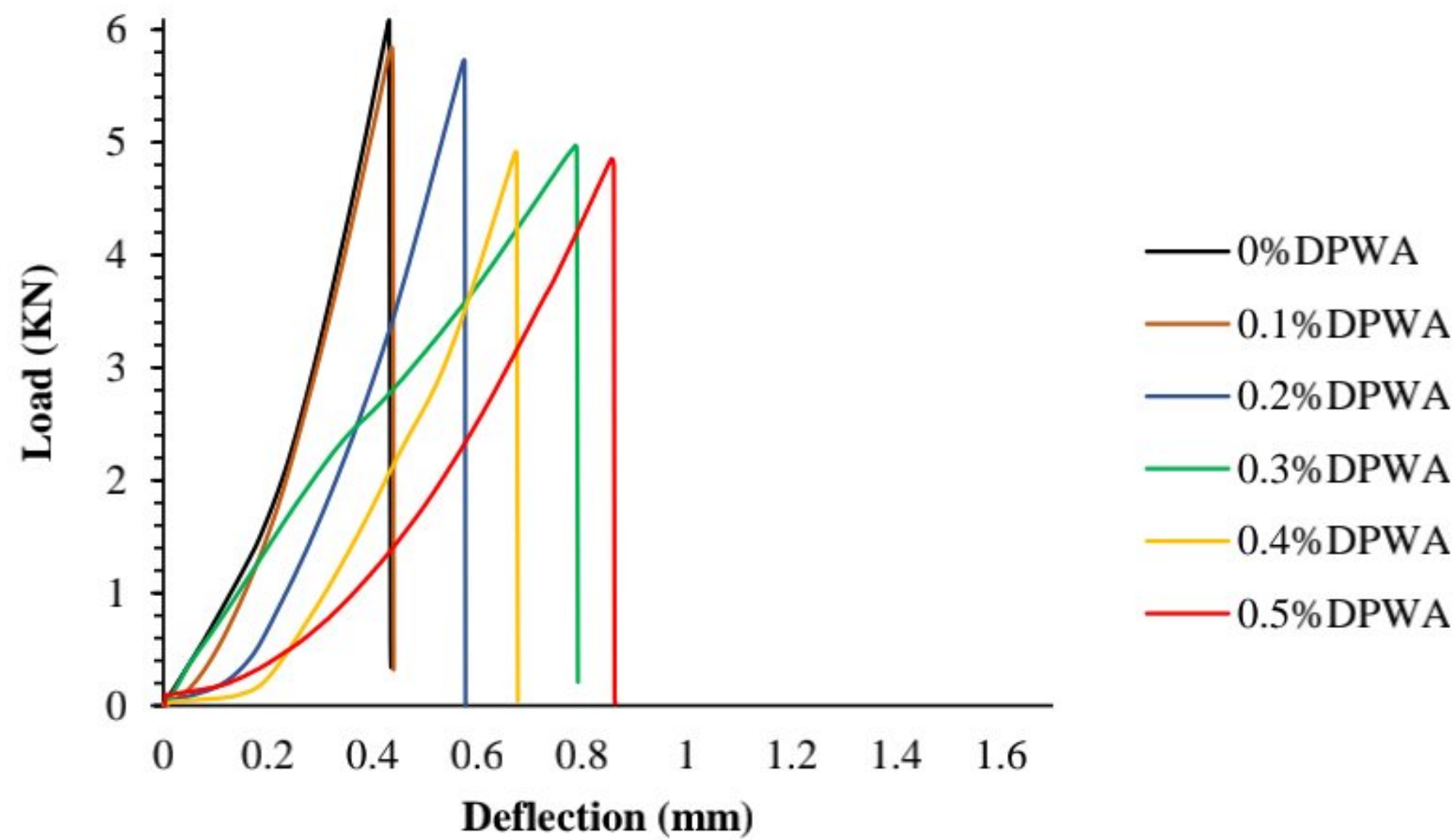
Fig 4. 3. Effect of DPWA content on the mechanical behavior of CEB: Typical load-deflection curves.
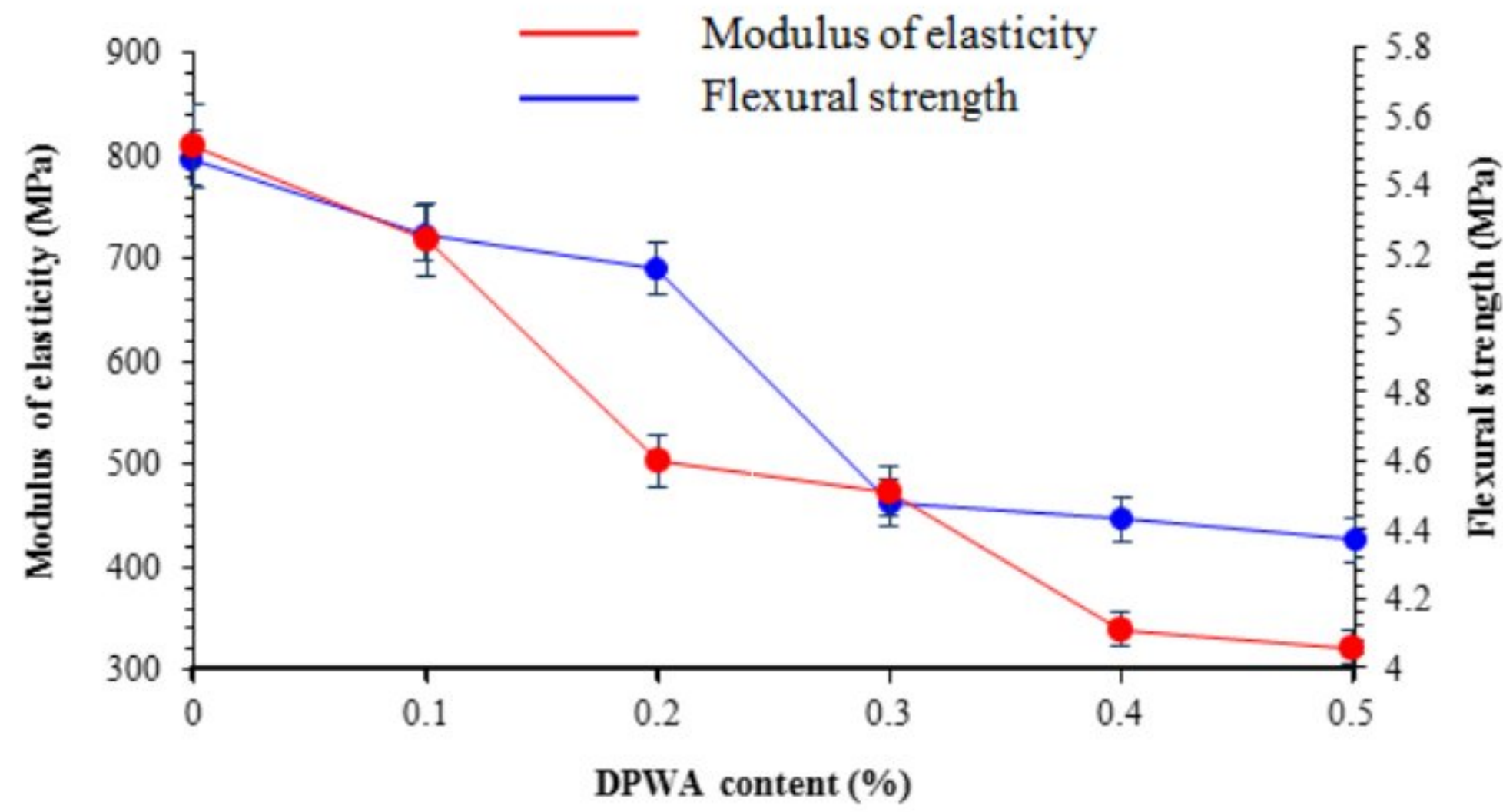
Fig 4. 4. Effect of DPWA content on the mechanical properties: elastic modulus and flexural strength of CEB.

Table 4. 1. Mechanical properties of the compressed earth blocks

DPWA content (%)	Flexural strength (MPa)	Modulus of elasticity (MPa)
0	5.48±0.14	809.37±44.23
0.1	5.26±0.20	717.59±34.88
0.2	5.16±0.11	504.13±23.05
0.3	4.48±0.26	473.79±31.28
0.4	4.43±0.34	339.57±56.51
0.5	4.37±0.09	321.52± 11.13
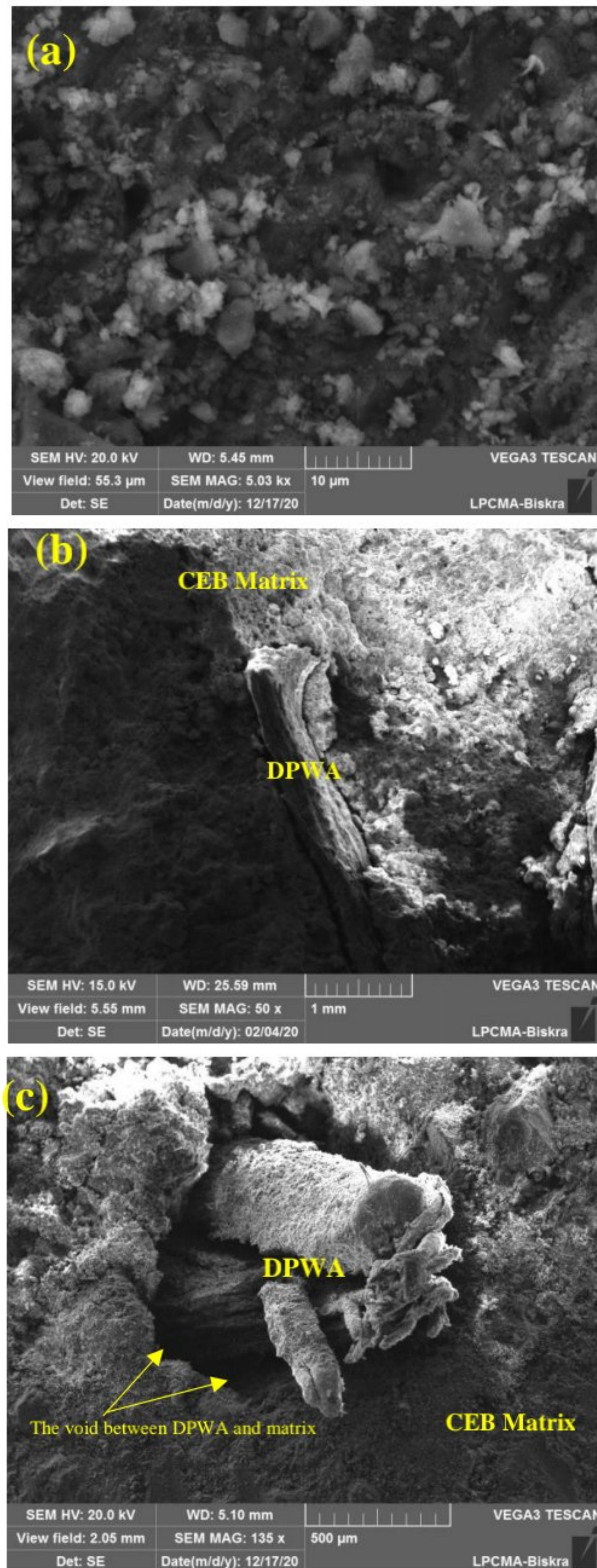
Fig 4. 5. SEM images of samples: (a) Without DPWA, (b, c) With DPWA.

```
cps/eV
(a)

El  AN  Series   unn. C norm. C Atom. C Error (1 Sigma)
                 [wt.%]  [wt.%]  [at.%]        [wt.%]
--------------------------------------------------------
O   8   K-series  29.86   46.32   65.93          4.09
Ca  20  K-series  23.37   36.25   20.60          0.71
Si  14  K-series   5.40    8.38    6.80          0.26
Al  13  K-series   2.04    3.17    2.67          0.13
Mg  12  K-series   1.62    2.51    2.35          0.12
Fe  26  K-series   1.19    1.84    0.75          0.07
K   19  K-series   0.99    1.53    0.89          0.06
--------------------------------------------------------
        Total:    64.47  100.00  100.00
```

```
cps/eV
(b)

El  AN  Series   unn. C norm. C Atom. C Error (1 Sigma)
                 [wt.%]  [wt.%]  [at.%]        [wt.%]
--------------------------------------------------------
O   8   K-series  34.31   51.75   70.40          4.56
Ca  20  K-series  21.71   32.76   17.79          0.67
Si  14  K-series   3.81    5.75    4.46          0.19
Mg  12  K-series   2.45    3.69    3.31          0.17
Al  13  K-series   2.29    3.46    2.79          0.14
K   19  K-series   0.97    1.46    0.81          0.06
Fe  26  K-series   0.74    1.12    0.44          0.06
--------------------------------------------------------
        Total:    66.29  100.00  100.00
```

Fig 4. 6. Energy-dispersive X-ray (EDX) spectroscopy of CEB: (a) Without DPWA, (b) With DPWA.

4.4 Effect of DPWA content on the ultrasonic pulse velocity

Fig. 4.7 depicts the results of the ultrasonic pulse velocity (UPV) test performed on CEB. One may easily see that the ultrasonic pulse velocity test values were affected by the integration of DPWAs. Indeed, it was found that the ultrasonic pulse velocity decreased as the DPWA content rose up; the UPV values passed from 2556.67 m/s (0% DPWA) to 2110 m/s (0.5% DPWA). Actually, the block including 0.5% DPWA showed the lowest ultrasonic pulse velocity value among all blocks; this value decreased by about 17.47% in comparison with the block without DPWA. This decrease may

98

certainly be assigned to the slower ultrasonic pulses when they pass through the air-filled pores resulting from the incorporation of date palm waste aggregates. It should be pointed out that the sound insulation coefficient of plant aggregates is higher than that of earth concrete or cement concrete.

Fig. 4.7 illustrates the evolution of the ultrasonic pulse velocity as a function of DPWA content. This variation may be expressed in the form of the equation below:

$$UPV = 2511.6 - 841.9 \, (DPWA) \qquad (4.1)$$
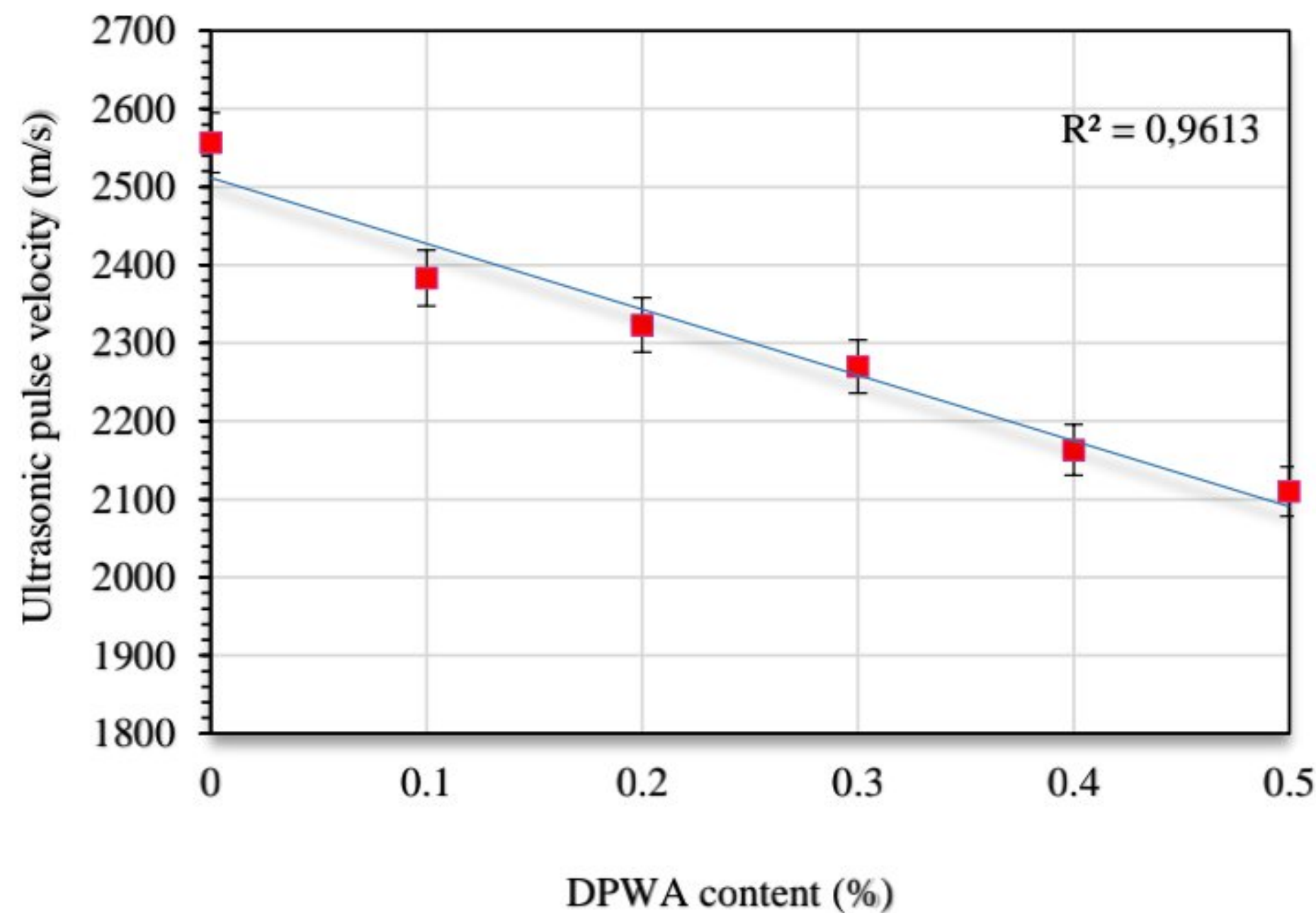
Fig 4. 7. Effect of DPWA content on the ultrasonic pulse velocity of CEB.

Further, the correlation between the dry compressive strength and ultrasonic pulse velocity of CEB is clearly depicted in Fig. 4.8. Note that the CEB dry compressive strength dropped when the ultrasonic pulse velocity (UPV) decreased; this can undoubtedly be attributed to the increase in CEB porosity following the incorporation of DPWA into the CEB mixture. In fact, it was found that when the CEB ultrasonic pulse velocity dropped from 2556.67 m/s to 2110 m/s, the dry compressive strength also decreased from 15.84 to 9.81MPa. As a matter of fact, when this UPV

diminished by 17.47%, the dry compressive strength dropped by 38.09%. Fig. 13 indicates, in fact, that there is a good correlation between the ultrasonic pulse velocity (UPV) of a compressed earth block and its dry compressive strength (DCS).

Fig. 4.8 clearly indicates that there is a linear relationship between the dry compressive strength (DCS) and the ultrasonic pulse velocity (UPV); it may be expressed as follows:

$$DCS = 0.0128\ (UPV) - 16.676 \qquad (4.2)$$
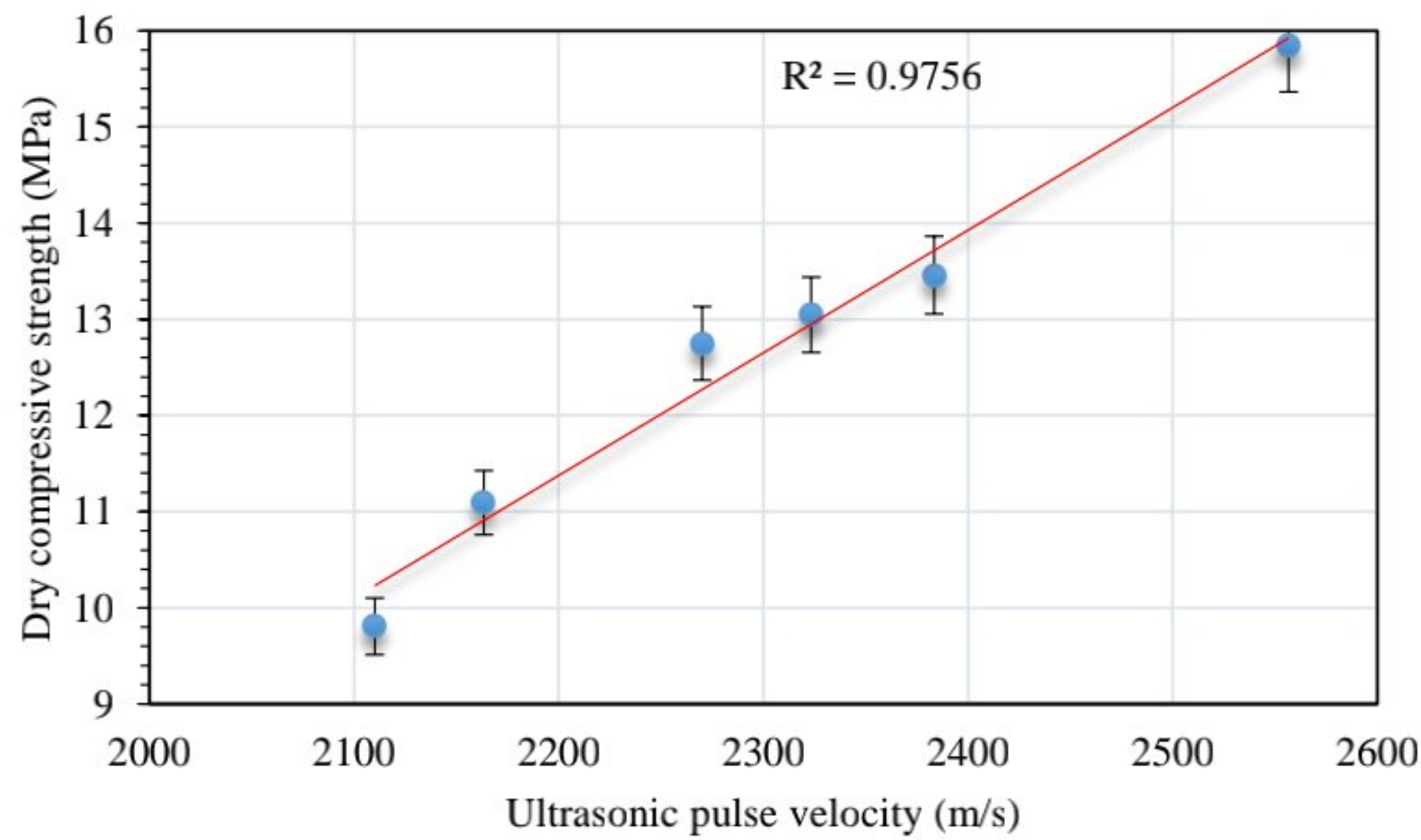
Fig 4. 8. Relationship between the dry compressive strength and ultrasonic pulse velocity of CEB.

4.5 Effect of DPWA content on the physical and thermal properties of CEB

4.5.1 Bulk density

Fig. 4.9 depicts the variation of the bulk density as a function of the DPWA content. It is clearly indicated that the bulk density decreased as the DPWA content increased. In this context, numerous authors reported that the bulk density decreased when plant fibers or plant aggregates were integrated into the formulation of the compressed earth blocks[19], [101]. Note also that increasing the DPWA content in the CEB mixture caused the bulk density to drop. Consequently, the low bulk density of plant aggregates induced a decrease in the CEB bulk density. It was found that the bulk

density value dropped from 2069.57 kg m^{-3} (0% DPWA) to 2033 kg m^{-3} (0.5% DPWA). As can be observed, these values are within the usual interval of CEB bulk density interval that ordinarily extends from 1800 to 2100 kg.m^{-3} [62]. It is also worth adding that augmenting the DPWA content from 0.1% to 0.5% caused a bulk density drop from 0.17% to 1.77% with respect to CEB without DPWA. As can be seen, the bulk density diminution is very small, which can certainly be due to the high compaction pressure applied to the sample during its manufacture (10 MPa) [19]. Similarly, Fig. 4.9 indicates that the evolution of the bulk density as a function of DPWA content can be deduced from the expression given below:

$$\rho = 2073.2 - 77.746(\text{DPWA}) \tag{4.3}$$
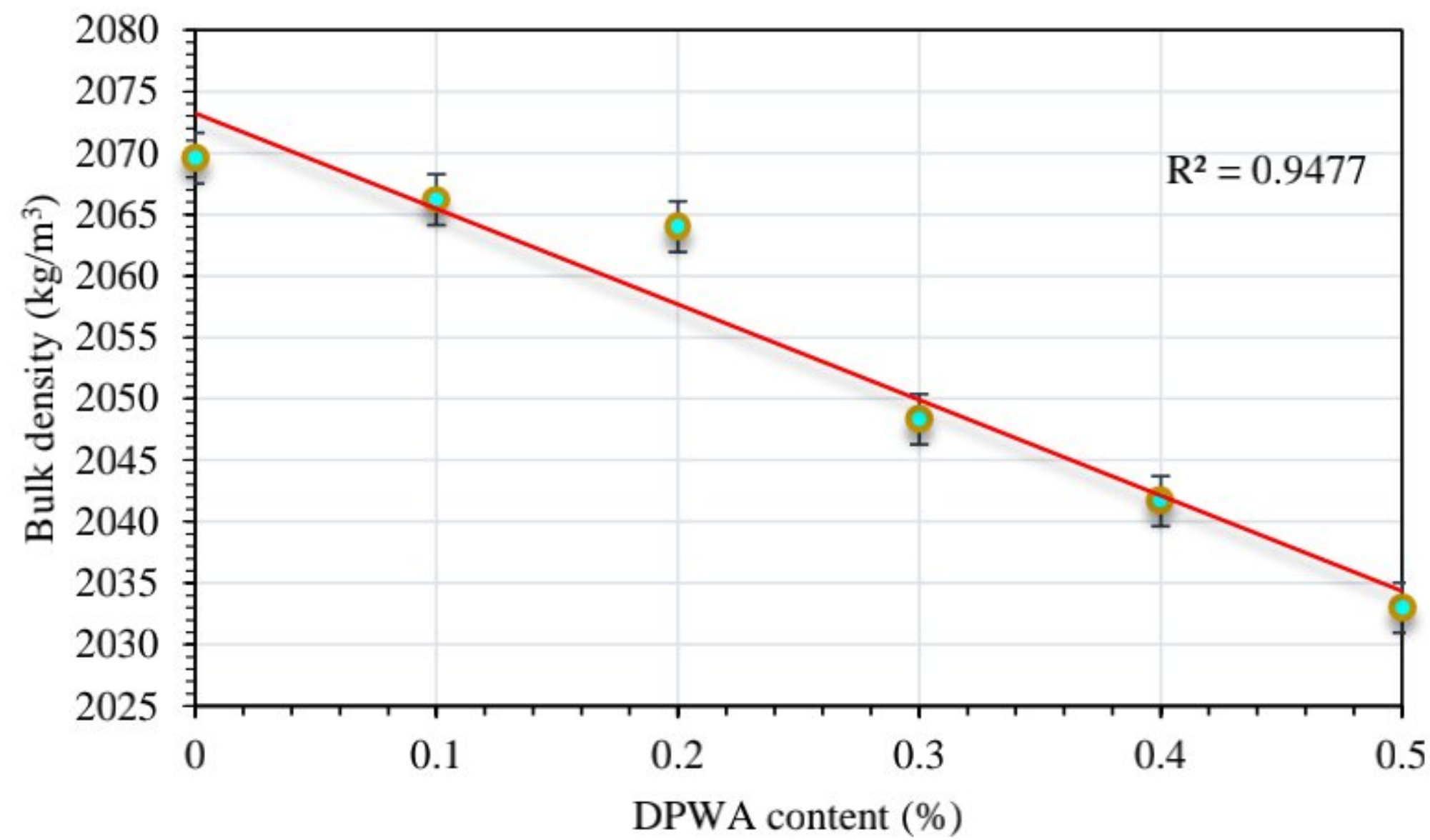
Fig 4. 9. Effect of DPWA content on CEB bulk density.

4.5.2 Thermal conductivity

The thermal conductivity of any material is defined as the rate of heat transfer by conduction through a unit cross-section area of that material. The thermal conductivity is a bulk property that describes the ability of a material to transfer heat. It is widely admitted that materials with low thermal conductivity values are used for thermal insulation. In this regard, Fig. 4.10 summarizes

the thermal conductivity values corresponding to various DPWA contents. One may easily see that the thermal conductivity of CEB with DPWA decreases when the amount of plant waste aggregates rises. Indeed, the block with 0.5% DPWA exhibited the lowest thermal conductivity value among all blocks; this value dropped by about 13.28% with respect to that of DPWA-free blocks. The results obtained showed that date palm waste aggregates helped to enhance the thermal conductivity of CEB. It is interesting to mention that this reduction might have been caused by the low date palm waste thermal conductivity which was found equal to 0.0738 ± 0.0006 (W/m.K) [25]. This small conductivity value was indubitably engendered by the higher volume of voids created by the addition of DPWA into the CEB mixture. Therefore, the larger the void ratio, the lower the thermal conductivity of the specimen [131]. Note that these voids are generally filled with air [132], which means that the thermal conductivity progressively diminishes as the volume of air in voids goes up as a result of the increasing amount of DPWA within the mixture. Moreover, it was shown that plant-based aggregates have a much higher thermal insulation coefficient than that of earth concrete or cement concrete. Low thermal conductivity materials are preferred for buildings as they allow saving a lot of energy and ensure better thermal comfort for residents. These findings are in good agreement with those previously reported in the literature[19], [25], [99], [100], [133]–[135]. The lowest thermal conductivity value was found with 0.5% DPWA content. Furthermore, the lowest dry and wet compressive strength values were obtained for this same DPWA content. Although these compressive strength values are low, they are still acceptable for the use of these blocks in earthen construction. Note that these values exceed the minimum threshold of 1 MPa as recommended by Van Damme and Houben [1].

Furthermore, the results depicted in Fig. 4.10 allow deducing an approximate relation, for calculating the thermal conductivity as a function of the DPWA content for the blocks stabilized with 12% of quicklime and compacted at 10 MPa stress, as follows:

$$\lambda = 0.975 - \frac{DPWA}{4} \tag{4.4}$$
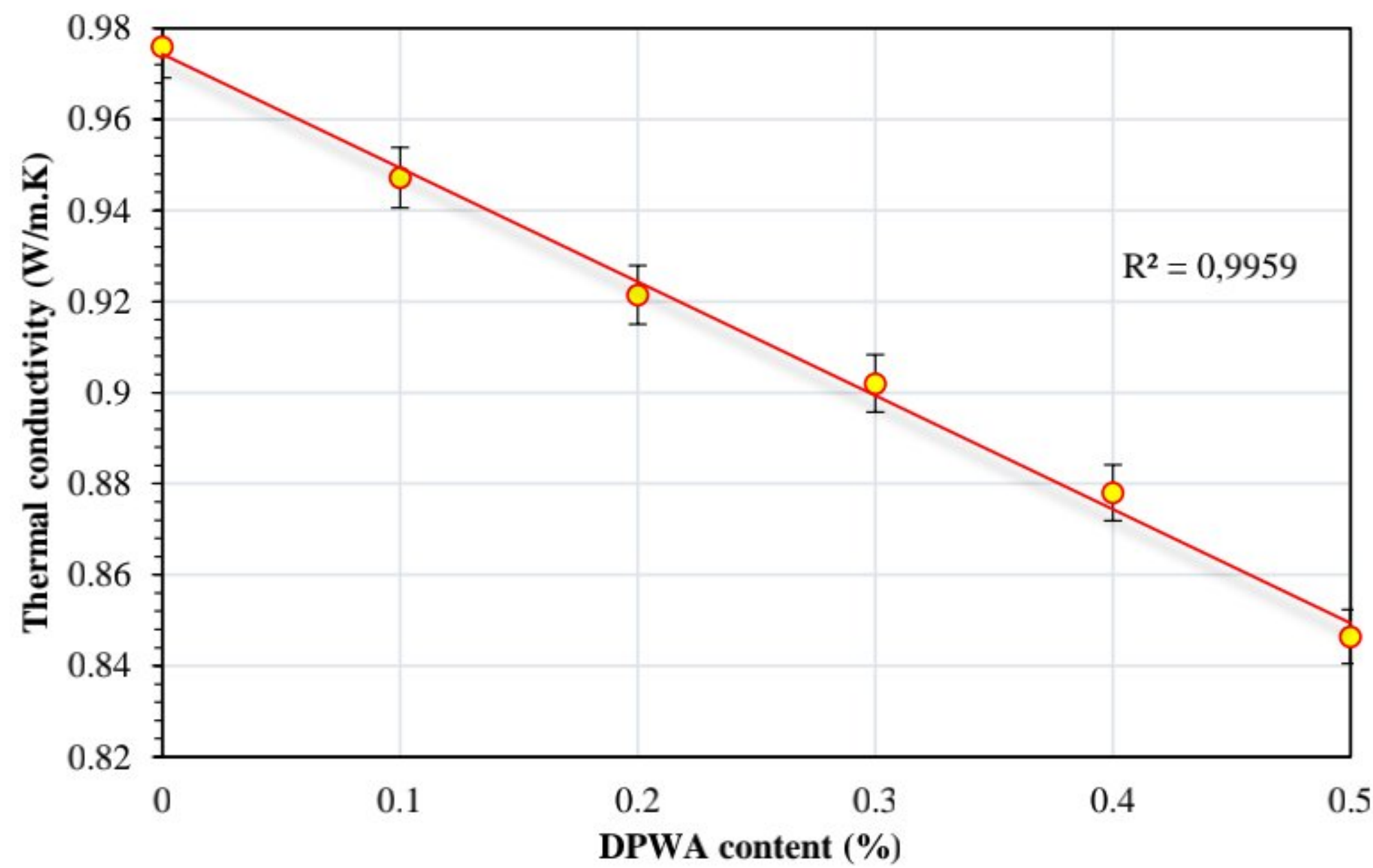
Fig 4. 10. Effect of DPWA content on the thermal conductivity of CEB.

4.5.3 Thermal diffusivity

Fig. 4.11 depicts the variation of thermal diffusivity as a function of the amount of DPWA incorporated into the formulation of CEB. It was found that the thermal diffusivity values were within the interval extending from 7.096×10^{-7} m^2/s to 7.386×10^{-7} m^2/s. Also, when the DPWA content increased, the thermal diffusivity went down. In comparison with the control block (free of DPWA), when the DPWA content passed from 0.1% to 0.5%, the thermal diffusivity dropped from 0.21% to 3.69%. Fig. 4.11 shows that date palm waste aggregates affect positively the thermal diffusion damping in the blocks. It should be noted that the increase in the porosity of compressed earth blocks, as a result of the integration of these aggregates into the CEB mixture and the alveolar

structure of plant wastes, both contribute to the heat diffusion-related damping process inside the blocks [136].

On the basis of the results presented in Fig. 4.11, and using the least squares method, an approximate relationship could be developed to compute the thermal diffusivity in terms of the DPWA content for the blocks stabilized with 12% quicklime and compacted at 10 MPA stress. The thermal diffusivity evolution followed the pattern described by Equation (4.5) within the waste content interval under study, with no need to perform the tests. Following the same path one can develop other relationships on CEB mixture performed with different conditions.

$$\alpha = (7.37 - 1.614(DPWA)^{2.61}) \times 10^{-7} \tag{4.5}$$
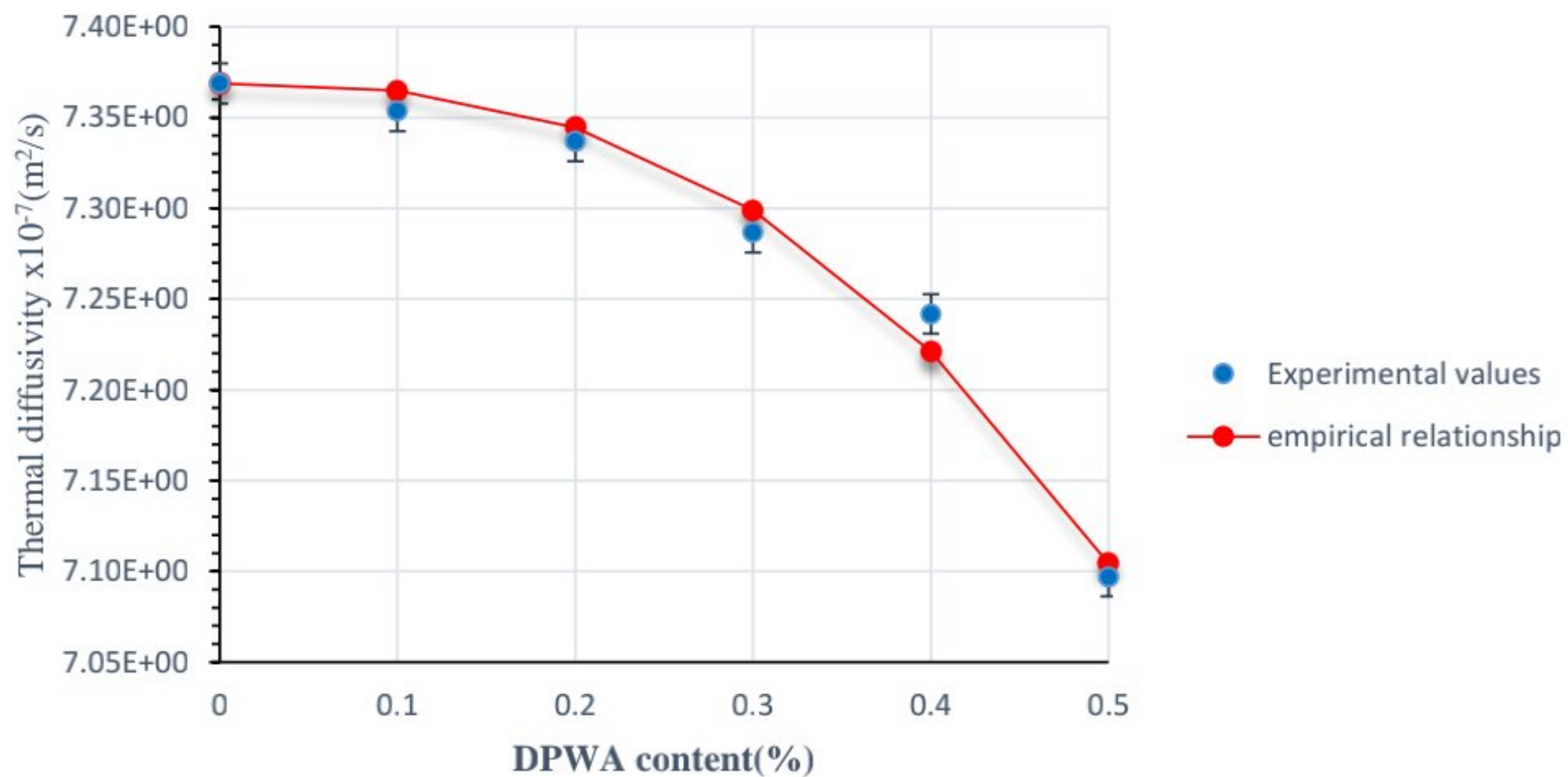
Fig 4. 11. Effect of DPWA content on the thermal diffusivity of CEB.

4.5.4 Thermal effusivity

The thermal effusivity of a material is defined as its ability to absorb and release heat through its surface and to exchange the thermal energy with its environment [132]. In this context, Fig. 4.12 displays the variation of thermal effusivity as a function of DPWA content. As can be observed,

when the DPWA content increased in the mixture, the thermal effusivity of CEB specimens decreased. In comparison with the control sample (block without DPWA), when the DPWA ratio passed from 0.1% to 0.5%, the thermal effusivity decreased from 2.85% to 11.63%. Consequently, the compressed earth blocks that contained DPWA exhibited a lower ability to exchange heat with their environment in comparison with the reference block [132]. The results obtained are in agreement with those previously published by Boumhaout et al. [132] who conducted a study on cement mortar containing palm mesh fibers, as well as those found by Djoudi et al. [136] who investigated gypsum integrating date palm fibers.

Fig. 4.12 illustrates the variation of the thermal effusivity (e) as a function of DPWA content; it can be deduced from the expression below:

$$e = 1132.6 - 256.71(\text{DPWA}) \qquad (4.6)$$
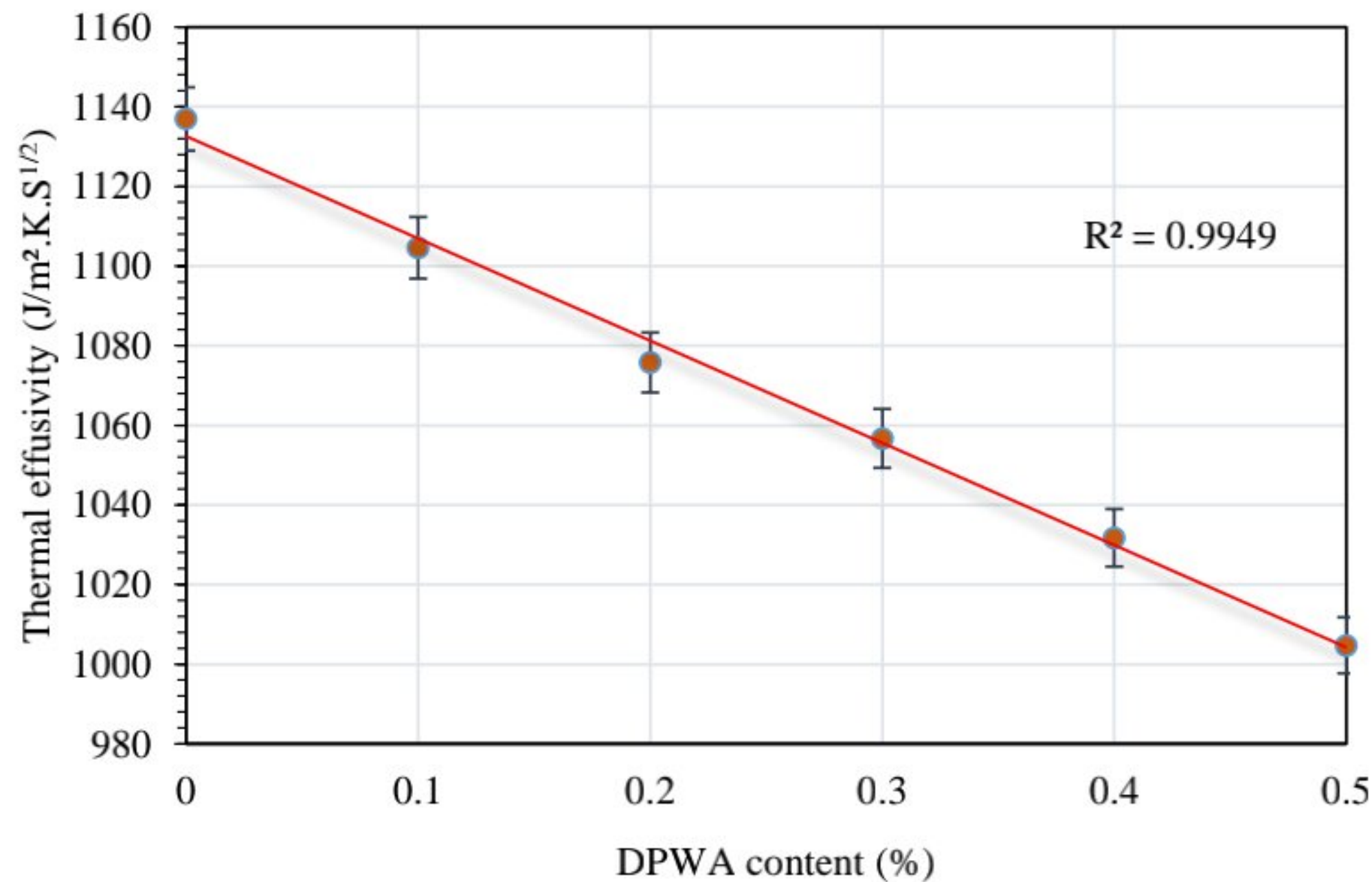
Fig 4. 12. Effect of DPWA content on the thermal effusivity of CEB.

4.5.5 Volumetric heat capacity and specific heat

The volumetric heat capacity is defined as the amount of thermal energy needed to increase the temperature of 1 m^3 of material by 1°C [10]. Fig. 4.13 presents the relationship between the DPWA content and volumetric specific heat. It is clearly indicated that the volumetric heat capacity varies between 1.3244 Mj/m^3.K (for 0% DPWA content) and 1.1926 Mj/m^3.K (for 0.5% DPWA content). Indeed, it was found that increasing the DPWA content from 0.1% to 0.5% engendered a decrease in the volumetric heat capacity from 2.75% to 9.95% in comparison with the block free of DPWA. This decrease was due to the combined effects of thermal diffusivity and thermal conductivity [132]. Similar findings have been reported in the literature [132], [137].

Fig. 4.13, which presents the variation of the volumetric heat capacity (C) as a function of DPWA content, can be used to deduce that parameter from the following expression:

$$C = 1.3165 - 0.2583(\text{DPWA}) \qquad (4.7)$$
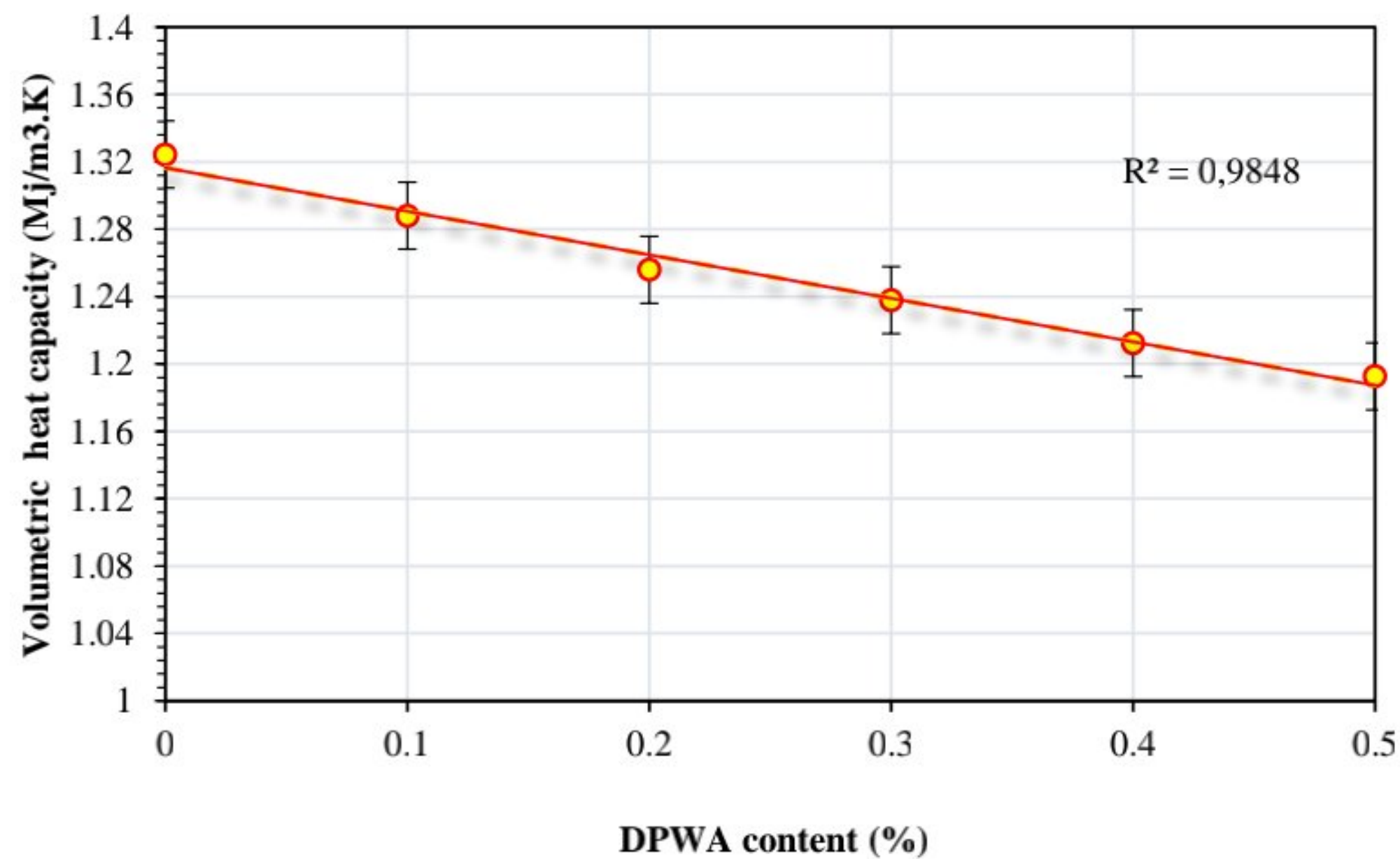
Fig 4. 13. Effect of DPWA content on the volumetric heat capacity of CEB.

Regarding the specific heat, it is defined as the amount of heat that is necessary to raise the temperature of 1 kg of a material by 1°C. The evolution of the specific heat as a function of the

DPWA content is depicted in Fig. 4.14. The specific heat value of CEB without DPWA was found within the interval [545 - 712 J kg^{-1} K^{-1}] of unfired earth bricks as reported by El Fgair et al. [138]. It was also revealed that when the DPWA content increased from 0.1% to 0.5%, the specific heat dropped from 2.56% to 8.33% in comparison with the block without DPWA. This decrease was certainly due to the combined effects of the volumetric heat capacity and bulk density. It should be noted that when the density and volumetric heat capacity both decreased, the specific heat of CEB dropped too.

Fig. 4.14, which presents the evolution of the specific heat as a function of DPWA content, can be used to evaluate Cp following the equation (4.8).

$$Cp = 635.12 - 102.69(\text{DPWA}) \tag{4.8}$$
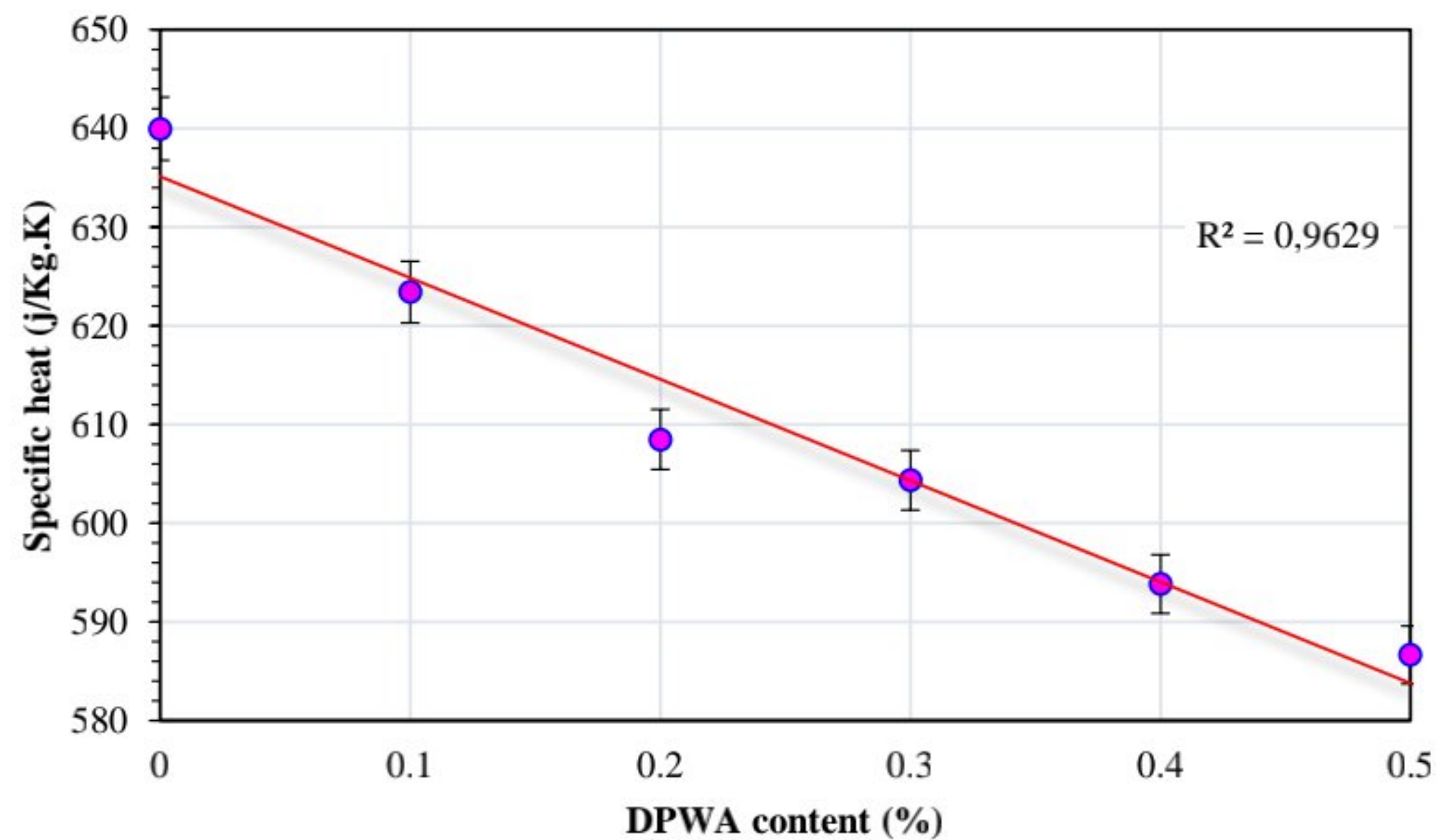
Fig 4. 14. Effect of DPWA content on the specific heat of CEB.

The thermos-physical parameters of the tested blocks and other building materials are summarized in the table 4.2. The addition of palm waste aggregates improved thermo-physical properties, particularly thermal conductivity, which is the most important characteristic. Furthermore, CEB containing 0.5% DPWA and compressed at 10 MPa outperformed plaster concrete, sand concrete, and CEB stabilized by 8% cement.

Table 4. 2. Thermal properties of CEB based on DPWA and similar construction materials.

Reference	Materials	Thermal conductivity (λ) (W/m. K)	Thermal diffusivity (α) (m^2/s)	Thermal effusivity (E) (J/m².K.s$^{1/2}$)	Specific heat (Cp) (J /Kg. K)
This work	CEB without DPWA	0,975952753	7.36877 x10^{-7}	1136.923	639.961
This work	CEB with 0.1%DPWA	0,94720092	7.35352 x10^{-7}	1104.572	623.411
This work	CEB with 0.2%DPWA	0,921449624	7.33692 x10^{-7}	1075.758	608.482
This work	CEB with 0.3%DPWA	0,902018415	7.28662 x10^{-7}	1056.701	604.351
This work	CEB with 0.4%DPWA	0,878000209	7.2418 x10^{-7}	1031.742	593.830
This work	CEB with 0.5%DPWA	0,846423149	7.0969 x10^{-7}	1004.738	586.653
[71]	CEB with 8% cement	1.22	5.75 x10^{-7}	1598	1106.87
[100]	unfired earth bricks	0.57	3.9 x10^{-7}	913	774
[132]	Cement mortar	0.795	3 x10^{-7}	1414	1229.91
[139]	Sand concrete	1.40	5.78 x10^{-7}	1862.8	1209.07
[136]	Plaster concrete	0.895	3 x10^{-7}	1600	1470.34

4.5.6 Total water absorption

The results presented in Fig. 4.15 show the effect of DPWA content on the total water absorption of compressed earth blocks. It can clearly be observed that the total water absorption increases as the DPWA content rises. It turned out that the total water absorption of these blocks varied between 12.21% (0% DPWA on the first day) and 13.15% (0.5% DPWA on the fourth day). These are favorable results and within acceptable limits in comparison with to the total water absorption of clay bricks (from 0% to 30%), calcium silicate bricks (from 6% to 16%) and concrete blocks (from 4% to 25%) [18]. It is worth indicating that increasing the DPWA level from 0.1% to 0.5% caused the total water absorption to augment on the first day from 1.19% to 6.12%, on the second day from 1.30% to 6.15%, on the third day from 1.38% to 5.80%, and on the fourth day from 1.41 % to 5.82%. Obviously, the absorption rate was more rapid when the material was exposed to water, but it started slowing down over time, until attaining the equilibrium point. These results may certainly be attributed to the fact that date palm waste, which is a type of wood waste, is a very hygroscopic material and presents a high water absorption capacity [23]. Similar results were observed in several previously published studies [18], [23], [24], [108].
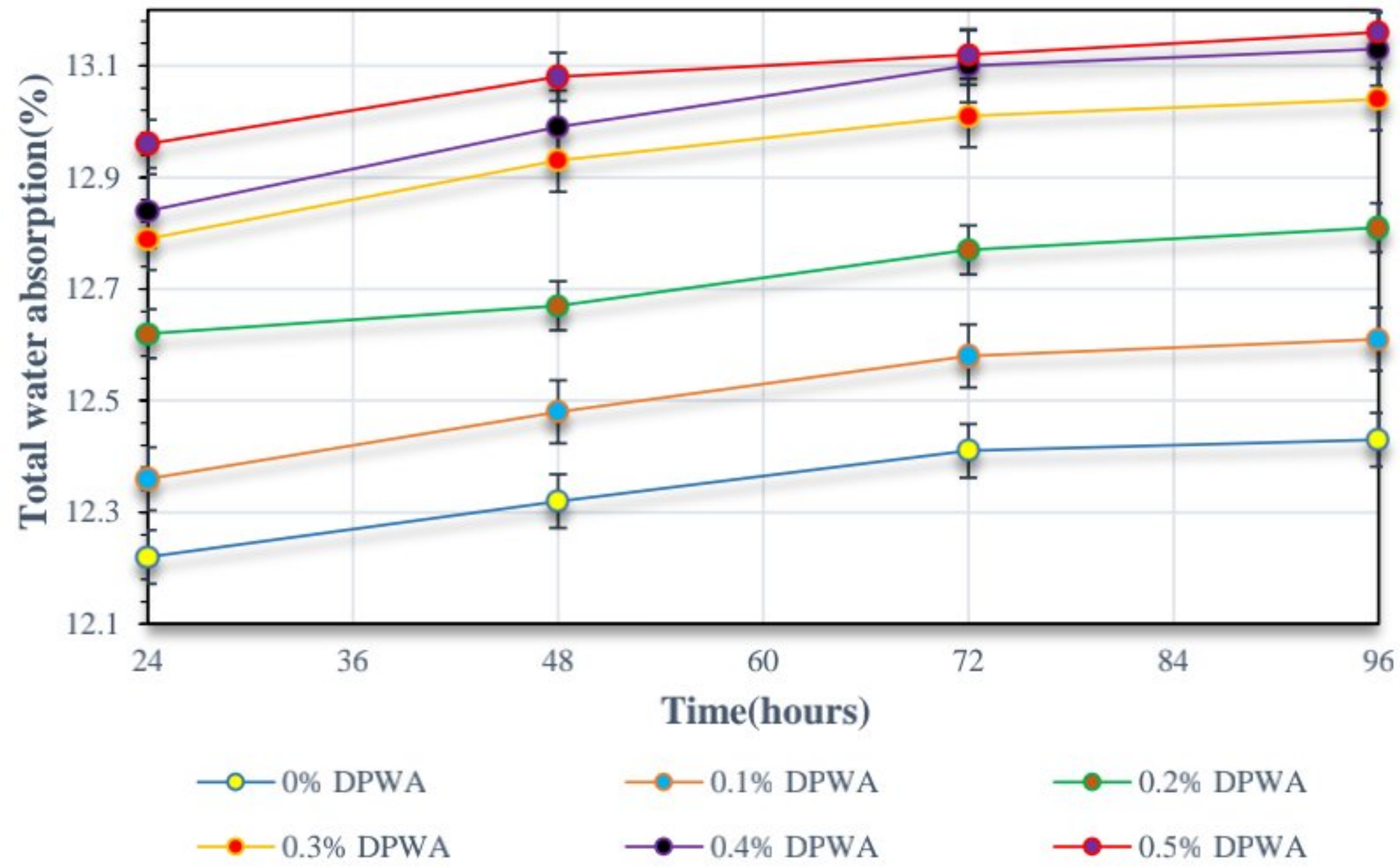
Fig 4. 15. Effect of the DPWA content on total water absorption over time.

4.5.7 Capillary water absorption

The results regarding the effect of DPWA content on the capillary water absorption of compressed earth blocks are presented in Fig. 4.16, which suggests that the capillary water absorption increased as the DPWA content increased. The capillary water absorption of the block comprising 0.5% DPWA was found equal to 13.10 g/cm min$^{1/2}$ which is a quite acceptable value as it is smaller than the recommended one of 20 g/cm min$^{1/2}$ [19]. It was found that increasing the DPWA level from 0.1% to 0.5% engendered a capillary absorption increase from 5.62% to 56.91%. This increase in the capillary water absorption of CEB may be assigned to the higher percentage of date palm wastes in the CEB mixture. It should be noted that the increase in capillary absorption is due to two main reasons which are first the hydrophilicity of plant waste, and second the increase in the porous network due to the presence of waste in the mixture. These findings are in good agreement with those previously reported by Taallah and Guettala [19].
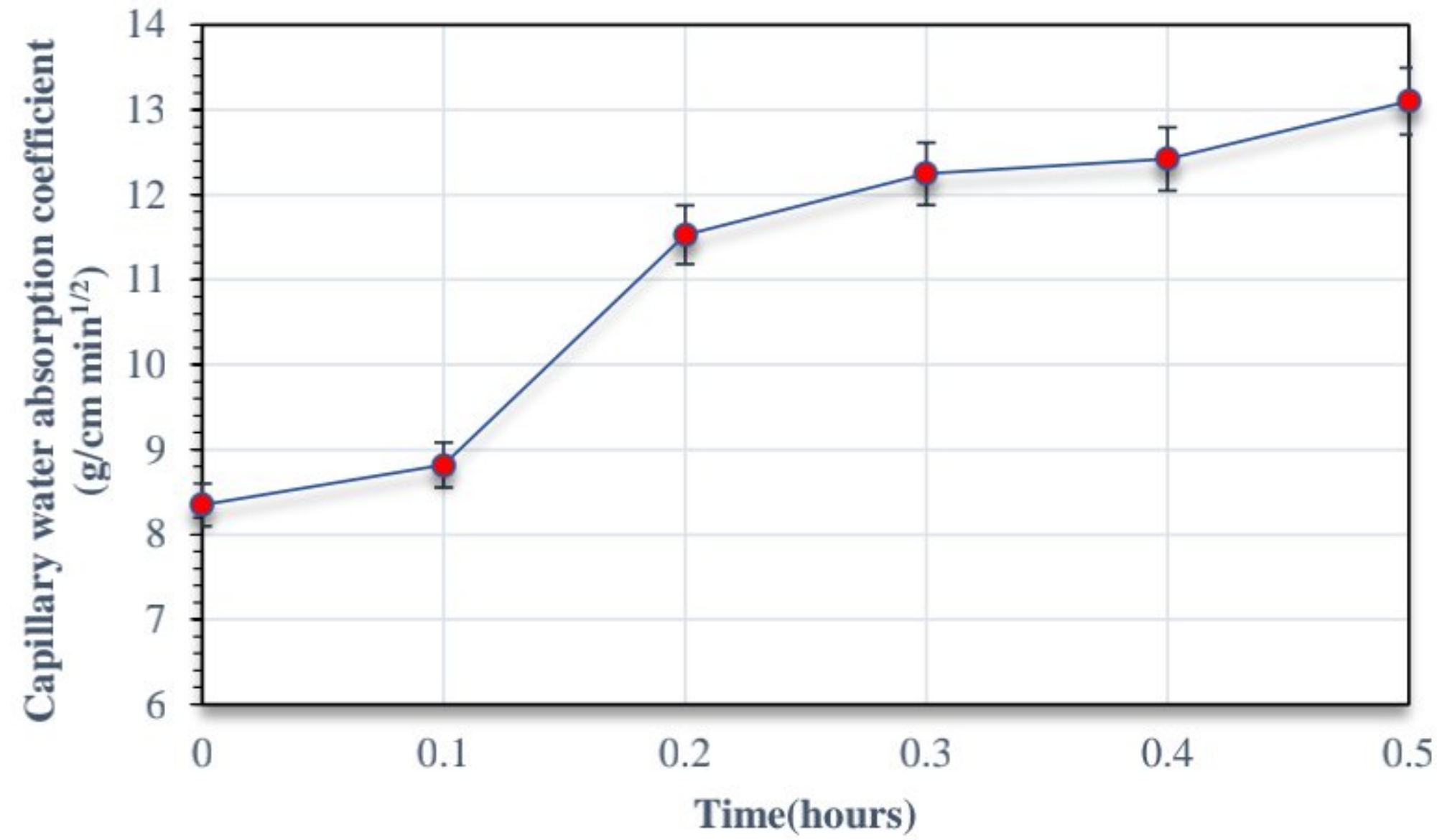
Fig 4. 16. Effect of DPWA content on capillary water absorption over time.

4.5.8 Swelling

Fig. 4.17 depicts the swelling data regarding compressed earth blocks containing date palm waste aggregates. It is clearly observed that the swelling of the block increases as the DPWA content grows. Indeed, the swelling ranged between 0.43mm/m (for 0% DPWA on the first day) and 0.96 mm/m (for 0.5% DPWA on the third day). The swelling values on the fourth day were similar to those observed on the third day. Moreover, increasing the DPWA content from 0.1% to 0.5% caused the swelling to increase from 14.82% to 51.29% on the first day, from 5.41% to 26.82% on the second day, and from 4.65% to 14.49% on the third day. It was established that the swelling rate in the block were influenced by many factors, like the quality of the clay mineral (kaolin, illite, …) present in the soil used, the percentage of voids, and the amount and type of chemical stabilizer used. When the quantity of DPWA in the mixture increases, the number of pores inside the sample as well as the quantity of water absorbed by the sample increase, which explains the growing swelling of the sample. Several studies reported comparable outcomes in the literature [18], [108].
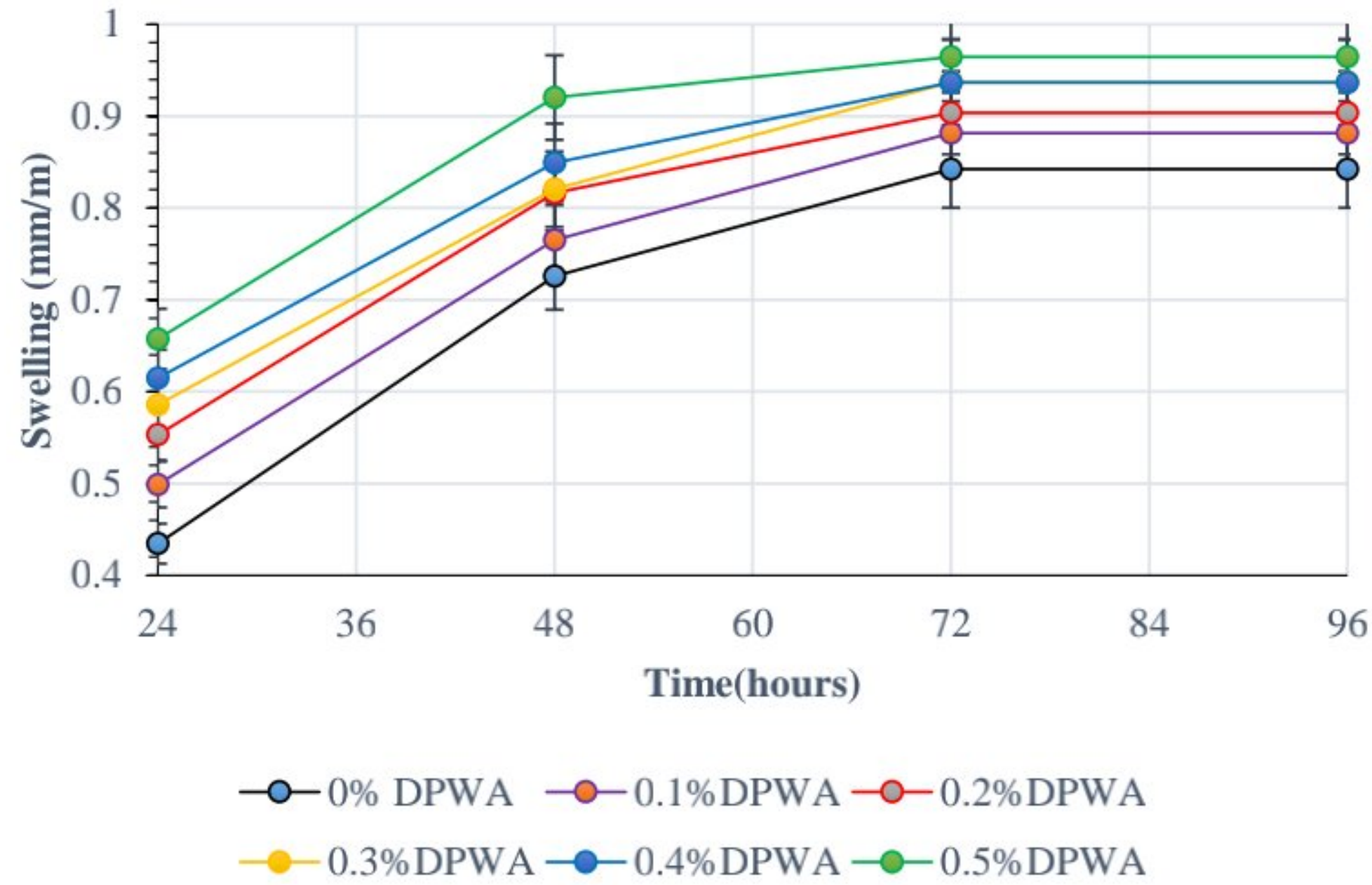
Fig 4. 17. Effect of DPWA content on swelling over time.

4.6 Correlation between the bulk density of blocks and their most important mechanical and thermal properties

It is broadly admitted that density is among the most important physical properties affecting the characteristics of materials, particularly the compressive strength and thermal conductivity. In the present study, the relationships between the bulk density and other properties, such as the compressive strength, thermal conductivity, thermal diffusivity and thermal effusivity of compressed earth blocks including palm tree wastes, were investigated.

Fig. 4.18 illustrates the relationship between the dry compressive strength and bulk density of the block samples. This same figure clearly indicates that the dry compressive strength of the blocks augments as the density goes up, which reveals a direct correlation between the density and the dry compressive strength. As clearly indicated, when the bulk density of CEB decreases from 2069.57 to 2033 Kg /m^3, the dry compressive strength diminishes from 15.84 to 9.81 MPa. Moreover, the increased CEB porosity, engendered by the incorporation of DPWA into the CEB mixture, induced

a decrease in the bulk density, which in turn led to lower compressive strength of the compressed earth blocks (CEBs).

Fig. 4.19 displays the relationship between thermal conductivity and apparent density of CEB. It was found that its thermal conductivity decreased as its bulk density dropped. It should be noted that the thermal conductivity decrease due to the bulk density drop can be attributed to the rise in the CEB porosity as a result of the incorporation of DPWA aggregates into the CEB mixture. Note that when the CEB bulk density decreased from 2069.57 to 2033 Kg /m^3, its thermal conductivity diminished from 0.976 to 0.846 W/m. K.

Figs 4.20 and 4.21 show the variations of the thermal diffusivity and thermal effusivity, respectively, as a function of the apparent density of CEB. These two figures suggest that the thermal diffusivity and thermal effusivity of CEB decreased as the bulk density of CEB went down. This decline in thermal conductivity, thermal diffusivity and thermal effusivity is due to the slower heat transfer when heat passes through the air-filled pores which are created by the incorporation of DPWA. It is worth adding that the air in pores between aggregates plays the role of an insulating medium [62]. Several authors have reported similar findings in the literature [19], [23], [24].

The linear relationships between the different properties of CEB and its bulk density (ρ) have a good correlation coefficient and are given by the equations (4.9, 4.10, 4.11 and 4.12).

$$DCS = 0.1271\,\rho - 248.38 \qquad (4.9)$$

$$\lambda = 0.003\,\rho - 5.2934 \qquad (4.10)$$

$$\alpha = 6\text{x}10^{-10}\,\rho - 6\text{x}10^{-7} \qquad (4.11)$$

$$e = 3.0792\,\rho - 5255.7 \qquad (4.12)$$
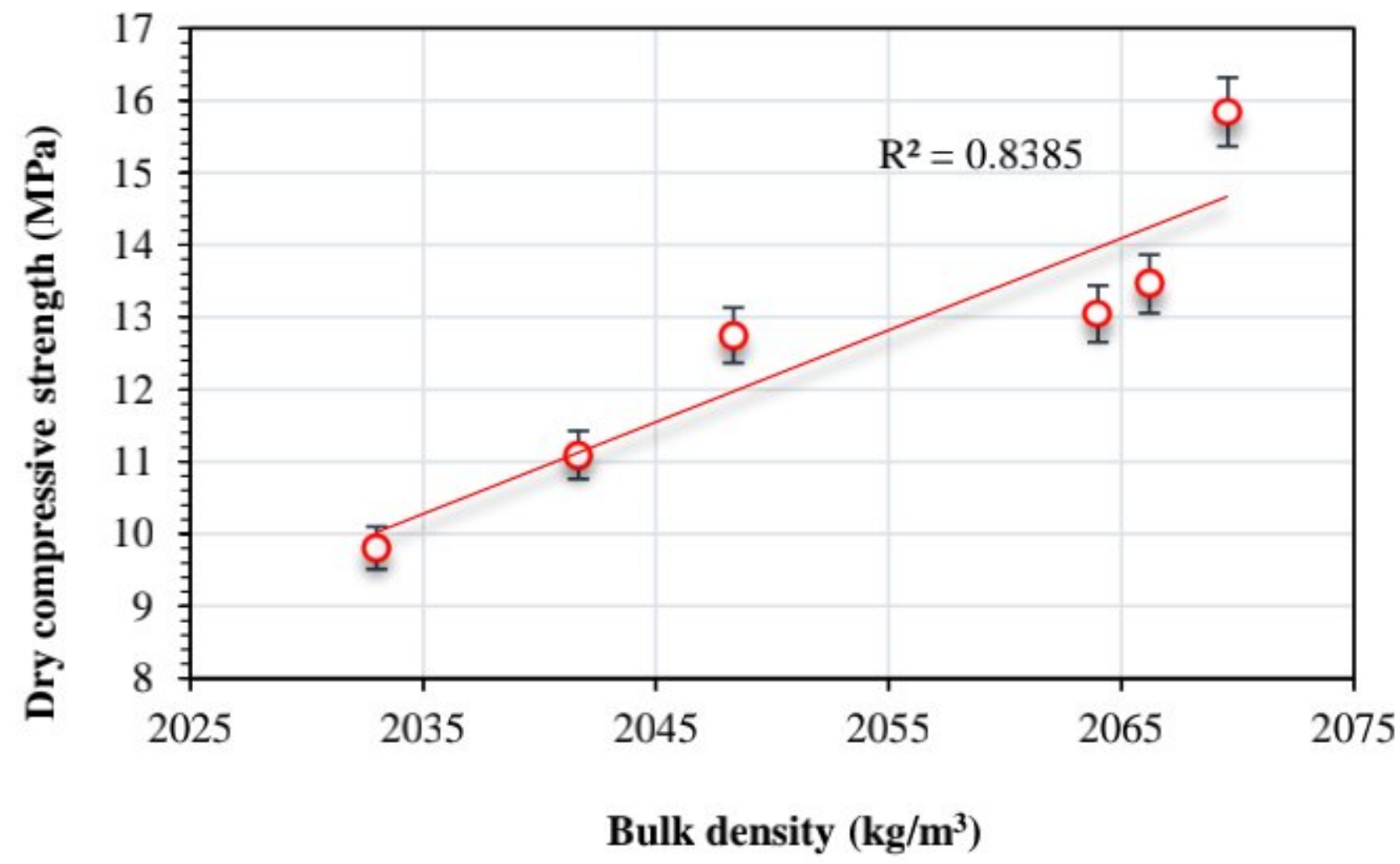
Fig 4. 18. Relationship between the dry compressive strength and bulk density of CEB.
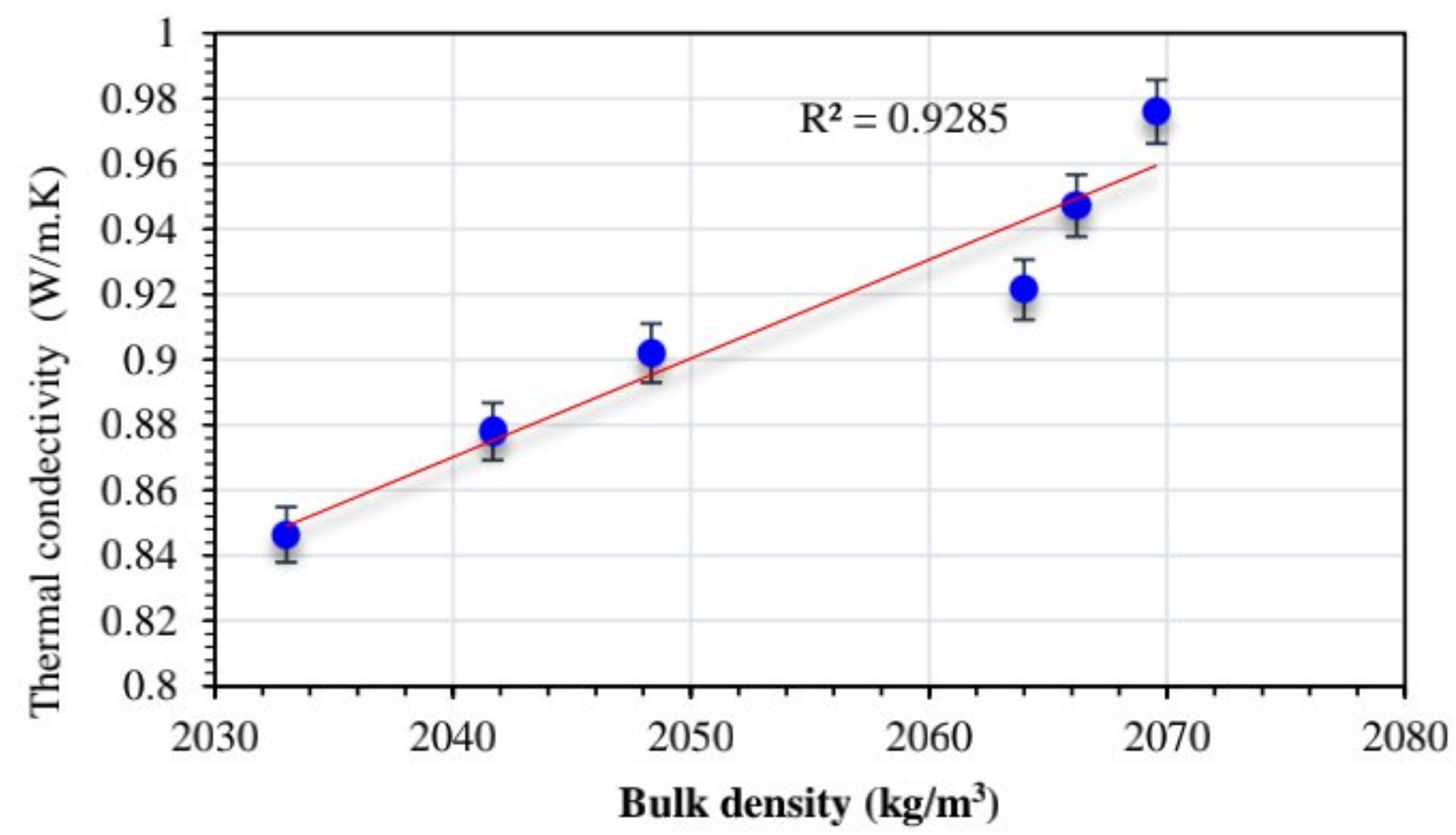
Fig 4. 19. Relationship between the thermal conductivity and bulk density of CEB.
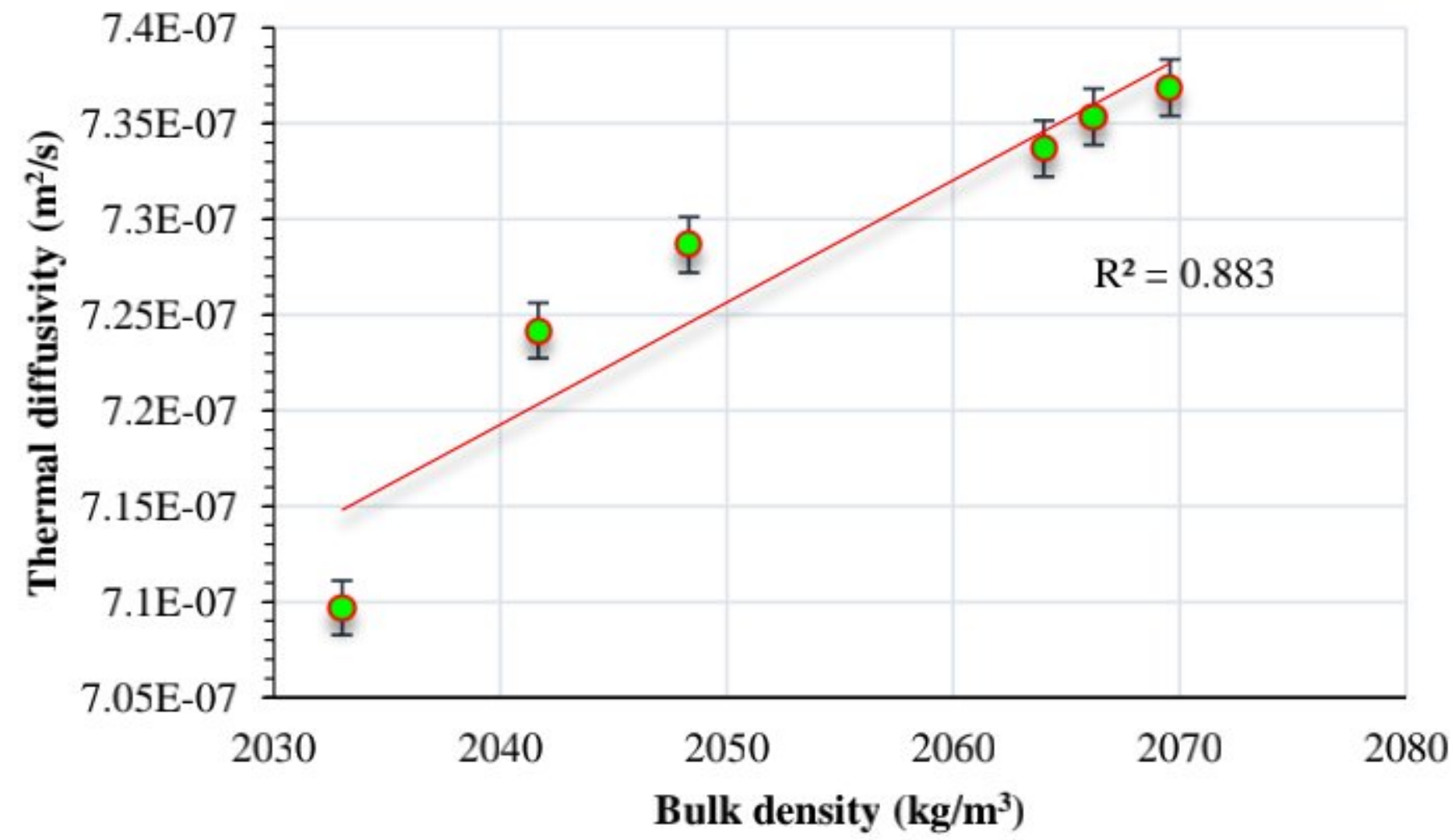
Fig 4. 20. Relationship between the thermal diffusivity and bulk density of CEB.
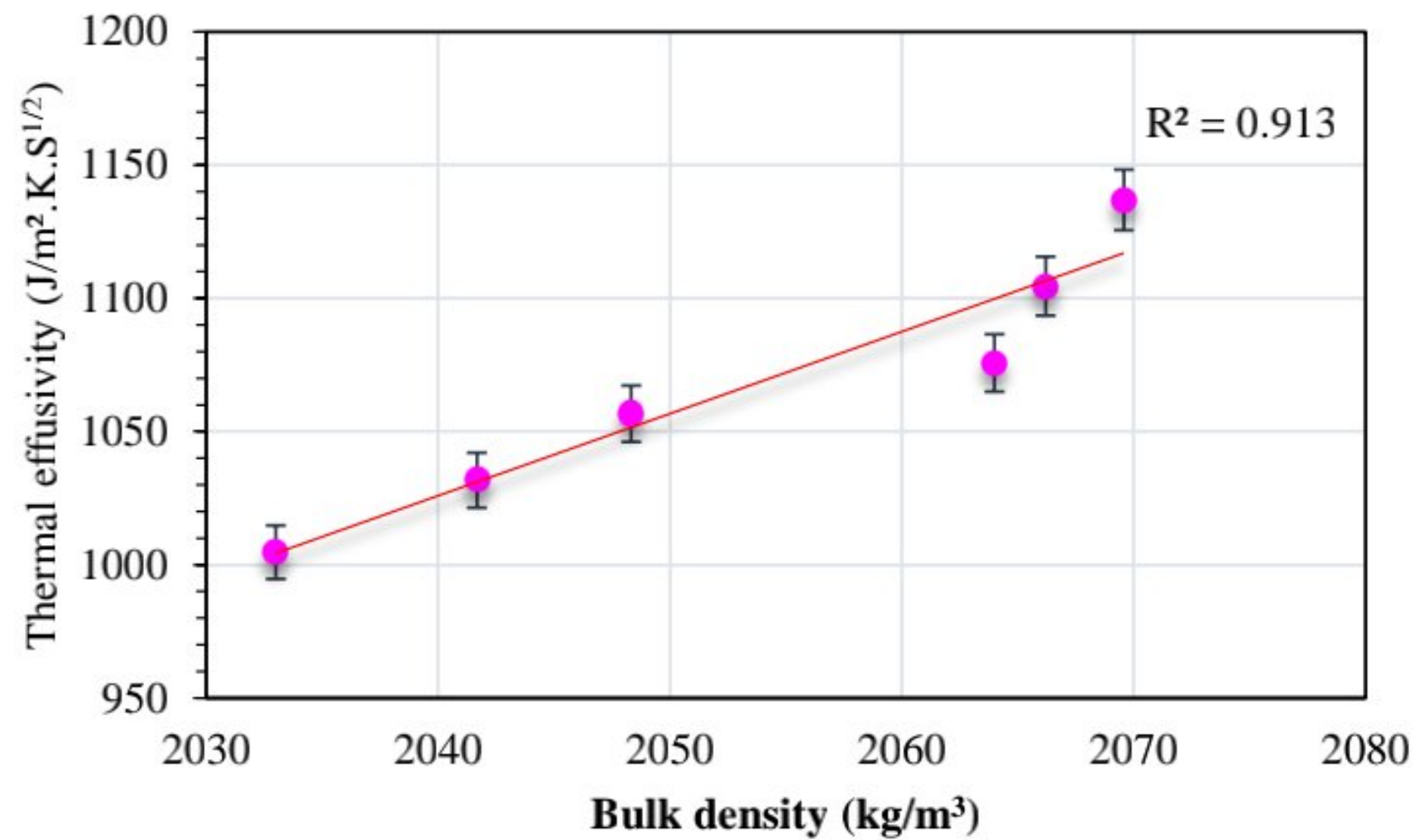
Fig 4. 21. Relationship between the thermal effusivity and bulk density of CEB.

4.7 Evaluation of flexural behavior of compressed earth blocks (CEBs) using digital image correlation technique (DIC): effect of different type of date palm waste fibers and compaction pressure

4.7.1 Effect of date palm waste content and different compaction pressure on load-deflection behavior of compressed earth bricks (CEBs)

Figs. 4.22 and 4.23 show load-deflection curves for unreinforced and reinforced samples with different DPW types as well as for compressed earth bricks with different compaction pressures. It

can be seen from the figures that the degradation of force values was related to an increase in DPW content and a decrease in compaction pressure. All blocks presented quasi-linear elastic behavior up to maximum load, followed by a sudden brittle failure of the block matrix, where samples could not take any residual load resulting in immediate failure. The same behavior was seen in the control blocks (without DPW) and the blocks with 2% DPW in the research by Khoudja et al. [25]. The brittle fracture is explained as brittle materials and the introduction of low contents of DPW into the mineral matrix did not contribute to improving the ductility of the tested materials. However, the sample with 0.5 percent DPS, exhibited a two-phase behavior. The first phase is defined by a quasi-linear load-deflection relationship up to a maximum value, followed by a second phase characterized by a decrease in flexural load, accompanied by plastic deflection and an increase in residual flexural force. The addition of 0.5%DPS increases the ductility of the bricks, resulting in some residual force and increasing the deflection at failure (see Table 4.3). In addition, the ultimate deflection of blocks values augmented when DPW fibers and aggregate content increased. Similar findings have been observed in previous researches [101].
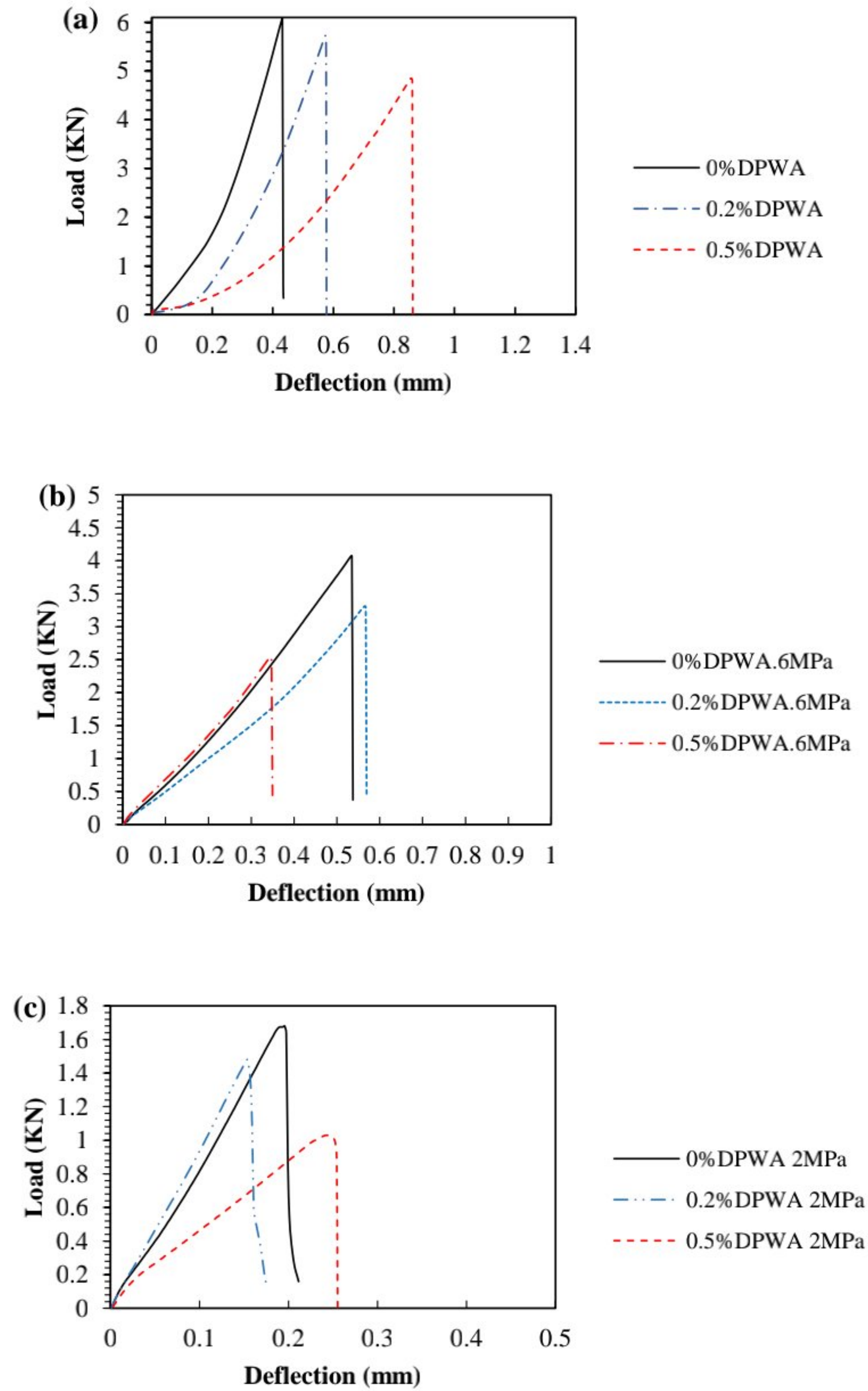
Fig 4. 22. Effect of DPWA content on mechanical behavior of CEB: (a) typical load-deflection curves; (b) typical load-deflection curves of CEB compacting by 6 MPa; (c) typical load-deflection curves of CEB compacting by 2MPa.
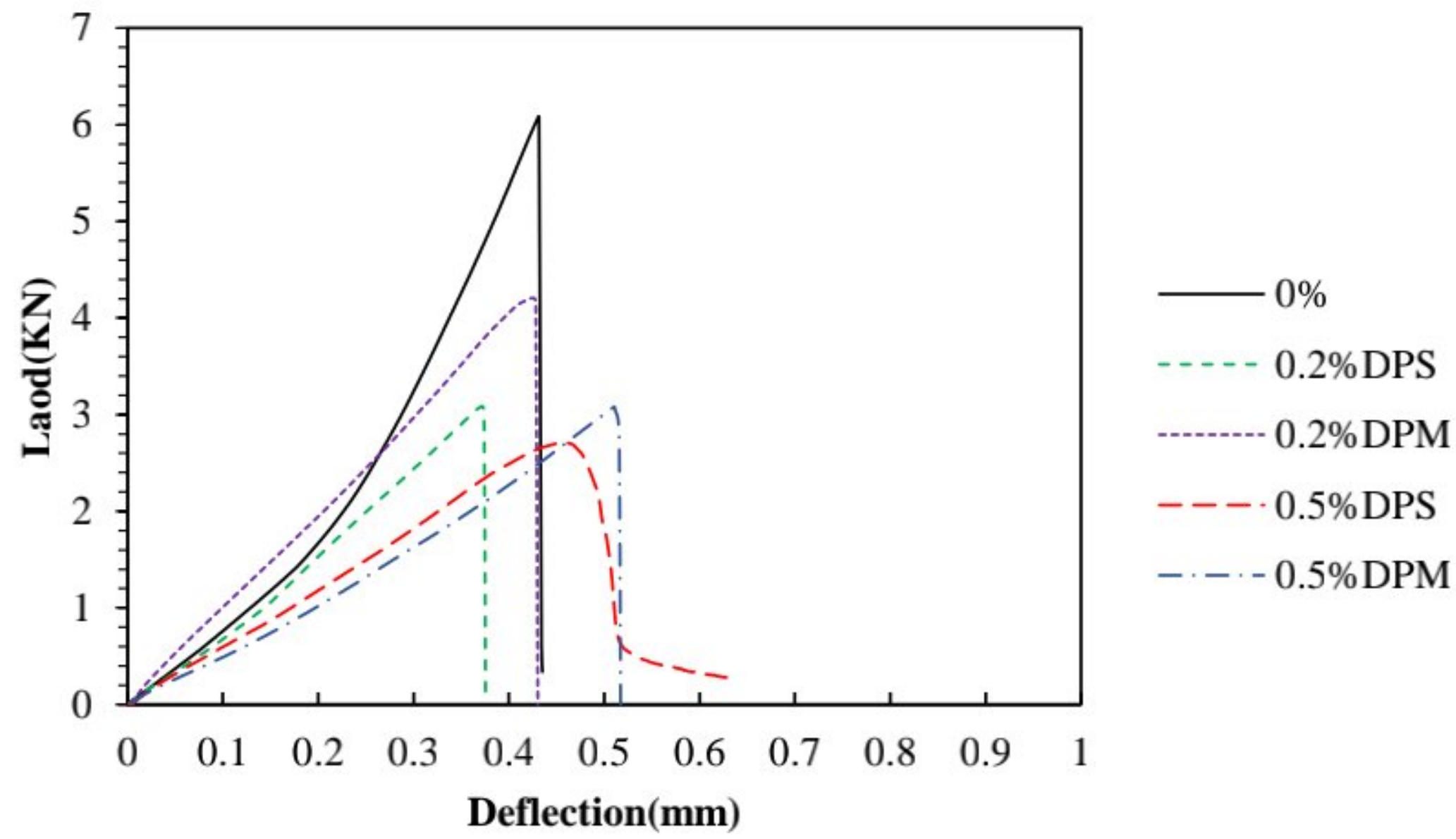
Fig 4. 23. Effect of date palm type and content on mechanical behavior: typical load-deflection curves of CEBs compacting by 10MPa.

Table 4. 3. Mechanical properties of CEBs with various DPW percentages and various compaction pressure.

DPW (%)	Compaction pressure (MPa)	Maximum load (KN)	Maximum deflection (mm)
0% DPWA	2	1.678	0.211
	6	4. 076	0.537
	10	6.085	0.435
0.2%DPWA	2	1.479	0.175
	6	3.312	0.569
	10	5.729	0.577
0.5%DPWA	2	1.029	0.255
	6	2.544	0.349
	10	4.85	0.864
0.2%DPS	10	3.084	0.375
0.5%DPS	10	2.708	0.631
0.2%DPM	10	4.205	0.430
0.5%DPM	10	3.079	0.510

4.7.2 Effect of date palm waste content on flexural strength and modulus of elasticity

The flexural strengths of CEB filled by different DPW types are summarized in Fig.4.24. The bending strength of the CEB without DPW is greater than other samples. The flexural strength values range between 2.25 to 5.48 MPa. The results reveal that by increasing the DPW content, the flexural strength of all blocks decreased. Furthermore, in comparison with the reference CEB, the decreasing percentage in the flexural strength was about 5.83%, 20.25%, 30.83%, 49.27%, 49.42% and 55.52% for CEB containing 0.2% DPWA, 0.5% DPWA, 0.2% DPM, 0.2% DPS, 0.5% DPM and 0.5% DPS, respectively. The results also show that the flexural strength values were higher for the mixtures with DPWA than for those with DPM or DPS. This drop can be caused by poor adhesion between the fibers and the earth matrix.
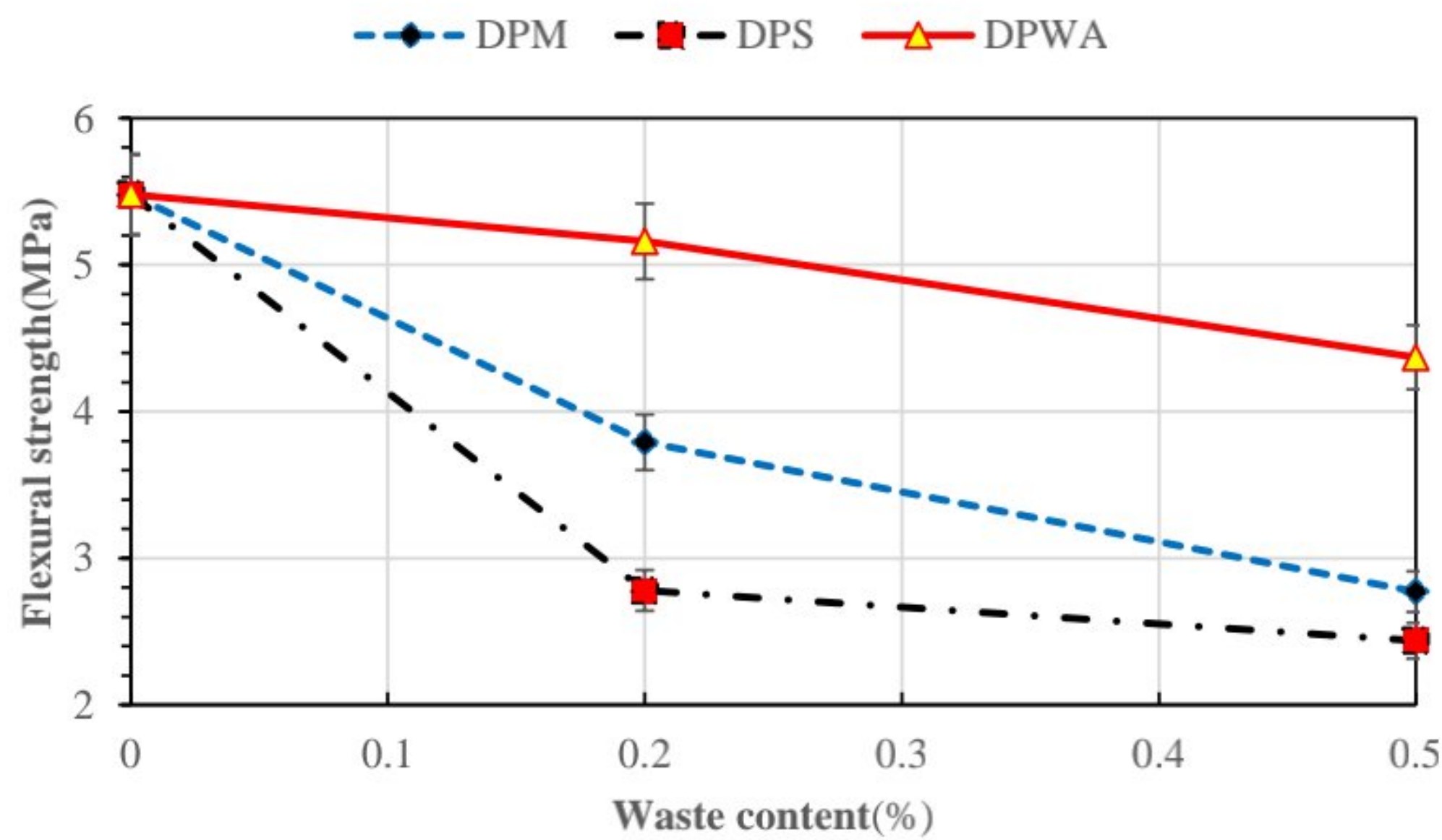
Fig 4. 24. Effect of DPW type content on flexural strength of CEB.

The apparent modulus of elasticity of CEB filled by different DPW types is summarized in Fig.4.25. The apparent modulus of elasticity values range between 321.52 to 809.37MPa. The apparent modulus of elasticity of the specimen of CEB without waste is higher than that of all the others. The results show that increasing the palm waste content from 0% to 0.5% leads to a decrease in the apparent modulus of elasticity of blocks in all types of palm waste. Compared to the block without DPW fibers of CEB, the increase of the DPW content from 0.2% to 0.5% affects the accompanying decrease of the apparent modulus of elasticity at DPM type from 16.38% to 57.36%, at DPWA type from 37.71% to 60.27%, at DPS type from 37.86% to 51.04%. This decrease in

119

flexural strength and apparent modulus can be related to the significant reduction of C-S-H in CEB, which is mainly responsible for strength. This decrease of C-S-H due to a decrease SiO_2 in the mixture, which decreased due to the decrease in the amount of soil that has been replaced by DPW[26].
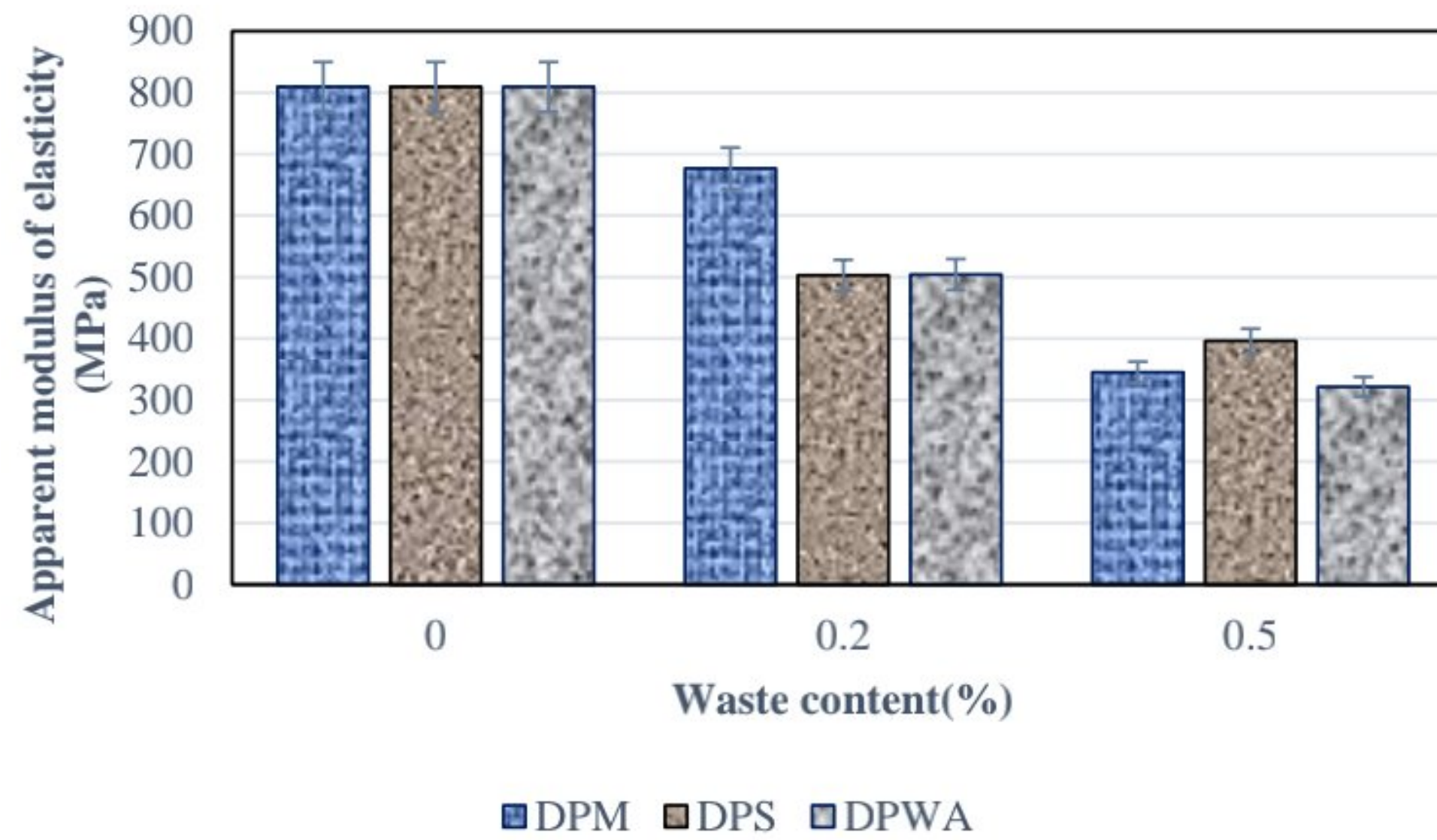
Fig 4. 25. Effect of DPW type content on apparent modulus of elasticity.

4.7.3 Effect of date palm waste content on dry compressive strength

The dry compressive strengths of CEB filled by different date palm waste type are summarized in Fig.4.26. The compressive strength of the specimen of CEB without waste is higher than that of all the others. The dry compressive strengths values ranging between 9.54 to 15.84 MPa. the results show that the increasing the palm waste content from 0% to 0.5% lead to a decrease in compressive strength of blocks in all types of palm waste. In addition, this reduction of compressive strength, linked to the incorporation of plant waste with low compressive strength and stiffness[101]. The results also show that the values of the compressive strength was higher for the mixtures with DPM than for those with DPWA or DPS. Compared to the block without DPWA of CEB, the increase of the date palm waste content from 0.1% to 0.5% affects the accompanied decrease of the compressive strength at DPM type from 6% to 34.42%, at DPWA type from 15.03% to 38.09%, at DPS type from 17.03% to 39.75%. This decrease can be due to the significant reduction of C-S-H in CEB, which is mainly responsible for compressive strength. This decrease of C-S-H due to decrease SiO_2 in the mixture, which decreased due to the decrease in the amount of soil which has

been replaced by date palm waste. The results were obtained in accordance with those published in the literature[19], [101].
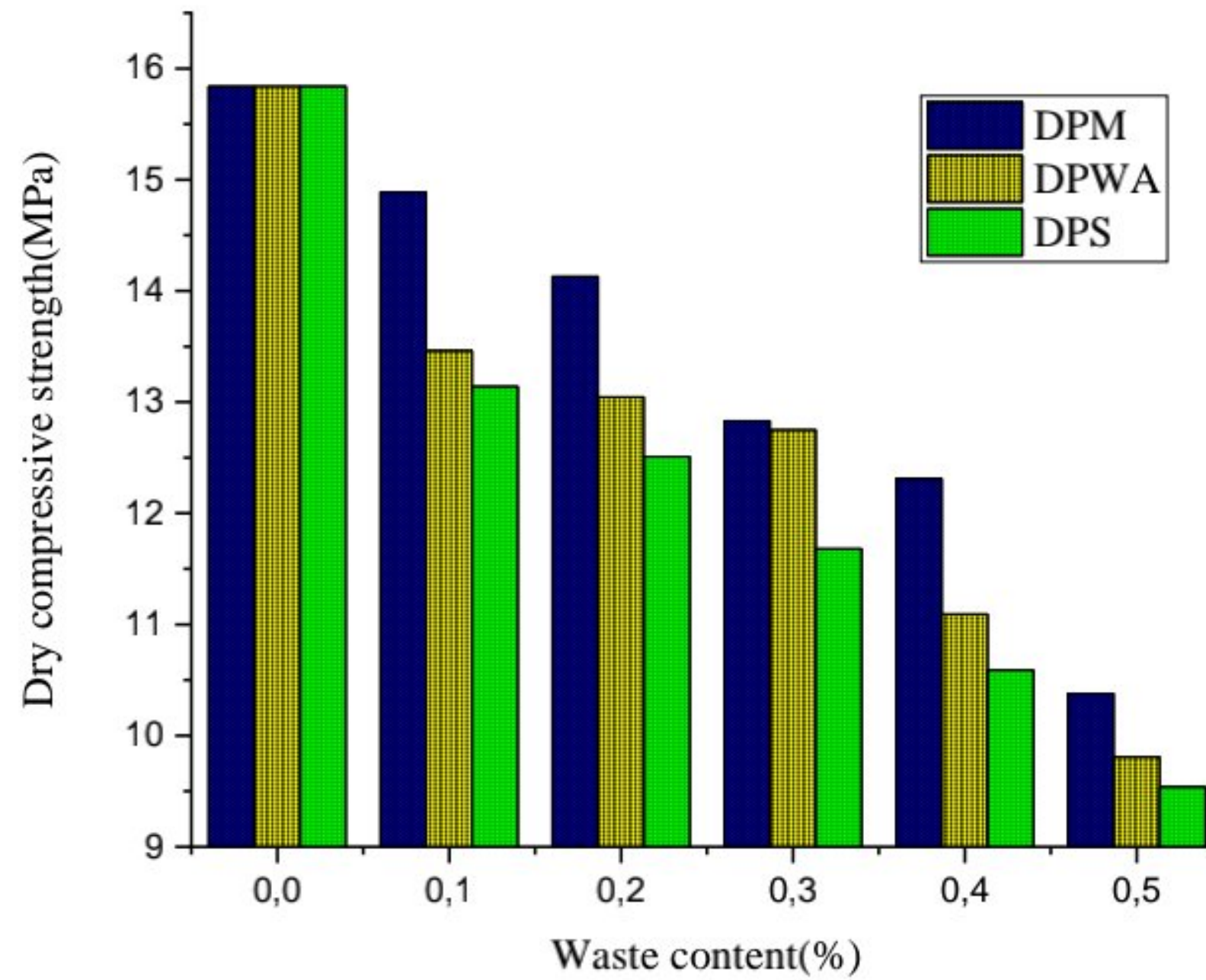
Fig 4. 26. Effect of waste type content on dry compressive strength of CEB.

4.7.4 Effect of date palm waste content on Ultrasonic Pulse Velocity (UPV)

The results of ultrasonic pulse velocity of CEB presented in Fig. 4.27. It is clear that the ultrasonic pulse velocity was affected by the incorporation of date palm waste, and it was observed that the ultrasonic pulse velocity decrease with an increase in date palm waste content at all palm waste types. The pulse velocity values ranged from 2556.67 m/s (0% palm waste content) to 1936.67m/s (0.5%DPM). This decrease is due to the slowing down of ultrasonic pulses when they pass through pores filled with air, these pores are caused by the addition of palm waste. In addition, the plant waste have higher sound insulation coefficient than earth concrete. The results show that the block filled with 0.5% of DPM are recorded the lowest value of ultrasonic pulse velocity compared to all blocks with DPWA or DPS cases use. This result indicate that DPM have best sound insulation than DPWA or DPS.
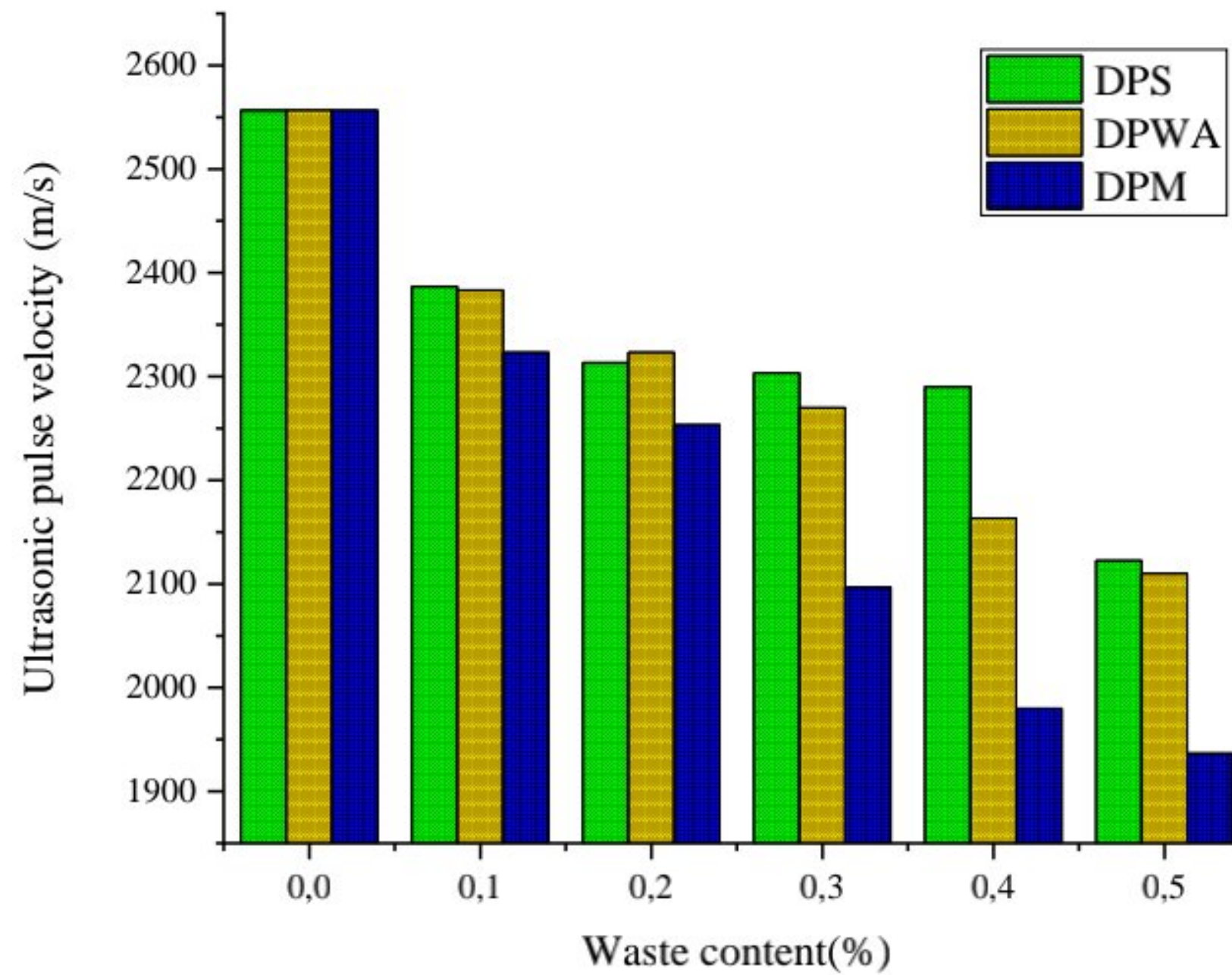
Fig 4. 27. Effect of waste type content on ultrasonic pulse velocity of CEB.

4.7.5 Effect of date palm waste content on thermal conductivity of CEB

As has been frequently reported in the literature, the primary motivation for incorporating a bio-resource into an earth matrix is to improve the material's thermal insulating properties[84], [100], [140]–[143]. In order to optimizing thermal performance of compressed earth blocks (CEB) based on different date palm waste (DPW) types, the thermal conductivity of CEBs incorporating different DPW types was performed. The results of the thermal conductivity of CEB are shown in Fig. 4.28. The values of the thermal conductivity are between 0.846 and 0.976 W/m. K. These results show that an addition of plant aggregates and fibers in an earth matrix decreases the thermal conductivity of the material. The addition of 0.5% of DPWA decreased the thermal conductivity by 13.27% in comparison with the specimen without plant waste whereas the decrease was only 9.63% in the case of an addition of 0.5% of DPS, and 6.6% in the case of an addition of 0.5% of DPM. The most efficient plant aggregate for improving the thermal insulation of the material seems to be DPWA.
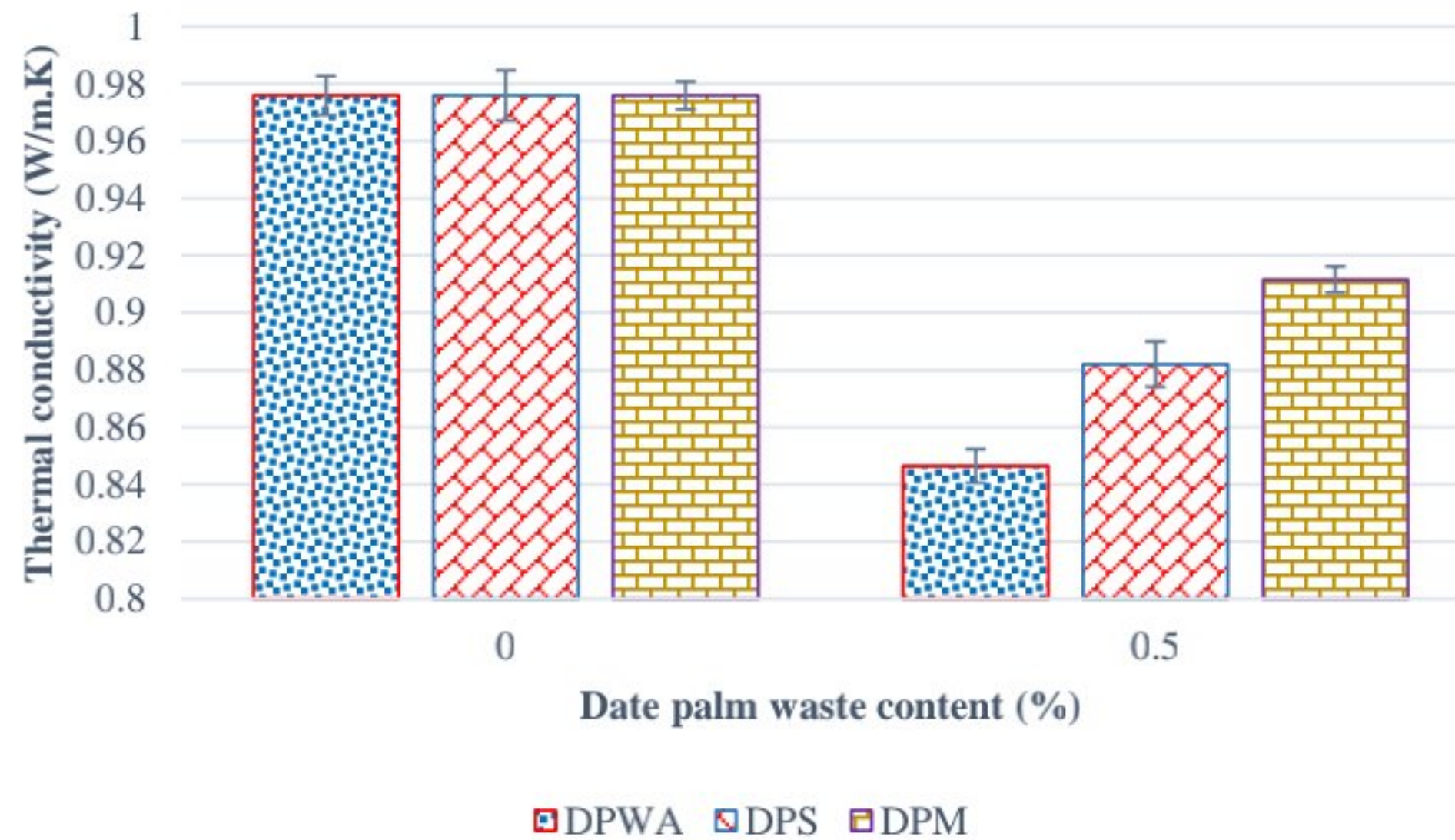
Fig 4. 28. Effect of DPW type on thermal conductivity of CEB.

4.7.6 Effect of compaction pressure on properties of compressed earth blocks (CEBs) based on date palm waste aggregates (DPWAs)

4.7.6.1 Effect of compaction pressure on bulk density and ultrasound plus velocity

The results of the bulk density and ultrasonic pulse velocity of CEB are presented in Table 4.4. Increasing the DPWA content in the mixture of CEB subsequently decreases the specimen's bulk density and ultrasonic pulse velocity. The light bulk density of the plant aggregate can explain the decreased bulk density of the CEB. Generally, the increase in porosity and decrease in density and ultrasonic pulse velocity is due to the weak bond between date palm aggregates and the matrix. In addition, This can be explained that the decrease of compaction pressure reduces the number of contact between grains[62].The increase in compaction pressure leads to an increase in bulk density and ultrasonic pulse velocity of CEB. The compaction pressure helps to reduce voids and therefore to increase the density of the blocks[18].

Table 4. 4. Bulk density and ultrasound plus velocity of CEB.

DPWA (%)	Compaction pressure (MPa)	Bulk density (kg/m^3)	Ultrasonic pulse velocity (m/s)
0	2	1668.41±2.53	1526.67±118.46
	6	1864.42±12.82	1863.33±115.03
	10	2069.57±17.90	2556.67±58.59
0.2	2	1667.83±2.16	1333.33±35.11
	6	1862.54±5.33	1783.33±83.26
	10	2064±10.53	2323.33±35.11
0.5	2	1662.38±2.91	1310±91.65
	6	1858.06±2.80	1680±86.60
	10	2033±6.56	2110±70

4.7.6.2 Effect of compaction pressure on dry compressive strength and dynamic modulus of elasticity

Compressive strength is one of the most important mechanical properties of materials. Fig. 4.29 and Fig.4.30 shows the effect of DPWA content and compacting pressure on the compressive strength of CEB. Compared with the CEB block without DPWA, increasing the DPWA content from 0.2% to 0.5% led to a decrease in compressive strength. In addition, the reduction of compressive strength that was observed in this study is connected to the incorporation of plant aggregate that has low compressive strength and stiffness[101].

The equations shown on the figure:

$$y = 5.2444e^{0.1091x}$$
$$R^2 = 0.9966$$

$$y = 4.3133e^{0.1115x}$$
$$R^2 = 0.9989$$

$$y = 4.3469e^{0.0815x}$$
$$R^2 = 1$$
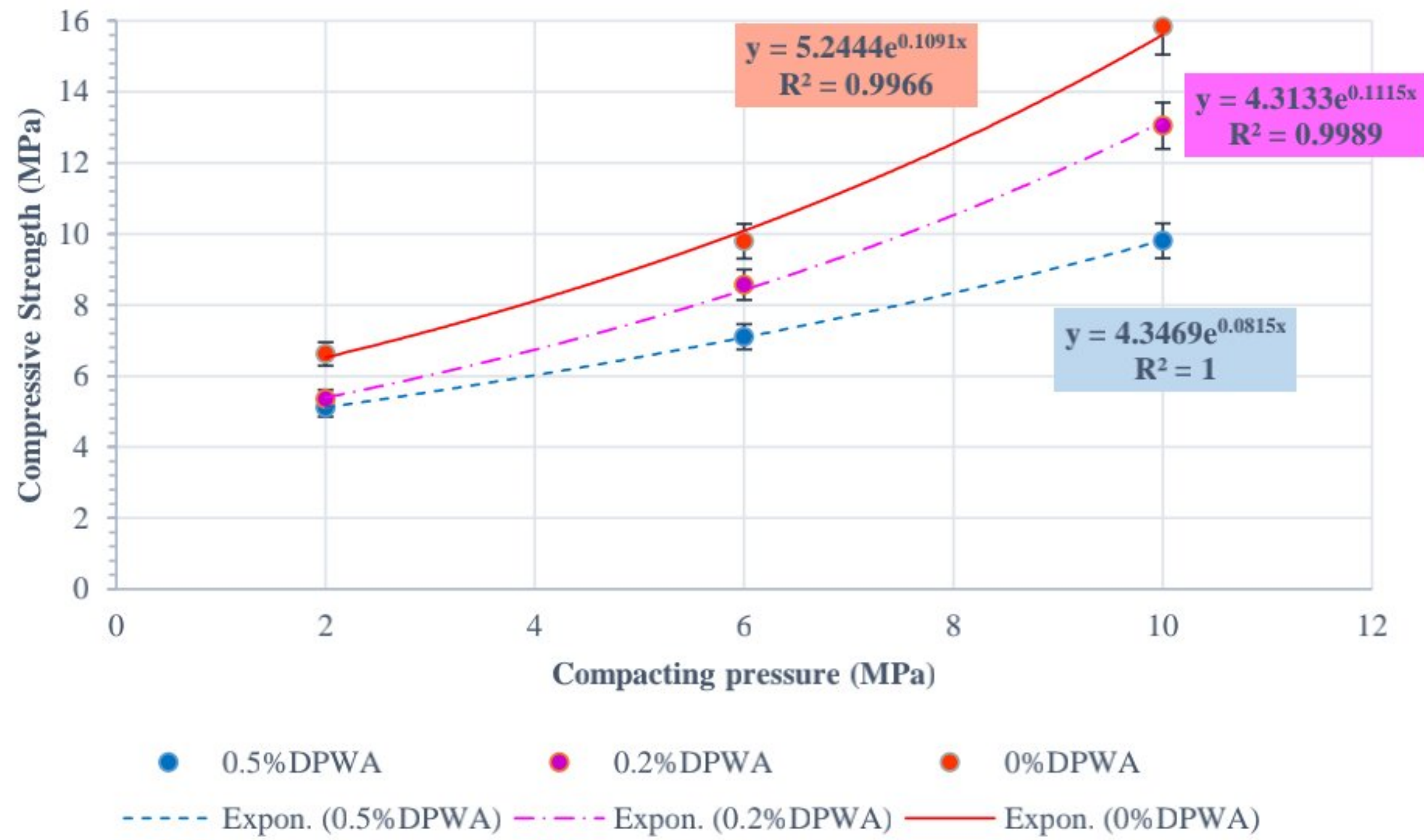
Fig 4. 29. Influence of the compacting pressure on the compressive strength of CEB.
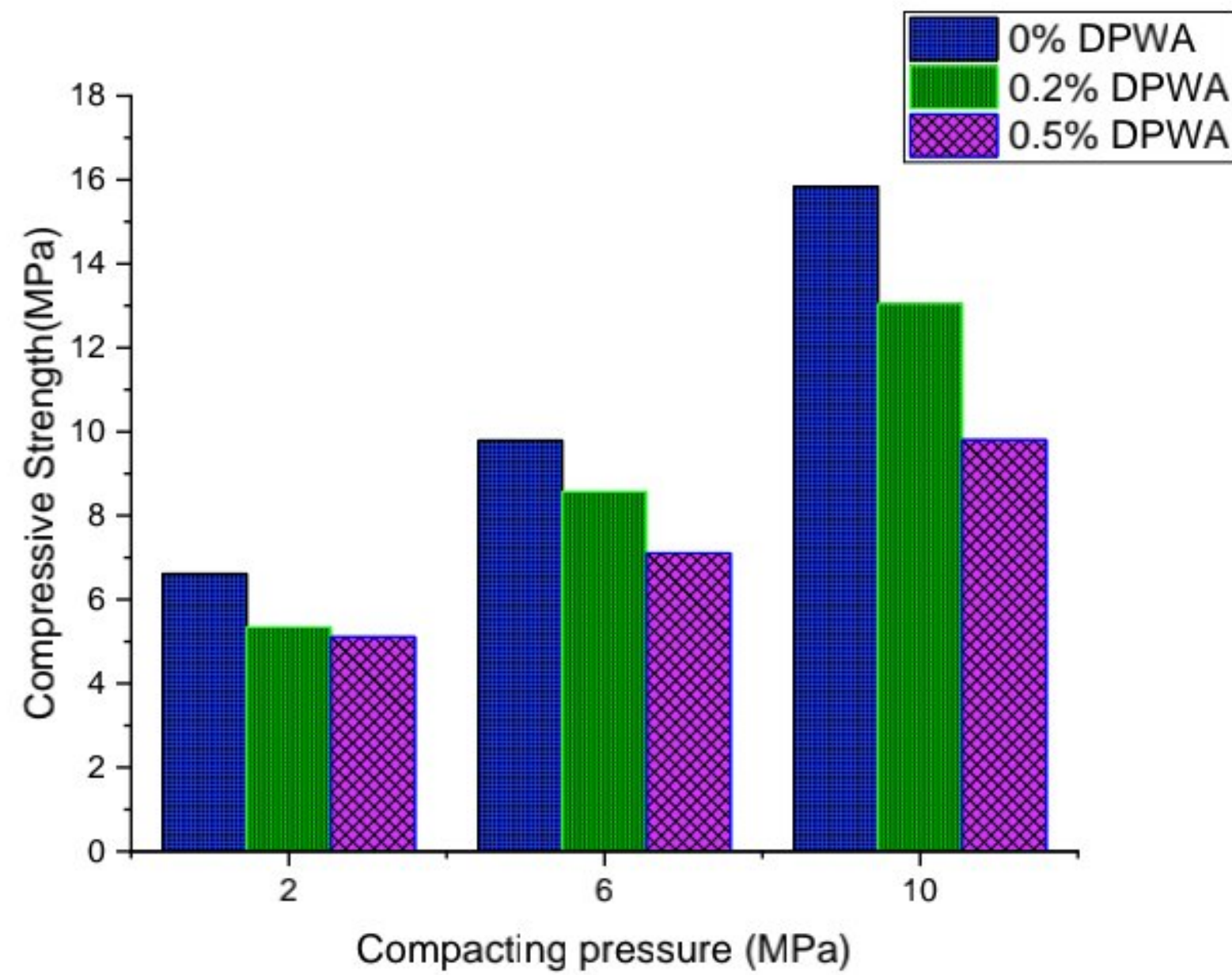
Fig 4. 30. Effect of DPWA content and compaction pressure on the compressive strength of CEB.

Fig.4.31 shows the influence of DPWA content and compacting pressure on the dynamic modulus of elasticity. The dynamic modulus of elasticity decreases when the percentage of date palm waste aggregate (to replace natural soil and sand) increases. The incorporation of plant particles into composite materials results in reduced dynamic elastic modulus[124]. Latroch et al. [124]reported

that the dynamic modulus of elasticity decreases as the percentage of waste from expanded PVC sheets (EPVC) increases.

The increase in compaction pressure leads to an increase in dynamic modulus of elasticity and compressive strength of CEB. The increase of the compressive strength with the dynamic modulus of elasticity is mainly explained by the decrease of porosity of the CEB as shown in Fig.3 and Fig.4.31. Increasing the applied compacting stress and thus increasing bulk density leads to CEB with higher mechanical performance.
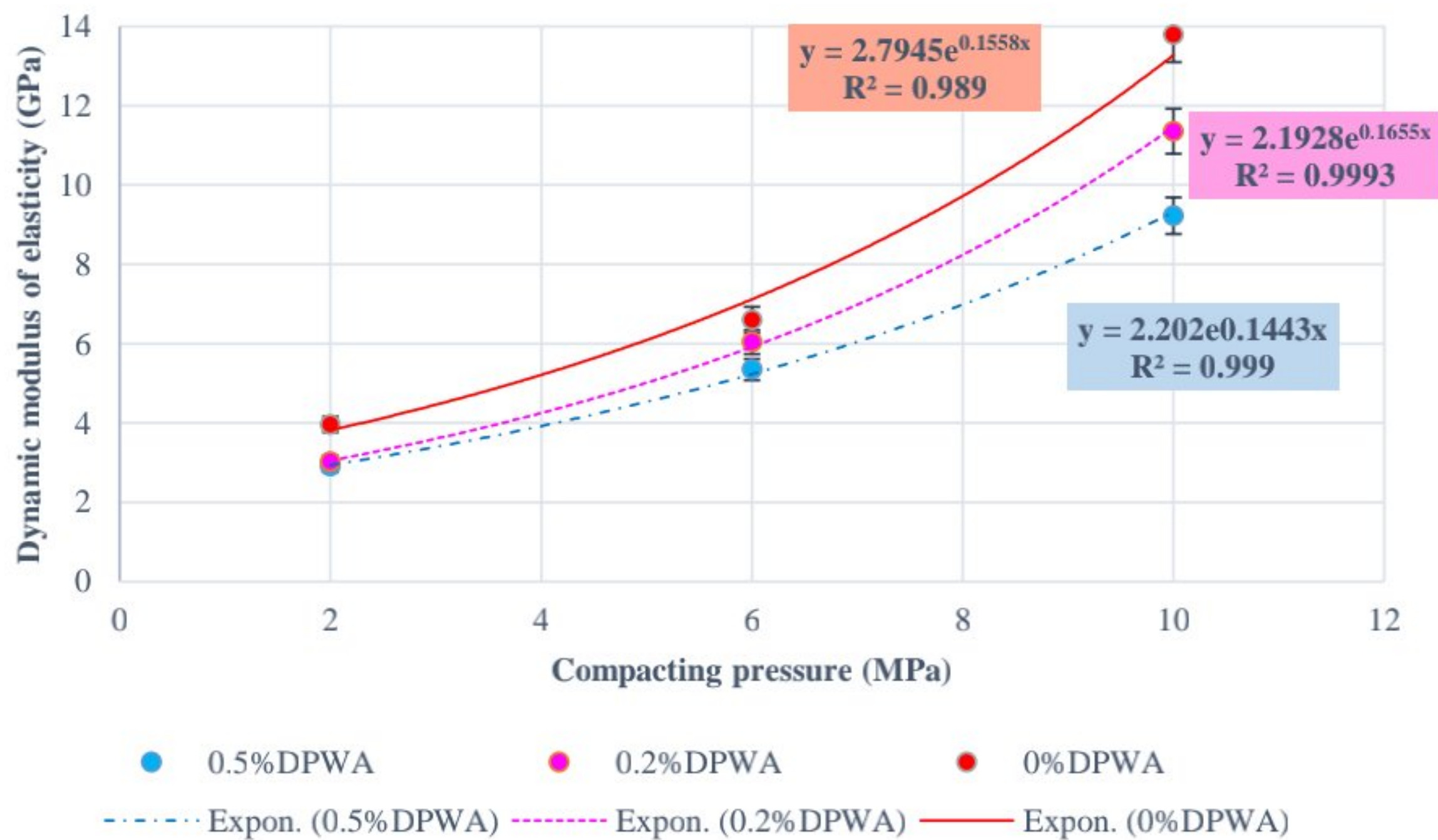
Fig 4. 31. Influence of the compacting pressure on the dynamic modulus of elasticity of CEB.

4.7.6.3 Effect of compaction pressure on apparent modulus of elasticity, flexural strength and microstructure (SEM) of CEB

In order to know the effect of increasing the compacting pressure on the mechanical properties, apparent modulus of elasticity, flexural strength and microstructure, various CEBs containing DPWA types are considered. Figs. 4.32 and 4.33 show the effect of DPWA content and the compacting pressure on the flexural strength and apparent modulus of elasticity of CEBs. One can see from the figures that, when the compaction pressure is increased from 2MPa to 10MPa, the modulus of elasticity and bending strength of CEB increases. In fact, the increase in compaction

pressure from 2 MPa to 6 MPa resulted in a very significant increase in flexural strength of about 142.83% and from 2 MPa to 10 MPa compaction pressures resulted in an increase in flexural strength of about 262.73% for the control block (samples without DPW). In addition, it was found that samples containing 0.5% DPWA increased the bending strength by about 371.68% with an increase in the compaction pressure from 2 MPa to 10 MPa. When the compaction pressure increases from 2MPa to 10MPa, the apparent modulus of elasticity increases from 393.31MPa to 809.37MPa for a block without DPWA, and from 214.22 MPa to 321.52MPa for a block containing 0.5% DPWA. The results obtained in the present investigation confirm the previous findings of the authors[18] regarding the effect of compaction pressure on the mechanical performance of CEB.
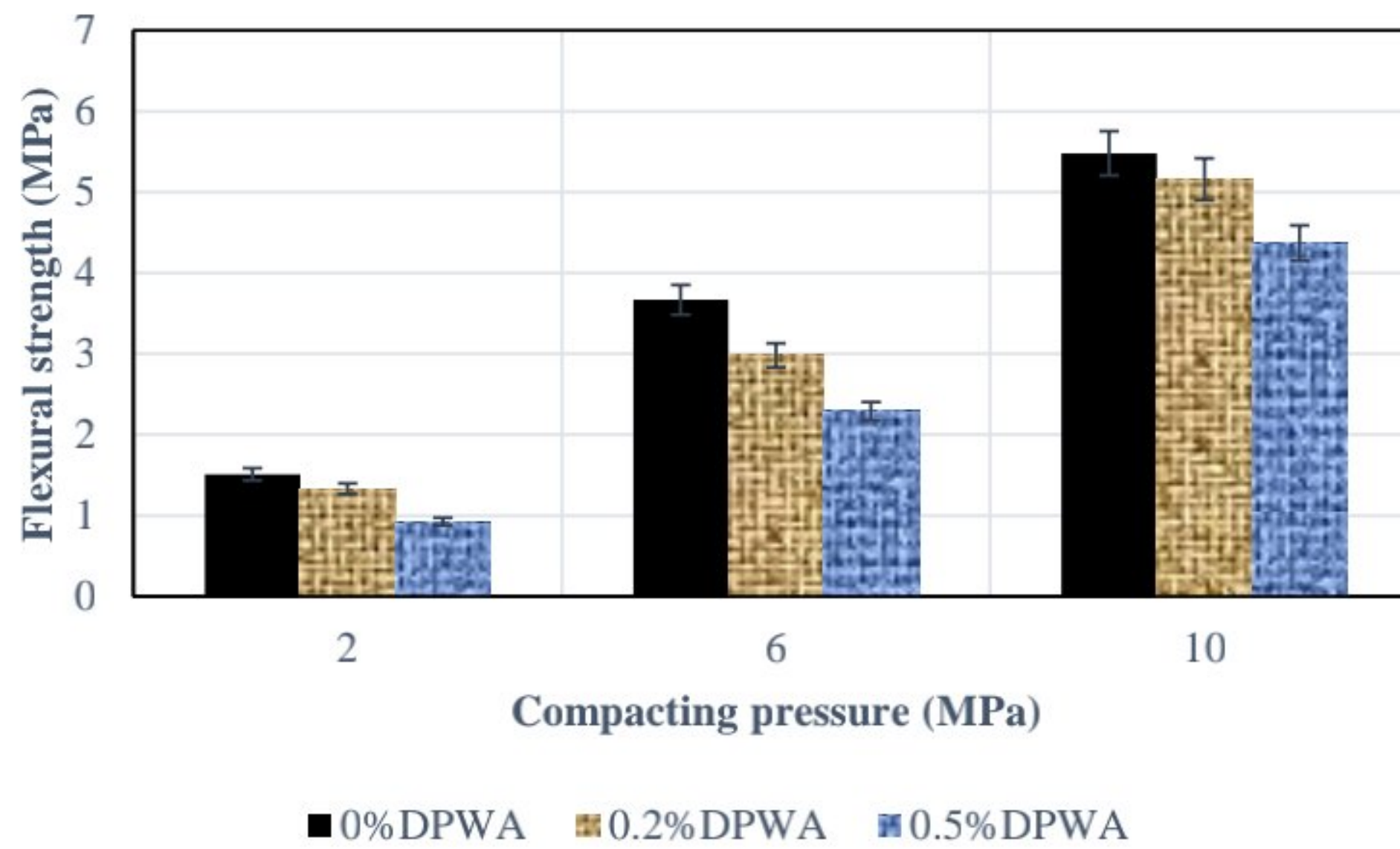
Fig 4. 32. Effect of compacting pressure on flexural strength of CEB based on DPWA.
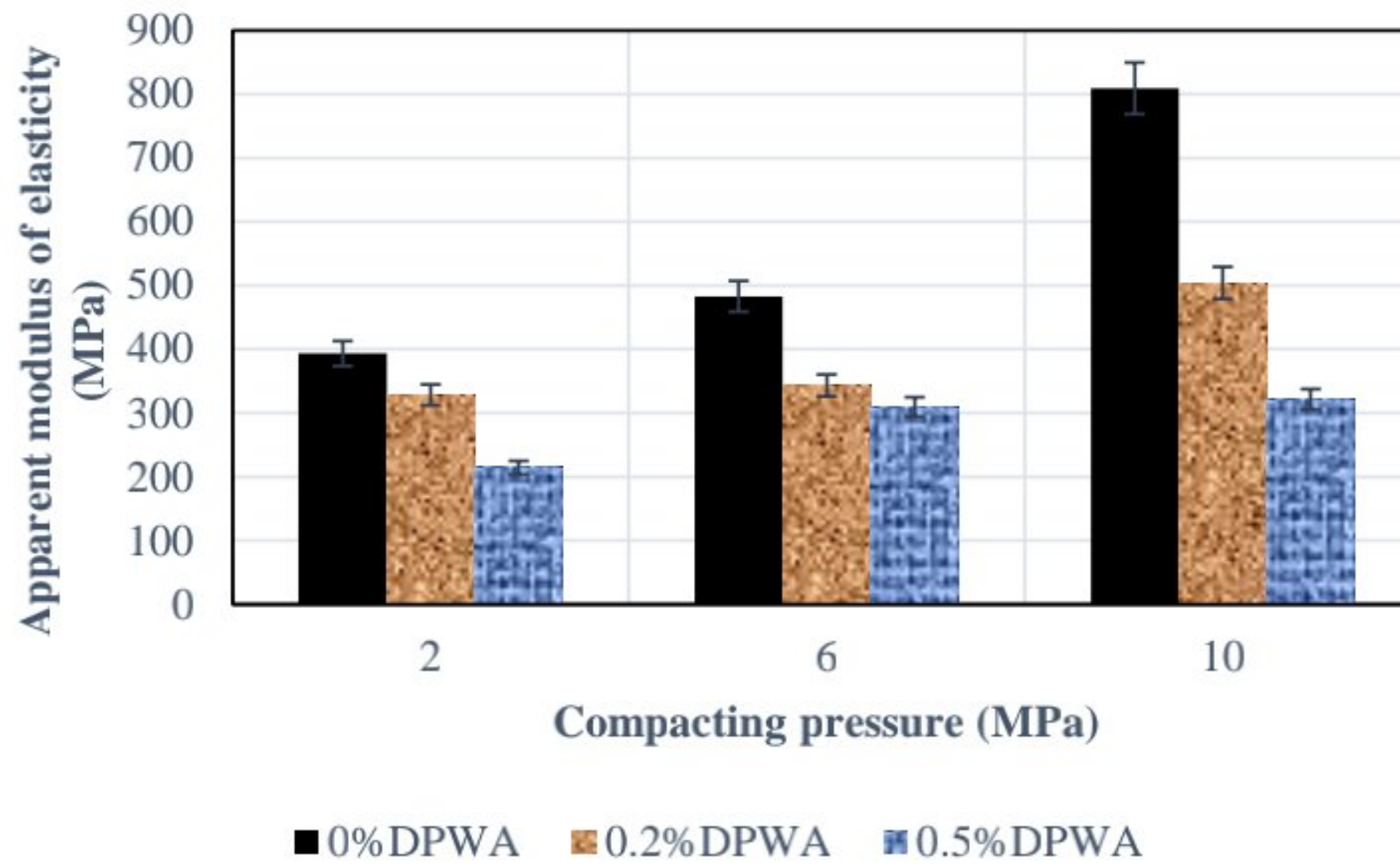
Fig 4. 33. Effect of compacting pressure on modulus of elasticity of CEB based on DPWA.

On the other hand, Fig. 4.34 shows the decreased porosity of CEB and this explains the increase in flexural strength and the modulus of elasticity. Microstructural analysis of the samples with different compaction stress level was performed by scanning electron microscopy (SEM) and they are presented in Fig.4.34. As it can be seen from Fig.4.34, CEB samples contain microscopic pores, as evidenced by SEM scans. The block with a compacting pressure of 2 MPa has more micro-pores than those with compacting pressures of 6 and 10 MPa. When the applied compacting pressure rose from 0.39 MPa to 3.16 MPa, the porosity values decreased from 41.6% to 21.7%, according to Ben Mansour et al.[62]. On the other hand, the block with compaction pressure of 10MPa has lower micro-voids than the rest of the samples. Indeed, the internal structure of the fluid phase and the solid phase (granular packing) was regulated by reducing the amount of macroscopic and microscopic pores and this is due to the increased compaction pressure[62].

Building materials used in structural applications must have a minimum flexural strength of 0.65 MPa, according to British Standard BS 6073[144]. On the other hand, the Masonry Standards Joint Committee requires that clay and concrete blocks have a minimum flexural strength of 0.21 MPa [101], [145]. The sample integrated by 0.5% DPWA and compacted by 2MPa has the lowest flexural strength of about 0.93 MPa. However, it stayed within the acceptable building materials range, and all of the samples evaluated in this study have bending strengths that exceed these two minimal requirements.
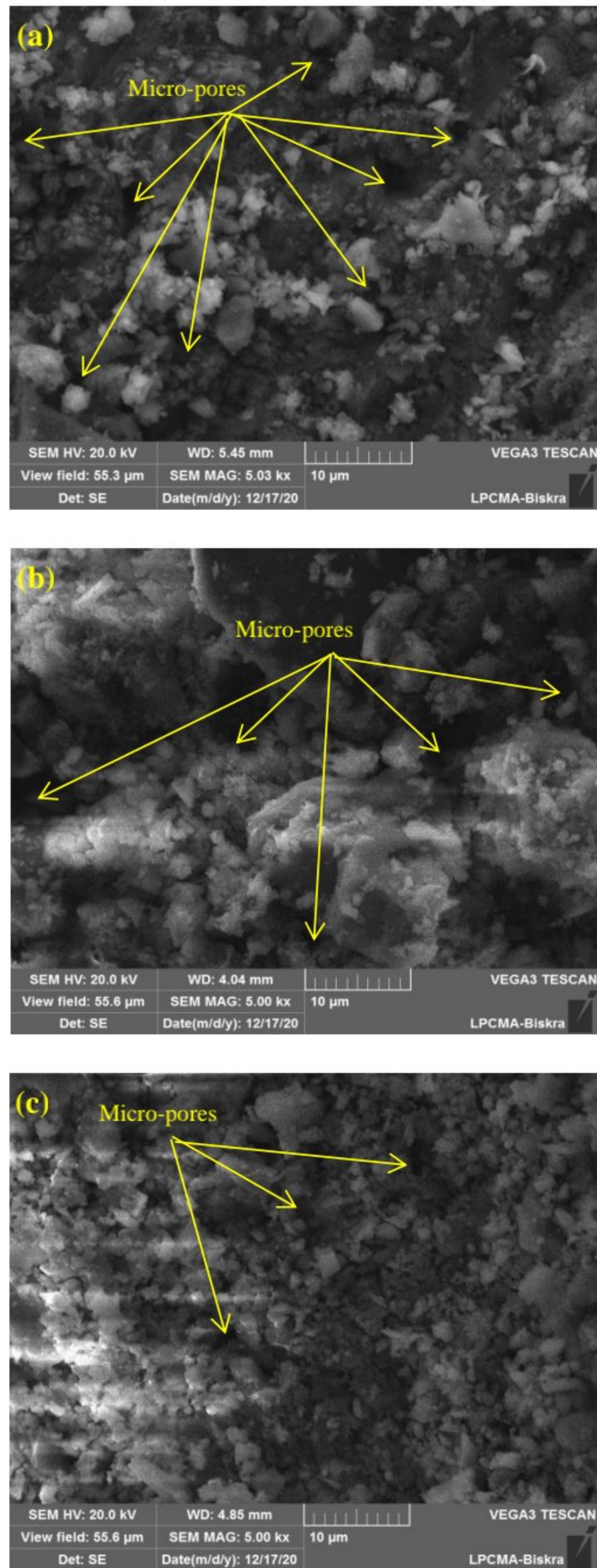
Fig 4. 34. SEM observation of CEB with different compacting stress levels: a) 2MPa, b) 6MPa and c) 10MPa.

4.7.6.4 Influence of the compacting pressure on the thermal conductivity of CEB based on DPWA

The variation of thermal conductivity as a function of the compaction pressure is shown in Fig. 4.35. When the compaction pressure of CEB is reduced, the thermal conductivity is decreased. In fact, the thermal conductivity has reached a value of 0.694 W/m.K at a compaction pressure of 2 MPa. The decrease in the thermal conductivity is mainly explained by the increase in the porosity (micro-pores) of the CEB, as shown in SEM observation (Fig. 4.34). In fact, the decrease in compaction pressure from 10 MPa to 6 MPa resulted in a significant decrease in thermal conductivity of about 7.21%, and the decrease from 10 MPa to 2 MPa resulted in a decrease in thermal conductivity of about 21.96% for the block containing 0.5% DPWA. In addition, it was found that a sample containing 0% DPWA decreased the thermal conductivity by about 26.17%, with a decrease in the compaction pressure from 10 MPa to 2 MPa. The results of Khoudja et al's[25] studies on thermal conductivity revealed that the adobe block without date palm waste (DPW) has a thermal conductivity of 0.677 W/m.K. Fortunately, the CEB block combined with 0.5% DPWA and compressed by 2 MPa gives approximately the same result (0.694 W/m.K).
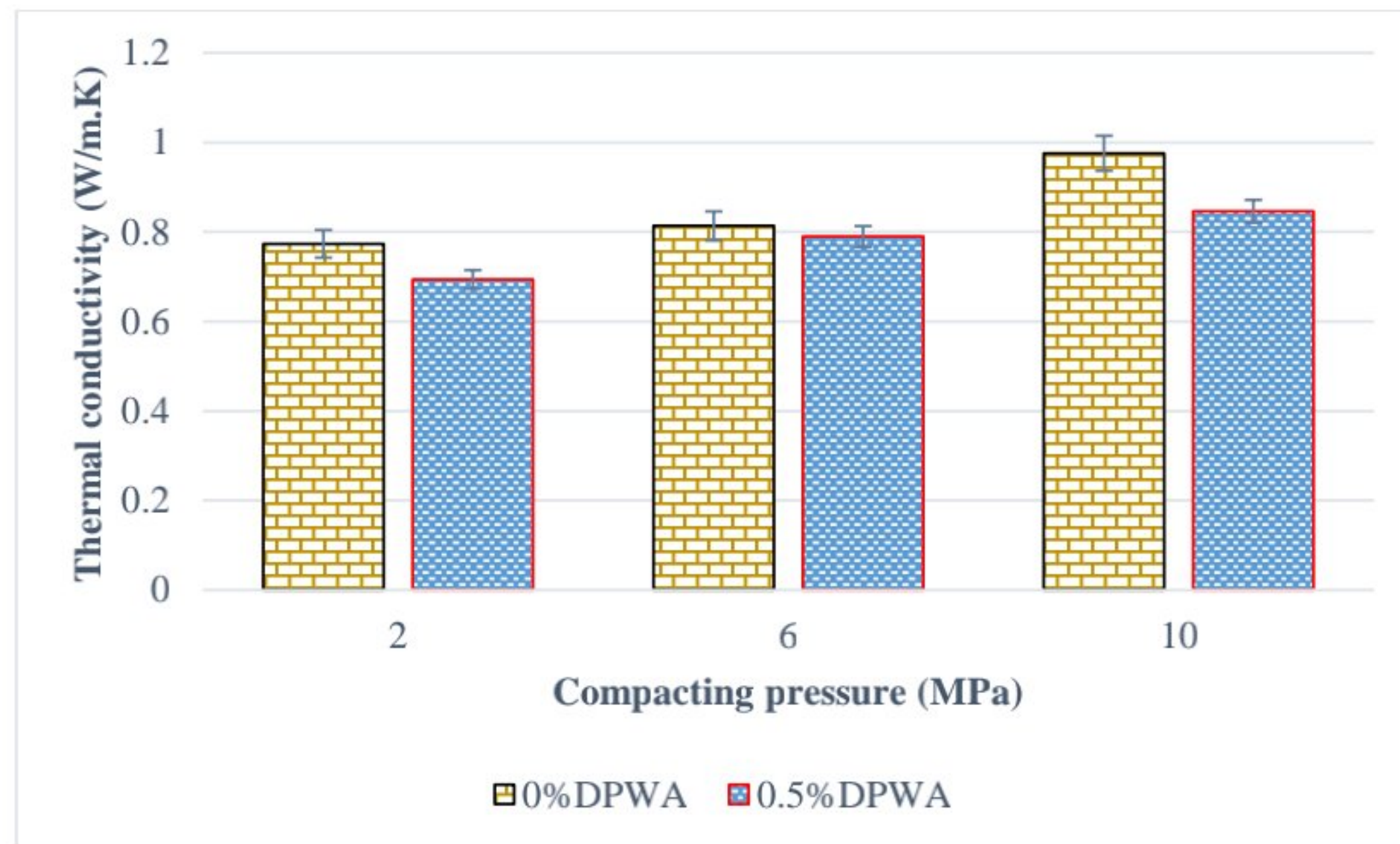
Fig 4. 35. Influence of the compacting pressure on the thermal conductivity of CEB based on DPWA.

4.7.7 DIC analysis (Strain field distributions)

The in-plane strain fields (ε_{xx} (transverse direction), ε_{yy} (force direction), and ε_{xy}) obtained by the DIC technique, for different samples under flexural applied load are depicted in Figs. 4.36–4.50. All DIC images were taken right before the collapse. In this study, the most important strain is the horizontal strains (ε_{xx}), because the samples are under a bending load. Many researchers [40], [113], [120] have focused their analysis on understanding the ε_{xx} behavior while studying the failure mechanism of construction materials under bending tests by using the DIC method.

Figs. 4.36, 4.39, 4.40, 4.45, and 4.48 show the horizontal strains (ε_{xx}) of the CEBs beams just before collapse. In particular, Fig. 4.36(a) demonstrates that the control CEB beam had low ε_{xx} values, and with increasing the fiber doses for CEB beams (see Fig. 4.36 (b) to Fig. 4.36 (c)) the values of ε_{xx} increased just before the crash (compared to the control CEB). The results of ε_{xx} show that the samples have very high-localized strains in the middle of the block and the strain concentration increases with increasing fiber content. This can be explained by the bending load being applied in the middle of the block. These results are consistent with the destructive experimental results, as the higher the palm fiber or the plant aggregates content, the higher the value of the ultimate deflection.

In addition, when the compaction pressures of CEBs are increased, the values of ε_{xx} are increased. The block integrated by 0.5%DPWA and compacted by 10MPa has a high ε_{xx} value (around 0.04 as seen in Fig. 4.36 (c)) at the tensioned bottom part compared to all other blocks. This is consistent with the experimental results. From Fig.4.22 (a), it can be seen that this sample has the highest ultimate displacement value. The fields of ε_{yy} strain are shown in Figs. 4.37, 4.43, 4.44, 4.47 and 4.49. As shown in these figures, the strain fields at the bottom of blocks are tensioned, while most of the samples are compressed at the top. Since the beams are subject to bending forces, according to the beam theory, there are two types of deformations, compression deformations, and tensile deformations. It can be clearly seen from the shear strains (ε_{xy}) that the shear band is diagonal and in the middle of the blocks in most cases (see Fig.4.38, 4.41, 4.42, 4.46 and 4.50). The ε_{xy} results show high-localized strains at the bottom of the samples under two types of deformation: (1) caused by tension stress and (2) by compressive stress.

🔸 **CEBs incorporating DPWA and compacting by 10MPa**
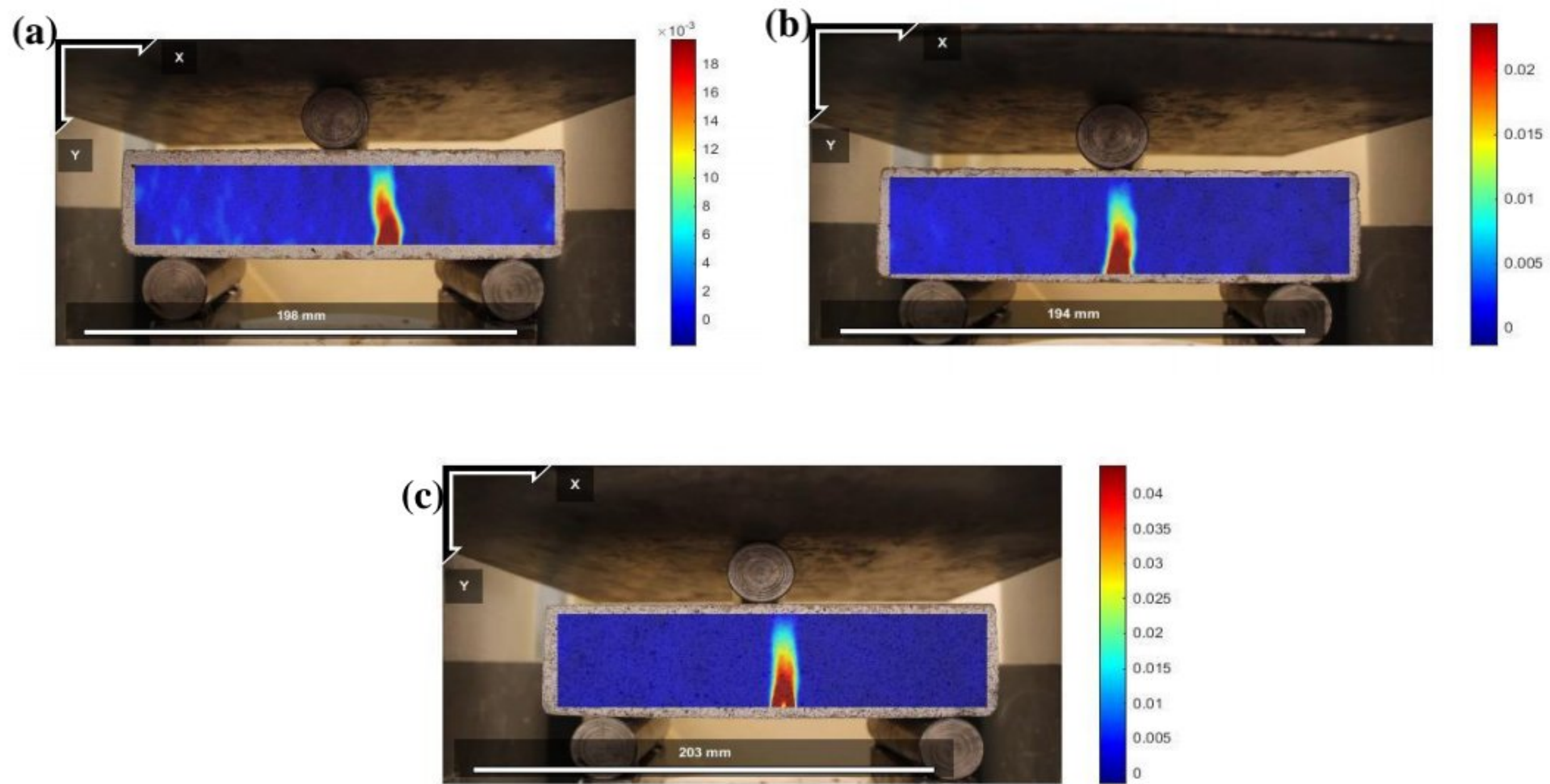
Fig 4. 36. (a) ε_{xx} DIC of 0%DPWA.10MPa, (b) ε_{xx} DIC of 0.2%DPWA.10MPa, and (c) ε_{xx} DIC of 0.5%DPWA.10MPa.
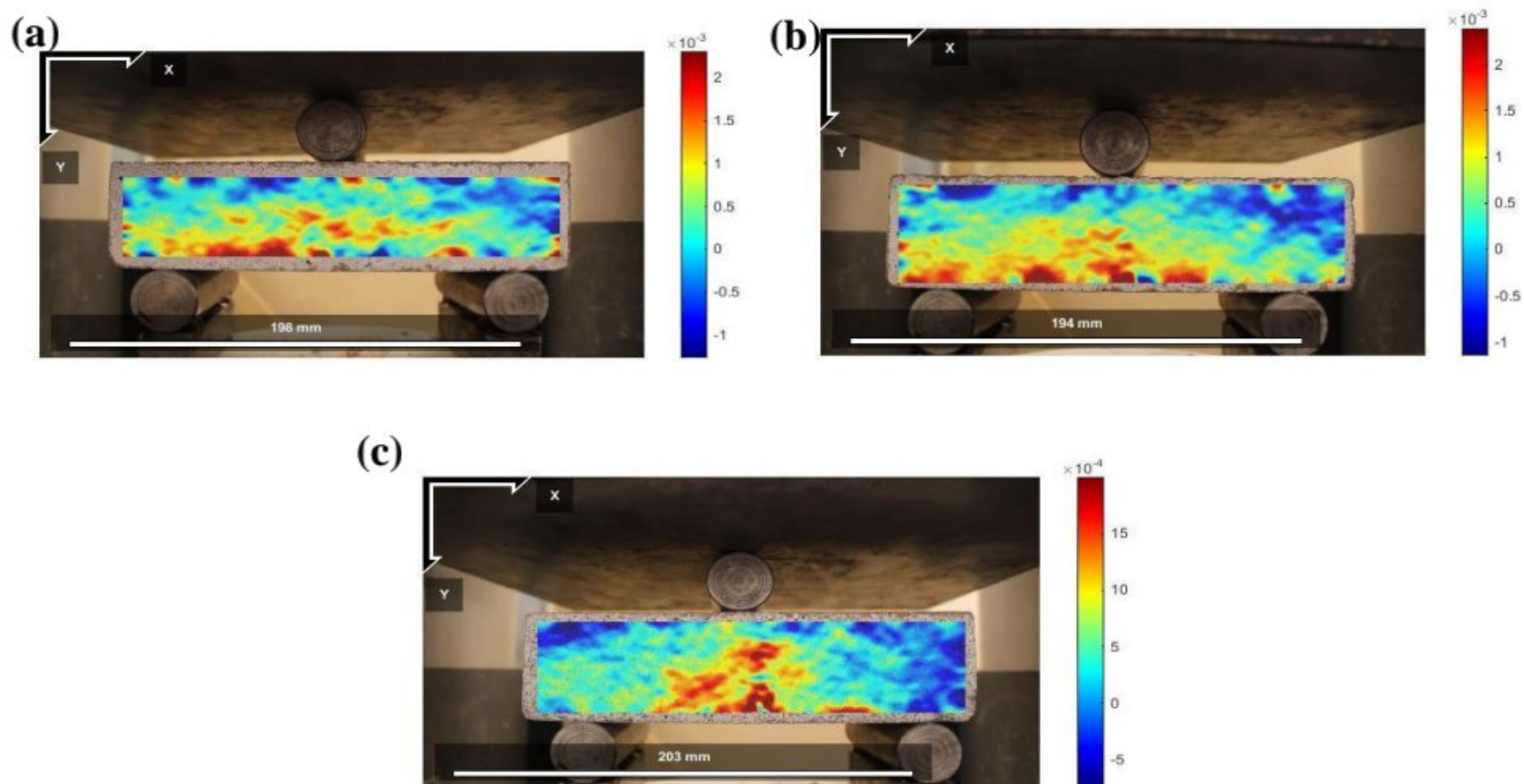
Fig 4. 37.(a) ε_{yy} DIC of 0%DPWA.10MPa, (b) ε_{yy} DIC of 0.2%DPWA.10MPa, and (c) ε_{yy} DIC of 0.5%DPWA.10MPa.
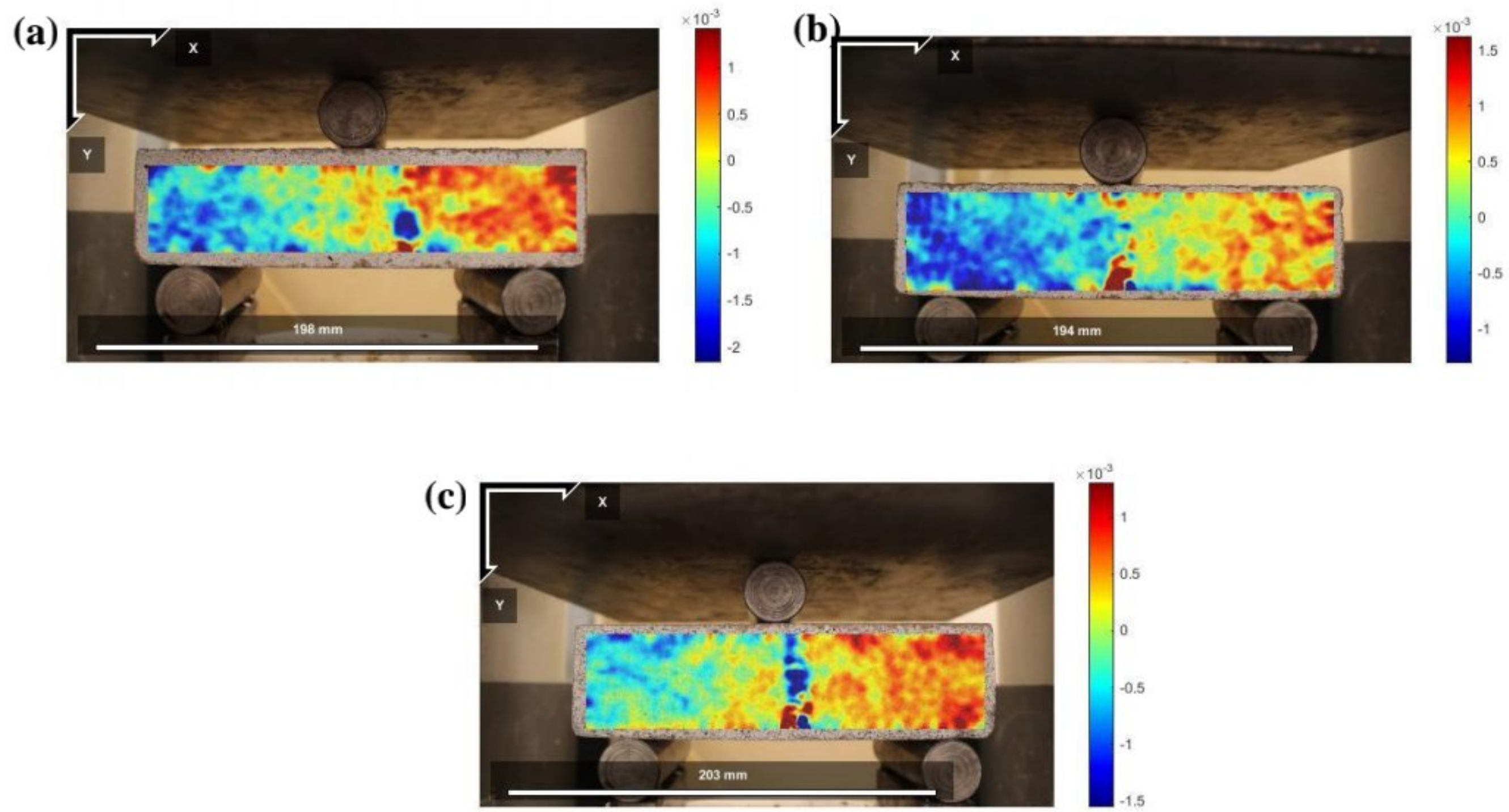
Fig 4. 38. (a) ε_{xy} DIC of 0%DPWA.10MPa, (b) ε_{xy} DIC of 0.2%DPWA.10MPa, and (c) ε_{xy} DIC of 0.5%DPWA.10MPa.
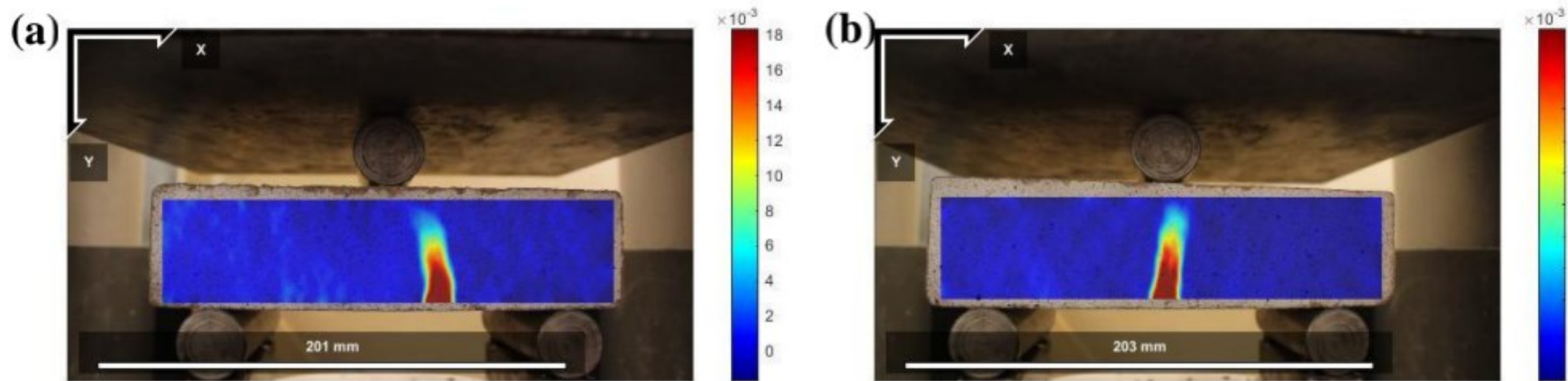
Fig 4. 39. (a) ε_{xx} DIC of 0.2%DPM.10MPa, (b) ε_{xx} DIC of 0.2%DPS.10MPa.
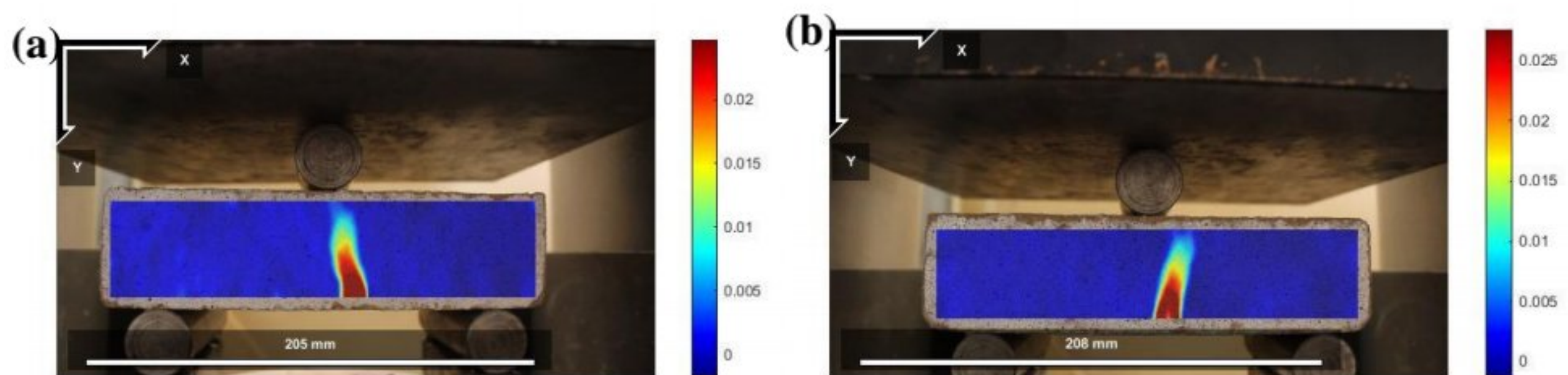
Fig 4. 40. (a) ε_{xx} DIC of 0.5%DPM.10MPa ;(b) ε_{xx} DIC of 0.5%DPS.10MPa.
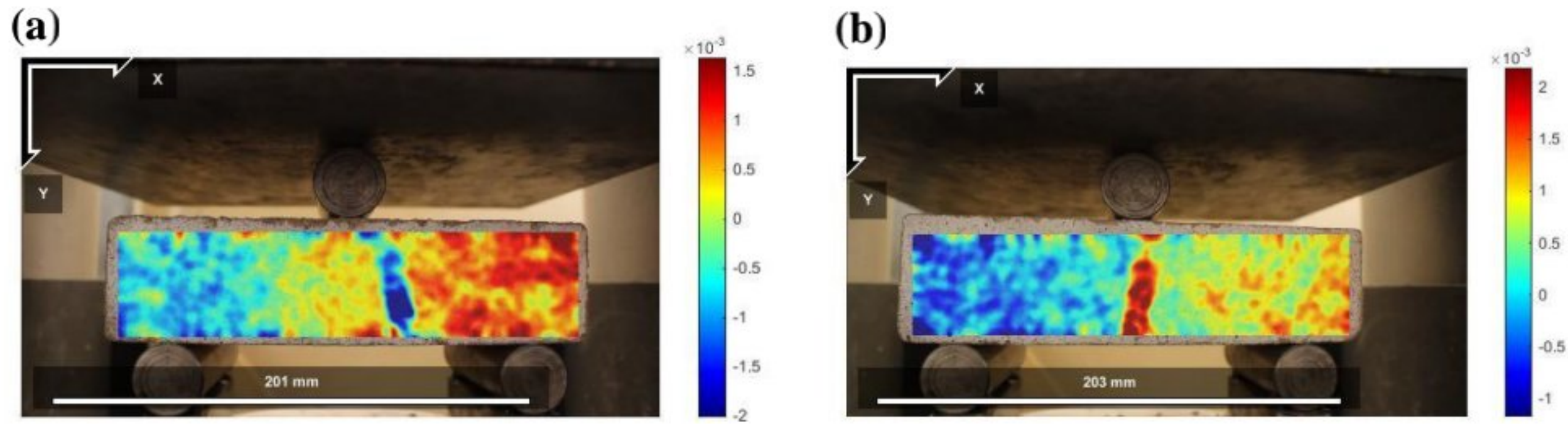
Fig 4. 41. (a) ε_{xy} DIC of 0.2%DPM.10MPa, (b) ε_{xy} DIC of 0.2%DPS.10MPa.
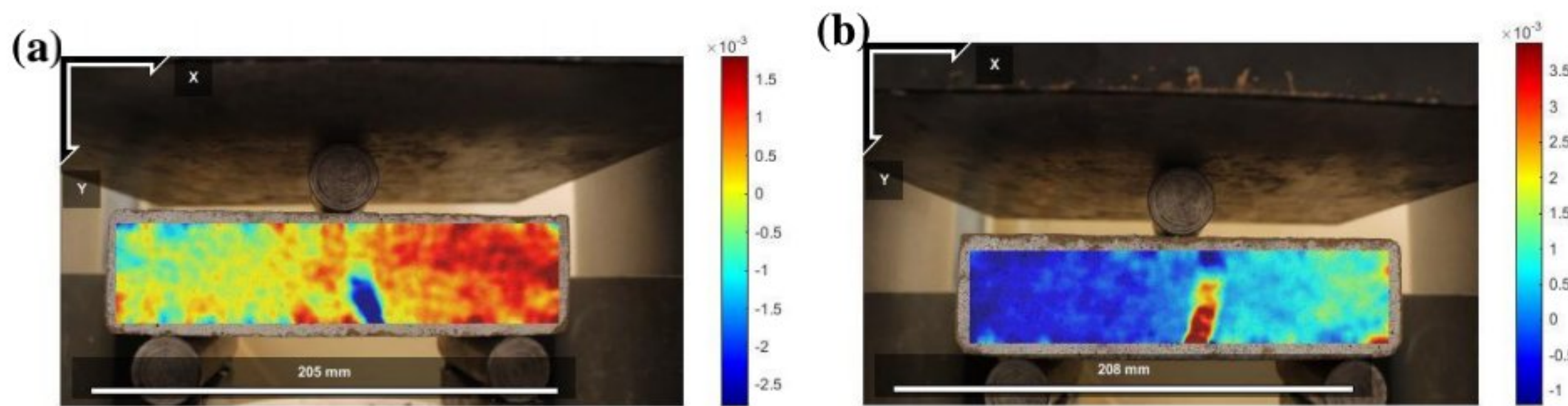
Fig 4. 42. (a) ε_{xy} DIC of 0.5%DPM.10MPa; (b) ε_{xy} DIC of 0.5%DPS.10MPa.
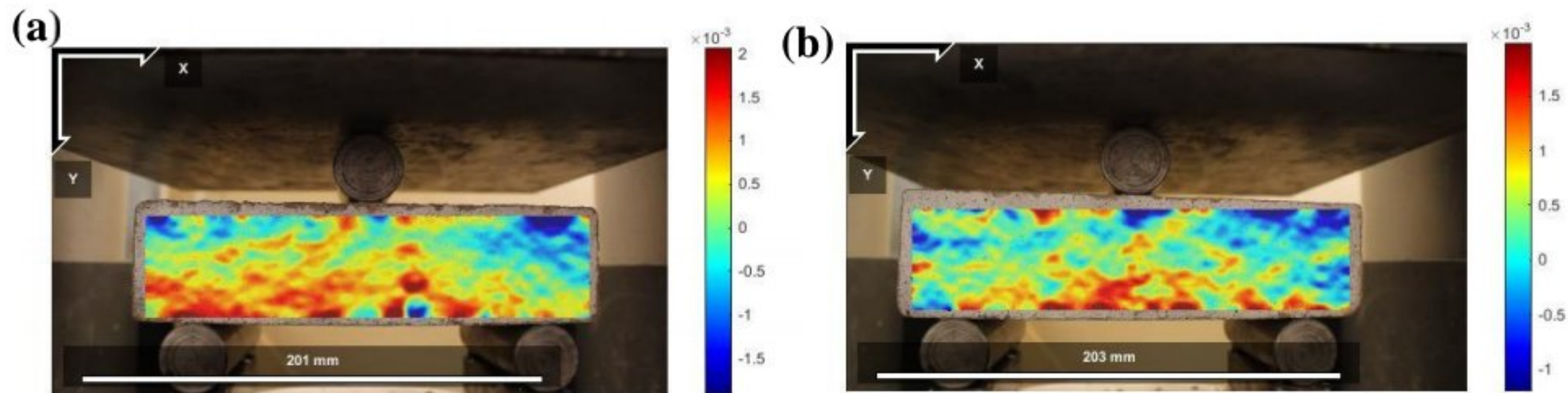
Fig 4. 43. (a) ε_{yy} DIC of 0.2%DPM.10MPa, (b) ε_{yy} DIC of 0.2%DPS.10MPa.
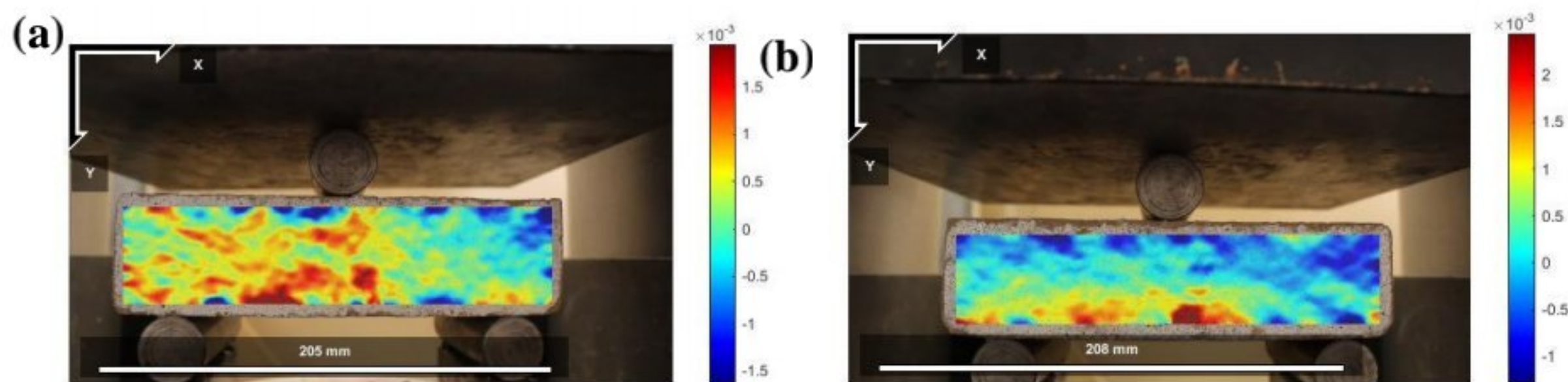
Fig 4. 44. (a) ε_{yy} DIC of 0.5%DPM.10MPa; (b) ε_{yy} DIC of 0.5%DPS.10MPa.

⬥ **CEBs incorporating DPWA and compacting by 6 MPa**
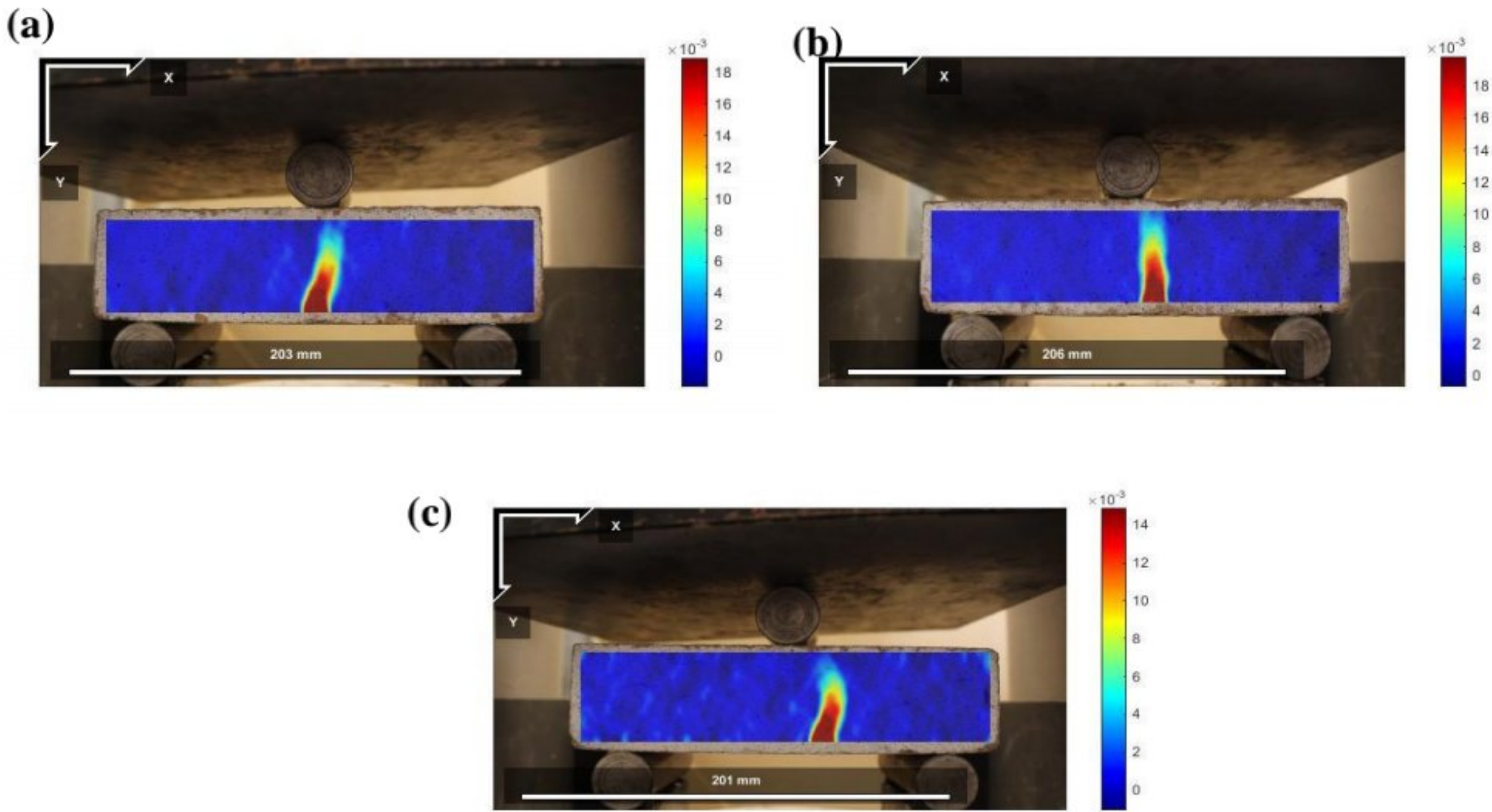
Fig 4. 45. (a) ε_{xx}DIC of 0%DPWA.6MPa, (b) ε_{xx} DIC of 0.2%DPWA.6MPa, and (c) ε_{xx} DIC of 0.5%DPWA.6MPa.
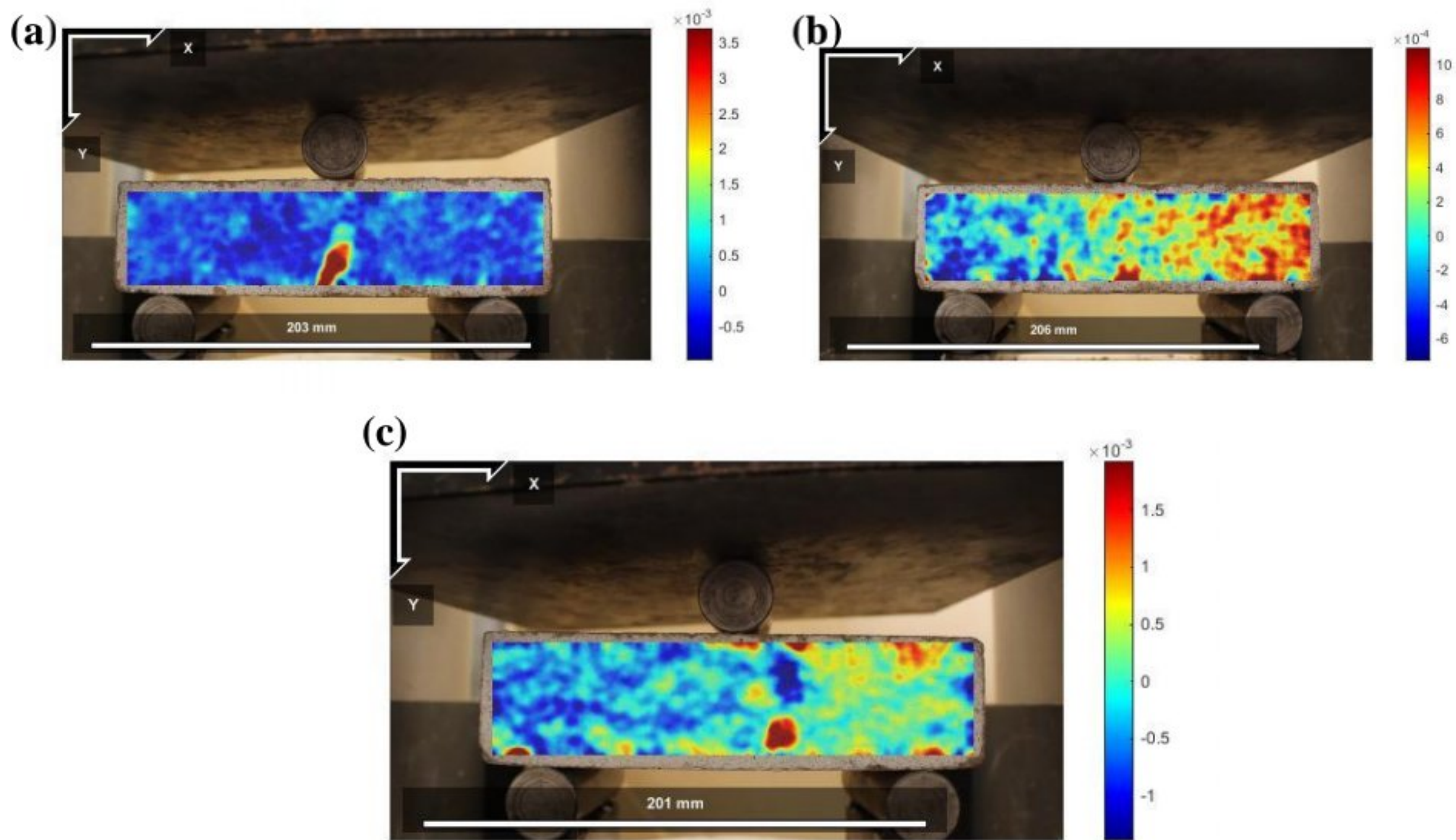
Fig 4. 46. (a) ε_{xy}DIC of 0%DPWA.6MPa, (b) ε_{xy} DIC of 0.2%DPWA.6MPa, and (c) ε_{xy} DIC of 0.5%DPWA.6MPa.
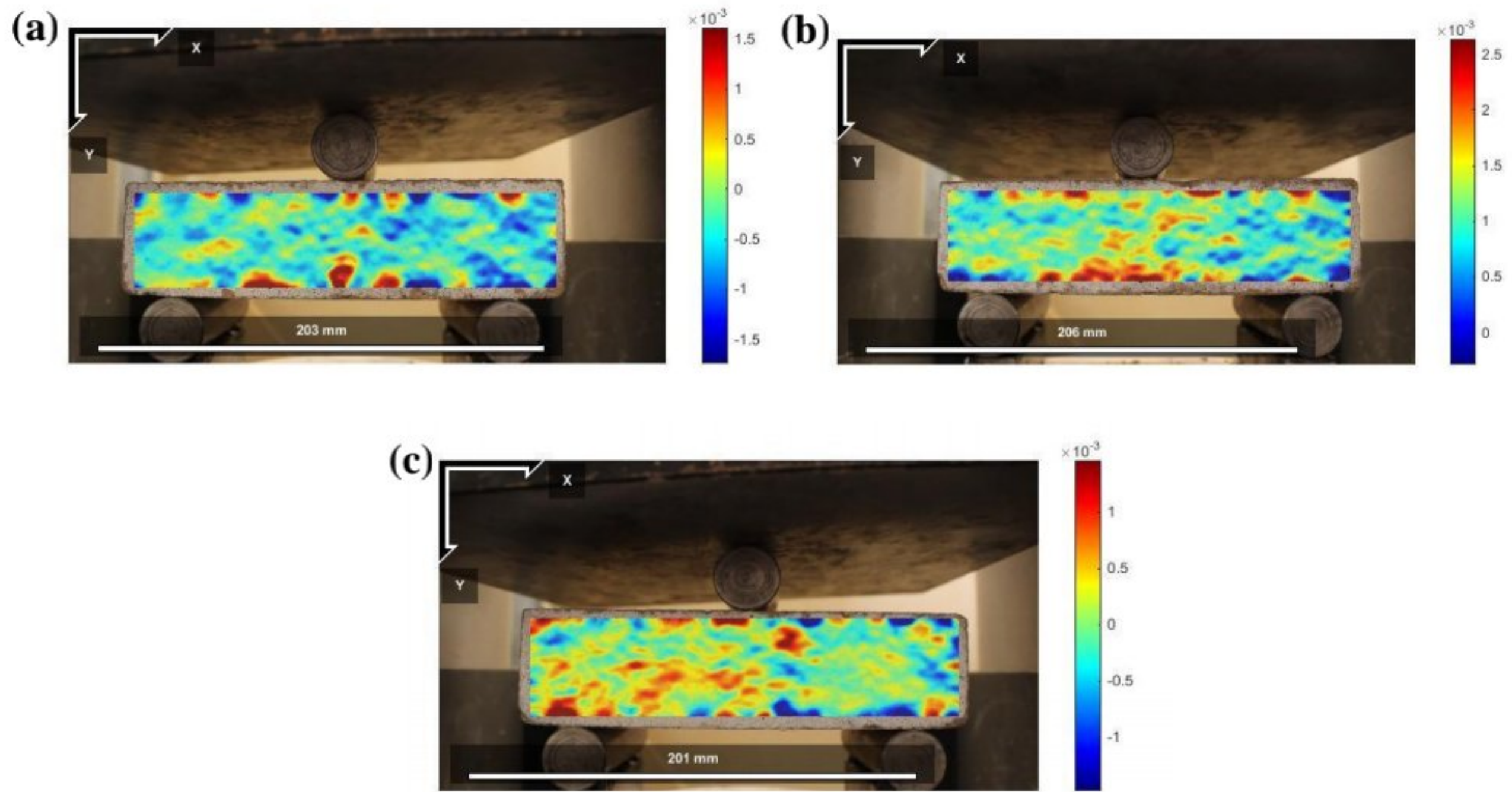
Fig 4. 47. (a) ε_{yy}DIC of 0%DPWA.6MPa, (b) ε_{yy} DIC of 0.2%DPWA.6MPa, and (c) ε_{yy} DIC of 0.5%DPWA.6MPa.

🔸 **CEBs incorporating DPWA and compacting by 2MPa**
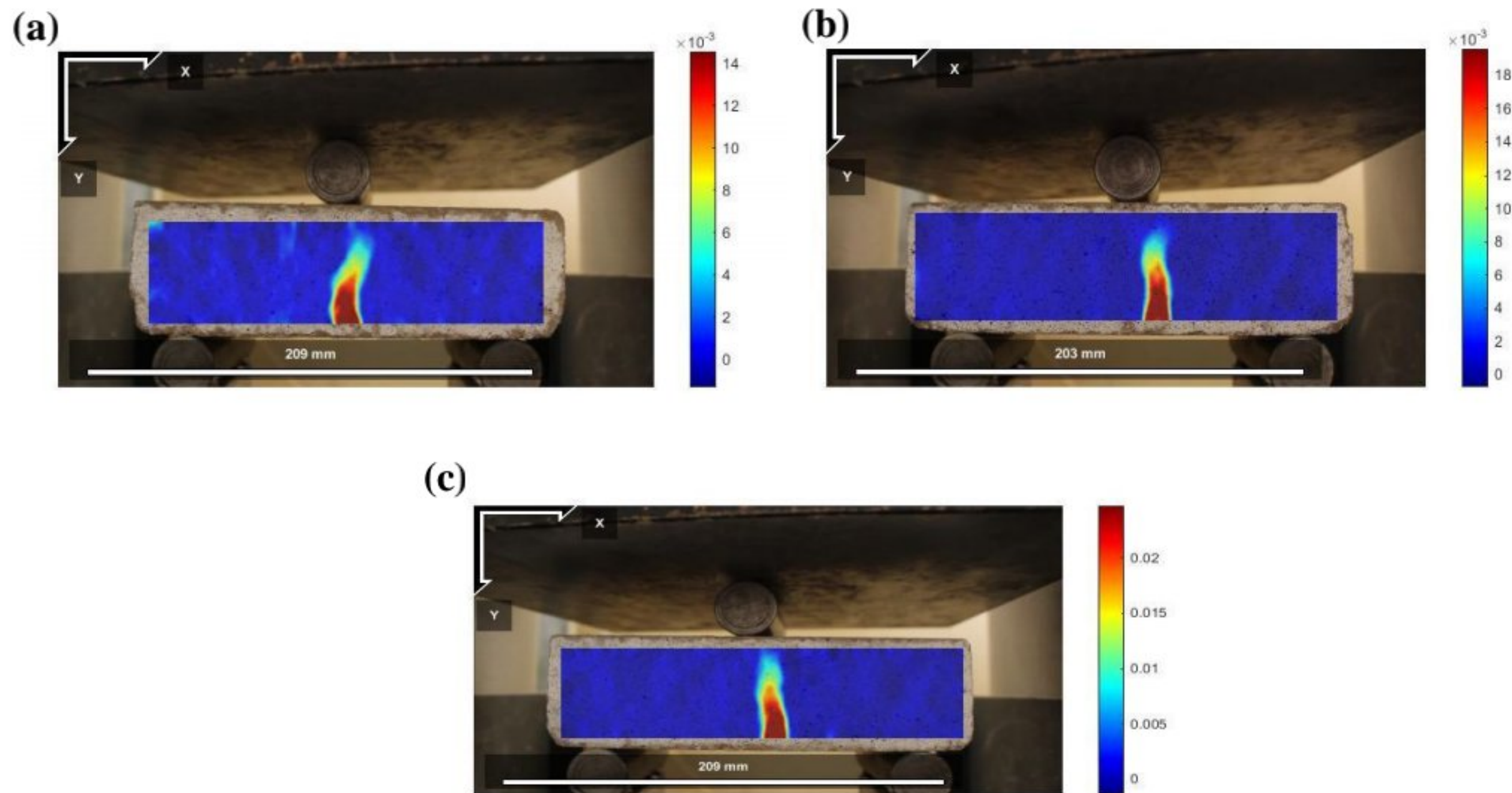
Fig 4. 48. (a) ε_{xx}DIC of 0%DPWA.2MPa, (b) ε_{xx} DIC of 0.2%DPWA.2MPa, and (c) ε_{xx} DIC of 0.5%DPWA.2MPa.
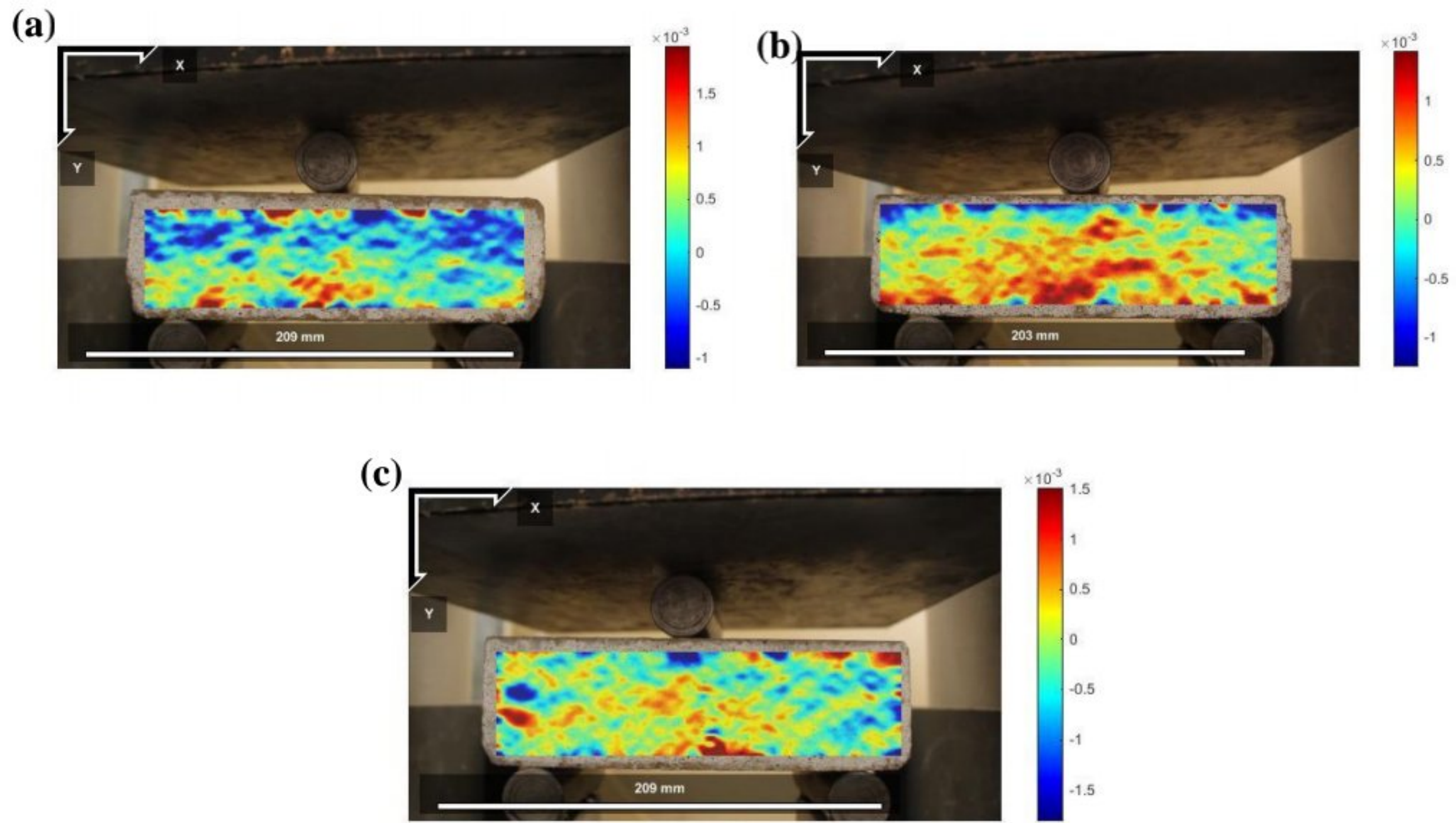
Fig 4. 49. (a) ε_{yy}DIC of 0%DPWA.2MPa, (b) ε_{yy} DIC of 0.2%DPWA.2MPa, and (c) ε_{yy} DIC of 0.5%DPWA.2MPa.
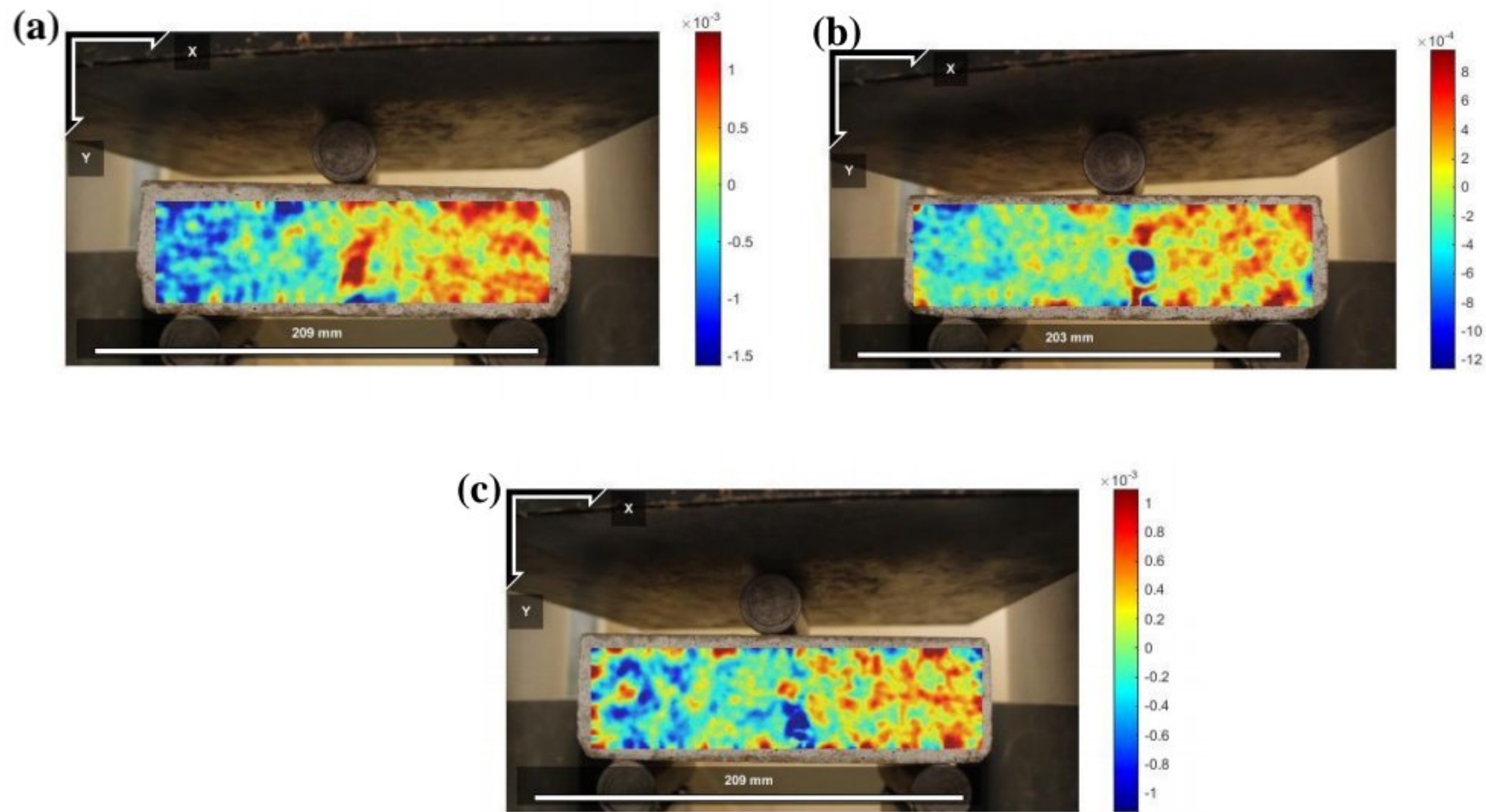
Fig 4. 50. (a) ε_{xy}DIC of 0%DPWA.2MPa, (b) ε_{xy} DIC of 0.2%DPWA.2MPa, and (c) ε_{xy} DIC of 0.5%DPWA.2MPa.

4.8 Conclusion

Based on the experimental results mentioned above, the following conclusions can be drawn:

- The incorporation of date palm waste aggregates (DPWAs) in compressed earth blocks (CEBs) improved their thermal behavior. Indeed, adding 0.5% by weight of DPWA decreased the thermal conductivity, thermal diffusivity, and thermal effusivity respectively by 13.28%, 3.69%, and 11.63% in comparison with the reference block (without DPWA).

- Increasing the DPWA content in the CEB mixture caused the specimen's bulk density to go down. The lightweight block exhibited a lower thermal conductivity as compared to that of the other compressed earth blocks.

- In fact, the decrease in compaction pressure from 10 MPa to 2 MPa resulted in a significant decrease in thermal conductivity of about 21.96% for the block containing 0.5% DPWA. Fortunately, this block gives approximately the same result (0.694 W/m.K) as the adobe block without date palm waste (0.677 W/m.K).

- The dry and wet compressive strengths decreased while the waste content increased but still remained within the range recommended for compressed earth blocks. In addition, increasing the Date palm Waste (DPW) content decreased the flexural strength of all blocks. The values of the flexural strength was higher for the mixtures with DPWA than for those with DPM or DPS.

- All of the samples evaluated in this study have bending strengths that exceed those minimal requirements. The specimen integrated by 0.5% DPWA compacted with a static loading by applying a compacting stress of 2MPa has the lowest flexural strength of about 0.93 MPa. However, it stayed within the acceptable CEB range.

- Increasing the percentage of DPW in the formulation of CEB directly affected the modulus of elasticity. It turned out that the higher this percentage, the smaller the modulus of elasticity.

- The addition of 0.5% DPS increases the ductility of the bricks, resulting in some residual force and increasing the deflection at failure.

- The increase in compaction pressure from 2 MPa to 6 MPa resulted in a very significant increase in flexural strength of about 142.83%, and the increase from 2 MPa to 10 MPa resulted in an increase in flexural strength of about 262.73% for the control block (samples

without DPW). In addition, it was found that for a block containing 0.5% DPWA, increasing the compaction pressure from 2 MPa to 10 MPa leads to an increase in the bending strength of about 371.68%. Furthermore, as the compaction pressure rises, the modulus of elasticity and compressive strength of CEB rise as well.

- The total water absorption, swelling, and capillary absorption of the blocks increase with the increase in the DPWA ratio. However, these hygroscopic properties can be qualified as acceptable as they have not exceeded the limits recommended by standards and literature.

- Microstructural analysis by SEM show that the block with a compacting pressure of 2 MPa has more micro-pores than those with compacting pressures of 6 and 10 MPa.

- The SEM microstructural analysis showed the presence of voids between the DPWA aggregates and the matrix. These SEM observations allowed confirming the previously reported mechanical and thermal characterization results.

- The EDX results indicated that the incorporation of DPWA as a substitute for soil and crushed sand in the formulation of CEB caused a decrease in the C-S-H content, which engendered a decrease in compressive and flexural strength of the blocks.

- The results of ε_{xx} show very high localized strains at the middle of block at the bottom of the samples under tension. The strain concentration zone increases as the fiber content increases.

CHAPTER 5

GENERAL CONCLUSION AND PERSPECTIVES

5.1   General conclusion

Earth construction is an older technique in human history. It has been used in most countries of the world, especially in ancient civilizations on a worldwide scale, and it is still widely used today. Algeria contains many Ksour (local name) of earthen buildings that are among the heritage of the country and have remained as a witness to this type of construction. Among the many earth materials techniques, compressed earth block (CEB) has several advantages, notably its compressive strength. In addition, CEB technology is a relatively recent development in construction and has become more popular over the last 50 years. Fortunately, CEBs are used as elements in the construction of load-bearing walls or partition walls of residential or industrial buildings.

This work is a part of a general problem of developing innovative building materials with limited environmental and health impacts. In this context, we proposed to develop and characterize an eco-material for construction formulated from an innovative earth and crushed sand matrix in which conventional additives, fibers and aggregates would be substituted by renewable resources: agro-resources. This research contributes to a feasibility study on the use of renewable natural resources in the production of compressed earth bricks made from date palm waste. Quicklime was used as a stabilizer to improve the strength and durability of the blocks against water.
The targeted applications were of two types:

✓ Compressed earth blocks reinforced with date palm mesh fiber (DPM) and date palm spikelet fiber (DPS) are intended for application in the construction of load-bearing walls, where flexural performance and ductility are most important.

✓ Compressed earth blocks incorporating date palm waste aggregates (DPWAs) as light plant aggregates, for which the mechanical and thermal properties are important, and whose final application would be, for example, the manufacture of self-supporting blocks also providing a distributed insulation function. Thus, these developed blocks possessing attractive mechanical properties, with enhanced thermal insulation features to provide highly insulating walls intended for housing construction.

In the field of civil engineering, the use of plant fibers and aggregates remains relatively new, and this prompted us first to review in depth the literature on the use of plant fibers and aggregates in soil matrices and on its more widespread applications. According to literature the compressive

strength of earth blocks materials is negatively affected by the incorporation of raw plant fibers. However, the incorporation of plant waste for making construction materials reduces heat transfer in buildings. It was found that, during quicklime stabilization of soils, four types of reactions may occur between lime, silica and alumina. These reactions are: (1) Cation exchange, (2) Flocculation and particle aggregation, (3) Lime carbonation, and (4) Pozzolanic reaction.

The third chapter is devoted to the characterization of many of the raw materials used in this work. In our study, local materials were used for make date palm waste-based CEB as follows: soil and crushed sand, quicklime as chemical stabilizer, three kinds of date palm waste (DPWA, DPM and DPS) and water. The mineralogical composition shows that the soil has a high content of calcite, dolomite and quartz and a low concentration of illite and gypsum. The chemical composition shows that the soil has a high content of SiO_2 and CaO. Crushed sand (0/3), for grain size correction. Its chemical composition is mainly composed CaO. Quicklime produced by the lime unit of Saida (Algeria) was used in this study.

All of the findings and debates are presented in the fourth chapter. In this chapter, we studied the effect of date palm waste. This study assessed the valorization of aggregates and fibers of date palm waste (DPWA, DPM, and DPS) as thermal insulator and as fibers reinforcement of compressed earth bricks mixtures. Firstly, the mechanical, thermal and microstructure properties of CEB filled with date palm waste aggregate (DPWA) as thermal insulator were investigated. Secondly, the effect of the kind of date palm waste on the mechanical properties of CEB were studied using DIC method to assess the influence of different date palm type and different compaction pressure in terms of the mixtures: (i) mechanical performance (flexural strength, compressive strength and elastic modulus); and (ii) damage performance (strains concentration). Based on the experimental results, the following conclusions can be drawn:

The incorporation of date palm waste aggregates (DPWAs) in compressed earth blocks (CEBs) improved their thermal behavior. Indeed, adding 0.5% by weight of DPWA decreased the thermal conductivity, thermal diffusivity, and thermal effusivity respectively by 13.28%, 3.69%, and 11.63% in comparison with the reference block (without DPWA). Increasing the DPWA content in the CEB mixture caused the specimen's bulk density to go down. The lightweight block exhibited a lower thermal conductivity as compared to that of the other compressed earth blocks. In fact, the decrease in compaction pressure from 10 MPa to 2 MPa resulted in a significant

decrease in thermal conductivity of about 21.96% for the block containing 0.5% DPWA. Fortunately, this block gives approximately the same result (0.694 W/m.K) as the adobe block without date palm waste (0.677 W/m.K).

The dry and wet compressive strengths decreased while the waste content increased but still remained within the range recommended for compressed earth blocks. In addition, increasing the Date palm Waste (DPW) content decreased the flexural strength of all blocks. The values of the flexural strength was higher for the mixtures with DPWA than for those with DPM or DPS. All of the samples evaluated in this study have bending strengths that exceed those minimal requirements. The specimen integrated by 0.5% DPWA compacted with a static loading by applying a compacting stress of 2MPa has the lowest flexural strength of about 0.93 MPa. However, it stayed within the acceptable CEB range. Increasing the percentage of DPW in the formulation of CEB directly affected the modulus of elasticity. It turned out that the higher this percentage, the smaller the modulus of elasticity. The addition of 0.5% DPS increases the ductility of the bricks, resulting in some residual force and increasing the deflection at failure. The increase in compaction pressure from 2 MPa to 6 MPa resulted in a very significant increase in flexural strength of about 142.83%, and the increase from 2 MPa to 10 MPa resulted in an increase in flexural strength of about 262.73% for the control block (samples without DPW). In addition, it was found that for a block containing 0.5% DPWA, increasing the compaction pressure from 2 MPa to 10 MPa leads to an increase in the bending strength of about 371.68%. Furthermore, as the compaction pressure rises, the modulus of elasticity and compressive strength of CEB rise as well.

The total water absorption, swelling, and capillary absorption of the blocks increase with the increase in the DPWA ratio. However, these hygroscopic properties can be qualified as acceptable as they have not exceeded the limits recommended by standards and literature.

Microstructural analysis by SEM show that the block with a compacting pressure of 2 MPa has more micro-pores than those with compacting pressures of 6 and 10 MPa. The SEM microstructural analysis showed the presence of voids between the DPWA aggregates and the matrix. These SEM observations allowed confirming the previously reported mechanical and thermal characterization results. The EDX results indicated that the incorporation of DPWA as a substitute for soil and crushed sand in the formulation of CEB caused a decrease in the C-S-H content, which engendered a decrease in compressive and flexural strength of the blocks.

The results of ε_{xx} show very high localized strains at the middle of block at the bottom of the samples under tension. The strain concentration zone increases as the fiber content increases.

In conclusion, these findings suggested that this novel Date Palm Waste-based Compressed Earth Bricks may be used as an interesting alternative to produce an environmentally bricks for the construction of walls with interesting mechanical properties and better thermal insulation properties as best as possible than those built with conventional compressed earth blocks.

5.2 Perspectives

This study was conducted using different raw materials, unconventional in our field. It therefore constituted a first step in characterizing these constituents, understanding their interactions and verifying the feasibility of developing composites for buildings from these agro-resources.

The perspectives of this work are therefore numerous and could be the subject of additional studies in each of the axes explored.

1. Study of the real-scale mechanical properties of walls built by compressed earth blocks reinforced by date palm waste fibers.

2. Study of the real-scale dynamic behavior of walls built by compressed earth blocks reinforced by date palm waste fibers.

3. Development of numerical and analytical models for the study of composite structures built by compressed earth bricks reinforced by date palm waste fibers and aggregate.

4. Study of the durability in aggressive environments of compressed earth blocks "CEB" reinforced with date palm waste.

5. Study of the microstructure by x-ray micro-tomography of compressed earth blocks with and without date palm fiber.

References

[1]   H. Van Damme and H. Houben, "Earth concrete. Stabilization revisited," *Cem. Concr. Res.*, vol. 114, pp. 90–102, 2018.

[2]   S. A. Miller and F. C. Moore, "Climate and health damages from global concrete production," *Nat. Clim. Chang.*, vol. 10, no. 5, pp. 439–443, 2020.

[3]   S. Fawzy, A. I. Osman, J. Doran, and D. W. Rooney, "Strategies for mitigation of climate change: a review," *Environ. Chem. Lett.*, vol. 18, pp. 2069–2094, 2020.

[4]   S. A. Miller, A. Horvath, and P. J. M. Monteiro, "Impacts of booming concrete production on water resources worldwide," *Nat. Sustain.*, vol. 1, no. 1, pp. 69–76, 2018.

[5]   S. A. Miller, V. M. John, S. A. Pacca, and A. Horvath, "Carbon dioxide reduction potential in the global cement industry by 2050," *Cem. Concr. Res.*, vol. 114, no. August 2017, pp. 115–124, 2018.

[6]   M. Missoum, A. Hamidat, L. Loukarfi, and K. Abdeladim, "Impact of rural housing energy performance improvement on the energy balance in the North-West of Algeria," *Energy Build.*, vol. 85, pp. 374–388, 2014.

[7]   F. Touloum, A. Younsi, A. Kaci, and A. Benchabane, "Formulation of a composite of date palm wood-cement," *J. Appl. Eng. Sci. Technol.*, vol. 2, no. 2, pp. 57–63, 2016.

[8]   S. H. Ghaffar, M. Al-Kheetan, P. Ewens, T. Wang, and J. Zhuang, "Investigation of the interfacial bonding between flax/wool twine and various cementitious matrices in mortar composites," *Constr. Build. Mater.*, vol. 239, p. 117833, 2020.

[9]   J. Fernandes, M. Peixoto, R. Mateus, and H. Gervásio, "Life cycle analysis of environmental impacts of earthen materials in the Portuguese context : Rammed earth and compressed earth blocks," *J. Clean. Prod.*, vol. 241, p. 118286, 2019.

[10]   G. Minke, *Building With Earth:Design and Technology of a Sustainable Architecture*. Birkhäuser, Basel, Switzerland., 2006.

[11]   B. Medvey and G. Dobszay, "Durability of Stabilized Earthen Constructions: A Review,"

Geotech. Geol. Eng., vol. 38, no. 3, pp. 2403–2425, 2020.

[12] A. Guettala, A. Abibsi, and H. Houari, "Durability study of stabilized earth concrete under both laboratory and climatic conditions exposure," *Constr. Build. Mater.*, vol. 20, pp. 119–127, 2006.

[13] Y. Millogo, M. Hajjaji, and R. Ouedraogo, "Microstructure and physical properties of lime-clayey adobe bricks," *Constr. Build. Mater.*, vol. 22, no. 12, pp. 2386–2392, 2008.

[14] R. Eires, A. Camões, and S. Jalali, "Enhancing water resistance of earthen buildings with quicklime and oil," *J. Clean. Prod.*, vol. 142, pp. 3281–3292, 2017.

[15] M. M. Barbero-Barrera, F. Jové-Sandoval, and S. González Iglesias, "Assessment of the effect of natural hydraulic lime on the stabilisation of compressed earth blocks," *Constr. Build. Mater.*, vol. 260, p. 119877, 2020.

[16] S. A. A. Khattab, M. Al-Mukhtar, and J. Fleureau, "Long-Term Stability Characteristics of a Lime-Treated," *J. Mater. Civ. Eng.*, vol. 19, no. 4, pp. 358–366, 2007.

[17] S. Abdelaziz, S. Guessasma, A. Bouaziz, R. Hamzaoui, J. Beaugrand, and A. A. Souid, "Date palm spikelet in mortar: Testing and modelling to reveal the mechanical performance," *Constr. Build. Mater.*, vol. 124, pp. 228–236, 2016.

[18] B. Taallah, A. Guettala, S. Guettala, and A. Kriker, "Mechanical properties and hygroscopicity behavior of compressed earth block filled by date palm fibers," *Constr. Build. Mater.*, vol. 59, pp. 161–168, 2014.

[19] B. Taallah and A. Guettala, "The mechanical and physical properties of compressed earth block stabilized with lime and filled with untreated and alkali-treated date palm fibers," *Constr. Build. Mater.*, vol. 104, pp. 52–62, 2016.

[20] O. Benaimeche, A. Carpinteri, M. Mellas, C. Ronchei, D. Scorza, and S. Vantadori, "The influence of date palm mesh fibre reinforcement on flexural and fracture behaviour of a cement-based mortar," *Compos. Part B*, vol. 152, pp. 292–299, 2018.

[21] A. Kriker, G. Debicki, A. Bali, M. M. Khenfer, and M. Chabannet, "Mechanical properties of date palm fibres and concrete reinforced with date palm fibres in hot-dry climate," *Cem.*

Concr. Compos., vol. 27, pp. 554–564, 2005.

[22] T. Djoudi, M. Hecini, D. Scida, Y. Djebloun, and H. Djemai, "Physico-Mechanical Characterization of Composite Materials Based on Date Palm Tree Fibers," *J. Nat. Fibers*, pp. 1–14, 2019.

[23] N. Benmansour, B. Agoudjil, A. Gherabli, A. Kareche, and A. Boudenne, "Thermal and mechanical performance of natural mortar reinforced with date palm fibers for use as insulating materials in building," *Energy Build.*, vol. 81, pp. 98–104, 2014.

[24] M. Chikhi, B. Agoudjil, A. Boudenne, and A. Gherabli, "Experimental investigation of new biocomposite with low cost for thermal insulation," *Energy Build.*, vol. 66, pp. 267–273, 2013.

[25] D. Khoudja, B. Taallah, O. Izemmouren, S. Aggoun, O. Herihiri, and A. Guettala, "Mechanical and thermophysical properties of raw earth bricks incorporating date palm waste," *Constr. Build. Mater.*, vol. 270, p. 121824, 2021.

[26] E. Atiki, B. Taallah, S. Feia, K. S. Almeasar, and A. Guettala, "Effects of Incorporating Date Palm Waste as a Thermal Insulating Material on the Physical Properties and Mechanical Behavior of Compressed Earth Block," *J. Nat. Fibers*, vol. 00, no. 00, pp. 1–18, 2021.

[27] K. S. Almeasar, B. Taallah, O. Izemmouren, E. Atiki, and A. Guettala, "Effect of Addition Date Palm Ash on Physical and Mechanical Properties and Hygroscopicity Behavior of Earth Mortars Effect of Addition Date Palm Ash on Physical and Mechanical Properties and," *Int. J. Archit. Herit.*, vol. 00, no. 00, pp. 1–19, 2021.

[28] F. Pacheco-Torgal and S. Jalali, "Earth construction: Lessons from the past for future eco-efficient construction," *Constr. Build. Mater.*, vol. 29, pp. 512–519, 2012.

[29] N. Fezzioui, M. Benyamine, N. Tadj, B. Draoui, and S. Larbi, "Performance énergétique d'une maison à patio dans le contexte maghrébin (Algérie, Maroc, Tunisie et Libye)," *Rev. des Energies Renouvelables*, vol. 15, no. 3, pp. 399–405, 2012.

[30] C. Magniont, "Contribution à la formulation et à la caractérisation d'un écomatériau de construction à base d'agroressources," Ph.D. Thesis; UNIVERSITÉ DE TOULOUSE,

2010.

[31] T. A. Phung, "Formulation et caractérisation d'un composite terre-fibres végétales : la bauge," Ph.D. Thesis;, 2018.

[32] G. Habert *et al.*, "Environmental impacts and decarbonization strategies in the cement and concrete industries," *Nat. Rev. Earth Environ.*, vol. 1, pp. 559–573, 2020.

[33] N. Toubal Seghir, M. Mellas, Ł. Sadowski, and A. Żak, "Effects of marble powder on the properties of the air-cured blended cement paste," *J. Clean. Prod.*, vol. 183, pp. 858–868, 2018.

[34] N. Toubal Seghir, M. Mellas, Ł. Sadowski, A. Krolicka, and A. Żak, "The Effect of Curing Conditions on the Properties of Cement-Based Composites Blended with Waste Marble Dust," *Jom*, vol. 71, no. 3, pp. 1002–1015, 2019.

[35] S. Ramdani, A. Guettala, M. L. Benmalek, and J. B. Aguiar, "Physical and mechanical performance of concrete made with waste rubber aggregate, glass powder and silica sand powder," *J. Build. Eng.*, vol. 21, no. June 2018, pp. 302–311, 2019.

[36] G. Araya-Letelier, J. Concha-Riedel, F. C. Antico, C. Valdés, and G. Cáceres, "Influence of natural fiber dosage and length on adobe mixes damage-mechanical behavior," *Constr. Build. Mater.*, vol. 174, pp. 645–655, 2018.

[37] A. N. Raut and C. P. Gomez, "Utilization of waste as a constituent ingredient for enhancing thermal performance of bricks - A Review paper," *Indian J. Sci. Technol.*, vol. 9, no. 37, 2016.

[38] C. Thomas, I. Sosa, J. Setién, J. A. Polanco, and A. I. Cimentada, "Evaluation of the fatigue behavior of recycled aggregate concrete," *J. Clean. Prod.*, vol. 65, pp. 397–405, 2014.

[39] M. Sutcu, E. Erdogmus, O. Gencel, A. Gholampour, E. Atan, and T. Ozbakkaloglu, "Recycling of bottom ash and fly ash wastes in eco-friendly clay brick production," *J. Clean. Prod.*, vol. 233, pp. 753–764, 2019.

[40] G. Araya-Letelier *et al.*, "Waste-based natural fiber reinforcement of adobe mixtures:

Physical, mechanical, damage and durability performance assessment," *J. Clean. Prod.*, vol. 273, p. 122806, 2020.

[41] W. Ahmad, A. Ahmad, K. A. Ostrowski, F. Aslam, and P. Joyklad, "A scientometric review of waste material utilization in concrete for sustainable construction," *Case Stud. Constr. Mater.*, vol. 15, no. September, p. e00683, 2021.

[42] G. L. Gontijo, "Thermal Behaviour of Compressed Earth Blocks with Municipal Organic Waste Incorporation," School of Technology and Management of Bragança, 2020.

[43] L. Guettatfi, A. Hamouine, K. Himouri, and B. Labbaci, "Mechanical and Water Durability Properties of Adobes Stabilized with White Cement, Quicklime and Date Palm Fibers," *Int. J. Archit. Herit.*, vol. 00, no. 00, pp. 1–15, 2021.

[44] CRAterre, "CRAterre- map of historical earth construction. Around the World, 8.26.21.," 2021.

[45] K. A. J. Ouedraogo, "Stabilisation de matériaux de construction durables et écologiques à base de terre crue par des liants organiques et/ou minéraux à faibles impacts environnementaux," Université Paul Sabatier-Toulouse III, 2019.

[46] M. Bouhicha, F. Aouissi, and S. Kenai, "Performance of composite soil reinforced with barley straw," *Cem. Concr. Compos.*, vol. 27, pp. 617–621, 2005.

[47] M. Gomaa, W. Jabi, V. Soebarto, and Y. Min, "Digital manufacturing for earth construction : A critical review," *J. Clean. Prod.*, vol. 338, no. January, p. 130630, 2022.

[48] H. Danso, "Use of Agricultural Waste Fibres as Enhancement of Soil Blocks for Low-Cost Housing in Ghana," School of Civil Engineering and Surveying University of Portsmouth, 2016.

[49] M. Mostafa and N. Uddin, "Experimental analysis of Compressed Earth Block (CEB) with banana fibers resisting flexural and compression forces," *Case Stud. Constr. Mater.*, vol. 5, pp. 53–63, 2016.

[50] K. Terzaghi, R. B. Peck, and G. Mesri, *Soil Mechanics in Engineering Practice*, Third Edit. John Wiley & Sons, 1996.

[51] M. Budhu, *Soil mechanics and foundations*, 3rd ed. John Wiley & Sons, 2008.

[52] C. Turco, A. C. Paula Junior, E. R. Teixeira, and R. Mateus, "Optimisation of Compressed Earth Blocks (CEBs) using natural origin materials: A systematic literature review," *Constr. Build. Mater.*, vol. 309, no. September, p. 125140, 2021.

[53] R. E. Grim, "Clay Mineralogy," vol. 135, pp. 890–898, 1962.

[54] A. Benchabane, "Etude du comportement rhéologique de mélanges argiles - polymères. Effets de l'ajout de polymères," Université Louis Pasteur – Strasbourg I, 2006.

[55] O. Izemmouren, "Effet des ajouts minéraux sur la durabilité des briques de terre comprimée," Université de Biskra.

[56] V. N. . Murthy, *Geotechnical Engineering: Principles and practices of Soil Mechanics and Fondation Engineering.* 2002.

[57] H. H. Hurray, "Applied clay mineralogy today and tomorrow," *Clay Miner.*, vol. 34, pp. 39–49, 1999.

[58] H. E. Gaudette, J. L. Eades, and R. E. Grim, "The nature of illite," *Clays Clay Miner.*, vol. 13, no. 1, pp. 33–48, 1964.

[59] A. A. Firoozi, A. A. Firoozi, and M. S. Baghini, "A Review of Clayey Soils," *Asian J. Appl. Sci.*, vol. 04, no. 06, p. 13, 2016.

[60] M. C. J. Delgado and I. C. Guerrero, "The selection of soils for unstabilised earth building : A normative review," vol. 21, pp. 237–251, 2007.

[61] A. L. Murmu and A. Patel, "Towards sustainable bricks production: An overview," *Constr. Build. Mater.*, vol. 165, pp. 112–125, 2018.

[62] M. Ben Mansour, A. Jelidi, A. S. Cherif, and S. Ben Jabrallah, "Optimizing thermal and mechanical performance of compressed earth blocks (CEB)," *Constr. Build. Mater.*, vol. 104, pp. 44–51, 2016.

[63] B. V Venkatarama Reddy and K. S. Jagadish, "The static compaction of soils," . *Ghotechnique*, vol. 43, no. 2, pp. 337–341, 1993.

[64]   A. Guettala, H. Houari, B. Mezghiche, and R. Chebili, "Durability of Lime Stabilized Earth Blocks," *Courr. du Savoir*, pp. 61–66, 2002.

[65]   Y. Millogo, J. E. Aubert, E. Hamard, and J. C. Morel, "How Properties of Kenaf Fibers from Burkina Faso Contribute to the Reinforcement of Earth Blocks," vol. 8, no. 5, pp. 2332–2345, 2015.

[66]   H. F. W. Taylor, *Cement Chemistry*, vol. 2. London: Thomas Telford, 1997.

[67]   B. Taallah, "Etude du comportement physico-mécanique du bloc de terre comprimée avec fibres," Université de Biskra, 2014.

[68]   J. Locat, M. A. Bérubé, and M. Choquette, "Laboratory investigations on the lime stabilization of sensitive clays: shear strength development," *Can. Geotech. J.*, vol. 27, no. 3, pp. 294–304, 1990.

[69]   S. Chaib eddra, "Etude de la durabilite d'un beton de terre stabilisee dans son environnement," UNIVERSITE DES SCIENCES ET DE LA TECHNOLOGIE HOUARI BOUMEDIENE, 2019.

[70]   T. Davidenko, "Hydratation D'un Système Cimentaire Binaire Contenant Des Cendres Volantes de Biomasse," Université de Sherbrooke, 2015.

[71]   S. Omar Sore, A. Messan, E. Prud'homme, G. Escadeillas, and F. Tsobnang, "Stabilization of compressed earth blocks (CEBs) by geopolymer binder based on local materials from Burkina Faso," *Constr. Build. Mater.*, vol. 165, pp. 333–345, 2018.

[72]   R. K. Preethi and B. V. V. Reddy, "Experimental investigations on geopolymer stabilised compressed earth products," *Constr. Build. Mater.*, vol. 257, p. 119563, 2020.

[73]   G. Furtos, L. Molnar, L. Silaghi-Dumitrescu, P. Pascuta, and K. Korniejenko, "Mechanical and thermal properties of wood fiber reinforced geopolymer composites," *J. Nat. Fibers*, vol. 00, no. 00, pp. 1–16, 2021.

[74]   A. Celik, K. Yilmaz, O. Canpolat, M. M. Al-mashhadani, Y. Aygörmez, and M. Uysal, "High-temperature behavior and mechanical characteristics of boron waste additive metakaolin based geopolymer composites reinforced with synthetic fibers," *Constr. Build.*

Mater., vol. 187, pp. 1190–1203, 2018.

[75] A. E. Losini, A. C. Grillet, M. Bellotto, M. Woloszyn, and G. Dotelli, "Natural additives and biopolymers for raw earth construction stabilization – a review," *Constr. Build. Mater.*, vol. 304, no. November 2020, p. 124507, 2021.

[76] C. Udawattha, D. E. De Silva, H. Galkanda, and R. Halwatura, "Performance of natural polymers for stabilizing earth blocks," *Materialia*, vol. 2, 2018.

[77] L. Duo, T. Kan-liang, Z. Hui-li, W. Yu-yao, N. Kang-yi, and Z. Shi-can, "Experimental investigation of solidifying desert aeolian sand using microbially induced calcite precipitation," *Constr. Build. Mater.*, vol. 172, pp. 251–262, 2018.

[78] O. Benaimeche, N. T. Seghir, Ł. Sadowski, and M. Mellas, *The Utilization of Vegetable Fibers in Cementitious Materials*. Elsevier, 2020.

[79] S. O. Bamaga, "A Review on the Utilization of Date Palm Fibers as Inclusion in Concrete and Mortar," *Fibers*, vol. 10, pp. 1–10, 2022.

[80] M. Sood and G. Dwivedi, "Effect of fiber treatment on flexural properties of natural fiber reinforced composites: A review," *Egypt. J. Pet.*, vol. 27, no. 4, pp. 775–783, 2018.

[81] N. Kouta, J. Saliba, and N. Saiyouri, "Effect of flax fibers on early age shrinkage and cracking of earth concrete," *Constr. Build. Mater.*, vol. 254, p. 119315, 2020.

[82] D. Asprone, M. Durante, A. Prota, and G. Manfredi, "Potential of structural pozzolanic matrix-hemp fiber grid composites," *Constr. Build. Mater.*, vol. 25, no. 6, pp. 2867–2874, 2011.

[83] A. Kriker, A. Bali, G. Debicki, M. Bouziane, and M. Chabannet, "Durability of date palm fibres and their use as reinforcement in hot dry climates," *Cem. Concr. Compos.*, vol. 30, no. 7, pp. 639–648, 2008.

[84] M. Lahouioui, R. Ben Arfi, M. Fois, L. Ibos, and A. Ghorbal, "Investigation of Fiber Surface Treatment Effect on Thermal, Mechanical and Acoustical Properties of Date Palm Fiber-Reinforced Cementitious Composites," *Waste and Biomass Valorization*, vol. 11, no. 8, pp. 4441–4455, 2020.

[85] W. Abdelmajeed Labib, "Utilisation of date palm fibres in cement-based composites: A feasibility study," *IOP Conf. Ser. Mater. Sci. Eng.*, vol. 596, no. 1, 2019.

[86] S. Amroune, A. Bezazi, A. Belaadi, C. Zhu, and F. Scarpa, "Composites : Part A Tensile mechanical properties and surface chemical sensitivity of technical fibres from date palm fruit branches (Phoenix dactylifera L .)," *Compos. PART A*, vol. 71, pp. 95–106, 2015.

[87] A. Jesudass, V. Gayathri, R. Geethan, M. Gobirajan, and M. Venkatesh, "Earthen blocks with natural fibres - A review," *Mater. Today Proc.*, 2021.

[88] A. Laborel-Préneron, J. E. Aubert, C. Magniont, C. Tribout, and A. Bertron, "Plant aggregates and fibers in earth construction materials: A review," *Construction and Building Materials*, vol. 111. pp. 719–734, 2016.

[89] B. Chihaoui, F. Serra-Parareda, Q. Tarrés, F. X. Espinach, S. Boufi, and M. Delgado-Aguilar, "Effect of the fiber treatment on the stiffness of date palm fiber reinforced PP composites: Macro and micromechanical evaluation of the young's modulus," *Polymers (Basel).*, vol. 12, no. 8, pp. 1–21, 2020.

[90] S. Awad, Y. Zhou, E. Katsou, Y. Li, and M. Fan, *A Critical Review on Date Palm Tree (Phoenix dactylifera L.) Fibres and Their Uses in Bio-composites*, vol. 12, no. 6. Springer Netherlands, 2021.

[91] N. Bouhemame *et al.*, "Tensile Properties Optimization of Date Palm Leaflets Using Taguchi Method," *J. Nat. Fibers*, vol. 00, no. 00, pp. 1–17, 2021.

[92] K. Almi, A. Benchabane, S. Lakel, and A. Kriker, "Potential utilization of date palm wood as composite reinforcement," *J. Reinf. Plast. Compos.*, vol. 34, no. 15, pp. 1231–1240, 2015.

[93] F. M. AL-Oqla and M. S. Salit, *Material selection of natural fiber composites*. Amsterdam, 2017.

[94] J. Biagiotti, D. Puglia, and J. M. Kenny, "A review on natural fibre-based composites - Part I: Structure, processing and properties of vegetable fibres," *J. Nat. Fibers*, vol. 1, no. 2, pp. 37–68, 2004.

[95] C. Álvarez, F. M. Reyes-Sosa, and B. Díez, "Enzymatic hydrolysis of biomass from wood," *Microb. Biotechnol.*, vol. 9, no. 2, pp. 149–156, 2016.

[96] D. . Stokke, Q. Wu, and G. Han, *Introduction to Wood and Natural Fiber Composites*. 2013.

[97] D. Tarek, "Elaboration Et Caractérisation De Composites Bio-Sourcés À Base De Fibres De Palmier Dattier," Université Mohamed Khider – Biskra, 2019.

[98] B. Agoudjil, A. Benchabane, and M. Fois, "Renewable materials to reduce building heat loss : Characterization of date Renewable materials to reduce building heat loss : Characterization of date," *Energy Build.*, vol. 43, no. 2–3, pp. 491–497, 2011.

[99] A. B. Laibi, P. Poullain, N. Leklou, M. Gomina, and D. K. C. Sohounhloué, "Influence of the Length of Kenaf Fibers on the Mechanical and Thermal Properties of Compressed Earth Blocks (CEB)," *KSCE J. Civ. Eng.*, vol. 22, pp. 785–793, 2018.

[100] A. Laborel-Préneron, C. Magniont, and J. E. Aubert, "Hygrothermal properties of unfired earth bricks: Effect of barley straw, hemp shiv and corn cob addition," *Energy Build.*, vol. 178, pp. 265–278, 2018.

[101] A. Laborel-Préneron, J. E. Aubert, C. Magniont, P. Maillard, and C. Poirier, "Effect of Plant Aggregates on Mechanical Properties of Earth Bricks," *J. Mater. Civ. Eng.*, vol. 29, no. 12, p. 04017244, 2017.

[102] H. Omrani, L. Hassini, A. Benazzouk, H. Beji, and A. ELCafsi, "Elaboration and characterization of clay-sand composite based on Juncus acutus fibers," *Constr. Build. Mater.*, vol. 238, p. 117712, 2020.

[103] A. Mesbah, J. C. Morel, P. Walker, and K. Ghavami, "Development of a Direct Tensile Test for Compacted Earth Blocks Reinforced with Natural Fibers," *J. Mater. Civ. Eng.*, vol. 16, no. 1, pp. 95–98, 2004.

[104] D. C. Ngo, J. Saliba, N. Saiyouri, and Z. M. Sbartaï, "Design of a soil concrete as a new building material – Effect of clay and hemp proportions," *J. Build. Eng.*, vol. 32, p. 101553, 2020.

[105] I. Bouchefra, F. Z. EL Bichri, H. Chehouani, and B. Benhamou, "Mechanical and thermophysical properties of compressed earth brick rienforced by raw and treated doum fibers," *Constr. Build. Mater.*, vol. 318, p. 126031, 2022.

[106] A. Laborel-Préneron, C. Magniont, and J. E. Aubert, "Characterization of Barley Straw, Hemp Shiv and Corn Cob as Resources for Bioaggregate Based Building Materials," *Waste and Biomass Valorization*, vol. 9, no. 7, pp. 1095–1112, 2018.

[107] M. Segetin, K. Jayaraman, and X. Xun, "Harakeke reinforcement of soil-cement building materials: Manufacturability and properties," *Build. Environ.*, vol. 42, no. 8, pp. 3066–3079, 2007.

[108] K. Ghavami, R. D. Toledo Filho, and N. P. Barbosa, "Behaviour of composite soil reinforced with natural fibres," *Cem. Concr. Compos.*, vol. 21, no. 1, pp. 39–48, 1999.

[109] J. Blaber, B. Adair, and A. Antoniou, "Ncorr: Open-Source 2D Digital Image Correlation Matlab Software," *Exp. Mech.*, vol. 55, pp. 1105–1122, 2015.

[110] B. Pan, "Recent Progress in Digital Image Correlation," *Exp. Mech.*, vol. 51, pp. 1223–1235, 2011.

[111] A. Khechai, A. Tati, B. Guerira, A. Guettala, and P. M. Mohite, "Strength degradation and stress analysis of composite plates with circular, square and rectangular notches using digital image correlation," *Compos. Struct.*, vol. 185, pp. 699–715, 2018.

[112] A. H. Salmanpour, N. Mojsilović, and J. Schwartz, "Displacement capacity of contemporary unreinforced masonry walls: An experimental study," *Eng. Struct.*, vol. 89, pp. 1–16, 2015.

[113] A. Madadi, H. Eskandari-Naddaf, R. Shadnia, and L. Zhang, "Digital image correlation to characterize the flexural behavior of lightweight ferrocement slab panels," *Constr. Build. Mater.*, vol. 189, pp. 967–977, 2018.

[114] S. Rouchier, G. Foray, N. Godin, M. Woloszyn, and J. J. Roux, "Damage monitoring in fibre reinforced mortar by combined digital image correlation and acoustic emission," *Constr. Build. Mater.*, vol. 38, pp. 371–380, 2013.

[115] A. El Hajjar, T. Ouahbi, S. Taibi, J. Eid, M. Hattab, and J. M. Fleureau, "Assessing crack initiation and propagation in flax fiber reinforced clay subjected to desiccation," *Constr. Build. Mater.*, vol. 278, p. 122392, 2021.

[116] N. Kouta, J. Saliba, and N. Saiyouri, "Fracture behavior of flax fibers reinforced earth concrete," *Eng. Fract. Mech.*, no. August, p. 107378, 2020.

[117] F. Stazi, M. Serpilli, G. Chiappini, M. Pergolini, E. Fratalocchi, and S. Lenci, "Experimental study of the mechanical behaviour of a new extruded earth block masonry," *Constr. Build. Mater.*, vol. 244, p. 118368, 2020.

[118] S. Y. Alam, J. Saliba, and A. Loukili, "Fracture examination in concrete through combined digital image correlation and acoustic emission techniques," *Constr. Build. Mater.*, vol. 69, no. February 2016, pp. 232–242, 2014.

[119] A. Farsi *et al.*, "Full deflection profile calculation and Young's modulus optimisation for engineered high performance materials," *Sci. Rep.*, vol. 7, no. March, pp. 1–13, 2017.

[120] G. Araya-Letelier *et al.*, "Experimental evaluation of adobe mixtures reinforced with jute fibers," *Constr. Build. Mater.*, vol. 276, p. 122127, 2021.

[121] C.D.E, "Centre for Development of Enterprise (C.D.E). Compressed earth blocks: Testing procedures. In: C.D.E., ENTPE et CRATerre Coed." Belgique: Bruxelles, p. 121, 2000.

[122] Y. He, "Rapid thermal conductivity measurement with a hot disk sensor: Part 2. Characterization of thermal greases," *Thermochim. Acta*, vol. 436, pp. 130–134, 2005.

[123] E. Ouedraogo, O. Coulibaly, A. Ouedraogo, and A. Messan, "Caractérisation mécanique et thermophysique des blocs de terre comprimée stabilisée au papier (cellulose) et / ou au ciment," *J. Mater. Eng. Struct.*, vol. 2, pp. 68–76, 2015.

[124] N. Latroch, A. S. Benosman, N. E. Bouhamou, Y. Senhadji, and M. Mouli, "Physico-mechanical and thermal properties of composite mortars containing lightweight aggregates of expanded polyvinyl chloride," *Constr. Build. Mater.*, vol. 175, pp. 77–87, 2018.

[125] T. Cheboub, Y. Senhadji, H. Khelafi, and G. Escadeillas, "Investigation of the engineering properties of environmentally-friendly self-compacting lightweight mortar containing olive

kernel shells as aggregate," *J. Clean. Prod.*, vol. 249, p. 119406, 2020.

[126] B. Pan, K. Qian, H. Xie, and A. Asundi, "Two-dimensional digital image correlation for in-plane displacement and strain measurement: A review," *Meas. Sci. Technol.*, vol. 20, pp. 1–17, 2009.

[127] B. Pan, A. Asundi, H. Xie, and J. Gao, "Digital image correlation using iterative least squares and pointwise least squares for displacement field and strain field measurements," *Opt. Lasers Eng.*, vol. 47, no. 7–8, pp. 865–874, 2009.

[128] S. Yoneyama and G. Murasawa, "Digital image correlation," *Exp. Mech.*, vol. 207, 2009.

[129] O. Benaimeche, "Elaboration et caractérisation d' un bio-composite destiné à la construction," Mohamed Khider University- Biskra, 2019.

[130] A. G. Kerali, "Durability of compressed and cement-stabilised building blocks," Ph.D. Thesis; School of Engineering, University of Warwick, 2001.

[131] J. Khedari, B. Suttisonk, N. Pratinthong, and J. Hirunlabh, "New lightweight composite construction materials with low thermal conductivity," *Cem. Concr. Compos.*, vol. 23, no. 1, pp. 65–70, 2001.

[132] M. Boumhaout, L. Boukhattem, H. Hamdi, B. Benhamou, and F. Ait Nouh, "Thermomechanical characterization of a bio-composite building material: Mortar reinforced with date palm fibers mesh," *Constr. Build. Mater.*, vol. 135, pp. 241–250, 2017.

[133] T. Ashour, H. Wieland, H. Georg, F. J. Bockisch, and W. Wu, "The influence of natural reinforcement fibres on insulation values of earth plaster for straw bale buildings," *Mater. Des.*, vol. 31, no. 10, pp. 4676–4685, 2010.

[134] F. Naiiri, A. Lamis, S. Mehdi, Z. Redouane, and Z. Mondher, "Performance of lightweight mortar reinforced with doum palm fiber," *J. Compos. Mater.*, 2020.

[135] T. Djoudi, H. Djemai, M. Hecini, and A. Ferhat, "Physical, Thermal and Mechanical Characterization of a New Material Composite Based on Fibrous Wood Particles of Date Palm Tree," *Rev. des Compos. des matériaux avancés*, vol. 32, no. 1, pp. 45–52, 2022.

[136] A. Djoudi, M. M. Khenfer, A. Bali, and T. Bouziani, "Effect of the addition of date palm fibers on thermal properties of plaster concrete : experimental study and modeling," *J. Adhes. Sci. Technol.*, vol. 28, no. 20, pp. 2100–2111, 2014.

[137] A. . . Cherki, A. Khabbazi, B. Remy, and D. Baillis, "Granular cork content dependence of thermal diffusivity, thermal conductivity and heat capacity of the composite material / Granular cork bound with plaster," *Energy Procedia*, vol. 42, pp. 83–92, 2013.

[138] F. El Fgaier, Z. Lafhaj, E. Antczak, and C. Chapiseau, "Dynamic thermal performance of three types of unfired earth bricks," *Appl. Therm. Eng.*, vol. 93, pp. 377–383, 2016.

[139] B. Belhadj, M. Bederina, N. Montrelay, J. Houessou, and M. Quéneudec, "Effect of substitution of wood shavings by barley straws on the physico-mechanical properties of lightweight sand concrete," *Constr. Build. Mater.*, vol. 66, pp. 247–258, 2014.

[140] F. A. Al-sulaiman, "Date palm fibre reinforced composite as a new insulating material," vol. 1297, no. February, pp. 1293–1297, 2003.

[141] S. Benaniba, Z. Driss, M. Djendel, E. Raouache, and R. Boubaaya, "Thermo-mechanical characterization of a bio-composite mortar reinforced with date palm fiber," *J. Eng. Fiber. Fabr.*, vol. 15, 2020.

[142] D. Taoukil, A. El bouardi, T. Ajzoul, and H. Ezbakhe, "Effect of the incorporation of wood wool on thermo physical proprieties of sand mortars," *KSCE J. Civ. Eng.*, vol. 16, no. 6, pp. 1003–1010, 2012.

[143] S. Ajouguim *et al.*, "Effect of Alfa fibers on the mechanical and thermal properties of compacted earth bricks," *Mater. Today Proc.*, no. xxxx, 2020.

[144] H. M. Algin and P. Turgut, "Cotton and limestone powder wastes as brick material," *Constr. Build. Mater.*, vol. 22, no. 6, pp. 1074–1080, 2008.

[145] M. C. N. Villamizar, V. S. Araque, C. A. R. Reyes, and R. S. Silva, "Effect of the addition of coal-ash and cassava peels on the engineering properties of compressed earth blocks," *Constr. Build. Mater.*, vol. 36, pp. 276–286, 2012.

List of publications and communications

List of publications and communications

International Journal Papers

■   **Atiki, E.**, Taallah, B., Feia, S., Almeasar, K. S., & Guettala, A. (**2021**). ''**Effects of Incorporating Date Palm Waste as a Thermal Insulating Material on the Physical Properties and Mechanical Behavior of Compressed Earth Block**''. *Journal of Natural Fibers*, 1-18.

■   K. S. Almeasar, B. Taallah, O. Izemmouren, **E. Atiki**, and A. Guettala. "**Effect of Addition Date Palm Ash on Physical and Mechanical Properties and Hygroscopicity Behavior of Earth Mortars**" *International Journal of Architectural Heritage*. (2021): 1–19.

International Conference Papers

• **E. Atiki,** B. Taallah , S. Feia, K. S. Almeasar, A. Guettala. ''Experimental evaluation of dynamic modulus of elasticity and hygroscopicity behavior of compressed earth blocks (CEBs) based on date palm wastes aggregates (DPWAs)''. First international conference on geotechnical, structural and advanced materials, 05-07 December **2021**,Biskra, Algeria.

• **E. Atiki**, B. Taallah , S. Feia, K. S. Almeasar, A. Guettala. ''Effect of compaction pressure on dynamic modulus of elasticity and compressive strength of compressed earth blocks (CEBs) based on date palm waste aggregates (DPWA)''. Construction Materials of The first International Conference on Energy, Thermofluids and Materials Engineering, ICETME 2021 held online from 18 to 20 December, **2021,** Biskra, Algeria.

• **E. Atiki**, B. Taallah , S. Feia, K. S. Almeasar, A. Guettala. ''The relationship between porosity and dynamic modulus of elasticity of CEB based on date palm waste fibers''. 8th International Conference on Materials Science and Nanotechnology For Next Generation (MSNG-2021) July 14-16, **2021** / TURKEY.

• **E. Atiki**, B. Taallah, K. S. Almeasar, D. Khoudja, A. Guettala. ''Relationship between density and thermal properties of Compressed Earth Block (CEB) based on date palm waste aggregates''.

3rd International Conference on Applied Engineering and Natural Sciences. July 20-23, 2022, Konya, Turkey.

- D. Khoudja, B. Taallah, O. Izemmouren, **E. Atiki**, K. S Almeasar, and A. Guettala.''Compressive and flexural strength of adobe bricks filled with date palm waste aggregates (DPWA) and the relationship between their water absorption and thermal properties". 1st International Conference on Engineering and Applied Natural Sciences. May 10-13, 2022, Konya, Turkey.

- K. S Almeasar, B. Taallah, O. Izemmouren, **E. Atiki**, and A. Guettala "Mechanical properties of earth mortars stabilized with date palm ash (DPA) and lime". International Conference on Geotechnical, Structural and Advanced Materials Engineering: From Research to Practice. 05-07 December 2021, University of Biskra, ALGERIA.

- K. S Almeasar, B. Taallah, **E. Atiki**, O. Izemmouren, and A. Guettala "Relationship Between Ultrasonic Pulse Velocity and Mechanical Strength for Earth Mortars with Date Palm Ash". International Conference on New Trends in Science and Applications (NTSA) 12-13 October 2021, TURKEY.

- K. S Almeasar, B. Taallah, **E. Atiki**, D. Khoudja, O. Izemmouren, and A. Guettala. ''Effect of date palm ash on shrinkage of earth mortar". Conference: 3rd International Conference on Applied Engineering and Natural Sciences. July 20-23, 2022, Konya, Turkey.

- K. S Almeasar, B. Taallah, O. Izemmouren, **E. Atiki**, and A. Guettala. ''Effects of sand type on the mechanical properties of earth mortars'', 8th International conference on Materials Science and Nanotechnology for next Generation (MSNG2021), July 14-16/ 2021, Elazig, Turkey.